

**Biodegradation of Poly (Ethylene Terephthalate) by  
Bacteria Isolated from Soil**



By  
**Salah Ud Din**

**Department of Microbiology  
Faculty of Biological Sciences  
Quaid-I-Azam University  
Islamabad  
2023**

**Biodegradation of Poly (Ethylene Terephthalate) by  
Bacteria Isolated from Soil**

*A thesis submitted in partial fulfillment of the requirements for the*

*Degree of*

**Doctor of Philosophy**

**In**

**Microbiology**



**By**

**Salah Ud Din**

**Department of Microbiology  
Faculty of Biological Sciences  
Quaid-i-Azam University  
Islamabad  
2023**

*In the name of Allah, the Most Gracious,  
the Most Merciful*

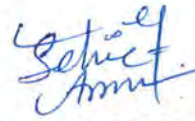
*To*

*My beloved parents, Wife,  
and brother for their love,  
support and prayers*

**Author's Declaration**

I **Mr. Salah Ud Din** hereby state that my Ph.D. thesis titled "**Biodegradation of Poly (Ethylene Terephthalate) by Bacteria Isolated from Soil**" is my own work and has not been submitted previously by me for taking any degree from Quaid-i-Azam University, Islamabad, Pakistan.

At any time if my statement is found to be incorrect even after I Graduate, the University has the right to withdraw my Ph.D. degree.



**Mr. Salah Ud Din**  
**Date: 31-10-2023**

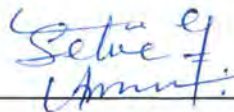
### Plagiarism Undertaking

**“Biodegradation of Poly (Ethylene Terephthalate) by Bacteria Isolated from Soil”** is solely my research work with no significant contribution from any other person. Small contribution / help wherever taken has been duly acknowledged and that complete thesis has been written by me.

I understand the zero tolerance policy of the HEC and Quaid-i-Azam University towards plagiarism. Therefore I as an Author of the above titled thesis declare that no portion of my thesis has been plagiarized and any material used as reference is properly referred/cited.

I undertake that if I am found guilty of any formal plagiarism in the above titled thesis even after award of Ph.D degree and that HEC and the University has the right to publish my name on the HEC/University Website on which names of students are placed who submitted plagiarized thesis.

Student / Author Signature: \_\_\_\_\_




Name: **Mr. Salah Ud Din**

### Certificate of Approval

This is to certify that the research work presented in this thesis, entitled titled "**Biodegradation of Poly (Ethylene Terephthalate) by Bacteria Isolated from Soil**" was conducted by **Mr. Salah Ud Din** under the supervision of **Prof. Dr. Aamer Ali Shah**. No part of this thesis has been submitted anywhere else for any other degree. This thesis is submitted to the Department of Microbiology, Quaid-i-Azam University, Islamabad in partial fulfillment of the requirements for the degree of Doctor of Philosophy in field of **Microbiology**.

Student Name: **Mr. Salah Ud Din**

Signature: 

#### Examination Committee:

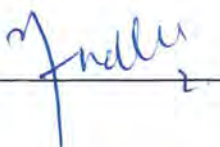
a) External Examiner 1:

Signature: 

**Prof. Dr. Ijaz Ali**

Department of Biosciences  
COMSATS University Islamabad Campus  
Chak Shehzad Islamabad.

b) External Examiner 2:

Signature: 

**Prof. Dr. Saadia Andleeb**

Atta-ur-Rehman School of Applied Biosciences,  
National University of Science & Technology,  
NUST, Islamabad.

Supervisor Name: **Prof. Dr. Aamer Ali Shah**

Signature: 

Name of HOD: **Prof. Dr. Naeem Ali**

Signature: 

## Contents

S. No	Title	Page No
	<b>List of Tables</b>	<b>i</b>
	<b>List of Figures</b>	<b>iii</b>
	<b>List of Acronym/abbreviations</b>	<b>xi</b>
	<b>Acknowledgments</b>	<b>xv</b>
	<b>Summary</b>	<b>xvii</b>
	<b>Introduction</b>	<b>1</b>
	Research Questions	<b>6</b>
	Aim and Objectives	<b>7</b>
	<b>Literature review</b>	<b>8</b>
<b>2.1</b>	A brief overview on plastic	<b>8</b>
<b>2.2</b>	Plastics in Environment	<b>9</b>
<b>2.3</b>	Production and use of Plastic	<b>9</b>
	2.3.1 Production	<b>9</b>
	2.3.2 Plastic Consumption	<b>11</b>
<b>2.4</b>	Plastic Waste Generation	<b>11</b>
<b>2.5</b>	The Marine Plastic Pollution	<b>13</b>
<b>2.6</b>	Plastics in freshwater	<b>14</b>



<b>2.7</b>	Environmental and Other Hazards of Plastic	<b>14</b>
	2.7.1 Plastic Waste Deposition in the Natural Environment	<b>15</b>
	2.7.2 Animals' Risks of Entanglement and Ingestion	<b>16</b>
	2.7.3 Toxicity Transfer through the Food Chain	<b>17</b>
	2.7.4 Human Health Hazards of Plastic	<b>18</b>
<b>2.8</b>	Plastic Disposal Methods	<b>19</b>
	2.8.1 Landfill	<b>19</b>
	2.8.2 Incineration	<b>19</b>
	2.8.3 Recycling	<b>19</b>
<b>2.9</b>	Biotic and Abiotic Mechanisms of Polymer Degradation	<b>20</b>
	2.9.1 Abiotic degradation	<b>21</b>
	2.9.1.1 Mechanical Process	<b>21</b>
	2.9.1.2 Thermal Degradation	<b>21</b>
	2.9.1.3 Photodegradation	<b>22</b>
	2.9.1.6 Chemical Process	<b>23</b>
<b>2.9.2</b>	Biotic degradation	<b>23</b>
	2.9.2.1 Biological process	<b>23</b>
	2.9.2.2. Depolymerization	<b>24</b>
	2.9.2.3 Biodeterioration	<b>25</b>

	2.9.2.4 Bio-fragmentation	25
	2.9.2.5 Mineralization	26
<b>2.10</b>	Classification of plastics	26
	2.10.1 Non-biodegradable plastics	26
	2.10.2 Biodegradable plastics: A green alternative	27
	2.10.3 Bioplastics	28
	2.10.3.1 Bioplastics from renewable resources	29
	2.10.3.1 Bioplastics from non-renewable resources	29
<b>2.11</b>	Enzymes and Microorganisms able to Biodegrade Polymers	30
	2.11.1 Microbial Population	31
<b>2.12</b>	Different typed of synthetic plastic	31
	2.12.1 Polyurethanes	32
	2.12.2 Polyethylene	32
	2.12.3 Polyamide	33
	2.12.4 Polystyrene	33
	2.12.5 Polyvinylchloride PVC and polypropylene PP	33
	2.12.6 Polyethylene terephthalate PET	34
<b>2.13</b>	Properties and Applications of PET	35

<b>2.14</b>	Chemical Structure and Synthesis of PET	<b>36</b>
<b>2.15</b>	PET in the Environment	<b>37</b>
<b>2.16</b>	Biodegradation of PET	<b>38</b>
<b>2.17</b>	Role of enzyme in Degradation of PET	<b>39</b>
	2.17.1 Extracellular Enzymes	<b>41</b>
	2.17.1.1 Carboxylesterases	<b>41</b>
	2.17.1.2 Lipases	<b>42</b>
<b>3.1</b>	2.17.1.3 Cutinase	<b>43</b>
<b>2.18</b>	Application of Cutinase in Industry	<b>44</b>
	<b>Material and Method</b>	<b>45</b>
	Overview of material and methods	<b>45</b>
<b>3.1</b>	Collection of Samples	<b>46</b>
<b>3.2</b>	Isolation of bacteria	<b>46</b>
<b>3.3</b>	Screening of bacterial isolates for PET degradation by selective enrichment	<b>46</b>
	3.3.1 Inoculum preparation	<b>47</b>
	3.3.2 Screening experiment	<b>47</b>
	3.3.3 Determination of Bacterial growth	<b>47</b>
<b>3.4</b>	Identification and Characterization of PET degrading Bacterial Strain PRS8	<b>48</b>

	3.4.1 Microscopic and macroscopic characterization	<b>48</b>
	3.4.1.1 Macroscopic examination	<b>48</b>
	3.4.1.2 Microscopic examination (Gram's Staining)	<b>48</b>
	3.4.2 Biochemical identification	<b>49</b>
	3.4.2.1 Catalase test	<b>49</b>
	3.4.2.2 Oxidase test	<b>50</b>
	3.4.2.3 Triple sugar iron test (TSI)	<b>50</b>
	3.4.2.4 Urease test	<b>51</b>
	3.4.2.5 MacConkey Agar Test	<b>51</b>
	3.4.2.6 Indole Test	<b>52</b>
	3.4.2.7 Citrate Utilization Test	<b>52</b>
	3.4.3 Molecular Identification of Bacterial Strain PRS	<b>53</b>
	3.4.3.1 Genomic DNA extraction	<b>53</b>
	3.4.3.2 Preparation of agarose gel and Confirmation of Genomic DNA	<b>54</b>
	3.4.3.3 Phylogenetic analysis	<b>54</b>
<b>3.5</b>	Biofilm assay for Bacterial Strain PRS8	<b>55</b>
	3.5.1 Congo red agar	<b>55</b>
	3.5.2 Microtitre Plate Assay	<b>55</b>

<b>3.6</b>	Evaluation of bacterial Hydrophobicity	<b>56</b>
<b>3.7</b>	Qualitative screening of cutinase by <i>Stenotrophomonas maltophilia</i> PRS8	<b>57</b>
	3.7.1 Polycaprolacton Agar for cutinase activity	<b>57</b>
<b>3.8</b>	Extracellular Protein determination	<b>57</b>
	3.8.1 Standard Stock Solution of Bovine Serum Albumin Procedure	<b>58</b>
	3.8.2 Standard Curve Development	<b>58</b>
<b>3.9</b>	Reagents for Enzyme Assay	<b>60</b>
	3.9.1 Stock Preparation of substrate	<b>60</b>
	3.9.2 Potassium phosphate buffer	<b>60</b>
	3.9.3 Standard curve development for <i>p</i> -nitrophenol ( <i>p</i> NP)	<b>61</b>
<b>3.10</b>	Biodegradation of PET by <i>S. maltophilia</i> PRS8	<b>62</b>
	3.10.1 Quantitative assay for total protein and cutinase activity from degradation experiment	<b>63</b>
<b>3.11</b>	Analysis of Degradation of PET by <i>S. maltophilia</i> PRS8	<b>63</b>
	3.11.1 Determination of dry weight of residual PET	<b>63</b>
	3.11.2. Fourier-transform Infrared (FT-IR) Spectroscopy	<b>64</b>
	3.12.3. Scanning Electron Microscopy (SEM)	<b>64</b>
<b>3.12</b>	Cutin Extraction from tomato peel	<b>64</b>
<b>3.13</b>	Standardization of Cutinase Assay Conditions	<b>65</b>

	3.13.1 Enzyme production media	<b>65</b>
	3.13.2 Optimization of Temperature for enzyme assay	<b>65</b>
	3.13.3 Optimization of pH for enzyme assay	<b>66</b>
	3.13.4 Optimization of Substrate concentration for enzyme assay	<b>66</b>
	3.13.5 Optimization of Enzyme Solution Concentration for enzyme assay	<b>66</b>
	3.13.6 Optimization of incubation time for enzyme assay	<b>66</b>
<b>3.14</b>	Optimization of physico-chemical parameters for Cutinase Production <i>S. maltophilia</i> PRS8	<b>66</b>
	3.14.1 Preparation of Inoculum	<b>67</b>
	3.14.2 Effect of temperature	<b>67</b>
	3.14.3 Effect of pH	<b>67</b>
	3.14.4 Effect of incubation time	<b>67</b>
	3.14.5 Effect of Inoculum size	<b>67</b>
<b>3.15</b>	Plackett Burman Design for optimizing of nutritional condition	<b>68</b>
<b>3.16</b>	Central Composite Design (CCD) Experiment	<b>68</b>
<b>3.17</b>	Bulk production of crude Cutinase	<b>69</b>
<b>3.18</b>	Purification of Cutinase from <i>S. maltophilia</i> PRS8	<b>69</b>
	3.18.1 Ammonium sulfate precipitation	<b>69</b>
	3.18.2 Dialysis of crude enzyme	<b>70</b>

<b>3.19</b>	Protein purification by gel permeation (Sephadex G-100) column chromatography	<b>70</b>
<b>3.20</b>	Molecular Weight determination Through SDS-PAGE	<b>71</b>
	3.20.1 15% Resolving gel preparation	<b>71</b>
	3.20.2 8% Stacking gel Preparation	<b>71</b>
	3.20.3 Cutinase Treatment	<b>71</b>
	3.20.4 Electrophoresis buffer Preparation	<b>71</b>
	3.20.5 Separation of cutinase	<b>71</b>
	3.20.6 Staining of Gel	<b>72</b>
	3.20.7 Zymograph for Cutinase activity	<b>72</b>
<b>3.21</b>	Characterization of Purified Cutinase	<b>72</b>
	3.21.1 Effect of Temperature on the activity and stability	<b>73</b>
	3.21.2 Effect of pH on the activity and stability	<b>73</b>
	3.21.3 Effect of Metals ions	<b>73</b>
	3.21.3. Effect of organic solvents	<b>73</b>
	3.21.4. Effect of organic surfactant	<b>74</b>
<b>3.22</b>	Kinetic parameters of purified cutinase enzyme	<b>74</b>
<b>3.23</b>	Enzymatic Depolymerization of PET by purified cutinase	<b>74</b>
	3.23.1. Sample preparation and investigation of depolymerization products	<b>74</b>

	3.23.2 Specifications for LC-MS equipment	75
<b>3.24</b>	Analysis of Degradation of enzymatically treated PET	75
	3.24.1 Differential Scanning Calorimetry Analysis	75
	3.24.2 Quantitative assay for cutinase activity and Determination of dry weight of residual PET	76
	3.24.3 Fourier-transform Infrared (FT-IR) Spectroscopy of Enzymatically treated PET	76
	3.24.3 Scanning Electron Microscopy (SEM) of Enzymatically treated PET	76
<b>3.25</b>	Cloning and expression of PET degrading enzyme	77
	3.25.1 Preparation of culture media	77
	3.25.2 Preparation of antibiotic	77
	3.25.3 Isopropyl- $\beta$ -D-thiogalactoside stock Preparation	77
	3.25.4 X-Gal Stock Preparation	78
	3.25.5 Selection of recombinant Strains	78
	3.25.6 Vectors and plasmids	78
	3.25.7 Deigning of primers	79
<b>3.26</b>	Isolating Genomic DNA extraction of PRS8 by QIAamp® DNA Mini Kit (QIAGEN)	79
	3.26.2 Preparation of agarose gel and confirmation of genomic DNA	80
	3.26.3 Nucleic acid quantification by NanoDrop (ND-100)	81
<b>3.27</b>	Polymerase Chain Reaction (PCR) to Amplify PET Hydrolase Gene	81



	3.27.1 Purification of DNA from polyacrylamide gel by QIAEX II® Gel Extraction Kit (QIAGEN)	82
	3.27.3 Ligation of PCR purified Products	82
<b>3.28</b>	Cloning and expression experiments	83
	3.28.1 Preparation of competent cells	83
	3.28.2 Transformation of <i>E. coli</i> competent cells by heat shock method	83
	3.28.3 Plasmid extraction of transformed cell by QIAprep® Spin Miniprep Kit -QIAGEN	84
	3.28.4 Confirmation of Cloning with NdeI and XhoI restriction enzymes	85
	3.28.5 Purification of double digested band from polyacrylamide gel by QIAEX II® Gel Extraction Kit (QIAGEN)	85
<b>3.29</b>	Ligation of purified pET2b plasmid and cloned gene	86
	3.29.1 Transformation of Insert + pET21b plasmid <i>E. coli</i> DH5α competent cells by heat shock method	86
	3.29.2 Plasmid extraction of transformed cell by QIAprep® Spin Miniprep Kit -QIAGEN	86
	3.29.3 Verification of PET hydrolase gene Cloning	87
	3.29.3 Confirmation of Cloning with NdeI and XhoI restriction enzymes	87
	3.29.4 Sequencing of cloned PET hydrolase gene	87
<b>3.30</b>	Bioinformatics analysis	88
<b>3.31</b>	Growth Conditions and Expression of PET hydrolase gene <i>E. coli</i> BL21	88
<b>3.32</b>	Purification of Recombinant Protein	88

	3.32.1 Protein purification by HiPrep 16/60 Sephacryle S-300 High resolution Gel filtration column Chromatography	<b>88</b>
	3.32.2 Mini- protein TGX Staining-free SDS polyacrylamide gels of protein	<b>89</b>
<b>3.33</b>	Characterization of Purified recombinant enzyme	<b>89</b>
	3.33.1 Effect of Temperature on the activity and stability	<b>89</b>
	3.33.2 Effect of pH on the activity and stability	<b>90</b>
	3.33.3. Effect of Metals ions	<b>90</b>
	3.33.4. Effect of Organic Solvents	<b>90</b>
	3.33.5. Effect of Surfactant	<b>90</b>
<b>3.34</b>	Enzymatic Depolymerization of PET by Recombinant Enzyme	<b>91</b>
	2.34.1. Sample preparation	<b>91</b>
	3.34.2 Analysis of de-polymerization products by HPLC	<b>91</b>
	2.34.3 LC-MS analysis of Depolymerization products	<b>91</b>
<b>3.35</b>	Degradation Analysis of Enzymatically Treated PET	<b>92</b>
	3.35.1 Differential Scanning Calorimetry Analysis	<b>92</b>
	3.35.2 Determination of dry weight of residual PET	<b>92</b>
	3.35.3 Fourier-transform Infrared (FT-IR) Spectroscopy of Enzymatically treated PET	<b>92</b>
	<b>Results</b>	<b>93</b>
<b>4.1</b>	Collection of Sample	<b>93</b>

<b>4.2</b>	Isolation of bacteria	<b>93</b>
<b>4.3</b>	Screening of bacterial isolates for PET degradation	<b>93</b>
<b>4.4</b>	Identification of PET degrading bacterial strain PRS8	<b>93</b>
	4.4.1 Growth of Bacterial strain	<b>93</b>
	4.4.2 Macroscopic and Microscopic Characteristics	<b>94</b>
	4.4.3 Biochemical characteristics	<b>94</b>
	4.4.4 Molecular identification os strain PRS8	<b>94</b>
<b>4.5</b>	Biofilm Assays of <i>S. maltophilia</i> PRS8	<b>98</b>
	4.5.1 Congo red agar	<b>98</b>
	4.5.2 Microtitre Plate Assay	<b>98</b>
<b>4.6</b>	Evaluation bacterial Hydrophobicity	<b>98</b>
<b>4.7</b>	Qualitative Cutinase assay using PCL agar plate	<b>102</b>
<b>4.8</b>	Analysis of Degradation of PET by <i>S. maltophilia</i> PRS8	<b>102</b>
	4.8.1 Determination of dry weight of residual PET	<b>102</b>
	4.8.2 Fourier-transform infrared (FT-IR) spectroscopy	<b>102</b>
	4.8.3 Scanning Electron Microscopy (SEM)	<b>102</b>
	4.8.4 Quantitative Assay for Cutinase activity and total protein by <i>S. maltophilia</i> PRS8	<b>103</b>
<b>4.9</b>	Standardization of enzyme assay conditions	<b>106</b>

<b>4.10</b>	Optimization of physico-chemical parameters for Cutinase production by <i>S. maltophilia</i> PRS8	<b>106</b>
	4.10.1 Effect of temperature	<b>106</b>
	4.10.2 Effect of pH	<b>106</b>
	4.10.3 Effect of Incubation Time	<b>106</b>
	4.10.4 Effect of inoculum size	<b>107</b>
<b>4.11</b>	Plackett Burman Design for optimizing of nutritional condition	<b>110</b>
<b>4.12</b>	Optimization of significant variable using Central Composite Design (CCD)	<b>110</b>
<b>4.13</b>	Purification of Cutinase from <i>S. maltophilia</i> PRS8 strain	<b>119</b>
	4.13.1 Precipitation with ammonium sulfate	<b>119</b>
	4.13.2 Protein purification (Sephadex G-100) column Chromatography	<b>119</b>
	4.13.3 Purification steps	<b>119</b>
	4.13.4 Molecular Weight determination (SDS-PAGE)	<b>119</b>
<b>4.14</b>	Characterization of purified Cutinase	<b>122</b>
	4.14.1 Effect of temperature on the activity and stability	<b>122</b>
	4.14.2 Effect of pH on the activity and stability	<b>122</b>
	4.14.3 Effect of Metal Ions on the activity of enzyme	<b>122</b>
	4.14.4 Effect of Surfactants on the activity of enzyme	<b>123</b>
	4.14.5 Effect of organic solvents on the activity of enzyme	<b>123</b>

	3.14.6. Kinetic parameter of Cutinase	<b>123</b>
<b>4.15</b>	Cutinase activity on PET and analysis of Depolymerization by HPLC	<b>128</b>
	4.15.1 Identification of Degradation Products by LC-MS	<b>128</b>
	4.15.2 Fourier-transform infrared (FT-IR) spectroscopy of enzymatically treated PET	<b>129</b>
	4.15.3 Scanning Electron Microscopy (SEM) of enzymatically treated PET	<b>129</b>
	3.15.4. Thermal properties and crystallinity of PET after treated with purified Enzyme	<b>129</b>
<b>4.16</b>	Cloning and Expression of PET hydrolase gene	<b>135</b>
	4.16.1 Isolation of genomic DNA	<b>135</b>
	4.16.2 PCR optimization for PET hydrolase gene	<b>135</b>
	4.16.3 PCR amplification of PET hydrolase gene	<b>135</b>
	4.16.4 Purification of amplified band from polyacrylamide gel	<b>135</b>
	4.16.5 Cloning of PET hydrolase gene in cloning vector	<b>135</b>
	4.16.6 Preparation of pET21b and PET hydrolase gene product for expression	<b>136</b>
	4.16.7 Purification of amplified band from polyacrylamide gel	<b>136</b>
	4.16.8 Cloning of PET hydrolase gene in expression vector	<b>136</b>
<b>4.17</b>	Bioinformatics analysis	<b>137</b>
<b>4.18</b>	Induction of recombinant PET hydrolase enzyme	<b>145</b>

<b>4.19</b>	Protein purification by HiPrep 16/60 Sephacryle S-300 High resolution Gel filtration column Chromatography	<b>146</b>
	4.19.1 Purification steps	<b>146</b>
	4.19.2 Recombinant enzyme Molecular Weight determination (SDS-PAGE)	<b>146</b>
<b>4.20</b>	Characterization of Recombinant PET hydrolase	<b>149</b>
	4.20.1 Temperature effect on the activity and stability	<b>149</b>
	4.20.2 pH effect on the activity and stability	<b>149</b>
	4.20.3 Effect of Metal Ions	<b>149</b>
	4.20.4 Effect of Surfactants	<b>149</b>
	4.20.5 Effect of organic solvents	<b>150</b>
	3.20.6. Kinetic parameter of Cutinase	<b>150</b>
<b>4.21</b>	Recombinant enzyme Activity on PET and degradation analysis by HPLC	<b>155</b>
	4.21.1 Identification of degradation product by LCMS	<b>155</b>
	4.21.2 Fourier-transform infrared (FT-IR) spectroscopy	<b>156</b>
	4.21.3 Thermal properties and crystallinity of PET	<b>156</b>
	<b>Discussion</b>	<b>161</b>
	<b>Conclusion</b>	<b>172</b>
	<b>Future prospects</b>	<b>173</b>
	<b>References</b>	<b>174</b>

	<b>Appendices</b>	<b>198</b>
	<b>Published Paper</b>	<b>215</b>

## List of Tables

Table No	Title	Page No
2.1	Microorganisms and their enzymes in biodegradation of plastics	30
2.3	Commonly used polyesters	32
3.1	Composition of MSM medium	48
3.2	Composition of BHI agar	55
3.3	PUM Buffer composition	56
3.4	Standard curve development for bovine serum albumin	59
3.5	Standard curve development for <i>p</i> -nitrophenol ( <i>p</i> NP)	61
3.6	Antibiotic used in the present study	77
3.7	<i>E. coli</i> strains used for cloning in the present work	78
3.8	List of vectors used for cloning	79
3.9	Primer for gene amplification	79
3.10	The ligation reaction mixture	83
3.11	Digestion of PET hydrolase gene	85
3.12	Ligation of PET hydrolase gene into pET21b	86



<b>3.13</b>	Digestion of PET hydrolase gene	87
<b>4.1</b>	Soil physical characteristics at the time of sampling	95
<b>4.2</b>	Physiological and biochemical characteristics of bacterial strain PRS8	96
<b>4.3</b>	Placket Burman design of factors with specific enzyme activity (U/mg) as response	113
<b>4.4</b>	ANNOVA for Placket-Burman Design	114
<b>4.5</b>	Central Composite design of factors with specific activity (U/mg)	117
<b>4.6</b>	ANNOVA for Central Composite design	118
<b>4.7</b>	Purification steps of cutinase by <i>S. maltophilia</i> PRS8 strain	121
<b>4.8</b>	PET depolymerization activity of the cutinase of <i>S. maltophilia</i> PRS8 compared with enzymes. The reaction time was between 72 and 73 hours.	132
<b>4.9</b>	Properties and crystallinity of the untreated PET and enzymatically treated PET	134
<b>4.10</b>	Purification steps of recombinant PET hydrolase by <i>S. maltophilia</i> PRS8 strain	148
<b>4.11</b>	PET depolymerization activity of the recombinant PET hydrolase of <i>S. maltophilia</i> PRS8 compared with enzymes after 72 hours	158

<b>4.12</b>	Properties and crystallinity of the untreated PET and treated with recombinant PET hydrolase enzyme	160
-------------	---	-----

## List of Figures

S. No.	Titles	Page. No.
2.1	The most common synthetic polymers were developed around the world. The numbers in the graph represent the global annual output of the mentioned synthetic polymer (in millions of tons).	10
2.2	Polymer degradation mechanisms by biotic and abiotic factor	21
2.3	Main stages that involved in biotic degradation process	24
2.4	Enzymatic hydrolysis of polymer chain	25
2.5	Classification of biodegradable plastics	28
2.6	Chemical structure of PET	37
2.7	Water soluble product obtained from PET film degraded by polyester hydrolase	40
2.8	Extracellular enzymes that degrade PET plastic derived from esters	41
3.1	Standard curve development for bovine serum albumin (BSA)	60
3.2	Standard curve development for <i>p</i> -nitrophenol ( <i>p</i> NP)	62
4.1	Samples from plastic disposal site for isolation of PET degrading bacteria	95
4.2	Bacterial growth in the minimal salt medium containing PET as the sole carbon source after 28 days of incubation	96
4.3	Neighbour-joining tree based on 16S rRNA gene sequences showing the phylogenetic position of PRS8 strain and representatives of some other related taxa. For out group <i>Halomonas elongata</i> was used. Bootstrap standards were analyzed as % of 1200 replications not <50% are shown at the branching points bar 0.02 substitutions per nucleotide position was identified <i>Stenotrophomonas maltophilia</i>	97

4.4	<i>S. maltophilia</i> strain PRS8 biofilm on the surface of BHI Congo red agar	99
4.5	<i>S. maltophilia</i> PRS8 strain biofilm forming on Microtiter plate and on PET piece after crystal violet fixation(A) The biofilm forming ability of <i>S. maltophilia</i> PRS8 on Microtiter plate after treatment with crystal violet, (Lane 1), Negative control; (Lane 2), Positive control <i>Pseudomonas aeruginosa</i> ; (Lane 3), <i>S. maltophilia</i> PRS8 biofilm in the wells (B) The biofilm forming ability of PRS8 strain on the surface of PET	99
4.6	The biofilm forming ability of <i>S. maltophilia</i> PRS8 strain on microtiter plate and on PET piece	100
4.7	Hydrophobicity of <i>S. maltophilia</i> PRS8 strain resulted by the bacterial cells adhesion to hexadecane hydrocarbon. (A) Phase separation of aqueous phase and organic phase after the addition of hexadecane in comparison with control. (B) The transfer of hydrophobic cells from the aqueous phase to the hexadecane reflected as a decreased in the turbidity of the bacterial suspension.	101
4.8	Expression of cutinase activity by <i>S. maltophilia</i> PRS8 strain, clear zone around colony on PCL agar showed cutinase activity	103
4.9	Percent of weight reduction in PET by <i>S. maltophilia</i> PRS8 strain	104
4.10	Expanded FT-IR spectra of PET after 28 days, abiotic control untreated (black solid curve) and PET treated with <i>S. maltophilia</i> PRS8 strain (Green dotted curve).	104
4.11	SEM images of <i>S. maltophilia</i> PRS8 treated PET compared with untreated PET 28 days (A) Control un-treated (x5.00K) (BCD) Micrographs of biodegraded PET (x1.0K, x2.5K, x5.00K)	105
4.12	Cutinase enzyme activity and total protein in cell free supernatant by <i>S. maltophilia</i> PRS8 strain during biodegradation of PET piece as a carbon source in MSM media.	105
4.13	Effect of temperature on production of cutinase from <i>S. maltophilia</i> PRS8 strain within 24–72 hours of incubation	108

4.14	Effect of pH on production of cutinase from <i>S. maltophilia</i> PRS8 strain within 24–72 hours of incubation	108
4.15	Effect of incubation time on production of cutinase from <i>S. maltophilia</i> PRS8 strain within 24–72 hours of incubation	109
4.16	Effect of inoculum size on production of cutinase from <i>S. maltophilia</i> PRS8 strain within 24–72 hours of incubation	109
4.17	Placket Burman design of residuals vs run showed color point by value of specific enzyme activity (U/mg) as response of run number	112
4.18	Pareto chart showing the effect of t value by important factors [J, cutin; D, NaNO <sub>3</sub> and L (NH <sub>4</sub> ) <sub>2</sub> SO <sub>4</sub> ] generated by Placket Burman design with respect to the effect on the cutinase enzyme production	112
4.19	Central Composite design of residuals vs run showed color point by value of specific enzyme activity (U/mg) as response of run number	115
4.20	Three-dimensional response surface plot between Cutin and NaNO <sub>3</sub> showing the significant factor with respect to the effect on the cutinase enzyme in terms of specific activity (U/mg)	115
4.21	Three-dimensional response surface plot between cutin and (NH <sub>4</sub> ) <sub>2</sub> SO <sub>4</sub> showing the significant factor with respect to the effect on the cutinase enzyme in terms of specific activity (U/mg)	116
4.22	Three-dimensional response surface plot between NaNO <sub>3</sub> and (NH <sub>4</sub> ) <sub>2</sub> SO <sub>4</sub> showing the significant factor with respect to the effect on the cutinase enzyme in terms of specific activity (U/mg)	116
4.23	Ammonium Sulfate precipitation of crude cutinase from <i>S. maltophilia</i> PRS8 and evaluation of specific activities of pellet at varying ammonium sulfate precipitation percentages	120
4.24	Total protein and cutinase activity profile by <i>S. maltophilia</i> PRS8 through Sephadex G-100 gel filtration column	120
4.25	SDS-PAGE of cutinase from <i>S. maltophilia</i> PRS8 strain after purification by column chromatography. Lane 1, Zymogram; Lane 2, eluate from Sephadex G 100; Lane 3, (Color Prestained Protein Standard) 11-245 kDa	121

4.26	Effect of temperature on the activity of purified cutinase <i>S. maltophilia</i> PRS8 strain	124
4.27	Effect of temperature on stability of purified cutinase from <i>S. maltophilia</i> PRS8 strain	124
4.28	Effect of pH on the activity of purified cutinase from <i>S. maltophilia</i> PRS8 strain	125
4.29	Effect of pH on stability of purified cutinase from <i>S. maltophilia</i> PRS8 strain	125
4.30	Effect of metals on the activity of cutinase from <i>S. maltophilia</i> PRS8 strain	126
4.31	Effect of surfactants on the activity of cutinase from <i>S. maltophilia</i> PRS8 strain	126
4.32	Effect of organic solvents on the activity of cutinase from <i>S. maltophilia</i> PRS8 strain	127
4.33	Kinetics analysis of cutinase-like enzyme from <i>S. maltophilia</i> PRS8 strain ( $K_m$ and $V_{max}$ ) value were calculating by Lineweaver-burk plot using <i>p</i> -nitrophenyl Butyrate ( <i>p</i> -NPB) as substrate	127
4.34	HPLC analysis of the degradation products of the cutinase enzyme activity on PET, The Chromatogram showed the time course of product profile where the main product is MHET, followed by TPA and a small fraction of BHET. (A) Un-treated (control) PET chromatogram. (B) PRS8 enzyme treated PET chromatogram	131
4.35	Analysis of the degradation products of the cutinase activity on PET (A) The Chromatogram showed the time course of product profile (B) The Mass spectrum confirmed the identity of TA, MHET, and BHET	131
4.36	The Fourier Transform Infra-Red (FT-IR) absorption pattern of PET (A) Control un-treated PET (B) Enzyme treated PET	133
4.37	SEM images of enzymatically treated PET compared with untreated PET (A) Control un-treated (x5.00K) (BCD) Micrographs of biodegraded PET (x2.5K, x5.00K, x7.5K)	133
4.38	DSC heating curves (first cycle, exo up) of untreated PET and PET treated with PRS8. The $T_g$ , $T_{cc}$ and $T_m$ are shown on the PET untreated curve	134

4.39	Gel electrophoresis of extracted genomic DNA; 1, DNA ladder (10 kb, GeneRuler); 2, <i>S. maltophilia</i> genomic DNA	138
4.40	PCR optimization for PET hydrolase gene (54 to 64°C); 1, DNA ladder (10 kb, GeneRuler); 2-11, Temperatures from 54°C to 62°C	138
4.41	PCR amplification of <i>S. maltophilia</i> PRS8 PET hydrolase gene; 1, DNA ladder (10 kb, GeneRuler); 2, PRS8 PCR amplified PET hydrolase gene product 1800 bp approximately	139
4.42	Purification of PCR amplified PET hydrolase gene product from polyacrylamide gel; 1, DNA ladder (10 kb, GeneRuler); 2, PRS8 PCR amplified PET hydrolase gene product 1800 bp approximately	139
4.43	White/blue screening of pUC19 with <i>S. maltophilia</i> PRS8 strain PET hydrolase gene	140
4.44	Confirmation of PET hydrolase gene into pUC19 vector; 1, DNA ladder (10 kb, GeneRuler); 2, Digested PET hydrolase clone; 3, Purified PRS8 gene amplicon; 4, Undigested PRS8 gene clone	140
4.45	Isolation of PET hydrolase cloned pUC19 plasmid; 1 DNA ladder (10 kb, GeneRuler); 2, PET hydrolase cloned pUC19 plasmid	141
4.46	Isolation of pET21b plasmid; 1 DNA ladder (10 kb, GeneRuler); 2, pET21b plasmid vector	141
4.47	Confirmation of double-digested PET hydrolase gene into pUC19 vector; 1, DNA ladder (10 kb, GeneRuler); 2, double-digested PET hydrolase gene into pUC19 product; 3, un-digested PET hydrolase gene into pUC19 vector; 4, un-digested pET21b plasmid; 5, double digested pET21b plasmid	142
4.48	Purification of double digested amplified PET hydrolase gene product and pET21b product from polyacrylamide gel; 1, DNA ladder (10 kb, GeneRuler); 2, PRS8 double digested PET hydrolase gene product; 3, DNA ladder (10 kb, GeneRuler); 4, double digested pET21b product	142
4.49	Recombinant colonies of pET21b with <i>S. maltophilia</i> PRS8 strain PET hydrolase gene	143

4.50	Confirmation of double-digested PET hydrolase gene into pET21b vector; 1, DNA ladder (10 kb, GeneRuler); 2, double-digested PET hydrolase gene into pET21b product; 3, un-digested PET hydrolase gene into pET21b plasmid	143
4.51	Phylogenetic relationship of <i>S. maltophilia</i> PRS8 PET hydrolase with other PET hydrolase available in NCBI database, Neighbor-joining tree showed maximum identity with polyethylene terephthalate hydrolase of <i>Stenotrophomonas</i> sp HBG88740	144
4.52	Recombinant PET hydrolase enzyme expression by SDS-PAGE. 1: Protein marker (10 – 250 kDa; 2, Induced protein of <i>E.coli</i> BL 21 (DE3) with pET21b; 3, Induced protein of <i>E.coli</i> BL21 (DE3) with pET21b and PET hydrolase	145
4.53	Total protein profile by <i>S. maltophilia</i> PRS8 through HiPrep 16/60 Sephacryle S-300 High resolution gel filtration column	147
4.54	PET hydrolase enzyme activity profile by <i>S. maltophilia</i> PRS8 through HiPrep 16/60 Sephacryle S-300 High resolution gel filtration column	147
4.55	SDS-PAGE of Recombinant PET hydrolase from <i>S. maltophilia</i> PRS8 strain after purification HiPrep 16/60 Sephacryle S-300 High resolution Gel filtration column Chromatography:1, Protein Standard (10-250 kDa). Eluate from Sephacryle S-300	152
4.56	Effect of temperature on activity of recombinant enzyme <i>S. maltophilia</i> PRS8 strain	151
4.57	Effect of temperature on stability of recombinant enzyme from <i>S. maltophilia</i> PRS8 strain	151
4.58	Effect of pH on activity of recombinant enzyme from <i>S. maltophilia</i> PRS8 strain	152
4.59	Effect of pH on stability of recombinant enzyme from <i>S. maltophilia</i> PRS8 strain	152
4.60	Effect of metals on the activity of recombinant enzyme from <i>S. maltophilia</i> PRS8 strain	153



4.61	Effect of surfactants on the activity of recombinant enzyme from <i>S. maltophilia</i> PRS8 strain	153
4.62	Effect of organic solvents on the activity of recombinant enzyme from <i>S. maltophilia</i> PRS8 strain	154
4.63	Kinetics analysis of recombinant enzyme from <i>S. maltophilia</i> PRS8 strain ( $K_m$ and $V_{max}$ ) value were calculating by Lineweaver-burk plot using <i>p</i> -nitrophenyl Butyrate ( <i>p</i> -NPB) as substrate	154
4.64	HPLC analysis of the degradation products of the recombinant enzyme activity on PET, The Chromatogram showed the time course of product profile where the main product is MHET, followed by TPA and a small fraction of BHET. (A) Un-treated (control) PET chromatogram. (B) PRS8 recombinant enzyme treated PET chromatogram	157
4.66	LC-MS analysis of the degradation products of recombinant PET hydrlase activity on PET. (A) The Chromatogram showed the time course of product profile. (B) The Mass spectrum confirmed the identity of TA, MHET, and BHET.	158
4.65	The Fourier Transform Infra-Red (FT-IR) absorption pattern of <i>S. maltophilia</i> PRS8 PET hydrolase treated PET after 72 hours	159
4.67	DSC heating curves (first cycle, exo up) of untreated PET and PET treated with PRS8 recombinant PET hydrolase. The $T_g$ , $T_{cc}$ and $T_m$ are shown on the PET untreated curve	159

## List of Acronym/abbreviations

%	Percentage
°C	Degree Celsius
AEG	Applied Environmental Geomicrobiology
ANOVA	Analysis of variance
Ba <sub>2</sub> SO <sub>4</sub>	Barium Sulfate
BATH	Bacterial adherence to hydrocarbons
BHET	Bis(beta-hydroxyethyl) terephthalate
BPA	bisphenol A
BSA	Bovine Serum Albumin
CaCl <sub>2</sub>	Calcium Chloride
CaSO <sub>4</sub>	Calcium sulphate
CCD	Central composite design
CD	Compact Disc
CH <sub>3</sub> COOH	Acetic Acid
CH <sub>4</sub>	Methane
CH <sub>4</sub> N <sub>2</sub> O	Urea
CO <sub>2</sub>	Carbon Dioxide
CoCl <sub>2</sub>	Cobalt chloride
CTAB	Cetyl tri-methyl ammonium bromide
CuCl <sub>2</sub>	Cooper chloride
CuSO <sub>4</sub>	Cooper Sulphate
CV-I	Crystal Violet Complex
DDT	Dichlorodiphenyltrichloroethane
DHA	Docosahexaenoic acid
DMAB	p- dimethylaminobenzaldehyde
DMSO	Dimethyl sulfoxide

DMT	dimethyl terephthalate
EC	Enzyme Commission
EDTA	Ethylene diamine tetra acetic acid
EG	ethylene glycol
EPA	Eicosapentaenoic acid
EPS	Exopolysaccharide
FeSO <sub>4</sub>	Iron sulphate
FTIR	Fourier-transform infrared spectroscopy
GNB	Gram Negative Bacteria
H <sub>2</sub> O	Water
HDPE	High Density Polyethylene
HgSO <sub>4</sub>	Mercuric sulphate
hrs	Hours
i.e	That is
K <sub>2</sub> HPO <sub>4</sub>	Dipotassium hydrogen phosphate
KH <sub>2</sub> PO <sub>4</sub>	Monopotassium phosphate
K <sub>2</sub> SO <sub>4</sub>	Potassium sulphate
KCl	Potassium chloride
kDa	Kilo Dalton
K <sub>m</sub>	Michaleous-Menton constant
kPa	Kilopascal
LDPE	Low Density Polyethylene
MAC agar	MacConkey Agar
MgSO <sub>4</sub>	Magnesium sulphate
MHET	mono(2-hydroxyethyl) terephthalic acid
min	Minutes
mM	Milli molar
MSM	Mineral Salts Medium
MSW	Municipal Solid Waste
Mt	Metric Ton
Na <sub>2</sub> CO <sub>3</sub>	Disodium carbonate

Na <sub>2</sub> HPO <sub>4</sub>	Disodium hydrogen phosphate
Na <sub>2</sub> SO <sub>4</sub>	Sodium sulphate
NaCl	Sodium chloride
NAFTA	North American Free Trade Agreement
NaH <sub>2</sub> PO <sub>4</sub>	Sodium dihydrogen phosphate
NaOH	Sodium hydroxide
NiCl <sub>2</sub>	Nickel chloride
NiSO <sub>4</sub>	Nickel sulphate
OD	Optical Density
OECD	Organization for economic cooperation and development
PA	Polyamide
PBA	Poly(butyl acrylate)
PBDE	2,2'-bis(p-chlorophenyl)
PBS	Polybutylene succinate
PCL	Polycaprolactone
PE	Polyethylene
PEG	Polyethylene glycol
PET	Polyethylene Terephthalate
pH	Power of hydrogen ion conc
PHB	Polyhydroxybutyrate
PBAT	poly(butylene adipate- co-terephthalate)
PLA	Polylactic Acid
PM	Plastic Material
p-NPB	p-Nitrophenyl Butyrate
POP	Persistent organic pollutants
PP	Polypropylene
PPC	Polypropylene carbonate
PS	Polystyrene
PUM buffer	Phosphate urea magnesium sulfate buffer
PUR	Polyurethane
PVC	Polyvinyl Chloride

PW	Plastic Waste
Rpm	Revolutions per minutes
SDS	Sodium dodecyl sulphate
SDS-PAGE	Sodium dodecyl sulphate-Polyacrylamide gel electrophoresis
SEM	Scanning Electron Microscopy
TSI	Triple sugar iron test
TEMED	Tetra methyl ethylene diamine
Tg	Glass transition temperature
Tm	melting temperature
TMPD	Tetra methyl-p- phenylene diaminedihydrochloride
TPA	Terephthalic acid
US	United States
UV	Ultraviolet
Vmax	Maximum velocity
ZnSO <sub>4</sub>	Zinc sulphate
μL	Microliter
(NH <sub>4</sub> ) <sub>2</sub> SO <sub>4</sub>	Ammonium sulfate
3 D	Three dimensional

## ACKNOWLEDGEMENTS

Starting with millions of thanks to **ALLAH**, the Omnipotent and the Omniscient, who is so kind to mankind and who enabled me for successfully completing this research and bestowed upon me the wealth of such nice, supportive, understanding and cooperative family. All the respect for the last and **Holy Prophet, Hazrat Muhammad** (peace be upon him) who enlightened the world with the essence of faith in Allah and guiding the mankind true.

I deem it a great honor and privilege to record my profound gratitude and indebtedness to my research supervisor, **Professor Dr. Aamer Ali Shah**, Department of Microbiology, Quaid-i-Azam University, Islamabad, who has supported and encouraged me throughout my thesis with his patience and knowledge whilst allowing me the room to work in my own way. I have no words to express my thanks to him for all of his kindness, constructive critical suggestions and consistent advice throughout the process in the incitation and completion of this thesis.

I express my deepest gratitude and sense of obligation to my research supervisor, **Professor Dr. Aamer Ali Shah**, Department of Microbiology, Quaid-i-Azam University, Islamabad, for his supervision and support. His constructive comments and suggestions throughout the experimental and thesis work have contributed to the success of this research.

I wish to thank **Professor Dr. Aamer Ali Shah** Chairperson, and grateful to the entire faculty and non-teaching staff at the Department of Microbiology, Quaid-i-Azam University, Islamabad. Words do not suffice for the ineffable gratitude I would like to extend to **Prof. Dr. Fariha Hasan** for her ever kind attitude, encouragement and guidance, which have been pivotal throughout the course of my Ph.D.

I take this opportunity to express my deep sense of gratitude to my foreign advisor **Dr. Javier Linares Pasten** and his research team (Lund University) for his kind cooperation, inspiration and guidance.

I take this opportunity to express my deep sense of gratitude to my foreign advisor **Prof. Dr. Sabriye Çanakçı** and her research team (Karadenez Technical University) for his kind cooperation, inspiration and guidance.

I would like to thank Turkey Burslari scholarship funded by Government of Turkey and Higher Education Commission, Pakistan for providing me grant under the project “International Research Support Initiative Program (IRSIP)” Scholarship.

Words are insufficient to express my thanks to my Ph.D fellow **Dr. Kalsoom** who support me financially and constantly present during my research work made it possible for me to complete this hard job quite smartly. It was because of her inspiring guidance and dynamic cooperation during entire research work that made it possible.

I would like to express my appreciations and sincere thanks to M. Phil and PhD Scholars especially **Risfa Mubarak, Asim ur Rehman, Adil Nawaz, Salah Ud Din** for their immense help and equally vital role that helped me to complete this project in due time.

I am extremely grateful to my father, who facilitated and encouraged me at every single step of my education.

I finally express my great gratitude and my deepest affection for my parents, wife, my sons, and daughter (**Amjad, Haseeb, Annayah, Muhtasib**) sisters and brother for their love, good wishes, inspiration and whose hands always rose in prayer for me. May I fulfill their expectations (Ameen).

Finally, I express my gratitude and apology to all those who provided me with the opportunity to achieve my endeavors, but I missed to mention them personally.

**Salah Ud Din**

## Summary

Polyethylene terephthalate (PET) is one of the most widely used synthetic polymers due to its desirable properties, including excellent mechanical strength, chemical resistance, and low production cost. However, the persistent accumulation of PET in the environment has raised concerns about its long-term impact on ecosystems. In recent years, there has been increasing interest in finding sustainable solutions for the management of PET waste through biodegradation. The aim of this study was to investigate the biodegradation of PET by bacteria and its enzyme from plastic contaminated soil. A polyethylene terephthalate (PET) degrading bacterium *Stenotrophomonas maltophilia* PRS8 was isolated from soil of a waste-dumping site located in Peshawar, Pakistan at N 34.0074° and E 71.6194°. The degradation of PET was evaluated using various qualitative assays such as weight loss, biofilm formation on PET pieces, Fourier-transform infrared (FTIR) spectroscopy and Scanning Electron Microscopy (SEM). *S. maltophilia* PRS8 strain demonstrated its ability to attach to PET pieces and form biofilm that could be helpful in its degradation. Approximately 1.2% reduction in weight of PET pieces was measured in comparison to control where no loss was found. A change in intensity of FTIR peaks of the treated PET was observed at wavenumber 722, 1098, 1242, and 1714  $\text{cm}^{-1}$  compared to the untreated PET that indicates polymer chain scission by *S. maltophilia* PRS8. SEM images also showed cracks and roughness on surface of PET pieces that clearly indicates its deterioration after treatment with *S. maltophilia* PRS8. The degradation medium was checked for presence of enzymes at the end of experiment, strain PRS8 expressed cutinase activity during PET degradation.

Different physico-chemical conditions were optimized for better enzyme yield using one time one factor and multiple factor one-time statistical models [Plackett-Burman Design (PBD) and Central Composite Design (CCD) software]. The involvement of each ingredient in production of cutinase is depicted in a Pareto chart acquired from PBD. Cutin,  $\text{NaNO}_3$ , and  $[(\text{NH}_4)_2\text{SO}_4]$  were discovered to have a considerable influence on cutinase synthesis. *S. maltophilia* PRS8 cutinase was optimized via PBD and CCD, which led to a 5-fold increase in enzyme activity. Cutinase was purified to homogeneity by column chromatography using Sephadex G-100 resin and molecular weight was found to be approximately 58 kDa. The specific activity of purified cutinase was estimated as 450.58



U/mg with 6.39-fold purification and 48.64% yield. The  $K_m$  and  $V_{max}$  values were determined as 0.703 mg.ml<sup>-1</sup> and 370.37  $\mu$ mol.mg<sup>-1</sup>min<sup>-1</sup>, respectively. The enzyme was stable at various temperatures (30-40°C) and pH (8.0-10.0). The cutinase activity was significantly enhanced by organic solvent (Formaldehyde), surfactants (Tween-40 and Triton X-100) and metals (NiCl<sub>2</sub> and Na<sub>2</sub>SO<sub>4</sub>). The purified cutinase hydrolyzed PET piece at 40°C and approximately 18.3% reduction in weight of PET was measured. The degradation products; terephthalic acid (TPA), mono(2-hydroxyethyl)-TPA (MHET) and bis(2-hydroxyethyl)-TPA (BHET) were confirmed through liquid-chromatography mass-spectrometry (LC-MS).

Furthermore, the activity of PET hydrolyzing enzyme was enhanced by cloning and expression of gene for PET hydrolyzing enzyme into expression host. The PET hydrolyzing enzyme was successfully cloned into PET-21b and expressed into BL21 (DE3). HiPrep 16/60 Sephacryle S-300 High resolution gel filtration column chromatography resin was used for the purification of recombinant enzyme and fractions were collected for measuring enzyme activity. The molecular weight of recombinant cutinase was found to be approximately 58 kDa. The specific activity of purified cutinase was estimated as 595.93 U/mg with 6.19-fold purification and 23.89% yield. The maximum PET hydrolyzing enzyme activity was observed at temperature 30-40°C and pH 8.0-9.0, while SDS, CTAB, ethanol and Hg<sup>+</sup> strongly inhibited its activity. The PET depolymerization products were detected by HPLC and LC-MS, and were identified as TPA, MHET, and BHET. However, an outstanding performance was achieved on PET reaching 22.5 % depolymerization activity after treated with recombinant PET hydrolyzing enzyme for 72 hours, while 18.3% depolymerization activity was achieved after PET treated with native enzyme which is lower than that of recombinant enzyme. The crystallinity of treated and untreated PET pieces with native and recombinant enzyme were analyzed by Differential Scanning Calorimetry (DSC). About 4.1 % reduction in crystallinity of PET pieces was observed after treatment with recombinant cutinase which was slightly higher than that of the native enzyme (3.4%). The recombinant PET hydrolyzing enzyme showed a depolymerization yield of the PET comparable to that of *Idonella skaiensis* IsPETase and significantly higher than that of *Humicola insolens* thermostable HiCut (HiC) cutinase. This study suggests that *S. maltophilia* PRS8 possesses

the ability to degrade PET at mesophilic temperature and could be further explored for sustainable management of plastic waste.

***CHAPTER 1***  
***INTRODUCTION***

## Introduction

Since the year 1950, plastics have been produced in large quantities. Plastics are widely used in a variety of industries and become indispensable to modern civilization (Thompson et al., 2009). Among the polymer materials, plastic has become the number one indispensable choice of the world and our everyday life. The reason, plastic is easy to handle, has low cost, availability, durability and has an incredible resistance to biological attack, chemical and mechanical aging. The word *plastikos*, a Greek word which is the basis of plastic literally means able to be deformed into various figures and have many opportunities in the market place such as by product like wood, leather, medical and food packaging, consumer goods, agriculture sector, automotive and construction parts (PlasticsEurope, 2021; Chinthapalli et al., 2021). The global annual production of plastic accumulation between 1950 and 2020, reached 9500 million metric tons (Geyer et al., 2017; PlasticsEurope, 2021). With the passage of time, people learned how to modify these materials. This was primarily done to enhance their properties. This is how synthetic polymers became the perfect substitutes for natural materials (Borrelle et al., 2020). The growth in this area was very rapid, and as a result, we got highly durable and resistant materials to environmental decay. Industries like food, agriculture, surgery, and engineering were the top users of these materials (Alqattaf, 2020). However, with their popularity and excessive use in daily life, these materials became problematic for the environment. This was due to the fact that they were used for a limited time, which was usually short, and thus they became waste very quickly. Around the world, 150 million metric plastics waste are produced annually. Sources of petroleum lead other industries in their production (Lau et al., 2020). Furthermore, these polymers are widely used in packing food, detergents, cosmetics, and chemicals (PlasticsEurope, 2021). With the introduction of biodegradable plastics, waste management strategies have been centered around them. People are constantly looking for best practices to degrade plastic resulting in minimum waste (Moog et al., 2019).

Moreover, polyethene (PE), polystyrene (PS), polyurethane (PU), polypropylene (PP), polyvinyl chloride (PVC) and polyethylene terephthalate (PET) are some others.

Together, their worldwide production was around fifty to 56 MT in 2013 (Samak et al., 2020). PET is mostly used in manufacturing films, fibers, bottles and containers. Various recovering systems are being used in countries. However, the ratio is not as high as it should be. Huge quantity of PET junk is dumped into waste disposing areas and left as disposed material. Effective and timely measures are required to recover the used PET waste using bio-physical and bio-chemical treatment. Also, efforts are needed to prevent PET waste from entering the environment. For the past 20 years, the Enzymatic recycling of PET is being investigated. The polyester PET is thought to be resistant to biodegradation. Environmentalists have focused their attention on the resilience of polymers, particularly in the cases of polystyrene, polyethylene, polypropylene and polyethylene terephthalate (PET), in order to develop an idea for proper disposal methods that are safer and more advantageous for society (Driedger et al., 2015; Tokiwa et al., 2009).

Biodegradation is the process by which microorganisms convert biochemical into compounds (Zheng et al., 2005). The major result of biotic degradation is the breakdown of the polymer into smaller fragments, which are then utilized as a carbon and energy source by microbes to produce end products like CO<sub>2</sub> and H<sub>2</sub>O under aerobic circumstances. Biodegradation is actively facilitated by microorganisms like bacteria and fungi. These microorganisms have its own ideal circumstances for growth, biotic degradation is a complicated process including the environment, microorganisms, and the polymer (Devi et al., 2016). Plastics degrade due to a variety of reasons, including those that are unique to plastics, like their mobility, molecular weight, crystallinity, kind of functional groups, and additives added to the polymers. The colonization of microbes on the plastic surface during biodegradation reduces the molecular weight of the plastic, which is followed by the conversion of the polymer to its monomers, followed by the mineralization of the monomers into carbon dioxide, water, and methane. (Shah et al., 2008; Krueger et al., 2015). There are numerous methods for plastics to degrade; one method is enzymatic degradation, which involves hydrolysis and enzyme assaults on the polymer substrate after hydrolytic cleavage. Extracellular enzymes produced by fungi and bacteria for biodegradation, hydrolyze polymers during this process, breaking them down into smaller molecules like oligomers, dimers, and

monomers. Microorganisms released enzyme such as lipase, esterase, cutinase, that degrade plastics (Mohee and Unmar, 2007; Danso et al., 2019).

Plastic materials, particularly polyethylene terephthalate (PET), give economic benefits because they are extensively used in our daily lives, and global production is rapidly growing due to the low-cost production, simple synthesis, and durability that are advantageous to the packaging manufacturing (Lebreton and Andrady, 2019). PET is an aromatic polyester that is difficult to degrade due to the availability of non-hydrolyzable covalent bonds with a substrate subunit called ethylene glycol (EG) and terephthalic acid (TPA) (Kawai et al. 2019). It is one of the most often used synthetic polymers. PET is a colorless, hygroscopic resin that is semi-crystalline and has excellent wear, impact resistance and good tensile strength. It is utilized for garments, textiles, storage containers, and some engineering applications. (Quartinello et al., 2017). It is normally utilized in the making of drinking bottles. It is due to its transparent and to process of degradation. It has a yield of over 50 million tons a year. Huge amounts of this have made their way to the natural environment and severely affected it. However, the use of enzymes to decompose PET is a great new way. It is a pollution free method to minimize public dispose and recycle petroleum-made initiating materials TPA and EG. It will ultimately discourage PET's production and recycling. Lipases, cutinases, and carboxylesterases can break ester linkages and have been found to hydrolyze PET in the last ten years (Ruan et al., 2018). Cutinases have shown remarkable activity against degrading PET, owing to the higher degrading ability and the absence of lid structure necessary for lipase for starting at lipid-water sites (Kim et al., 2020).

The biodegradation of PET into low molecular weight monomers or oligomers like mono(2-hydroxyethyl) terephthalate (MHET), terephthalic acid (TPA) and bis(2-hydroxyethyl) terephthalate (BHET) has been recently discovered in various fungal and bacterial strains (Wei et al., 2016). Bacteria known as saprophytic scavengers have the capacity to re-mineralize the hydrocarbons and organic carbon found in garbage, which are thought to be the constituents of plastics. *Thermobifida* and *Thermomonospora*, two genera of the Gram-positive phylum *Actinobacteria*, were identified as a potential

---

bacterial strain for whole-cell catalysis of PET (Ribitsch et al., 2012; Herrero Acero et al., 2011; Gong et al., 2018).

The PET hydrolyzing enzymes involved in the breakdown are typical serine hydrolases, e.g., lipases, cutinases, and carboxylesterases. *Ideonella sakaiensis* enzyme, PETase (PET-active enzyme) produces mainly MHET and in a lower amount, TPA and BHET as secondary products (Yoshida et al., 2016). One such plastic material is ironically both one of the most widely used materials and the one that can cause harmful pollution problems. PET degrading enzyme derived from PET degrading bacteria *I. sakaiensis* shows excellent hydrolytic action. It has an affinity for PET as substrate. It will remove the curtains from structural properties of PET degrading enzyme, the ones that are there in its catalytic process. Compared to enzymes which are homologous, PET degrading enzyme contains a disulfide bonding and an extended alpha and beta loop. Furthermore, the crystal like structures of PET provide vital facts for grasping the working action of PET degrading enzymes (Barth et al., 2016; Wei & Zimmermann, 2017). The new discoveries serve as vital important information for future detailed study and engineered development of PET degrading enzyme. Also, it will be helpful for the better implementation of plastic biodegradation strategy (Narancic et al., 2018).

Cutinases carry out ester bond hydrolysis using a canonical catalytic triad of Ser-His-Asp. Usually, PET and cutin share small structural characteristics, they have ester bonds, which are assaulted and cleaved by the enzyme (Danso et al., 2019). Cutinases-like enzymes are gaining interest because some showed activity on polyethylene terephthalate (PET). Although the first report on a PET active cutinase was published a long time ago Müller et al., (2005) the reports on PET-depolymerizing enzymes have significantly increased in the last years, after the publication on the *I. sakaiensis* bacterium able to grow using PET as a carbon source (Yoshida et al., 2016). It is worth emphasizing that amorphous PET can be more accessible to enzyme attack than crystalline forms. Indeed, thermostabilized PETase, acting at temperatures closer to the glass transition temperature of PET, has shown better depolymerizing performance (Kawai et al., 2021). However, mesophilic enzymes and microorganisms could play an important role in systems where high temperatures are not suitable, for

example, wastewater plants. Thus, cutinases play an important part in hydrolyzing polyesters (Kawai et al., 2019). They have the ester bonding, which is assaulted and cleaved by the enzyme. Although there have been massive reports of the working site through crystal graph studies and molecular designing, the genuine substrate-bonding mode of PET hydrolyzing enzyme has not been properly explored (Duan et al., 2017; Aristizábal-Lanza et al., 2022). Aliphatic-aromatic polyesters are difficult to degrade through the action of enzyme hydrolysis, but carboxylesterases, triacylglycerol lipase and cutinases have been identified as enzymes that can degrade PET. PET has recently been confirmed to be degraded by microbial enzymes which are related to the arylesterase (EC 3.1.1.2) family. Poly-esterase acting on polyesters which are aromatics (primarily PET) got reported for the time for *Thermobifida fusca* by a German scientists group (Kawai et al., 2019).

Plastic pretreatment is an important process before enzymatic depolymerization. Plastic crystallinity is one of the main obstacles to enzymatic attack (Wei and Zimmermann, 2017). Therefore, several pretreatment strategies focus on increasing amorphization. For example, extrusion and micronization are processes widely used in the plastic industries that amorphize and increase the exchange surface of plastics, facilitating enzymatic attack. These technologies have maximized PET depolymerization by using an outperforming engineered leaf-branch compost cutinase (LCC), resulting in an outstanding depolymerization yield in a few hours (Tournier et al., 2020). At the laboratory level and for research purposes, as in this work, PET and other polyesters can also be dissolved in organic solvents and then precipitated as powders (Wagner-Egea et al., 2021). These polyester powders are lower in crystallinity and suitable for assessing enzymatic activities. On the other hand, green plastic pretreatments should be developed for practical purposes and industrial processes.

In the present study, we isolated a total of 24 bacterial strains. A bacterial strain capable of growing in a saline medium containing PET as the sole carbon source was isolated from landfill soil. This strain was identified as *Stenotrophomonas maltophilia*. *S. melophilia* is a gram-negative bacterium and belongs to the  $\gamma$ -proteobacteria. This species has previously been reported to play a role in the bioremediation of various



contaminants, including xenobiotics, oils, dyes, and polyaromatic hydrocarbons (PAHs). However, to our knowledge, this is the first report of the PET-depolymerizing activity of an *S. melophilia* strain. The *S. melophilia* PRS8-degrading activity of the plastic was assessed using plastic weight loss, Fourier transform infrared spectroscopy (FTIR), and scanning electron microscopy (SEM). We also screened strain PRS8 for PET hydrolyzing enzymes and physico-chemical conditions were optimized employing Plackett Burman and Central Composite design. We also setup experiments for enzymatic depolymerization of PET and PET hydrolysis products were detected and quantified by HPLC and LC-MS. We also cloned and expressed PET hydrolyzing gene from *Stenotrophomonas maltophilia* PRS8 into a suitable host system for obtaining maximum degradation of PET waste. We analyzed the crystallinity and the glass transition thermal properties ( $T_g$ ) of treated PET with recombinant polyester hydrolase by Differential scanning calorimetry (DSC).

### **Research Questions**

1. Can we isolate PET degrading bacteria from plastic contaminated sites?
2. Can these isolate be employed for efficient degradation of PET plastic waste?
3. Can PET hydrolase enzyme prove to be an efficient tool in degradation of PET?
4. Can we improve the degradation rate through cloning and expression of polyester hydrolase genes into host cell?
5. Can recombinant PET hydrolase be effectively used for sustainable management of PET plastic waste?

**Aim and objectives****Aim**

To investigate the biodegradation of PET by bacteria and its enzyme from plastic contaminated soil

**Objectives**

1. Isolation and screening of PET degrading bacteria from plastic contaminated soil
2. Optimization of physico-chemical parameters for the enhanced production of enzyme from selected bacteria
3. Purification and characterization of PET hydrolyzing enzyme.
4. Cloning and expression of PET hydrolyzing gene in suitable microbial host.
5. Degradation of PET by recombinant PET hydrolase enzyme and determination of its degradation product

***CHAPTER 2***  
***REVIEW OF LITERATURE***

## Literature review

### 2.1 A brief overview on plastic

The per annum plastic production was recorded to be about 350 million tons in 2017 as per the figures reported in Plastics Europe, (2021) out of which 90 % was generated from fossil fuels (Geyer et al., 2017; Plastics-Europe, 2021). Polymeric materials have gained immense appreciation owing to their inexpensiveness, easy handling, lightweight, and excellent tolerance to physical, chemical, mechanical, and biological effects in the past sixty years (Chinthapalli et al., 2021). The global plastics production between 1950 and 2020, was estimated to be 9500 million metric tons (MMT) (Plastics-Europe, 2021). About 600 MMT are estimated for 2030. White pollution has been caused by plastics' capacity to persist in harsh environment (Geyer et al., 2017; Plastics-Europe, 2021; Chinthapalli et al., 2021). The term plastic has a Greek descent “Plastikos” which means ready to be shaped into various shapes (Shah et al., 2008). Initially, the material obtained naturally was studied first such as starch, protein, and their derived substances such as wood, leather, etc. Over the period, humans understood to chemically alter them to develop different products. These chemical alterations led to the immense growth of different kinds of products. These modifications led to an increase in the production of synthetic plastics, and they invaded each aspect of human life and their lifestyle as well (Jâms et al., 2020). The stable and durable nature of these synthetic polymers was a blessing and a curse as well, since their resistance to physical and chemical effects (Vethaak and Legler, 2021; MacLeod et al., 2021).

The biggest curse of synthetic polymers was their tolerance and resistance to degradation by any means. The continuous increase in their productivity caused a nuisance for the environment. Plastic is excellent material and its presence in the fields of medical, pharmacology, food industry is very alarming. They are only useful for a short time but become wasteful afterward. Polymers coming from petroleum resources are increasing at a rate of 150 million tons per annum internationally (Bher et al., 2022). Plastic is used majorly in food, packaging, pharmaceuticals, cosmetic and chemical industries (Shah et al., 2008). The growth in the use of polymeric substances is increasing at the rate of 12 % per year. These figures ensure that significant plastic

becomes waste and pollutes the environment (Borrelle et al., 2020; Plastics-Europe, 2021).

## **2.2 Plastics in Environment**

In 2020, per annum growth in the production of plastic has crossed 370 MMT. About 40 % of plastic production belongs to the packaging industry (PlasticsEurope, 2021). This packing material adds to the urban solid waste and synthetic plastic in the oceans, which is the most alarming situation on a global level for the environment (Danso et al., 2019). Plastics are dumped on land and are in direct contact with the oxygen and sunlight which causes breaking and fragmentation and eventually forming microplastics. These microplastics in water bodies are of major concern (Tulashie et al., 2020). These microplastics are taken up the aquatic life and birds as food. The presence of plastic in the digestive tracts of aquatic life has been brought to light by many researchers. Studies have shown that the ingestion of microplastic by the animals (land and aquatic) and birds is due to their scent, size and shape as food. This is a serious health risk that we are consuming microplastic contaminated with environmental toxins (Vaughan et al., 2017; Konieczna et al., 2018; Owczarek et al., 2018).

## **2.3 Production and use of Plastic**

### **2.3.1 Production**

Plastic production has hit an all-time high of 350 million tons (Hermabessiere et al., 2017; Alqattaf, 2020; Nielsen et al., 2020). By 2030, it is expected that it will rise to 590 million tons, plastic materials (PMs) have become part of daily life due to their increased usage and versatile nature (Wu et al., 2017; Cox et al., 2019). During the years 2011 to 2015, the usage of polymers has drastically increased from 300 million tons to 350 million tons. By 2050, the consumption of plastic is set to hit 12,000 million tons which is almost double the production in 2015, which was approximately 6300 million tons (Aryan et al., 2019; Heidbreder et al., 2019). Out of this figure, 9 % is reused, and 12 % of the rest is burned or 79 % is dumped in landfills (Figure 2.1) (PlasticsEurope, 2018). Another aspect to consider is that half the production of polymers is for single use. This means that they become a waste after being used for the initial purpose. Petro chemistry and fossil feedstock are constantly linked with the

production of plastics. Furthermore, studies show that 99% of the raw material to produce plastic is fossil fuel based. Out of this, 8–9% accounts for global oil and gas consumption. It is further estimated that 4–5% of this is used as raw material and 3–4% as energy (Prata, 2018). Petrochemical companies have a plan to make massive investments in new production facilities. They aim to expand and improve the infrastructure in places like America, Middle East, and South-East Asia. The US has already an established market, while the remaining two regions are growing rapidly to become top markets of the world. Moreover, according to current estimates, degradable and biobased plastic global production capacity reaches around 3.5 million tons per annum (Geyer et al., 2016). Nevertheless, this is only a small fraction of the recorded 380 million tons of total production. Broadly, PMs can be classified into two major groups: thermoplastics and thermoset. Formers are mostly branched and linear polymeric material. They are remolded easily and can also survive in a wide range of temperatures (Siracusa, 2019).

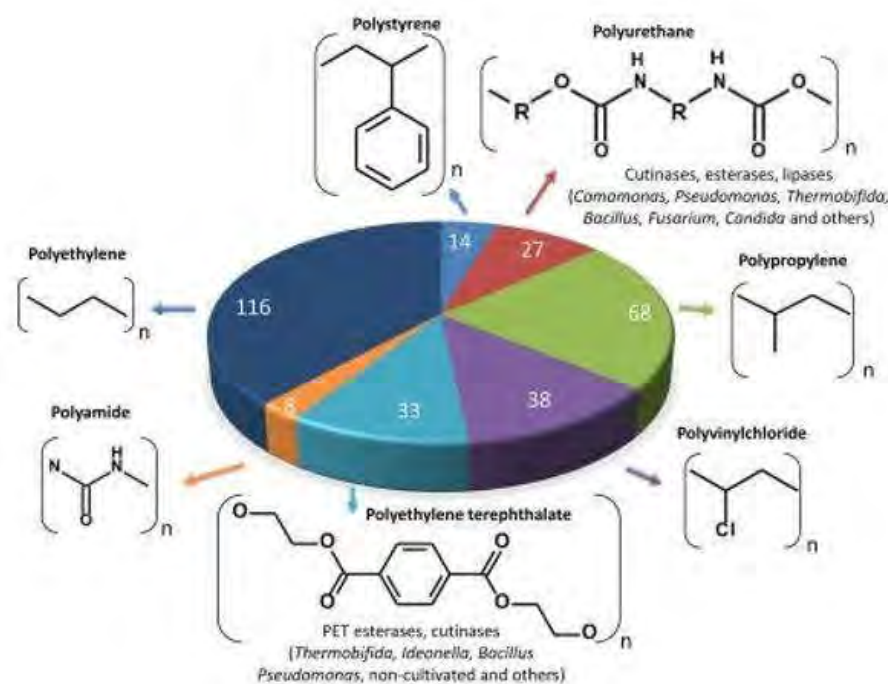


**Figure.2.1:** The most common synthetic polymers were developed around the world. The numbers in the graph represent the global annual output of the mentioned synthetic polymer (in millions of tons).

### **2.3.2 Plastic Consumption**

Past research and studies on the consumption of PMs have always focused on behavior in connection to products like plastic bags, plastic bottles, disposable cups, food packaging, and microbeads in cosmetics (Lahens et al., 2018; Anderson et al., 2016; Prata, 2018; Poortinga & Whitaker, 2018). However, the major product that has been in the spotlight is the plastic bag. It is the most heavily discussed product in studies related to plastic products (Nielsen et al., 2019). This behavior is different per various socio-economic factors, protection of the environment, and consumer demand (Lahens et al., 2018; Wei & Zimmermann, 2017). Analysts have proved that the packaging of products has several functions. These include protection and communicating with the customer by describing the properties. It has also been argued that the product and its production, transportation, and other marketing activities are a bigger influence on the environment apart from bad or careless packing may increase food wastage (Heidbreder et al., 2019; Cox et al., 2019). This is why researchers are of the view that packaging should be good as this will lessen environmental pollution (Willis et al., 2018). Furthermore, it has been observed that many studies have been focused on finding why plastic is used so much. The results are that characteristics like convenience, lightweight, cheap, tolerance, and protective characteristics are responsible for its large-scale usage (Dauvergne, 2018; Mendenhall, 2018; Steensgaard et al., 2017). Additionally, these studies suggest that synthetic plastic is still given preference over bio-based polymers (Barros et al., 2019; Prata, 2018). Also, bio-degradable plastic is preferred over conventional plastic. This new trend has been seen because the word biodegradable and others like it are perceived as more environmentally friendly materials. People usually think that these materials are less harmful to the environment and pose fewer health hazards (Danso et al., 2019).

### **2.4 Plastic Waste Generation**

The word Drivers means anthropogenic activities by humans because of human activities. These activities could affect socioeconomic factors. Unfortunately, such activities have an extremely adverse effect on the environment (Ayeleru et al., 2020). In recent years the utilization of plastic has increased significantly. As a result, the waste plastics are increasing by the day. This has led to numerous problems around the

globe. This has also contributed to the acute municipal solid waste (MSW) issue. As the waste by plastics is constantly rising, recycling, which should be at the same pace, is very low (Gawande et al., 2012; Werner et al., 2016). Littering on streets, beaches, and public places is a common thing to see in many countries. The plastic waste or PW is usually blown by the wind from the site it has been disposed of. This causes the PW to enter nearby places and water bodies and has caused mammals and marine life to die (Ayeleru et al., 2018; Siracusa, 2019). The reason behind this alarming number of marine issues is that sea animals tend to mistake these PW for food. Once they ingest the plastic, it sets in their alimentary canal and causes starvation. PW debris thrown around beaches, lakes, and ponds has caused massive loss to marine life (Barboza et al., 2020; Danso et al., 2019). Most of the plastics are non-biodegradable. This causes an excessive amount of debris in the environment. Other plastics do degrade, but it happens slowly, and this releases degradation products into the soil and water. Moreover, many plastics contain plasticizers and catalyst residues. These are normally added by the manufacturer. These materials have the tendency to stick to the soil and are not easy to dispose (Knoblauch et al., 2018). This is the core reason that PW is the major contributor to persistent organic pollutants (POPs). These POPs are known to be severely harmful to the endocrine systems and reproductive systems of both animals and humans (Browne et al., 2011). The additives also cause health issues which are those used in the manufacturing process. In addition to the plastic material itself, the additives used during its manufacturing (MoEFCC, 2018).

These materials include anti-microbial, flame inhibitors, preservatives, and plasticizers. For example, bisphenol A (BPA), a plasticizer that is a monomer for polycarbonates and epoxy resins. It has leaching qualities that make it difficult to degrade which is further improved by washing and reuse containers (Onundi et al., 2017). Bisphenol A is harmful to the human body because it can interfere with natural hormonal signals and damage the endocrine system. They are also the cause of multiple disorders and diseases in an adult human body (Konieczna et al., 2018). Some of the most common are obesity, type-2 diabetes, sudden puberty, chromosomal ovarian damage, prostate cancer, reduced production of sperms, causes changes in the immune system, increased



incidence of breast and metabolic disorders, frequent miscarriages, and cardiovascular disorder (Pelch et al., 2019; Vought and Wang, 2018).

### **2.5 The Marine Plastic Pollution**

Plastic waste is the main cause of water pollution as almost 60-90% of the marine litter consists of PW. In 2015, it was found that almost nine million tons of plastic are part of the water bodies. This makes 5-6 grocery bags per foot of the seashore. Moreover, it was also noticed that more than 80% of the marine litter came from the land. This situation had caused severe damage to marine life and caused some species to become endangered. Most of the waste of the land is disposed of in the water bodies (Bahl et al., 2020; Barboza et al., 2020). This practice is commonly observed in coastal areas. Such pollution hits the birds and the fish the most. Plastic waste becomes a great problem once these animals swallow it. This plastic pollution has many contributors. Some of the major sources of this type of pollution come from consumer packaging and products. For decades, almost all products have been using plastic packaging, for example soft drink and water bottles, packets, bottle caps, shopping food containers, straws, and cigarette butts. This also includes fishing gear which is also contributing to this plastic waste. Yet, it is still not clear how much of the produced plastic is a part of water bodies. As per the latest estimates, almost 200 million metric tons have seen their way to water bodies. This amounts to 2% of the total plastic production in the world since 1950. As a result, plastic debris can be found on beaches, city shores, and islands around the world (Prata, 2018; Idumah and Nwuzor, 2019).

In addition, plastic micro-beads and fibers have blocked the coral reefs in Arctic Sea ice (Barnes et al., 2009) This plastic waste is constantly swallowed by sea birds and fish (Cózar et al., 2014). Numerous studies have proved the fact that the bulk of marine pollutants come from the land. The waste from factories is mismanaged and dumped carelessly in the water bodies, killing hundreds of marine lives. Research has shown that the top five plastic-pollutants producing countries: Indonesia, the Philippines, Srilanka, Vietnam, and China. These states are collectively likely to account for all PW leaks that end up in the oceans (Cox et al., 2019; Willis et al., 2018). Nevertheless, a huge amount of this plastic from the top 5 countries was produced by OECD

(Organization for economic cooperation and development) countries. It is transported to South-East Asia, which is accountable for most plastic pollution in marine. Interestingly, the usage and dumping of plastic waste are complicated because companies around the world are going global. The responsibility or the blame for PW cannot be put on a single nation or a company (Gregson & Crang, 2019).

### **2.6 Plastics in freshwater**

Most of the waste from plastic production is disposed of in the water bodies. This makes up almost 80% of the total marine litter (Lebreton et al., 2018). Especially around the coastal areas, the ratio of this waste increases significantly. The most dangerous consequence of this disposal is when zooplankton ingest this microplastic waste. This disturbs their food web and causes problems (Eerkes-Medrano et al., 2015). It has been estimated that, on average, the plastic pellets in the waters are from 1000 to 4000 km in density around coastal and seabed areas. Studies show plastics that fish eat are harmful to the seabirds that feed on these fish. These end in detrimental effects that will affect the digestive system (Moss, 2017). The reason behind this situation is the low costs allocated to the recycling of plastics and improper waste management techniques. It has affected the coastal areas. Plastic waste has been found in large quantities in marine waters. Research about microplastics in Vembanad Lake's sediments that has small plastic pieces with a particle size of <5 mm was in the digestive system of marine animals (Lahens et al., 2018). These microplastics contain contains a low-density polyethylene as it is the dominant polymer in them. This situation poses a serious threat to the food business as fish is the major food source in the marine (Sruthy and Ramasamy, 2017).

### **2.7 Environmental and Other Hazards of Plastic**

Plastic packaging takes more than a thousand years to deteriorate completely. The bulk of this packaging consists of plastic bottles and plastic bags. Both materials contribute significantly to waste material. This waste is taken up by street animals and birds and causes harm to them (Sadri and Thompson, 2014). Furthermore, the materials that are released during the degradation of plastic are extremely harmful to the environment. The toxins and the pollutants get mixed up with the soil and pollute it. When the animals

swallow this plastic waste, it is trapped in their alimentary canal and ultimately causes the animal's death. Similarly, the polymers which are less in weight float on the surface of the water which is taken up by fish and other sea animals. These are consumed by fish and seabirds which gets blocked in their digestive system, causing in an animal's death. The digestion of such polymers also causes problems and even death in these animals (Warner et al., 2013).

So ultimately, the plastic contaminants are transmitted down the food chain. There have been studies that show the transmission of acetaldehyde from polyethylene terephthalate soft drink bottles into the water, styrene (from polystyrene -PS), plasticizer and antioxidants (Shafei et al., 2018). The total amount of plastic waste in the surrounding environment is increasing day by day without any controlled disposal, which is a great threat to human health and so is considered hazardous for human health (Kumar, 2018). There is an intense use of plastic materials and is manufactured in greater quantities but there is no well-organized procedure for its disposal and so as degradation. As plastic material shows greater stability in nature and is highly resistant towards degradation, its accumulation and thus quantity are increasing tremendously within the surrounding environment (Boucher and Billard, 2019). Plastic products are a threat to the life that exists on the land, ocean, and other habitats. The drainage system can also be blocked due to the resistant nature of plastic towards degradation. When chlorinated plastic accumulates in the soil, it results in the release of hazardous chemicals, which not only wash away the soil from the effective area but also pollute the water present underground. Out of the total wastes that are found in the marine ecosystem, 60-80% of the wastes comprises plastic products (Priyanka and Dey, 2018).

### **2.7.1 Plastic Waste Deposition in the Natural Environment**

Nowadays it is considered genuine information that unregulated plastic disposal can contaminate the number of natural habitats including water habitat both fresh water and marine and terrestrial habitat. Sometimes when thick sewage contaminated with plastic meets soil, automatically affects the soil, and imposes the same effect of contamination as that of sewage (Dauvergne, 2018). The same is the case with the mixture of decayed organic matter which is prepared from waste coming out of the city or town, through

water i.e., stream water or river water which carries plastic products. All these events can unintentionally pollute the soil with plastic material. Besides land contamination, plastic wastes can find their way to the ocean. It is reported that 60-80% of the marine pollutions caused by human beings themselves, and this pollution is comprised of plastic products (Jamieson et al., 2017).

Plastic products can float on the surface of the water but sometimes it comes in contact with marine creatures or rocks which takes these products to the bottom of water thus resulting in water pollution and results in the ultimate death of sea creatures. It has been documented that the water covering the European areas, the debris which results from plastic accumulation can reach or exceed 10000 items and can reach 1000 miles below the water surface (Lebreton et al., 2017). The data regarding the plastic debris that are found on the bed of the ocean is still missing. It is said that the rate of plastic degradation is slow deep inside water as compared to the outside environment. This reduced speed of plastic degradation in deep seawater is because of reduced temperature and due to the less amount of light reaching up to the bed of the ocean (Mason et al., 2018).

### **2.7.2 Animals' Risks of Entanglement and Ingestion**

Plastic products found floating on the water surface or deep seawater not only de-beautify the surrounding area but also impose an adverse effect on different activities i.e., trading through the sea, fishing, or tourism. Sometimes the fisherman discards the fishing nets in the ocean or sea which results in ghost gear, results in the death of many marine organisms, and thus adversely affects the area where fishing is carried out (Lahens et al., 2018). When plastic material is present in the water environment for a longer period, they become a substrate for different organisms to grow and thus give a reason for the movement of non-indigenous species (Barboza et al., 2020; Browne et al., 2011; Torres-Mura et al., 2015).

Nowadays, the greatest problem that arises within the marine ecosystem is the engulfment of plastic products by marine organisms. Marine species have different feeding such as some organism's feeds on sediments i.e., deposit feeders; some feeds on suspended materials in water i.e., filter feeders while other feed on organic materials

such as detritivores. All these organisms are said to ingest plastic materials. Among all these species, those organisms, which specifically select plastic for their source of food, can be more problematic as it can kill these organisms. There are a number of organisms that resides within water environments such as some invertebrates, fish, turtles, etc (Cózar et al., 2014; Wilcox et al., 2015), which take in plastic material and can result in a number of problems i.e., inability to reproduce, movement disabilities, sores, tearing of flesh and finally death. It is said that with time this type of situation might increase, for example, it was reported that in the North Sea, some dead fulmars were found dead onshore, and was reported that 95 % of the birds had plastic in their gut (Barboza et al., 2020; Jiang, 2018). Some other birds were reported for having a large amount of plastic in their gut (Moss et al., 2017).

### **2.7.3 Toxicity Transfer through the Food Chain**

Besides plastic ingestion by organisms, it is said that if these types of organisms having plastic debris inside their body are ingested by other organisms, can impose great harm and thus affect the whole food chain. Plastic material found within the marine environment is said to have different organic contaminants which have different concentrations from ng/g to ug/g. These contaminants include polycyclic aromatic hydrocarbon, polychlorinated biphenyl, petroleum hydrocarbon, organochlorine pesticide, alkylphenol and bisphenol etc. Out of these organic compounds, some of the compounds are absorbed from the environment whereas some are added to the plastic during manufacturing. Work was done in Japan, which shows that concerning the surrounding environment, plastic found within seawater can absorb the different types of organic pollutants on its surface and remain in the environment for a large period with adverse effects on the environment. Similarly, an experiment was carried out by a scientist named Teuten, who showed how these dangerous contaminants are transferred to fish, seabirds, and other mammals. This type of transport is different for different contaminants and polymers. It also varies accordingly with the weathering of debris in the environment. Some mathematical models were made which showed that even a small quantity of plastic is enough for the transport of contaminated debris from one organism to another followed by intake of plastic material (Wei & Zimmermann, 2017). In the same way, plastic can be transferred to higher organisms i.e sea birds, affecting

the whole food chain. All this transfer depends on the amount of plastic present in the environment (Horton et al., 2017).

Different types of plastic substances accumulate inside living organisms e.g., salts and ester of phthalate and BPA. The accumulation rate of plastic is greater inside invertebrates than vertebrates. Within invertebrates, still, there is variation among species with respect to plastic accumulation i.e., accumulation of plastic within mollusks and crustaceans are higher. All this plastic accumulation within species depends upon the type of plasticizer added to plastic or the procedure through which they are manufactured (Shafei et al., 2018).

#### **2.7.4 Human Health Hazards of Plastic**

Different types of abnormalities have been observed within the human population i.e. reproductive abnormalities; such problems arise because of different chemicals that are added to plastic during their manufacture. These chemicals are reported to have an adverse effect on human health (Aday and Yener, 2014; Danso et al., 2019; Willis et al., 2018). These adverse effects on human health were recorded from an experiment carried out on different animals in laboratories including mice and guinea pigs. Changes were reported in rat testis because of the effect of plastic (Jâms et al., 2020). It has been shown that many human health problems are directly related to the level of phthalate i.e. results would be more serious if humans are continuously exposed to the high level of phthalate mixtures (Konieczna et al., 2018; Owczarek et al., 2018).

Many articles have been published on Bisphenol A (BPA) in which it is reported that when BPA is administered to animals during their developmental stage, BPA can be harmful even if the dose is quite small. BPA greatly affects the brain of developing animal in which the brain fails to have sex differentiation within the very organism and also affect the behavior of that animal (Idumah & Nwuzor, 2019). Polyvinyl chloride that is used in the manufacture of water pipes, includes different types of chemicals such as Bisphenol A, phthalate, cadmium, lead, organotins, etc. all these products are reported to be very harmful to animals (Konieczna et al., 2018).

## **2.8 Plastic Disposal Methods**

Landfilling, chemical recycling, incineration, thermal treatment, and biodegradation are some common plastic disposal methods.

### **2.8.1 Landfill**

Approximately 60% of the waste (both plastic and other) is dumped in a landfill. This is a common practice in third-world countries and some of the developed nations as well. The reason behind such a huge percentage is that this method is considered to be the simplest way of disposing of solid waste (Qasaimeh et al., 2016). However, this is not a good practice as the waste disposed of by this method does not degrade easily. This PW is UV resistant, and because it has been manufactured, materials added to it make it impossible for even solar radiation to have any degradable effects on it (Simon et al., 2016). The anaerobic conditions around the landfill are another problem regarding degradation in landfills. These conditions make it difficult for the land to degrade any material, let alone plastics (Cleary, 2014).

### **2.8.2 Incineration**

Heating plastic at high temperature in the presence of oxygen to convert gases into heat that is further can be used as an energy source can be defined as incineration (Gug et al., 2015). On the other side, pyrolysis included converting plastic into specific chemicals when fuel is heated at a specific high temperature while keeping the oxygen absent (Badia et al., 2017). This one is considered the most effective method in Japan, and the reason for this popularity is the limitation of land. The main issue for utilizing this procedure is the emission of hazardous dioxins and furans during incineration. Another challenge of this process is the cleaning of gases that are emitted, which also includes desulphurization. Both these processes need a high level of investment, which is very time-consuming and takes years (Burnley et al., 2015).

### **2.8.3 Recycling**

Materials like glass or aluminum are recycled, then these are converted into products that can be reused so often. These types of processes are related to "closing the loop" and these processes do benefit not only the environment but also decrease the processes like extraction or mining of resources. This further leads to the saving of energy (Devi

et al., 2016). Plastic, commonly used in many applications, can be recycled multiple times. The recycling process involves collecting, cleaning, and shredding plastic items into small flakes, which are then melted and formed into new products. Recycling PET conserves energy and resources, lessening the environmental impact of plastic production. Promoting awareness and improving recycling infrastructure are key to maximizing the benefits of PET recycling. PET recycling can be done using the below-mentioned processes like chemical, thermochemical, mechanical and biological processes (Coates and Getzler, 2020; Law & Narayan, 2022).

### **2.9 Biotic and Abiotic Mechanisms of Polymer Degradation**

Polymer degradation entails the permanent modification of the chemical composition, physical properties, and visual attributes resulting from the chemical breakdown of the polymer's constituent macromolecules through one or more mechanisms (Shah et al., 2008). Because of external factors, multiple mechanisms may operate at once, with one mechanism occasionally dominating the others. (Laycock et al., 2017). The deterioration process and its rate may be altered by environmental elements such radiation, humidity, alkaline or acidic condition and heat. Polymer qualities like electrical, optical, discoloration, mechanical, phase separation or delamination, cracking, crazing and erosion can all be affected by the degradation process. (Shah et al., 2008). Mechanical, light (photo-oxidative), hydrolytic (chemical) and thermal (or thermo-oxidative), degradation are the four main abiotic mechanisms linked to polymer breakdown, some of which can be aided by catalysis. In addition, although it is less frequent, chemical ozone degradation of polymers is also thought to be a process of degradation. Biotic degradation is caused by the enzymatic activity of microorganisms (Figure 2.2) (Bher et al., 2022).



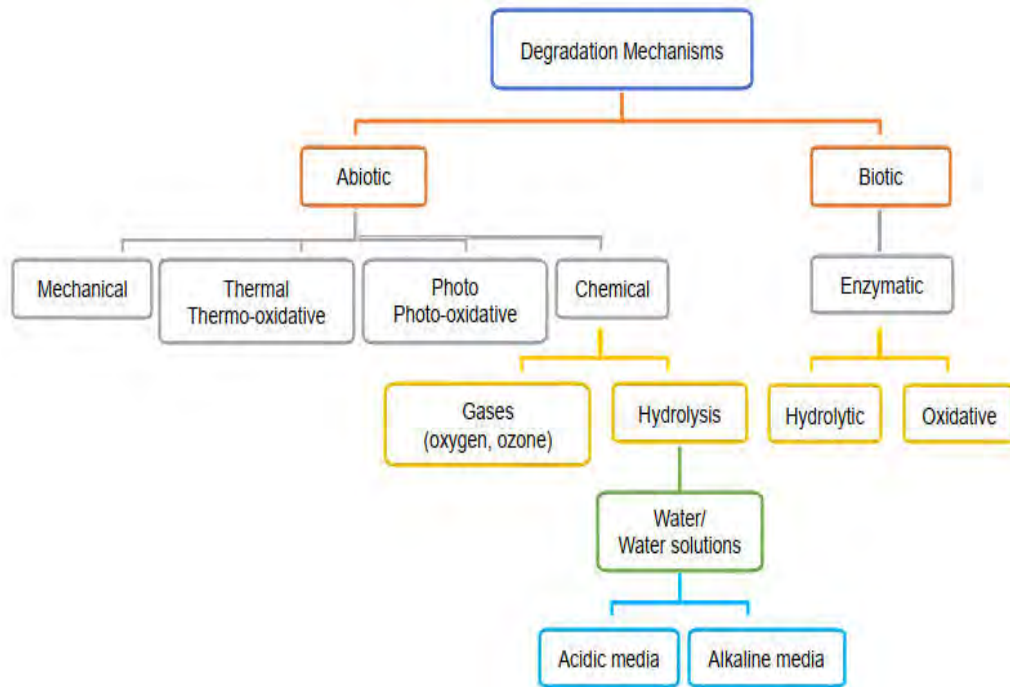


**Figure 2.2:** Polymer degradation mechanisms by biotic and abiotic factor

## 2.9.1 Abiotic degradation

### 2.9.1.1 Mechanical Process

Certain steps are followed by the plastic good when consumed during the mechanical processes. These steps include collect, handle, sort, densify, shred, melt and granulate. This process is then divided into two forms. One is primary recycling which is comprised of waste that is from the manufacturing factories. Then secondary is the product which is lesser in properties compared to the new ones (Kyaw et al., 2012). For example, plastic waste is not disposed of but shredded and reused in the raw plastic to produce dustbins or tables/chair (Lucas et al., 2008). Alternatively, physical forces like wetting, cooling, drying and heating brought on by water or air, can lead to mechanical degradation because of stress cracking (Laycock et al., 2017).

### 2.9.1.2 Thermal Degradation

A wide range of thermal treatments like pyrolysis, incineration and plasma arc gasification are involved in the plate waste management. Incineration is most frequently adopted waste treatment procedure. Raw or unprocessed garbage is heated in an air

chamber at a temperature of about 850 °C and releases CO<sub>2</sub>, H<sub>2</sub>O and fuel energy material (Joshi and Ahmed, 2016). Landfilling is replaced by incineration which generates more energy needed to be used for other advantages. Moreover, this results in the release of toxic and dangerous gases which pollutes the air (Badia et al., 2017)). However, the only positive side of this type of method is the generation of much greater amount of energy which is not possible to achieve in the process of landfilling (Becidan, 2007).

Another thermochemical treatment of plastic waste involves Pyrolysis which is the burning of solid waste in an anaerobic environment. The pyrolysis could be of two types: fast and slow. Fast pyrolysis results in the manufacturing of bio-oils, on the other hand, slow pyrolysis manufactures charcoal. Controlled oxygen and air environment is developed resulting in the production of gases such as CO, H<sub>2</sub>, and CO<sub>2</sub> from this gasification process. Hydrocarbons present in plastic polymers are oxidized and taken up as an energy source for future use. This occurs at an elevated temperature of >600°C (Nikolaidis and Poullikkas, 2017).

### **2.9.1.3 Photodegradation**

Rearrangement, cross-linking and chain scission are the results of photodegradation, which can take place in the presence or absence of oxygen (photolysis). The extent of photodegradation is correlated with the specific wavelengths of sunlight: visible light, ultraviolet (UV) and infrared (IR) radiation, The wavelength of the radiation that reaches the earth's surface ranges from 295 to 2500 nm, or from UV-C to IR. (Gardette et al., 2010). Polymers with high UV energy absorption tendencies are susceptible to oxidation and cleavage due to the activation of electrons at elevated energy levels (Shah et al., 2008; Yousif and Haddad, 2013). Photodegradation can result in a useless material by causing the polymer chains to break, radicals to be produced, changes to the optical and physical properties, a loss of mechanical qualities and yellowing effect and a reduction in Mw (Singh and Sharma, 2008; Yousif and Haddad, 2013). UV radiation can cause photooxidative degradation in polymers with or without the aid of a catalyst, and rising temperatures can increase the process. (Tsuji et al., 2006).

### **2.9.1.4 Chemical Process**

The approach of depolymerization of plastic waste and then using chemical processes is considered very attractive these days. Moreover, these chemical processes include glycolysis, hydrolysis, etc. In few studies, different approaches are discussed under the idea of degradation procedure and earring it by the reduction of labor and external effort (Cox et al., 2019; Jiang, 2018). Chemical treatment of plastic waste is not used on a large scale because of the fear of buildup of the chemical waste debris. The illegitimate disposal of plastic by chemical treatment is more harmful for environment. The municipal waste disposal of plastic is very unprofessional and it could cause leachates in the spoil after it enters the soil atmosphere (Browne et al., 2013).

## **2.9.2 Biotic degradation**

### **2.9.2.1 Biological process**

The process by which bacteria degrade organic materials enzymatically is known as biotic enzymatic degradation. When contributing to the possible solutions to the waste management caused by plastic, this approach is known to be the most effective process with the holding economic budget. Attention to building the waste management procedure that is safer for society is caught by the polymer's resistance and, more specifically for polyethylene, polystyrene, PET, and polypropylene. Many microbial families have proved to have the potential of degrading polymer, which has led to the finding that biodegradation is the eco-friendly approach. But a relative polymer leads to showing the resistance to multiple degradation processes (Jayasekara et al., 2005). Micro-organisms are the major reason for the problem because of the maintenance, cultivations, and enzyme extraction. This process mainly focuses on activity based on enzymes that catalyze the polymeric bonding into the monomer form for further processing. Hydrophilicity on the cell surface causes biofilm formation on the polyethylene surface; here, carbon is utilized as an energy resource which further enhances the degradation process. Complete biodegradation of the polymer is ensured by measuring the macroscopic changes, appearance, and microscopic readings of the microorganisms on the polymer's surface right after the treatment done by enzymes most effective method is quantifying the evolution of CO<sub>2</sub> is preferred. Different studies are conducted regarding aliphatic polyester on aromatic substances. Therefore, there

are greater chances of conducting research. One of the most universally recognized methods for the breakdown of plastic is biodegradation. It is highly accepted globally because of its ecofriendly nature and accessibility. A series of multiple environmental factors are involved in the biodegradation of plastic's dynamic structure in the marine ecosystem. The degradation of the polymer precedes biofilm production by microbiota. The polymers are broken into oligomers, dimers, and then monomers by enzymes' action (Figure 2.3) (Bhardwaj et al., 2013).

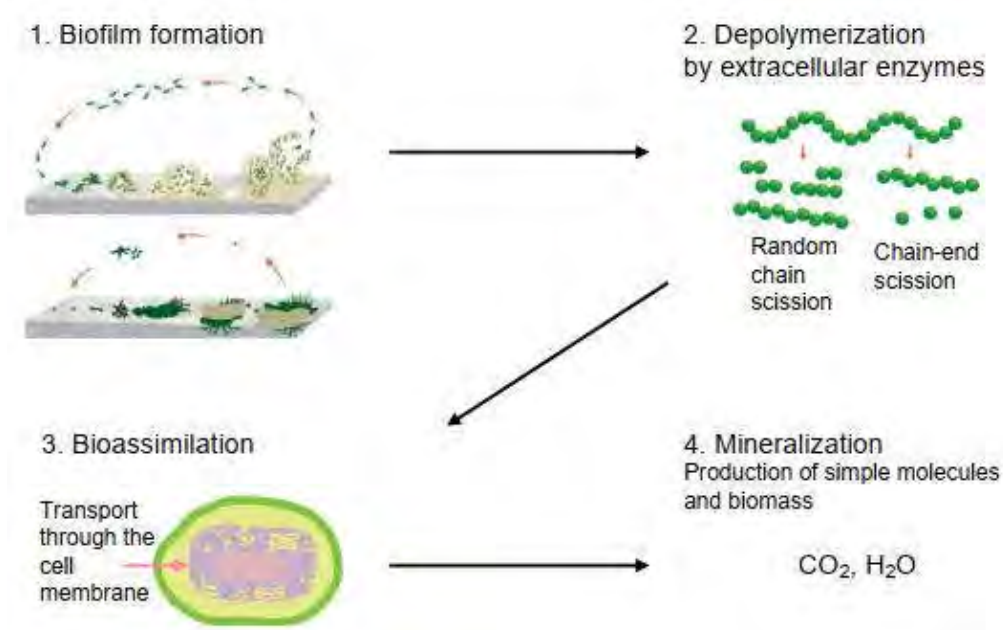


**Figure 2.3:** Main stages that involved in biotic degradation process

### 2.9.2.2 Depolymerization

The primary factor in the depolymerization stage is the enzymatic activity that follows biofilm development. Figure 2.4 shows that the hydrolytic and oxidative pathways of enzyme activity both involve random and end chain scission (Singh and Sharma, 2008; Devi et al., 2016). Enzymatic oxidation is called oxidative process. Due to the lack of hydrolysable groups in non-hydrolysable polymers, redox reactions are the most efficient method for rupturing the C-C bond backbone. Extracellular enzymes, on the other hand, must have high enough redox potentials to allow electron extraction from C-C bonds to ultimate polymer biodegradation (Krueger et al., 2015).

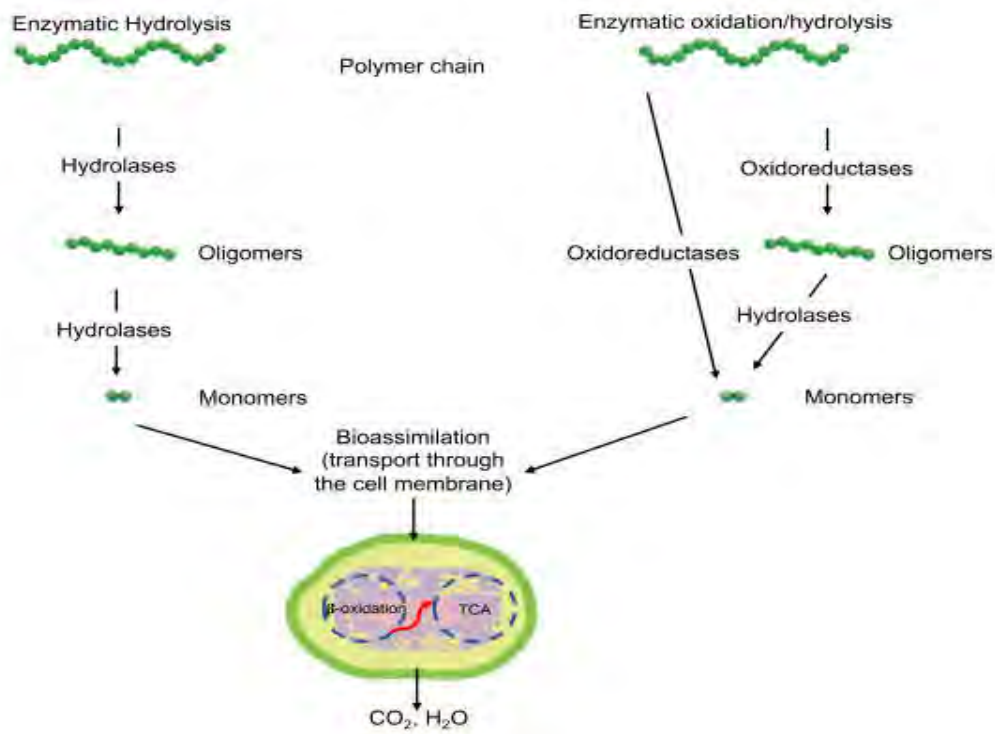


**Figure 2.4:** Enzymatic hydrolysis of polymer chain.

### 2.9.2.3 Biodeterioration

The pervasive nature and the staying power of microplastic in the marine environment provide an excellent space for the microbes to develop their niche. The progress of bio-deterioration is driven and determined by the proliferation of microorganisms and, ultimately, biofilm production. The enzymes (endo and exo-enzymes) produced by bacteria are the first responders to break down plastic polymers. Exopolysaccharides (EPS) is the glue that provides attachment and a bond between the biofilm and plastic layer. The process of bio-deterioration is affected by exopolysaccharides and enzymes. Research analysis on EPS of bacterium *Rhodococcus* rubber that degrades polyethylene reveals a concentration of 2.5 times higher than protein (Sivan, 2011).

### 2.9.2.4 Bio-fragmentation

The process of fragmentation works by converting the complex polymer into a simple form preceded by assimilation. The enzymes stimulate the fragmentation process to weaken the polymeric substance structure. The polymers are decomposed into

oligomers, dimers, and finally into monomers which cause the structure of carbon polymer to disrupt, enabling the fragmentation of plastic. The polymers are enzymatically depolymerized into monomers, which are then rapidly absorbed by microbes as carbon. This process contributes to a significant rise in bacterial biomass (Zubris & Richards, 2005; Barboza et al., 2020).

#### **2.9.2.5 Mineralization**

Mineralization is considered the end process for the degradation of plastic by microorganisms. At the point of biodegradation of plastic, the plastic polymers have entirely deteriorated to CO<sub>2</sub>, H<sub>2</sub>O, and CH<sub>4</sub>. The rate of degradation can be quantified depending on the levels of mineralization. With ever-increasing production and consumption of plastic has been estimated to about 5 to 15-million-ton plastic waste that has entered the oceans per year. This is an alarming situation and threat to human and animal health (Danso et al., 2019; Geyer et al., 2016; Willis et al., 2018).

### **2.10 Classification of plastics**

Plastics are divided into two types based on biodegradability, non-biodegradable and biodegradable plastics.

#### **2.10.1 Non-biodegradable plastics**

Non-biodegradable plastics are synthetic materials that cannot be broken down by natural processes into simpler, non-harmful components. These types of plastics, which are widely used in everyday items such as bottles, bags, packaging materials, and disposable products, pose significant environmental challenges due to their persistence in the environment (Ozen et al., 2002). When non-biodegradable plastics are discarded into the environment, they can take hundreds of years to decompose, during which time they can release toxic chemicals into the air, soil, and water (Krueger et al., 2015). These chemicals can have harmful effects on wildlife and human health, including cancer, reproductive problems, and hormonal imbalances. Furthermore, non-biodegradable plastics can accumulate in the environment and cause physical harm to wildlife, such as ingestion or entanglement. This can lead to a loss of biodiversity, as well as economic impacts on industries such as fishing and tourism (Shah et al., 2008). Despite the widespread use of non-biodegradable plastics, there are alternatives

available. Biodegradable plastics, which can decompose naturally and safely, are being developed and used in some applications (Ozen et al., 2002). Additionally, reducing the use of single-use plastics, such as straws and bags, and increasing recycling efforts can help to mitigate the negative impacts of non-biodegradable plastics on the environment. Non-biodegradable plastics pose significant environmental and health challenges due to their persistence in the environment, release of toxic chemicals, and harm to wildlife. While there are alternatives available, such as biodegradable plastics and reducing single-use plastics, a collective effort is needed to address the issue and minimize the harmful impacts on the human health and environment (Ozen et al., 2002).

### **2.10.2 Biodegradable plastics: A green alternative**

Degradable polymers in which microorganisms are involved in the primary degradation mechanisms are known as biodegradable polymers. (Leja and Lewandowicz, 2010). Biodegradable plastics (BPs) are sometimes completely degradable. Due to this sustainable nature of BPs, their demand has raised all over the world. To date, both aliphatic and aliphatic-aromatic co-polyesters have been produced. BPs are considered to be the potential solution for environmental pollution due to their degradability in natural environment. The degradability of these polymers is affected not only by their chemical structures but also by the ordered structures such as orientation and crystallinity (Chen et al., 2008). In bioactive environment, microorganisms could degrade BPs into water and CO<sub>2</sub> (Song et al., 2009). Although biodegradable plastics are biodegradable but the production of intermediates during their degradation in the environment or their incomplete degradation in the desired time, can cause environmental problems, as their consumption has been increased in the recent decades (Tokiwa et al., 2009).

The International Standards Organization (ISO) explains the biodegradability of polymeric materials as breakdown of larger molecules aided by microbial activity into smaller soluble intermediates such as carbon dioxide, methane, water and other inorganic molecules under optimal environmental conditions resulting in the alteration of chemical and physical properties (Mohee et al., 2008). The biodegradable polymers



such as aliphatic and aromatic polyesters are the derivatives of petrochemical based refined monomers (Figure. 2.5) (Song et al., 2009).

There are numerous applications of petroleum-based plastics but they are not ecofriendly and thus result in various environmental hazards. On the other hand, green plastics can be biodegradable with certain environmental benefits. Biodegradable plastics can also be derived from materials that breakdown into natural compounds upon fungal, bacterial or algal degradation resulting in the release of carbon dioxide, water and inorganic components (Harding et al., 2017).

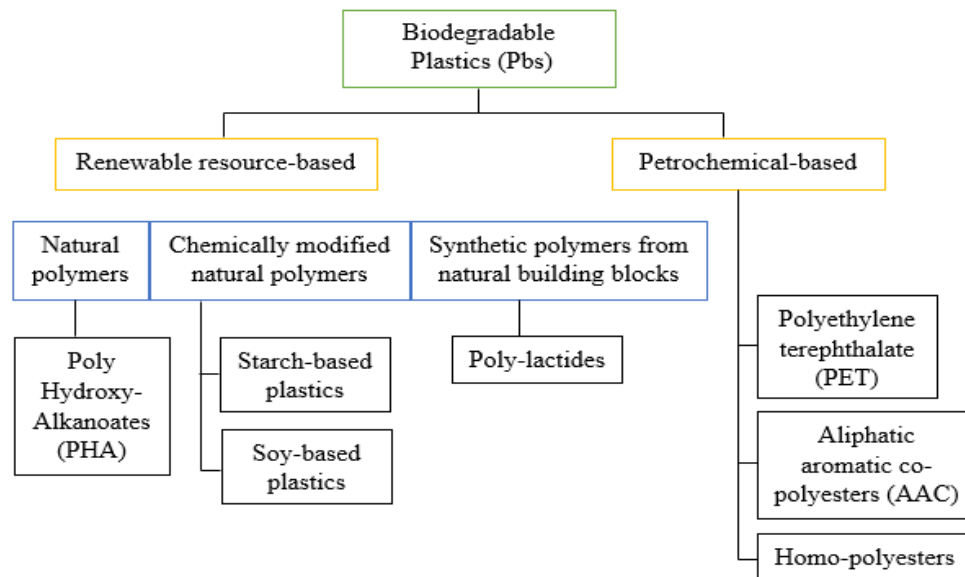


**Figure 2.5:** Classification of biodegradable plastics

### 2.10.3 Bioplastics

Plastics can be synthetic or natural sometimes also termed as bioplastics, manufactured by polymerizing smaller subunits called monomers resulting in a final product called polymer (Patel et al., 2015). The plastics generated so far are not biodegradable and it may persist in the environment for centuries. Majority of the biodegradable plastics generated so far take a substantial time for complete disruption into their harmless constituents depending on the availability of the optimum environmental and physical factors along with the existence of desired microbial population (Hopewell et al., 2009).



### **2.10.3.1 Bioplastics from renewable resources**

A type of plastic made from renewable resources is called bioplastic, such as cornstarch, sugarcane, and potato starch. Unlike traditional, non-biodegradable plastics, bioplastics are biodegradable and can decompose naturally into non-toxic components, leaving behind no trace in the environment. Bioplastics have a lower carbon footprint compared to non-biodegradable plastics, as they are made from renewable resources that require less fossil fuel energy to produce (Richert & Dąbrowska, 2021). Additionally, bioplastics are increasingly being used in various sectors, such as packaging materials, disposable cutlery, and textile fibers, as they are a more sustainable alternative to traditional plastics. However, the production of bioplastics requires large amounts of resources and energy, which can also have negative environmental impacts. As such, it is crucial to continue researching and developing new methods for producing bioplastics that minimize their environmental footprint while maintaining their biodegradability and functionality (Song et al., 2009). Starch blends, poly (lactide) (PLA) and Poly (hydroxybutyrate) (PHB) are other examples of polymers that have been manufactured from renewable resources and are biodegradable too but Nylon 11 (NY11) and polyethylene that are also produced from renewable resources, are non-biodegradable (Osman et al., 2018).

### **2.10.3.2 Bioplastics from non-renewable resources**

Plastics that are produced from non-renewable resources are synthetic polymers which can be synthesized from petroleum oil or can be made by scientists and engineers. Examples of these polymers comprise of Teflon, polyethylene, nylon, polyester and epoxy. Although these types of bioplastics are made from a similar chemical composition as traditional plastics, they are often marketed as being more eco-friendly since they are biodegradable (Smith, 2005). However, it is important to note that biodegradable plastics from non-renewable resources still rely heavily on fossil fuels and have a significant carbon footprint. Additionally, the production of bioplastics from non-renewable resources requires a large amount of energy, which contributes to greenhouse gas emissions and environmental degradation (Song et al., 2009). While biodegradable plastics from non-renewable resources may offer some advantages over traditional plastics, it is essential to continue investing in more sustainable alternatives

such as bioplastics made from renewable resources, which have a lower environmental impact and can help reduce our dependence on fossil fuels (Tokiwa et al., 2009).

### 2.11 Enzymes and Microorganisms able to Biodegrade Polymers

There is a vast range of capability across actinomycetes, fungi and bacteria, fungi regarding the capability to degrade biodegradable polymers. Microorganisms and their extracellular enzymes are capable of biodegrading polymers in various mesophilic environments are listed in Table 2.1.

**Table 2.1:** Microorganisms and their enzymes in biodegradation of plastics

Enzymes	Microorganism	Polymer	Reference
Carboxyl esterase (3.1.1.1)	<i>Alcanivorax borkumensis</i> (B)	PCL, PDLLA, PBSA, PCL, PES, PHBV, PDLLA	(Hajighasemi et al., 2016)
Cutinase	<i>Aspergillus oryzae</i> (F), <i>Humicola insolens</i> (F), <i>Aspergillus fumigatus</i> (F)	PCL, PET	(Baker et al., 2012)
Cutinase (21 kDa)	<i>Cryptococcus magnus</i> (F)	PDLLA, PLLA,	(Suzuki et al., 2012)
Cutinase (19.7 kDa)	<i>Paraphoma</i> strain B47-9 (F)	PBAT, PBS, PBSA, PCL, PDLLA	(Suzuki et al., 2014)
Cutinase-like enzyme (22 kDa)	<i>Cryptococcus flavus</i> GB-1 (Y)	PBSA, PBS, PLA, PCL, PET	(Watanabe et al., 2015)
Esterase (3.1.1.1)	<i>Aspergillus</i> sp. Strain S45 (F)	PU	(Osman et al., 2018)
Esterase	<i>Bacillus subtilis</i> (B), <i>Aspergillus tubingensis</i> (F), <i>Bacillus licheniformis</i> (B), <i>Alicyclophillus</i> sp. (B), <i>Leptothrix</i> sp. TB-71 (B)	PCL, PLA, PU, PLLA,	(Khan et al., 2017; Arena et al., 2011; Ocegüera-Cervantes et al., 2007; Nakajima-Kambe et al., 2009)
Esterase (62 kDa)	<i>Comamonas acidovorans</i> strain TB-35 (B)	PU	(Nakajima-Kambe et al., 1995)
Lipase (3.1.1.3)	<i>Rhizopus delemar</i> (F), <i>Candida rugosa</i> (F),	PLA	(Lee and Kim, 2010; Pérez-

---

Lipase (36 kDa)	<i>Pseudomonas aeruginosa</i> PBSA-2 (B)			Arauz et al., 2019)
	<i>Aspergillus niger</i> MTCC 2594 (F)		PCL, PLA	(Nakajima- Kambe et al., 2012)
Lipase (34 kDa)	<i>Pseudomonas</i> sp. DS04-T (B)	Strain	PLLA, PCL, PHB	(Wang et al., 2011)
Polyurethanase protease (29 kDa)	<i>Pseudomonas fluorescens</i> (B)		PU	(Howard and Blake, 1998)
Protease (3.4.21)	<i>Bacillus licheniformis</i> (B)		PLA	(Richert & Dąbrowska, 2021)
Proteinase K (3.4.21.64)	<i>Tritirachium album</i>		PLLA, PES, PEA, PBS, PBSA, PCL	(Lim et al., 2005)
co-polyester degrading enzyme (27–31 kDa)	<i>Roseateles depolymerans</i> TB-87 (B)		PBS, PBSA, PCL, PBST, PES	(Shah et al., 2013)

---

### 2.11.1 Microbial Population

In various environments, some microbes can break down a variety of polymer structures, and the efficiency of the breakdown rate can vary. Many papers that have been published have described the digesting activity of a particular microbe in the well-regulated environments of incubated or culture medium; in these environments, the polymer substrate is typically the bacterium's only source of nutrients. The complexity of the biological activity process rises in situations with less restrictions, such as home composting, soil, aquatic habitats or industrial composting and may be available. (Bher et al., 2022; Lefèvre et al., 2002).

### 2.12 Different typed of synthetic plastic

Different types of plastics are used commonly. Some widely used polyester are listed in table 2.2.

**Table 2.2:** Commonly used polyesters

Name	Abbreviations
Poly (Butylene-succinate)	PBS
Poly-caprolactone	PCL
Poly (ethylene-succinate)	PBS
Poly lactide	PL
Poly(hydroxyalkanoate)	PHB/PHBV
Poly (ethylene terephthalate)	PET
Polyurethane	PU
Poly (butyrate adipate- <i>co</i> -terephthalate)	PBAT
Poly ( $\beta$ -Propiolactone)	PBL
Poly (Butylene-succinate- <i>co</i> -adipate)	PBSA

### 2.12.1 Polyurethanes

PURs are manufactured in several ways; one of those is to use polyether or polyester polyols. It is a polymeric material made by organic units and concocted by carbamate (Skleničková et al., 2022). Furthermore, the physio-chemical characteristics of polymers are affected by the integration of aromatic ring structures. Also, PUR is widely used in producing polyurethane foam, thermal insulation, garment solvents, and paints (Aslam et al., 2018). It is 5th on the list of the most produced synthetic polymers according to the quantity produced. However, bioactivities focused on ester PUR have been studied. Bacteria or fungi were used to achieve biodegradation. As far as bacteria that can degrade PUR is concerned, *Betaproteobacteria* (Gram-negative), genus *pseudomonas* is found to be the most linked to PUR activities (Ghasemlou et al., 2019; Xie et al., 2019).

### 2.12.2 Polyethylene

Polyethylene (PE) is made up of repeating linking of the polymers of ethylene. It is prepared by chemical means for the polymerizing of ethane and it is extremely variable as the side-chains can be obtained by differing the production process. These changes

impact the molecular weight and crystallinity (Danso et al., 2019). The main and the most frequent packaging material used in the packing industry. The global annual production of polyethylene is around 100 million tons. A large number of bacterial genera have been affiliated with possible polyethylene degradation. Gram-negative with the genera *Ralstonia*, *Stenotrophomonas*, and *Pseudomonas* along with many Gram-positive taxa are among these bacterial genera. The fungi and insect including *Cladosporium*, *Aspergillus*, and *Galleria mellonella* are responsible for PE degradation (Jeon and Kim 2015; Konduri et al., 2011; Kong et al., 2019)

### **2.12.3 Polyamide**

Repeated units of semi-aromatic, aromatic, or aliphatic molecules that are linked through amide bonds are known as polyamide (PA). There are various types of synthetic polyamides as they are made up of monomers that are versatile, many of them are popular like nylon and Kevlar. In many industries, polyamides are used for automotive, textiles, sportswear, and carpets. Strangely proteins and natural silk are polyamides (PlasticsEurope, 2021). It can be expected that enzymes have emerged naturally that act on these polymers. Fully degrading an intact high molecular weight polymer and that too by microorganism has not been discovered yet (Samak et al., 2020).

### **2.12.4 Polystyrene**

This polymer comprises monomers of styrene. Apart from its extensive usage as a synthetic plastic in the packaging industry, polystyrene is also used in the production of daily use materials like CD cases, Petri dishes, plastic cutlery, and many others. Around 14 million tons were produced in the year 2016. In all these studies weight loss was mainly examined. No enzyme was found to be linked with the assumed depolymerization in these studies. A particular bacterium is not known for degrading, but multiple genera have been known to degrade PS (Poortinga and Whitaker, 2018)

### **2.12.5 Polyvinylchloride PVC and polypropylene PP**

Polyvinylchloride and polypropylene are termed as highly essential polymers which are generated at high levels as compared to the polymeric substances mentioned above

(Shah et al., 2008; Mowla and Ahmadi, 2007). PVC is made up of repeating units of chloroethyl while PP is made up of repeating units of propane-1,2-diyl units. Though both the polymers are produced in higher numbers globally, there is no information on the possible degradation of essential polymers (Tokiwa et al., 2009).

### **2.12.6 Polyethylene terephthalate (PET)**

PET, a thermoplastic co-polymer resin that is semi-aromatic and belongs to the polyester family, allow us to focus on its features. These include low permeability to gases, high strength, low density, durability against physical and chemical deterioration, and non-biodegradability (Sepperumal et al., 2013; Webb et al., 2013). Plastic materials, particularly Polyethylene terephthalate (PET), give economic benefits because they are extensively used in our daily lives, and global production is rapidly increasing due to the low-cost production, simple synthesis, and durability that are advantageous to the packaging manufacturing. (Lebreton and Andrady, 2019). PET is an aromatic polyester that is difficult to degrade due to the availability of non-hydrolyzable-covalent bonds with a substrate subunit called ethylene glycol (EG) and terephthalic acid (TPA) (Kawai et al., 2019). It is one of the most often used synthetic polymers. PET is a colorless, hygroscopic resin that is semi-crystalline and has excellent wear, impact resistance and good tensile strength. It is utilized for garments, textiles, storage containers, and some engineering applications. (Quartinello et al., 2017). It is normally utilized in the making of drinking bottles. In the textile market, PET has extensively used the production of soft drinks and water bottles, foils, and fibers (Barth et al., 2016). They are crystalline and thermoplastic by nature. The global generation of PET has surpassed 30 million tons in 2017. They can be collected and recovered through different means and systems that are being operated in multiple states, even though the recovery is about less than half and very limited polymeric plastic are recovered as new products (Kawai et al., 2019) Among the synthetic polymers that are being used for bottles and textiles, PET is indeed the most widely produced and used. It has a yield of over 50 million tons a year. Huge amounts of this have made their way to the natural environment and severely affected it. However, the use of enzymes to decompose PET is a great new way. It is a pollution free method to minimize public dispose and recycle petroleum-made initiating materials TPA and EG..

Lipases, cutinases, carboxylesterases, and esterases can break ester linkages and have been found to hydrolyze PET in the last ten years (Ruan et al., 2018). Cutinases have shown remarkable activity against degrading PET, owing to the higher degrading ability and the absence of lid structure necessary for lipase for starting at lipid-water sites (Kim et al., 2022). At present, multiple fungi and bacteria are reported to degrade PET to oligomers or monomers partially (Chen et al., 2010; Then et al., 2015; Wei & Zimmermann, 2017).

### **2.13 Properties and Applications of PET**

Polyethylene terephthalate is rendered as a plastic having high characteristic mechanical strength and low permeability to gases with an overall good aesthetic appearance; it's semi-crystalline thermoplastic polyester with such properties. PET is seen as a toxic or harmful material due to its prominent presence as waste in water bodies and also due to its strong resistance to atmospheric and biological agents despite the fact that it is mainly innocuous to the human body directly (Chen et al., 2010; Willis et al., 2018). PET time-controlled degradation by the environment is highly mandatory and desirable for certain applications such as packaging and farming biodegradable and consumable biomaterial. The PET is manufactured with different trade names by various companies. PET is gaining much more attention worldwide due to its use in a number of applications and its favorable characteristics durability and strength, chemical and thermal stability with low gas permeability, and easy manufacturing and handling. Above 50% of all synthetic fibers produced worldwide consists mainly of PET. Global consumption is reported to exceed \$17 billion per annum with 6.5% plastic demand in only Europe that is an excess of over 3000 tons (PlasticsEurope, 2021). PETs are generated by polymerization conditions for intended applications as desired properties. It is mainly utilized for films, fibers, and sheets which are used extensively in the food and packaging industry hence a very wide range of applications make use of this material (Danso et al., 2019).

### 2.14 Chemical Structure and Synthesis of PET

Two or more chemical reactions are required to carry out the synthesis of PET on a commercial level. For its manufacture, first Ethylene glycol is reacted either with dimethyl terephthalate DMT or with terephthalic acid. All this reaction is carried out at high temperatures about 250 to 260 °C and pressure of 350 to 500 kpa. For another reaction, the temperature is a bit low as compared to the first reaction i-e 140-220 °C and pressure of 100 kpa. These reactions result in the formation of BHET, depending on the molecular weight of PET which is required for a specific application, two or three polymerization reactions are carried out after completion of the initial reaction (Chen et al., 2013).

In the initial step of polymerization, the ethylene glycol is displaced due to transesterification between BHET molecules, at temperature of 250-280 °C and pressure of 2-3 kpa. Oligopolymers formed as a result of first reaction are then condensed at temperature 270-280 °C and at pressure of 50-100 kpa (Barth et al., 2016). This is the stage when the polymer is ready for use. But if high molecular weight polymers are required then further step is performed i-e third step in which polyesters 200–240°C and 100 kpa (Barth et al., 2016). Once the raw polymer is synthesized, the required form can be processed (Figure 2.6). It can be done by extrusion, injection molding or blow molding. During PET production, atmospheric CO<sub>2</sub> is emitted. The amount of this emitted carbon dioxide is reaches up to 2440 kg for every 1000kg of PET resin produced. Certain advances have been made in the production of P-xylene. These advancements have greatly helped to reduce environmental costs. Some new research has shown that P-xylene is a vital constituent while producing terephthalic acid. However, it may also be made from certain sources like cellulose and hemicellulose (Barth et al., 2016; Chen et al., 2013).



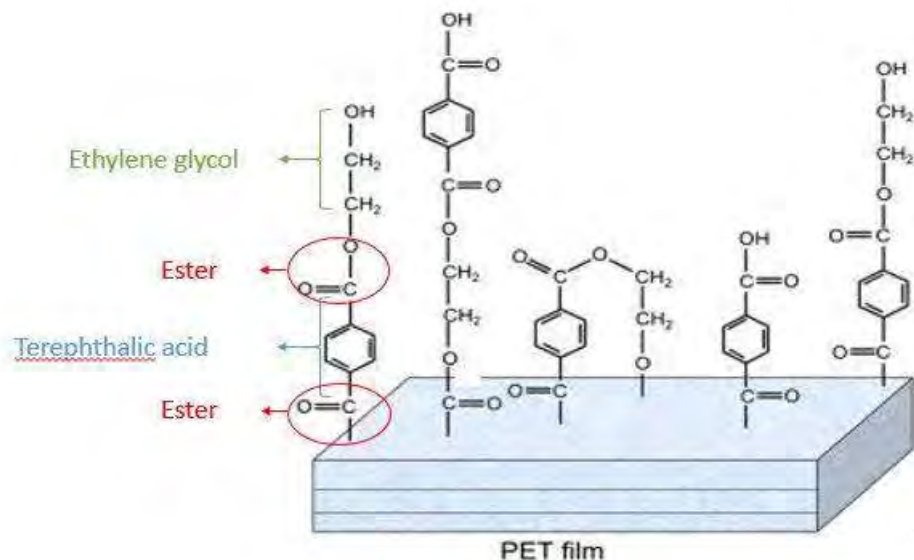


**Figure 2.6:** Chemical structure of PET

### 2.15 PET in the Environment

In 2017, there were 348 Mt of plastic produced globally (PlasticsEurope, 2018). Out of this, 90% came from fossil fuels (World Economic Forum, 2016). The yearly production of polyethylene terephthalate (PET) was found to be more than 30 million tons in 2017. It is known that packaging of products is the most prominent application sector. It makes up for approximately 40% of whole plastic demand (PlasticsEurope, 2018). These packaging materials which mostly consist of plastic are the major contributors towards the municipal solid waste and aquatic anthropogenic litter (Barnes et al., 2009). This has resulted in an extremely harmful worldwide environmental crisis. Plastics, including PET, that are thrown on land carelessly pose a danger to the environment. These materials break into smaller pieces when exposed to oxygen and intense sunlight. Ultimately, they form micro plastics which are the cause of many problems in the aquatic ecosystem (Thompson et al., 2009). Most micro plastics float over the oceans and seas which are then digested by marine animals and birds as food. Scientists have alerted that microplastics make their way to digestive system of birds and fishes. Therefore, when humans ingest seawater or consume fish, these plastics make their way to our digestive system as well. Moreover, recent reports suggest that

these micro plastics resemble the food of the fish and the birds which is why it is mistakenly swallowed by these creatures. Hence, it is an alarming issue that we humans may ingest microplastics through this food chain process (PlasticsEurope, 2021).

### 2.16 Biodegradation of PET

At present, only a few fungi and bacteria have been found to degrade PET partially to oligomers or monomers. Although, there are a few reports on the utilization of PET by microorganisms in many ecosystems to support their growth and development. Due to the rigid structure of PET, a number of difficulties are being experienced in the PET degradation by microbes and their relative enzymes. Furthermore, PET has a  $T_g$  of 75 °C and the crystallinity of biaxially oriented PET film is ~35%. All the PET hydrolases are known to have comparatively fewer turnover rates. Fascinatingly, the characteristic for degradation of PET seems to be for only some bacterial phyla. Amazing examples come from the genera *Thermobifida* and *Thermomonospora* (Gong et al., 2018).

Enzymes, PETase converts PET into two more monomers which are TPA and ethylene glycol (EG). The resulting enzymes are produced by *I. sakaiensis*. Moreover, they behave synergistically to hydrolyze PET. And further metabolizes these monomers to facilitate their growth (Geyer et al., 2016; Kawai et al., 2019; Yoshida et al., 2016). However, the bacterium's degradation of PET at 30°C is slow. Studies have revealed the structure and sequence of PETase show similar properties to the alpha and beta hydrolase enzymes which include lipases, cutinases and esterases. Fungi and bacteria have the same metabolic ways for the degradation and breakdown of esterases and cutinases as they degrade PET into terephthalic acid (TPA) (Wei et al. 2016; Duan et al., 2017; Aristizábal-Lanza et al., 2022). The microorganisms that have been reported until today can only metabolize PET to TPA and the further transformation of TPA is not yet clear, which makes it a nuisance to the environment and can cause Eco toxicity more than the PET products or materials (Barth et al., 2015). So therefore, to reduce and to eradicate PET from the environment and to define more clearly the mechanism of PET degradation. Hence, the degradation of PET by microbes needs further investigation. The molecular size of synthetic polymers and their hydrophobicity, crystallinity and surface topography are vital factors affecting their biodegradability.

---

Additional factors must be taken into consideration for PET hydrolysis (Aristizábal-Lanza et al., 2022; Narancic et al., 2018).

### **2.17 Role of enzyme in Degradation of PET**

TPA and EG join by ester bondage to form a polyethylene terephthalate polymer. The worldwide production and consumption of PET surpassed about 41.6 million tons in 2014 due to the extensive usage of plastic in packaging product lines, plastic containers for beverages, and the manufacturing sector. Normally the enzymes that are related to degradation are serine hydrolases. This means they are either cutinases, lipases and esterases.

The crystalline component of PET fiber is about forty percent, and PET beverage bottles have about thirty percent, making them highly reluctant to breakdown by the action of enzymes (Samak et al., 2020). The amorphous polymer structure component is affected by a temperature similar to the transition temperature of a glass of PET at about 65°C (Barros et al., 2019). This temperature makes the polymer's amorphous structure flexible, porous, and open to enzymes' action. Therefore, the degradation at such a high transition temperature needs enzymes that are stable to degrade the polymer (Samak et al., 2020; Then et al., 2015; Thompson et al., 2009). There has been a recent study that has shown the enzymatic breakdown of PET at 30°C temperature. Nevertheless, it has been reported that a very low degradation could be achieved at this temperature. Previous studies have demonstrated that a variety of lipase producing species of *actinomycetes*, and fungus could degrade amorphous PET and also affect the composition of PET films (Barth et al., 2016). *Thermobifida fusca*, *Bacillus subtilis*, and *Bacillus licheniformis* produce carboxylesterases that have shown to moderately degrade PET films and fibers. They also exhibited significant efficacy to degrade the oligomer of PET. Because of the lid-like configuration covering the lipases' hydrophobic catalytic center, they exhibit limited PET degradability, ultimately resulting in low availability for the polymers. On the contrary, Cutinases do not possess a lid structure, making them efficient in the breakdown of amorphous PET films and fibers, significantly decreasing the polymer's weight. Studies have indicated that the structures of bacterial and fungal cutinases

have accessible catalytic sites, unlike lipases (Chen et al., 2010). The open and accessible active sites provide the space for identification and association with the polymer substrates. Cutinases HiC from *Thermomyces* (formerly *Humicola*) *insolens* are thermostable and have a significant role in polyester hydrolases (Bahl et al., 2020). HiC has shown to entirely hydrolyze a low crystalline structure of PET film (7%) after a reaction time of 96 hours at 70°C, indicating the degradation of the crystalline part of the PET. Around the same reaction temperature, about 25 percent of low crystalline PET film is hydrolyzed by thermostable bacterial L-C cutinase (Aristizábal-Lanza et al., 2022).

The hydrolytic efficacy towards PET of a polyester hydrolase from *Thermobifida fusca* (Barth et al., 2016; Chen et al., 2008) and *Fusarium solani* (Chen et al., 2010; Melo et al., 2003) was improved by alerting the size and hydrophobicity of the residues. Major water-soluble products achieved through enzymatic hydrolysis of PET are ethylene glycol, terephthalate, MHET, and (BHET). MHET and BHT are hindered by a TfCut2, a polyester hydrolase (Figure.2.7) (Lahens et al., 2018).

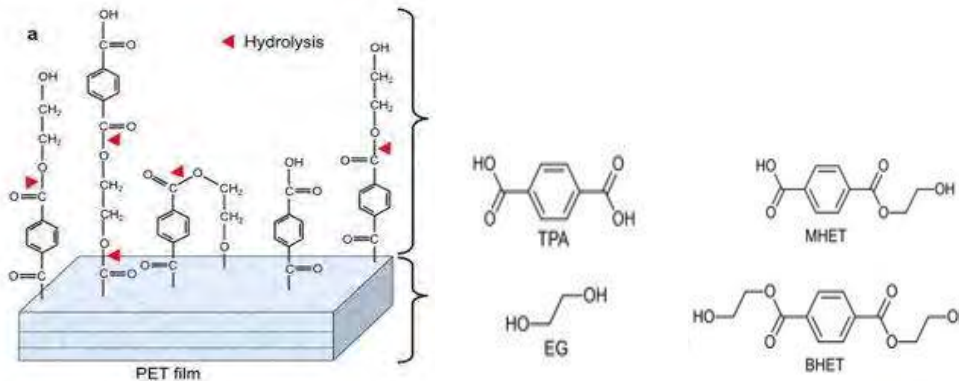


**Figure 2.7:** Water soluble product obtained from PET film degraded by polyester hydrolase

### 2.17.1 Extracellular Enzymes

The primary extracellular enzymes for depolymerizing aliphatic and aromatic/aliphatic polyesters, as well as PET generated from ester, are shown in figure 2.8; ester bond cleavage is thought to be the rate-determining step (Mueller, 2006).

The primary extracellular enzymes for the enzymatic hydrolysis of the ester group are lipases, esterases and cutinases are members of the hydrolase family and have structurally similar but functionally varied properties (Figure 2.8) (Marten et al., 2005).

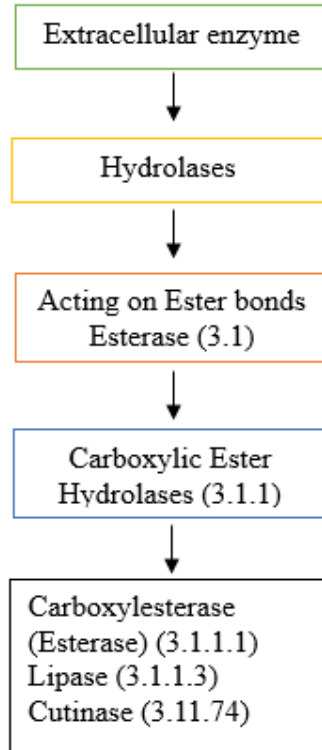


**Figure 2.8:** Extracellular enzymes that degrade PET plastic derived from esters

### 2.17.1.1 Carboxylesterases

Carboxylesterases are a class of enzymes that are capable of breaking down PET plastics. PET is a commonly used plastic that is widely used in food and beverage packaging due to its durability, transparency, and low cost. However, PET plastics are non-biodegradable and can persist in the environment for hundreds of years, contributing to the accumulation of plastic waste.

Carboxylesterases are found naturally in some bacteria and fungi and have been identified as potential candidates for degrading PET plastics. These enzymes work by breaking down the ester bonds that hold PET molecules together, resulting in the breakdown of the plastic into smaller, more biodegradable components. Research has

shown that carboxyesterases can effectively degrade PET plastics in laboratory settings, with some enzymes capable of breaking down up to 90% of PET within 10 hours. The discovery of carboxyesterases that degrade PET plastics holds significant promise in the fight against plastic pollution. By harnessing the power of these enzymes, we may be able to develop more effective and sustainable methods for managing plastic waste and reducing our impact on the environment (Gricajeva et al., 2022).

### **2.17.1.2 Lipases**

Lipases are a class of enzymes that have been shown to have the potential to degrade a variety of plastics, including polyethylene terephthalate (PET), polycarbonate (PC), and polyurethane (PU) (Singh and Mukhopadhyay, 2012). Lipase enzyme is commonly used in the food and detergent, due to their ability to catalyze the breakdown of fats and oils. Research has shown that lipases can effectively degrade plastics by breaking down the ester bonds that hold the plastic molecules together (Herzog et al., 2006; Mueller, 2006). In the case of PET, lipases have been shown to break down up to 60% of the plastic within 96 hours. Additionally, lipases have been shown to degrade PC and PU plastics, which are commonly used in electronic devices and other applications (Rizzarelli et al., 2004).

However, the use of lipases for plastic degradation is still in the early stages of development, and there are several challenges that must be addressed before this technology can be used on a large scale (Gricajeva et al., 2022). One of the major challenges is finding ways to optimize the effectiveness of the lipases and ensure their stability under the harsh conditions of industrial processes. Additionally, the cost of producing and using the enzymes must be carefully evaluated to determine whether this technology is economically viable. Despite these challenges, the discovery of lipases that can degrade plastics waste. By harnessing the power of these enzymes, we may be able to develop more sustainable and effective methods for managing plastic waste and mitigating the harmful effects of plastic pollution on the environment (Gricajeva et al., 2022).

### 2.17.1.3 Cutinase

The outer protective covering of the epidermis of terrestrial plant parts such as leaves, shoots, and other parts of the plant above the ground, is a plant cuticle. They are composed of waxes and lipid polymer. The composition of the cuticle is important in providing protection against dehydration and pathogenic infection. Cutin, an insoluble lipid polymer, largely comprised 16-18 hydroxylated carbon fatty acid joined together by ester bondage; this makes the most essential cuticle component. Fungus and bacteria secrete a hydrolyzing enzyme called cutinases, which can degrade PET polymer. Cutinases are a part of the  $\alpha/\beta$  hydrolase superfamily, which are serine esterases. The cutinases have a typical Ser-His-Asp catalytic triad those have their catalytic serine sites accessible to the solvent (Barth et al., 2016; Danso et al., 2019). Since cutinase's active site is not blocked by a hydrophobic covering active sites in true lipases and is available for all, even high molecular weight substrate cutin, some may even hydrolyze high molecular weight polymer polyester. Cutinases have a role to play in esterification and transesterification (Chen et al., 2013). According to research on the impact of pH on the surface charge surrounding the active site of cutinases, the activity toward polymers like PET is reduced as the active site becomes more positive when pH declines from alkaline to acidic levels. (Baker et al., 2012). The stabilization of the transition stage, the efficiency of the product release stage, and the interaction of the substrate with the enzyme are all impacted by the electrostatic surface potentials produced by charged residues (Baker et al., 2012; Pan et al., 2018; Shi et al., 2020).

Cutinases' activity toward polymers including PET, PCL, PBS, and PBSA increased when the cofactors  $\text{Ca}^{2+}$ ,  $\text{Na}^+$ , and  $\text{K}^+$  were present; however, the cofactors  $\text{Mg}^{2+}$  or  $\text{Zn}^{2+}$  had no discernible effect or considerably decreased the enzymes' activity (Suzuki et al., 2013; Mao et al., 2015; Shi et al., 2020). This enzyme has demonstrated some ability to depolymerize hydrophobic PET. They come from a plant pathogenic fungus, which helps the fungus enter the plant and hydrolyze the cutin. The hydrolyzing activity of *F. solani*, which is both exo and endo, is investigated (Woodard and Grunlan, 2018). PBURU-B5 strain hydrolysis increased dyeability and demonstrated improved moisture and water absorption capability (Jeon and Kim 2013; Woodard and Grunlan, 2018). One study found that adding hydrophobins to PET, which are

common in the *Tricoderma* genus, increases the action of the cutinases enzyme from *Humicola insolens*, causing PET to degrade. (Jeon and Kim, 2013; Kijchavengkul et al., 2008). Additionally, the thermophilic bacteria *T. fusca* was found to have cutinase activity, raising the possibility that it could biodegrade copolyesters of aromatic and aliphatic chemicals during the still-unstudied composting process (Coates and Getzler, 2020)

### **2.18 Application of Cutinase in Industry**

Cutinases are versatile in function, plus they can catalyze hydrolysis, esterification, and transesterification. These properties have significant potential to be utilized in chemical, food, detergent, and textile industries. They are effective precursors in the food industry for the processing of vegetables, milk products, flavor compounds, and essential fatty acids such as EPA (Eicosapentaenoic acid) and DHA (Docosahexaenoic acid) (Dhawan et al., 2019). They can be used for the manufacturing of biodiesel, phenolic substances, surfactants, and other chiral chemicals in the chemical sector. They have also shown huge assurance in polymer recycling and in the surface modification of polymers. They are considered huge in the detergent industry as lipolytic enzymes for dishwashing and laundry detergent. Cutinases have significant stabilization at temperatures ranging from 20°C to 50°C, and they show excellent results on the pH ranging from 8 to 11. They also have the ability to work in the presence of other enzymes such as H<sub>2</sub>O<sub>2</sub>. They are considered effective for extracting triacylglycerols and degrading fats lacking calcium instead of commercial lipase (Fett et al., 2000; Kawai et al., 2019; Wei et al., 2016). Cutinase is used in the environmental sector to aid in the breakdown of waste, including pesticide and polymer waste. The importance of cutinase has thoroughly increased in the textile industry as a biocatalyst in the previous years (Wei et al., 2016).

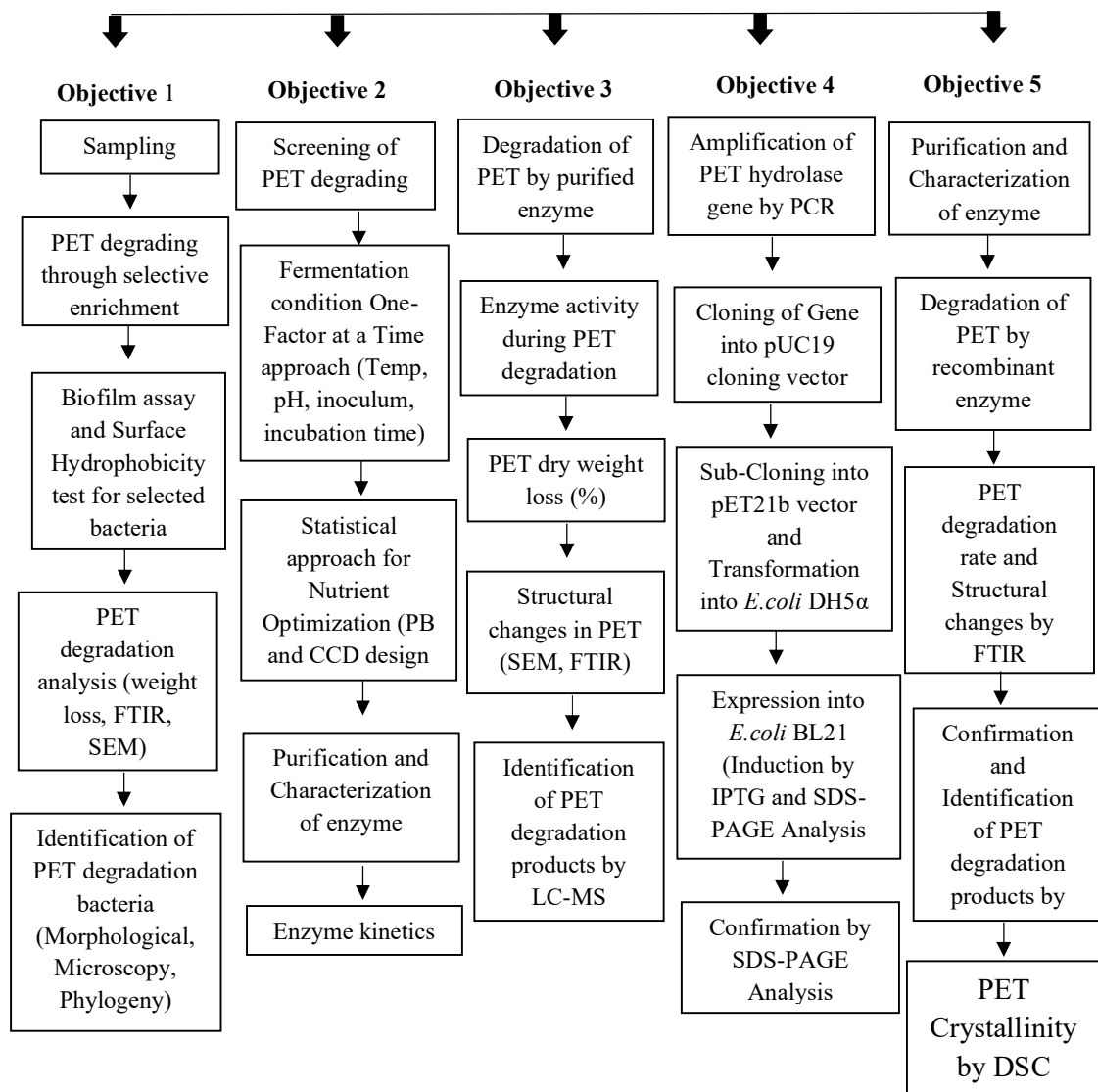


***CHAPTER 3***  
***MATERIALS & METHODS***

## Material and methods

The current research study was jointly conducted at Applied, Environmental and Geomicrobiology Laboratory, Department of Microbiology, Quaid-i-Azam University Islamabad, Pakistan; Molecular Biology laboratory, Karadeniz Technical University, Trabzon, Turkey and Department of Chemical Engineering, Division of Biotechnology, Lund University, Sweden. It included polyethylene terephthalate (PET) degradation by bacteria isolated from plastic waste disposal site as well as purification, characterization, cloning and expression of PET degrading enzyme.

### Overview of material and methods



### 3.1 Collection of Samples

Polyethylene terephthalate (PET) bottle and soil samples were aseptically collected from a garbage-dumping site located at Peshawar, Khyber Pakhtunkhwa, in sterile zipper bags. Temperature and pH at the sampling site were measured by means of thermometer and pH strips. Samples were transported carefully to Applied, Environmental and Geomicrobiology (AEG) laboratory, Department of Microbiology, Quaid-I-Azam University Islamabad and kept at 4°C for further analysis.

### 3.2 Isolation of bacteria

100 µL of 7-folds diluted soil sample ranging from  $10^{-1}$  to  $10^{-7}$  was transferred aseptically to nutrient agar (NA) plates and spread by mean of glass spreader. The inoculated plates were incubated for 24 hours at 35°C. The colonies on NA plates were counted and sub-cultured for purification on the basis of morphological differences.

The pieces of PET water bottle (2 x 2 cm and 50mg each) collected from garbage dumping site, were dropped into 100 mL nutrient broth (NB) in 250 mL Erlenmeyer flask. NB medium without PET pieces was run in separate as control. The flasks were incubated in shaker incubator at 35°C and 150 rpm for 2 days. After incubation, the broth medium was serially diluted and 100 µL of sample was shifted aseptically to NA plates and spread by sterile glass spreader in order to isolate bacteria. The inoculated plates were incubated at 35 °C for 24 hours. The colonies on NA plates were calculated and sub-cultured for purification on the basis of morphological differences.

### 3.3 Screening of bacterial isolates for PET degradation by selective enrichment

Total 24 bacterial strains, 19 from soil samples and 5 from PET sample were screened for PET degradation ability. Plastic pieces (2 x 2 cm) from a disposable PET bottle were sterilized by dipping in 70% ethanol for 30 minutes and rinsed twice with deionized distilled water to remove any residual ethanol and placed under UV for 5 minutes.

### 3.3.1 Inoculum preparation

The inoculum was prepared in nutrient broth. The isolated bacterial strains were sub-cultured in 5 mL nutrient broth (NB) in 20 mL test tube. Abiotic control was set up in NB without inoculum. The tubes were incubated in shaker incubator at 35°C and 150 rpm for 24 hours. After incubation, 2 mL of the freshly grown culture was subjected to centrifugation for 10 minutes at 8,000 rpm. The supernatant was removed, and the resulted pellet was re-suspended in 500 µL normal saline in order to remove all the nutrient from the pellet.

### 3.3.2 Screening experiment

PET pieces were aseptically transferred into an Erlenmeyer flask (250 mL) containing 100 mL of mineral salt medium (MSM), as sole source of carbon for bacterial growth. The composition of MSM medium in g/L shown in table 3.1. About 50 µL from the freshly prepared inoculum was transferred to MSM containing pieces of PET plastic. Abiotic control was set up with plastic pieces in the MSM without inoculum. Both the test and control flasks were incubated in a shaking incubator at 150 rpm and 35 °C for 4 weeks. After every one week, PET pieces were transferred aseptically to MSM in another flask with 1 mL culture from the previous flask and incubated at 35°C and 150 rpm for another week. Four consecutive shifts were performed to serially enrich the potential PET degrading bacteria in the medium.

### 3.3.3 Determination of Bacterial growth

The bacterial growth was observed on nutrient agar plate on weekly basis. Serial dilution was performed; it is a process, which reduces the concentration of a substance in a solution. It is basically the repetition of dilution to amplify the dilution factor quickly. 1 mL of MSM medium containing inoculum and PET pieces was transferred to a test tube containing 9 mL of autoclaved distilled water. After gentle mixing, 1 mL from tube 1<sup>st</sup> was transferred to 2<sup>nd</sup> tube and this process was carried till tube 6<sup>th</sup>. 50 µL from each tube was transferred to NB agar plates and was spread with the help of a sterile spreader. The plates were kept for incubation at 35°C for 24 hours. On the very next day CFU count and colony morphology was noted.

Similarly, 2mL from the MSM medium containing inoculum and PET pieces was taken and observed for bacterial growth by spectrophotometer after every 48 hours at 600 nm. A bacterial strain designated as PRS8 was selected on the basis of maximum growth in the presence of PET in MSM and further studies were conducted to confirm its role in PET degradation.

**Table. 3.1:** Composition of MSM medium

Constituents	g/L
CaCl <sub>2</sub> .2H <sub>2</sub> O	10.002
KH <sub>2</sub> PO <sub>4</sub>	0.2
MgSO <sub>4</sub> .7H <sub>2</sub> O	0.5
K <sub>2</sub> HPO <sub>4</sub>	1
FeSO <sub>4</sub> .7H <sub>2</sub> O	0.01
NaCl	1
(NH <sub>4</sub> ) <sub>2</sub> SO <sub>4</sub>	1

### 3.4 Identification and Characterization of PET degrading Bacterial Strain PRS8

PET degrading bacterial strain PRS8 was identified on the basis of microscopic examination, biochemical characteristics and molecular identification (16S rRNA gene sequence).

#### 3.4.1 Macroscopic and microscopic characterization

##### 3.4.1.1 Macroscopic examination

Bacterial strain PRS8 was grown on nutrient agar plates at 35°C for 16 hours and observed for colony morphology in terms of elevation, margin, shape and size.

##### 3.4.1.2 Microscopic examination (Gram's Staining)

**Principle:** Gram's staining was achieved to distinguish between a Gram-positive and Gram-negative because of the differences in the composition of cell membrane and cell wall. The gram-positive bacteria have a mesh and cross-linked peptidoglycan

layer which holds the crystal violet dye (Primary dye) after the mordant, iodine has been applied. The peptidoglycan layer develops a crystal violet and iodine (CV-I) complex. When ethanol is used the CV-I complex resides inside the high cross-linked peptidoglycan and gives the cell purple colored appearance. In the gram-negative bacteria, the thick peptidoglycan layer is missing and the structure of peptidoglycan is not as tightly packed as in gram-positive. So, with the application of CV-I complex, it is not trapped within the cell membrane and the decolorizer, ethanol removes the primary dye leaving it colorless. The secondary dye, safranin is applied to stain, making the gram negative cells appear pink.

***Gram's staining procedure:*** A drop of normal saline was placed on a sterile glass slide. A colony of strain PRS8 was placed on the drop and a smear was prepared by spreading colony on the slide. Strain PRS8 was heat-fixed by passing the slide through the flame 3-4 times, then allowed to cool before staining. The smear was stained for 2 minutes with crystal violet and carefully rinsed for 2 seconds with tap water. Afterward, the slide was saturated with Gram's iodine for 2 minutes and then gradually cleaned with tap water. Drop by drop ethanol was added to the slide to decolorize for 10-15 seconds until it runs clear. The slide was then saturated for 2 minutes with safranin counterstain, washed off with tap water until no color appeared. The slide was dried with absorbent paper and observed under 100X lens using light microscope.

### **3.4.2 Biochemical identification**

#### **3.4.2.1 Catalase test**

***Principle:*** Catalase was the first bacterial enzyme, described by Gottstein in 1893. To detect the presence of enzyme catalase in bacteria, a test is performed called a catalase test. The catalase test helps differentiate between catalase-negative *Streptococcaceae* from catalase-positive *Micrococcaceae*. This test is also useful in the speciation of certain gram-negative organisms from gram-positive organisms.

***Procedure:*** In the center of sterile glass slide, a loop-full of 14 hours fresh culture of strain PRS8 was mixed with a drop of 3% hydrogen peroxide. The slide was observed for bubble formation. The formation of bubbles indicated the presence of catalase,

which was observed as positive strain. Entire protocol was performed inside a laminar flow hood.

#### 3.4.2.2 Oxidase test

**Principle:** Use of dimethyl-*p*-phenylenediamine dihydrochloride solution to detect the presence of oxidase enzyme. The protocol was first described by Gordon and McLeod in 1928. If an organism contains enzyme cytochrome oxidase the color reagent is oxidized to a colored product. The enzyme cytochrome oxidase is required during the final stage of bacterial respiration for catalyzing the oxidation of cytochrome and reduction of oxygen thus forming water. These reactions take place at the electron transport chain.

**Procedure:** In order to observe oxidase enzyme activity, N,N-dimethyl-*p*-phenylenediamine oxalate was used as agent. 3 drops of freshly prepared reagent were transferred on a sterile filter paper (Whatmann No. 1). A colony of PET degrading bacterial strain PRS8 was picked through sterilized loop and placed over the filter paper surface. After 20 seconds, the positive result was noted as changed of color from pink to purple and then dark purple.

#### 3.4.2.3 Triple sugar iron test (TSI)

**Principle:** Kohn and Krunweide in 1917 modified Russell's double sugar by addition of a third sugar sucrose. Addition of sucrose allowed the detection of coliform bacteria that have the ability to ferment glucose more rapidly than lactose. TSI medium is used for detection of bacteria to ferment carbohydrate and produce hydrogen sulphide gas. TSI medium is composed of three different carbohydrates that are sucrose (1%), glucose (0.1%) and lactose (1%). For identification of gram-negative bacteria and especially *Enterobacteriaceae*, most frequently used medium is TSI. pH indicator present in this medium is phenol red. TSI agar is prepared as slants, which is aerobic, whereas butt is anaerobic. Drop in pH results as carbohydrate is fermented causing change in the color of medium from reddish orange to yellow. Whereas alkalization of peptone results in a deep red color. Production of black insoluble precipitates indicates production of hydrogen sulphide gas.

**Procedure:** TSI agar slants were prepared aseptically in a test tube. A colony of strain PRS8 was picked with the help of sterilized inoculating needle from a fresh 15 hours grown culture plate. TSI agar medium was inoculated first by stabbing the butt of agar to the bottom and without withdrawing the needle from test tube. Afterward, slant was streaked and incubated at 35°C for 24 hours. After incubation, the color of the slant changed from red to yellow, indicating carbohydrate fermentation.

#### 3.4.2.4 Urease test

**Principle:** In 1875 Reoch hypothesized that alkaline fermentation of urine resulted in production of ammonia by the action of microorganisms. Urease test is particularly used for identification of microorganisms that have ability to produce carbon dioxide and ammonia by hydrolyzing urea. Urease test is used to distinguish *enterobacteriaceae* from urease positive protease. Urease enzyme is produced constitutively by bacteria and breaks down CO<sub>2</sub> and ammonia. In urease test media (urea broth), phenol red is used as an indicator. Production of ammonia elevate the pH of media and color of indicator changes from yellow to bright pink as pH changes from 6.8 to 8.2. Urea agar contains both glucose and peptones.

**Procedure:** The primary objective of a urease test is to determine if a bacterium will degrade urea. Ammonia and carbon dioxide are produced when urea is degraded. A 40 % urea solution was prepared. It was transferred to urease broth and phenol red was used as an indicator. PRS8 bacterial strain was inoculated in the broth and incubated at 35°C for 24 hours. Based on ammonium carbonate formation, bacterial strain PRS8 showed positive result in pink-red color using phenol red dye as indicator.

#### 3.4.2.5 MacConkey Agar Test

**Principle:** MacConkey agar is a type of differential and selective medium, which is useful for the isolation of *Enterobacteriaceae*. The ability to distinguish enteric bacteria is by their capacity to ferment lactose. A pH indicator, neutral red is present, which appears red when the pH decreases below 6.9 and changes its color to colorless when pH increases above 6.9. The lactose fermenting bacterial isolates will appear pink in the presence of neutral red indicator. This shows that the bacterial isolate is a



lactose fermenter and the environment is acidic (pH below 6.9) by the leeching of bile salts in the medium around the bacterial colonies. In contrast to the non-lactose fermenters, the pH becomes basic and the bacterial colonies appear normal colored to colorless.

**Procedure:** MAC agar (5g) was weighed and added into distilled water (100mL). After autoclaving, the medium was poured into the petri dishes under sterile conditions. The MAC plates were streaked with overnight culture of bacterial strain PRS8 and incubated at 35°C for 24 hours. Bacterial strain PRS8 showed colorless to pink colonies, which deduced that they are non-lactose fermenting bacteria.

#### 3.4.2.6 Indole Test

**Principle:** Indole test is used for identification of bacteria that have the ability to degrade amino acid tryptophan and assemble indole. This test is a part of class of tests known as IMViC that is used in differentiating members of *Enterobacteriaceae* family. Bacteria that produce tryptophanase enzyme undergo deamination and hydrolysis of amino acid tryptophan. Indole is produced as a key product of tryptophan metabolism in addition with pyruvic acid and ammonia. Chemical reaction between indole and the Kovac's reagent *p*-dimethylaminobenzaldehyde (DMAB) produce red dye rosindole under acidic condition

**Procedure:** Trypton broth was prepared and autoclaved prior to inoculation. The tryptophan broth was inoculated with overnight culture of the bacterial strain PRS8 and incubated at 35°C for 24 hours. After incubation, 3 to 5 drops of Kovac's reagent were added to the inoculated test tubes using a sterilised dropper to observe indole formation. With the addition of reagent, pink to the cherry red ring in the reagent layer was observed in few seconds.

#### 3.4.2.7 Citrate Utilization Test

**Principle:** Citrate test is used to identify bacterial isolates that have the ability to employ citrate as an alternative carbon and energy source. Citrate metabolism results in the generation of alkaline by products resulting an increase in pH of medium. Citrate test is also used to identify gram-negative pathogens. Upon uptake, citrate lyase enzymes hydrolyses citrate yielding oxaloacetate and acetate. Oxaloacetate in

turn is metabolized to carbon dioxide and pyruvate. Production of sodium carbonate increases the pH and color of bromophenol blue changes from forest green to blue at pH above 7.6.

**Procedure:** The Simmons citrate agar slant was prepared in the sterilized test tube. The slant was streaked in a zig-zag pattern with freshly overnight culture of the bacterial strain PRS8 and incubated at 35°C for 24 hours. The color change from green to blue in the slants was observed after a period of incubation.

### 3.4.3 Molecular Identification of Bacterial Strain PRS8

#### 3.4.3.1 Genomic DNA extraction

The genomic DNA from strain PRS8 was extracted using DNA extraction kit (Eco-Pure-Genomi, Product Code # E1075) and evaluated by NanoDrop for concentration and purity (Thermo Scientific, 2000).

The bacterial strain PRS8 was cultured in Luria Bertani (LB) broth at 35°C for 24 hours. The fresh culture was transferred to 1.5 mL micro-centrifuged tube at 8000 rpm for 3 minutes. The pellet was re-suspended in 200 µL Eco-Pure re-suspension buffer and vortexed until no bacterial cells clumps remain. About 200 µL lysis buffer and 20 µL lysozyme solution was added and incubated for 5 minutes at room temperature. After incubation, 20 µL of RNase A and proteinase K was added to the mixture and again incubated in water bath at 55°C for about 45 minutes. After incubation, 400 µL of binding buffer was added and mixed in the Eppendorf tube. The mixture was shifted into the mini spin column (in a 2 mL collection tubes) and centrifuged at full speed, 14000 rpm for 60 seconds and the obtained flow through was discarded. The mini spin column was again kept in a fresh 2 mL tube and 500 µL of wash buffer 1 was added. The column was again centrifuged at 14000 rpm for 1 minute and flow through was discarded. The mini spin column was again placed in a new 2mL tube and 500 µL of wash buffer 2 was added. The column was again centrifuged at 14000 rpm for 1 minute and flow through was discarded. The mini spin column was transferred to a new 1.5 mL Eppendorf tube and 50 µL elution buffer was added and incubated for 5 minutes. Subsequently, the mini spin column in 1.5 mL Eppendorf tube was again centrifuged at 13000 rpm for 3 minutes to elute the DNA. The purified DNA obtained was stored at -20°C further analysis.

### 3.4.3.2 Preparation of Agarose Gel and Confirmation of Genomic DNA

About 1g agarose was added into 100 mL TBE buffer 1X (40 mM Tris buffer, 40 mM Boric acid, 1 mM EDTA and 40 mM Tris buffer) and boiled in microwave oven for 1 min at high speed to dissolve it completely. The flask containing agarose solution was cooled down to room temperature and then 5  $\mu$ L GelRed nucleic acid stain was added. The gel was poured into the gel tray (Bio-Rad) and a comb was placed for generation of wells. The gel tray was left undisturbed at room temperature for 15 minutes for solidification. DNA sample was prepared by adding 4  $\mu$ L of DNA into 1  $\mu$ L loading dye (Blue/Orange, promega). 3 $\mu$ L of DNA sample was loaded and the power supply turned on with volatage 90V and 400mA for 50 minutes. 1% agarose gel containing ethidium bromide was used to validate PCR product amplification. The band was then visualized by comparing it with DNA ladder (1 kb, GeneRuler™) and photograph was taken on a Bio-Rad Gel Doc imaging system (Universal Hood 2 – S.N. 76S/ 0.4186).

### 3.4.3.3 Phylogenetic analysis

The 16S rRNA region of genomic DNA was amplified using universal primers: F-(ATTCTAGAGTTTGATCATGGCTCA) and R-(TACACACCGCCCGTCACACGGTACCAT). The PCR mixture contained 1  $\mu$ L of each primer (10 mM), 10  $\mu$ L of Go-Taq buffer, 3  $\mu$ L of MgCl<sub>2</sub> (25 Mm), 1  $\mu$ L of dNTPs (10 mM), 0.5  $\mu$ L of Taq polymerase, 1  $\mu$ L of DNA template and 32.5  $\mu$ L of deionized water. PCR was carried out for amplification of 16S gene. The temperature cycles were for DNA denaturation at 95 °C for 3 minutes, annealing at 55 °C for 1 minute, and extension at 72 °C for 1 hour and 40 seconds per cycle for a total of 36 cycles. The reaction mixture was incubated at 72 °C for 7 minutes for the final elongation. 1% agarose gel containing ethidium bromide was used to validate PCR product amplification, and results were evaluated using a Bio-Rad Gel Doc imaging system (Universal Hood 2 – S.N. 76S/ 0.4186). The 16S rRNA sequence of our strain was determined using ezbiocloud program (<https://www.ezbiocloud.net/>) and sequences showing similarity index >95% were downloaded and aligned using BioEdit 7.2 software. A phylogenetic tree was constructed with the help of MEGA-X software using Neighbor-Joining method (Kumar et al., 2018).

### 3.5 Biofilm Assay for Bacterial Strain PRS8

#### 3.5.1 Congo red agar

The biofilm formation ability of PET degrading *Stenotrophomonas maltophilia* PRS8 was checked on brain heart infusion (BHI) agar plate supplemented with sucrose and using congo red dye as indicator (Table 3.2). The BHI agar plate was inoculated with strain PRS8 and incubated at 35°C for 48 hours.

**Table 3.2:** Composition of BHI agar

Constituents	g/L
BHI agar	52
Sucrose	36
Congo red dye	0.8

#### 3.5.2 Microtitre Plate Assay

Plastics-degrading bacteria need to attach to the surface of polymer for the purpose of its degradation. It tends to develop biofilm on polymer surface and enable the bacteria for efficient utilization of non-soluble polymer (Hadar and Sivan, 2004). A modified biofilm assay was performed to assess the potential of *Stenotrophomonas maltophilia* PRS8 to develop biofilms on the surface of PET pieces (Satti et al., 2017). Sterilized PET films were added to the wells of a microtiter plate. Plastic pieces (2 cm x 2 cm) from a disposable PET water bottle were sterilized by dipping in 70% ethanol for 30 minutes and rinsed twice with deionized water to remove any residual ethanol and placed under UV for 5 minutes.

Strain PRS8 was inoculated into wells of microtiter plate with pre-sterilized PET pieces and incubated at 35°C for 48 hours. A positive (biofilm-producing *Pseudomonas aeruginosa*) and a negative control (uninoculated wells) were run in parallel. After incubation, PET pieces were transferred into clean Eppendorf tubes and washed gently with sterilized deionized water three times. The microtiter plate and PET pieces were stained with 300 µL of 0.5% crystal violet for 15 minutes, and then washed three times with water. After air-drying, the plates and pieces were de-stained

with 30% acetic acid for 15 minutes and then transferred into clean microtiter plates. The microtiter plate and PET pieces were examined for biofilm using ELISA reader (Bio-Tek, Model EL 4308) at 600 nm.

### 3.6 Evaluation of Bacterial Hydrophobicity

The BATH (Bacterial adherence to hydrocarbons) assay, focus on the capacity of bacterial cells to adhere to the hydrocarbons such as hexadecane. Bacterial cells that are more hydrophobic have a stronger attraction for the hydrocarbon, which causes them to move from the aqueous suspension to the organic phase, reducing the turbidity of the culture as a result (Rosenberg et al., 1980).

For the Bacterial adherence to hydrocarbons (BATH) assay, In nutrient broth, *Stenotrophomonas maltophilia* PRS8 was grown to the mid-logarithmic phase, it was then subjected to centrifugation and washed (twice) with phosphate, urea, magnesium and sulphate (PUM) buffer (Table 3.3). The cells were suspended in PUM buffer until reaching an optical density (OD400) value ranging from 1.0 to 1.2. 1.2 mL of suspension was shifted to a number of test tubes and then Hexadecane was added to the tubes with an increasing volume (range 0.08-0.4 mL). The test tubes were kept in a shaker for 10 minutes and then allowed to stand for 2 minutes to facilitate phase separation. After the phase separation, the optical density was measured at 400nm. Cell-free buffer was served as a blank.

**Table 3.3:** PUM Buffer composition

Constituents	g/L
Urea	1.8
KH <sub>2</sub> PO <sub>4</sub>	7.26
K <sub>2</sub> HPO <sub>4</sub>	17
MgSO <sub>4</sub> ·7H <sub>2</sub> O	0.2

### 3.7 Qualitative Screening of Cutinase by *Stenotrophomonas maltophilia* PRS8

#### 3.7.1 Polycaprolacton Agar for cutinase activity

Polycaprolactone (PCL) agar plate was used to examine the hydrolytic activity of cutinase from *Stenotrophomonas maltophilia* PRS8 by the method as described previously (Adiguzel and Tuncer, 2017). The composition of PCL agar medium (g/L) was: [Peptone, 10; CaCl<sub>2</sub>.2H<sub>2</sub>O, 0.1; NaCl, 5; PCL, 1; agar-agar, 20]. About 0.5g of PCL was dissolved in 50 mL of acetone by sonication for 15 minutes to ensure homogeneity and then mixed with sterilized nutrient agar medium at final concentration of 0.1% (w/v). The medium was poured into the petri plates to make Polycaprolacton Agar Plates. Plates were inoculated with *S. maltophilia* PRS8 and incubated at 35°C for 48 hours. The plates were observed after incubation for clear zones around colonies that will indicate production of polyesterase enzyme by strain PRS8.

#### 3.8 Extracellular Protein Determination

Total proteins were determined by the method as previously described by Lowry et al. (1951). Protein was estimated by adding 1 mL sample and 1 mL solution D in a test tube by incubating at room temperature for 10 minutes. After incubation, 100 µL solution E was added and again incubated in dark at room temperature for 30 minutes. Absorbance was estimated at 650 nm. The composition of reagents is following:

##### **Reagents:**

Solution A (Na<sub>2</sub>CO<sub>3</sub> in 0.1 N NaOH, 2 %)

Solution B (potassium sodium tartrate, 1 %)

Solution C (CuSO<sub>4</sub>. 5H<sub>2</sub>O, 0.5 %)

Solution D (A+B+C = 48:1:1)

Solution E (Folin phenol + water = 1:1)

##### **Preparation of solution A**

Solution A was prepared by adding 4 g NaOH to 900 mL distilled water and dissolved properly. 20 g Na<sub>2</sub>CO<sub>3</sub> were added to the solution and made the final volume 1000 mL.

***Preparation of Solution B***

Solution B was prepared by adding 1 g potassium sodium tartrate into distilled water and

made the final volume 100 mL.

***Preparation of solution C***

Solution C was prepared by adding 0.5 g  $\text{CuSO}_4 \cdot 5\text{H}_2\text{O}$  into distilled water and made the final volume 100 mL.

***Preparation of solution D***

Solution D was prepared by mixing the solution A, B and C with following ratio: 48 ml solution A, 1 ml solution B, 1 ml solution C

***Preparation of solution E***

It is formed by combining Folin Phenol and water in a 1:1 ratio. Because it is light sensitive and cannot be stored, it was produced fresh.

**3.8.1 Standard stock solution of Bovine Serum Albumin procedure:**

In Lowry's method, copper and protein peptide bonds react in an alkaline environment to form  $\text{Cu}^+$ , which then interacts with the Folin reagent to produce a vibrant blue colour. 1 mL of test sample (supernatant) was mixed with 1 mL of solution C, shaken and was incubated for 10 minutes at room temperature. Then 0.1 mL of solution D was added to the reaction tube in dark condition and after shaking it was incubated for 30 minutes in dark. Absorbance was measured via spectrophotometer at 650 nm.

**3.8.2 Standard curve development:**

Bovine serum albumin (BSA) Stock solution was prepared with a concentration of 1mg/mL. Stock solution was diluted as given in table 3.4 and analyzed for protein estimation. The values were plotted in Microsoft Excel and a graph was plotted. A trend line was added to the graph and a formula was derived from the slope of graph for measuring unknown value of released sugars (Fig. 3.1).

**Table. 3.4:** Standard curve development for bovine serum albumin

<b>Test Tube #</b>	<b>Distilled Water (mL)</b>	<b>BSA Stock Solution (mL)</b>	<b>Protein Conc. (mg/mL)</b>	<b>Absorbance</b>
1	0.00	1	1	0.987
2	0.1	0.9	0.9	0.901
3	0.2	0.8	0.8	0.836
4	0.3	0.7	0.7	0.746
5	0.4	0.6	0.6	0.632
6	0.5	0.5	0.5	0.564
7	0.6	0.4	0.4	0.423
8	0.7	0.3	0.3	0.307
9	0.8	0.2	0.2	0.266
10	0.9	0.1	0.1	0.112
11	1	0.00	0.00	0



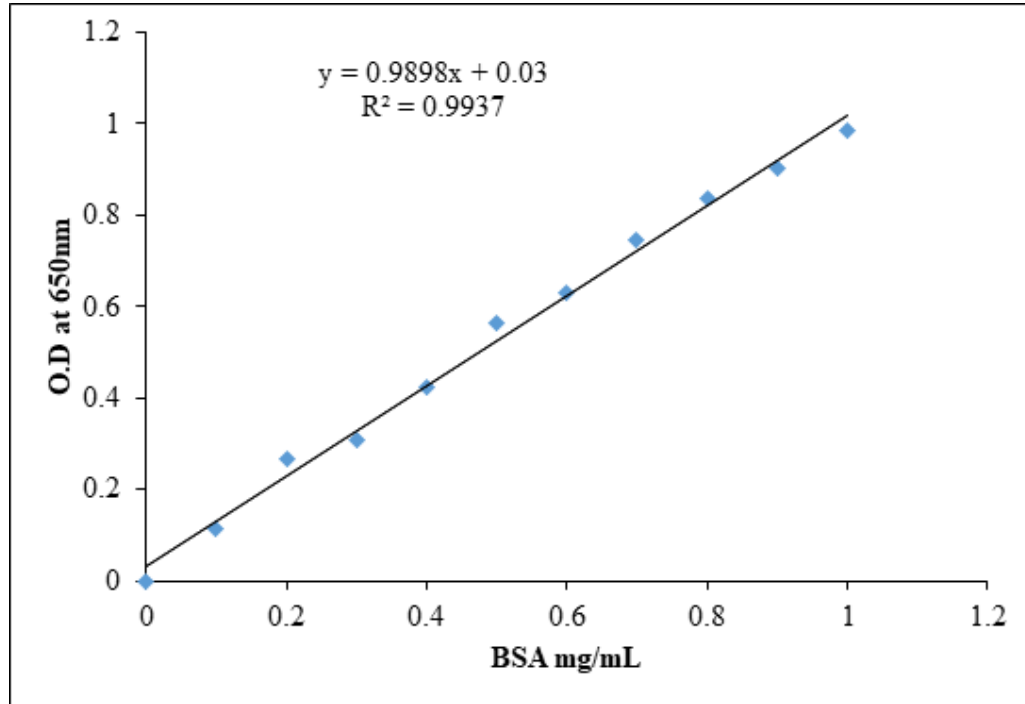


**Fig. 3.1:** Standard curve development for bovine serum albumin (BSA)

Formula:  $Y = 0.989x + 0.03$  was resulting from the slope of graph where X= Optical density of unknown protein in sample and Y= Concentration of known protein in known sample of BSA.

### 3.9 Reagents for Enzyme Assay

Following reagents were used in cutinase experiment; 100 mM Phosphate buffer with pH 8.0, Triton X-100 0.4%, 12mM 4-nitrophenyl butyrate (*p*NPB), culture supernatant.

#### 3.9.1 Stock preparation of substrate

A stock solution of (12 mM) *p*-nitrophenyl butyrate (*p*-NPB) was prepared in isopropanol for enzyme assay with the following composition: *p*-NPB 50  $\mu$ L was added to 50 mL of isopropanol and store at  $-20\text{ }^{\circ}\text{C}$  for further analysis.

#### 3.9.2 Potassium phosphate buffer

100mM potassium phosphate buffer (pH 8.0) was prepared by dissolving 13.6g  $\text{KH}_2\text{PO}_4$  and 17.4g  $\text{K}_2\text{HPO}_4$  in distilled water and made the final volume 1000 mL.

### 3.9.3 Standard curve development for *p*-nitrophenol (*p*NP)

*p*-nitrophenol (*p*NP) stock solution was prepared with a concentration of 1 mg/mL. Stock solution was diluted as given in table 3.5 and analyzed for phenol estimation. The values were plotted in Microsoft Excel and a graph was formed. A trend line was added to the graph and a formula was derived from the slope of graph for measuring unknown value of released *p*-nitrophenol (Fig. 3.2).

**Table. 3.5:** Standard curve development for *p*-nitrophenol (*p*NP)

Test Tube #	Distilled Water (mL)	<i>p</i> NP Stock Solution (μL)	<i>p</i> NP Conc. (μg/mL)	Absorbance
1	0.00	100	100	0
2	0.1	90	90	0.0506
3	0.2	80	80	0.1161
4	0.3	70	70	0.18514
5	0.4	60	60	0.2633
6	0.5	50	50	0.3297
7	0.6	40	40	0.4008
8	0.7	30	30	0.4636
9	0.8	20	20	0.514
10	0.9	10	10	0.5761
11	1	0.0	0.0	0.6664

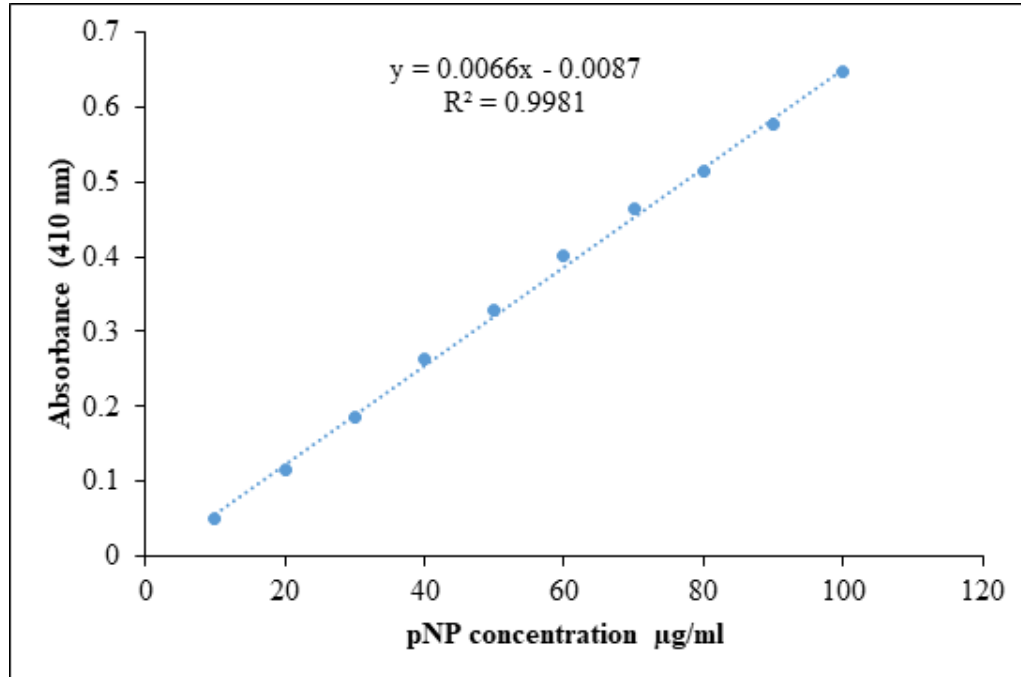


**Fig. 3.2:** Standard curve development for *p*-nitrophenol (*p*NP)

### 3.10 Biodegradation of PET by *S. maltophilia* PRS8

The bacterial strain *S. maltophilia* PRS8 was selected to be used for PET degradation. Plastic pieces (2 x 2 cm) from a disposable PET water bottle were sterilized by dipping in 70% ethanol for 30 minutes and washed twice with autoclaved distilled water to remove any residual ethanol and placed under UV for 5 minutes. About 2 mL of the overnight grown culture of *S. maltophilia* PRS8 in nutrient broth was centrifuged for 10 minutes at 10,000×g and the pellet was re-suspended in 500 µL normal saline (g/L) [NaCl, 9]. The sterilized PET water bottle pieces were added to 100 mL mineral salt medium (MSM) in Erlenmeyer flask and inoculated with cells of strain PRS8. A control with PET pieces in bacteria free MSM was run in separate. The flasks were incubated in shaker incubator at 35 °C and 150 rpm for 28 days. After every one week, one PET piece was recovered to analyze weight loss and other pieces were transferred aseptically to fresh MSM in another flask with 1 mL culture from the previous flask and incubated at 35°C and 150 rpm for another week. After every 48 hours 2 mL sample was taken for enzyme assay and protein estimation. Four

consecutive shifts were performed to serially enrich the potential PET degrading bacteria in the medium. Biodegradation was evaluated utilizing analytical techniques such as FTIR, and SEM, and percentage weight loss assessment by the end of the experiment.

### **3.10.1 Quantitative assay for total protein and cutinase activity from degradation experiment**

Samples were collected from degradation experiment after every 48 h and centrifuged at 10,000×g for 10 minutes at 4°C. The supernatant was assayed for cutinase activity using *p*-nitrophenyl butyrate (*p*-NPB) (12 mM) as substrate. 20 µL *p*-NPB was added to 1.38 mL of phosphate buffer (pH 8.0) with 0.2 mL of Triton X-100 and incubated in water bath at 40°C for 10 minutes for the removal of turbidity. 200 µL of the enzyme solution was added to the reaction mixture and again incubated in water bath at 37 °C for 1 hour. Finally, the reaction was stopped by incubating at -20 °C for 15 min and absorbance was measured at 410 nm. The reaction mixture without enzyme solution was used as blank. The *p*NP standard curve was plotted to calculate the amount of *p*-nitrophenol released as a result of enzymatic hydrolysis of substrate (Zhang et al., 2010). The protein concentration was estimated using bovine serum as standard (Lowery et al., 1951).

#### ***Enzyme Activity per Unit***

One unit of the enzyme was the quantity of enzyme necessary to release 1 mole of *p*-nitrophenol in 1 minute.

#### ***Specific Activity of Enzyme***

The specific activity of the enzyme was measured by dividing PET cutinase activity with the protein concentrations.

$$\text{Specific Activity (U/mg)} = \text{Enzyme Activity} / \text{Sample protein contents}$$

## **3.11 Analysis of Degradation of PET by *S. maltophilia* PRS8**

### **3.11.1 Determination of dry weight of residual PET**

PET pieces were recovered after incubation and re-suspended in 2% aqueous solution (v/v) of sodium dodecyl sulphate for 15 minutes in order to remove *S. maltophilia* PRS8 biofilm from their surface. They were then incubated for 4 hours at 50°C and

further washed with warm distilled water (Orr et al., 2004). After incubation, PET pieces were again rinsed with distilled water, dried overnight at 60°C and then weighed (Kyaw et al., 2012).

$$\text{Percentage of weight loss} = [(Initial\ weight - Final\ weight)/Original\ weight] \times 100.$$

### 3.11.2. Fourier-transform Infrared (FT-IR) Spectroscopy

PET pieces were analyzed for changes in functional groups after incubation with *S. maltophilia* PRS8 through Fourier-transform Infra-red (FTIR) Spectroscopy. The spectra of treated PET pieces were recorded in a frequency range 4000–400 cm<sup>-1</sup> wavenumber at a resolution of 4 cm<sup>-1</sup> at ambient temperature with a helium–neon laser lamp as a source of IR radiation. Abiotic control sample was run concurrently with test samples for comparison.

### 3.11.3. Scanning Electron Microscopy (SEM)

The changes in surface morphology of the PET pieces after incubation with *S. maltophilia* PRS8 was determined using a scanning electron microscope model JSM-IT100. The pieces were carefully rinsed for a few min with 2 % (v/v) aqueous SDS and distilled water, then flushed with ethanol (70%) to remove the cells and associated biofilm from the surface and finally gold-painted on copper stubs. To increase the conductivity of the samples, gold plating was done in a vacuum by evaporation. PET piece from control was examined alongside the test sample for comparison.

PET degradation by whole cell was performed up till this point, which is a more natural approach used by researchers. Now to get more precise and efficient degradation of PET, we employed an enzymatic approach using cutinase enzyme and cutin as a substrate. Cutin is not available commercially, it was extracted from tomato peel.

## 3.12 Cutin Extraction from tomato peel

### *Chemicals for cutin extraction:*

- Oxalate buffer (pH 3.5)

- Oxalic acid, 4g/L
- Ammonium oxalate, 16g/L
- Chloroform: Methanol (2:1)

Tomato was purchased from Kohsar Market F-6 Islamabad. The tomato peels were initially washed with distilled water to remove the pulp or any contaminants. The peels were sliced into small pieces and dried at 60°C for 12 hours in dry oven. The dried peels were added into boiling oxalate buffer pH 3.5 for 1 hour to remove any pectinaceous material. The peels were then filtered using cheesecloth. The resulting material was rinsed with distilled water multiple times to remove any residue of pectinaceous material and again dried at 60°C for 12 hours. The dried material is treated with a solution of chloroform and methanol with a ratio (2:1) and incubated in shaking incubator at 150 rpm at 30°C for 12 hours to yield dewaxed cutin. After incubation, the upper plastic-like thin layer was recovered and treated with pectinase (4000 PGNU/mL) and cellulase (1500 FPU/mL) in sodium acetate buffer (50 mM) at pH 4.5 at 60°C for 8 hours with continues agitation, and then filtered, washed and oven dried. The methanol: chloroform extraction step was repeated. The resulted material was dried in vacuum oven at 60°C and ground in a mortar and pestle and converted to powder to be utilized.

### 3.13 Standardization of Cutinase Assay Conditions

#### 3.13.1 Enzyme production media

The enzyme production medium consisted of the following composition (g/L); [Glucose, 10; FeSO<sub>4</sub>.7H<sub>2</sub>O, 0.01; K<sub>2</sub>HPO<sub>4</sub>, 1; MgSO<sub>4</sub>.7H<sub>2</sub>O, 0.5; KCL, NaNO<sub>3</sub>, 2;0.5; and Cutin, 4]. *S. maltophilia* PRS8 was grown in nutrient broth for 24 hours. Afterwards 6% of inoculum was added in 70 mL of growth medium in a 250 mL of Erlenmeyer flask and then incubated at 35°C at 150 rpm. Samples were taken after every 24 hours and centrifuged at 10,000 rpm for 10 minutes at 4 °C for enzyme assay.

#### 3.13.2 Optimization of Temperature for enzyme assay

Temperature optimization was carried out at different temperatures (20-60°C). 2 mL sample was centrifugation at 10,000 rpm for 10 minutes at 4°C. Enzyme assay

mixture was incubated at different temperatures and activity was calculated in term of U/mL.

### **3.13.3 Optimization of pH for enzyme assay**

pH optimization was carried out through enzyme assay at different pH ranges (5.0-10.0). Supernatant was obtained after centrifuging the samples at 10,000rpm for 10 minutes. Enzyme assay mixture was incubated at different pH and activity was calculated in term of U/mL.

### **3.13.4 Optimization of substrate concentration for enzyme assay**

Substrate optimization was carried out for enzyme assay using different concentration of substrate, ranging from 20 to 100  $\mu$ L. Supernatant was obtained after centrifuging the samples at 10,000rpm at 4°C for 10 minutes. Enzyme activity was calculated in term of U/mL.

### **3.13.5 Optimization of enzyme solution concentration for enzyme assay**

Enzyme solution optimization was carried out for enzyme assay using different concentration of enzyme solution, ranging from 20 to 100  $\mu$ L. Supernatant was obtained after centrifuging the samples at 10,000rpm at 4°C for 10 minutes. Enzyme activity was calculated in term of U/mL.

### **3.13.6 Optimization of incubation time for enzyme assay**

Time of incubation was optimized for enzyme assay using different time intervals ranging from 10 to 60 minutes. Samples were centrifuged and supernatant was collected. Enzyme activity was calculated in term of U/mL.

## **3.14 Optimization of Physico-chemical Parameters for Cutinase Production from *S. maltophilia* PRS8**

The submerged fermentation method was used in order to optimize various growth conditions such as temperature pH, incubation time, inoculum size and nutrients for bacterial strain *S. maltophilia* PRS8 for maximum cutinase production.

### 3.14.1 Preparation of Inoculum

*S. maltophilia* PRS8 was freshly cultured in nutrient broth with 0.4% cutin and incubated in a shaking incubator at 150rpm at 35°C for 24 hours.

### 3.14.2 Effect of temperature

The effect of temperature on production of cutinase was determined by growing *S. maltophilia* PRS8 at a wide range of temperature (25-45°C). The samples were taken after every 24 hours maximum up to 96 hours and centrifuged at 10,000 rpm for 10 minutes at 4°C. Supernatant was collected and processed for enzyme assay and protein estimation assay as described previously (section 3.11.1).

### 3.14.3 Effect of pH

The effect of pH on cutinase production was determined by incubating strain PRS8 in production medium having a wide range of pH (5.0-10.0). The samples were taken after every 24 hours maximum up to 96 hours and centrifuged at 10,000 rpm for 10 minutes at 4°C. Supernatant was collected and processed for enzyme assay and protein estimation assay. Specific activity was expressed in the term of U/mg.

### 3.14.4 Effect of incubation time

The effect of incubation time on production of cutinase was calculated by growing *S. maltophilia* PRS8 for different time intervals (24-96 hours). The samples were taken after every 24 hours maximum up to 96 hours and centrifuged at 10,000 rpm for 10 minutes at 4°C. Supernatant was collected and processed for enzyme assay and protein estimation assay. Specific activity was expressed in the term of U/mg.

### 3.14.5 Effect of Inoculum size

The effect of inoculum size on production of cutinase was determined by inoculating different concentration of *S. maltophilia* PRS8 ranging from 0.1 to 3.0%. The samples were taken after every 24 hours maximum up to 96 hours and centrifuged at 10,000 rpm for 10 minutes at 4°C. Supernatant was collected and processed for enzyme assay and protein estimation assay. Specific activity was expressed in the term of U/mg.



### 3.15 Plackett Burman Design for optimizing of nutritional condition

Plackett Burman's Design (PBD) is a critical method for identifying nutritional elements that influence any given process (Patil and Jena, 2015). The PBD developed by Design Expert 10.1 software (Stat-Ease Inc. Minneapolis) was used to screen various dietary ingredients for optimum cutinase production from *S. maltophilia* PRS8. The design was mathematically modelled using the first-order polynomial equation listed below (Eq. 1).

$$Y = \beta_0 + \sum \beta_i X_i \quad (\text{Eq.1})$$

Where Y represents specific activity (U/mg) of cutinase of the predicted response;  $\beta_0$  exhibited the intercept;  $\beta_i$  linear coefficient of the model; while  $X_i$  described the level of independent variable. A total of 10 components were optimized by Plackett Burman design which included glucose,  $(\text{NH}_4)_2\text{SO}_4$ , sucrose,  $\text{NaNO}_3$ ,  $\text{K}_2\text{HPO}_4$ , Yeast Extract,  $\text{MgSO}_4 \cdot 7\text{H}_2\text{O}$ , KCl,  $\text{FeSO}_4 \cdot 7\text{H}_2\text{O}$ , Cutin and  $\text{Na}_2\text{HPO}_4$ . The effect of these variables was studied on two levels. Table 2 of the Design Expert 7 software showed a total of 15 sets of experimentation with varying chemical ingredient concentrations. The fermentation was conducted at 35°C and 150 rpm. The crude enzyme activity was determined after 24 hours intervals up to maximum 72 hours and results were recorded in order to find out specific activity (U/mg) of cutinase. The significant factors were determined by evaluating the results and factors with  $p$ -value <0.05 were considered as significant and further analyzed by Central Composite design.

### 3.16 Central Composite Design (CCD) Experiment

Further analysis was conducted through Central Composite design (CCD) on the significant factors derived from the PBD to achieve a more extended optimization. These factors increased the enzyme yield. Each factor's significant impact on the enzyme activity and enhanced productivity as they interact with each other was assessed. Three significant factors (cutin,  $\text{NaNO}_3$ ,  $(\text{NH}_4)_2\text{SO}_4$ ) derived from PBD were further analyzed through second order polynomial equation and multiple regressions in order to achieve a more extended optimization for high enzyme yield. The effect of independent factors such as linear, quadratic, and mutual interactions on the dependent variable enzyme specific activity (U/mg) was investigated. The

mathematical relationship between the dependent variable and the significant independent variable is represented by the quadratic polynomial equation provided:

$$Y = \beta_0 + \sum_{i=1}^6 \beta_i X_i + \sum_{i=1}^6 \beta_{ii} X_i^2 + \sum_{i < j=2}^6 \beta_{ij} X_i X_j \quad (\text{Eq.2})$$

In this equation  $Y$ ,  $X_i$ ,  $\beta_i$ ,  $\beta_{ii}$ ,  $\beta_{ij}$ ,  $\beta_0$  are representing the specific activity, significant independent variables, coefficients for linear, interaction, quadratic, and regression, as well as a constant term, respectively. ANOVA was used to assess the model's feasibility (Siewe et al., 2021).

### 3.17 Bulk production of crude Cutinase

1000 mL production medium was prepared in 2 L Erlenmeyer flask with the following composition; (g/L) [Glucose, 13.0;  $(\text{NH}_4)_2\text{SO}_4$ , 5.5; sucrose, 11.0;  $\text{NaNO}_3$ , 11.0; Yeast Extract, 3.0;  $\text{K}_2\text{HPO}_4$ , 2.0;  $\text{MgSO}_4 \cdot 7\text{H}_2\text{O}$ , 2.0; KCl, 3.0; cutin, 9.0;  $\text{Na}_2\text{HPO}_4$ , 3.0; and pH 8.0]. The medium was inoculated with 2% of 16 hours fresh culture of *S. maltophilia* PRS8 and incubated in shaker incubator at 35 °C and 150 rpm for 48 hours. The cell free supernatant with crude cutinase was collected after centrifugation at 10,000×g for 10 minutes at 4 °C and further processed for enzyme purification.

### 3.18. Purification of Cutinase from *S. maltophilia* PRS8

#### 3.18.1 Ammonium sulfate precipitation

The production medium was subjected to centrifugation for 10 minutes at 10,000 rpm to get cell-free mixture. The required amount of ammonium sulfate was calculated via online calculator of EnCor Biotechnology Inc. Initially 10% ammonium sulfate was slowly added to the flask containing cell free supernatant (CFS) using magnetic stirrer at 4°C and incubated for 12 hours. This solution was subjected to centrifugation at 10,000rpm for 10 minutes. The resulted pellet and supernatant were obtained separately. After that pellet was dissipated in phosphate buffer having pH 8.0. Subsequently protein estimation and enzyme assay of the resulted pellet and supernatant was carried out followed by measuring specific activity. The supernatant

collected earlier was then further subjected to 30%, 40%, 50%, 60%, 70% and 80% ammonium sulfate treatment using the same protocol described earlier. The fractions resulted from these variations were stored at 4°C. Precipitation of bulk amount of production medium was carried out with optimum amount of ammonium sulfate at which the enzyme activity was maximum.

### **3.18.2 Dialysis of crude enzyme**

After precipitation, the enzyme solution's that contained ammonium sulphate was eliminated by dialysis. The crude enzyme dissolved in 50 mL phosphate buffer (pH 8.0) was shifted to dialysis tube and then placed in the same buffer (2 L) at 4°C for 24 hours.

### **3.19 Protein purification by gel permeation (Sephadex G-100) column chromatography**

The principle of gel permeation chromatography is the separation of proteins based on their sizes (Determann, 2012).

**Procedure:** For this process Sephadex G-100 gel was prepared by appropriately mixing 2.3g of Sephadex G-100, 0.03g sodium-azide (antibacterial) and 0.03g fluconazole (antifungal) in 150 mL of phosphate buffer (pH 8.0) and incubated at 40°C for 24 hours. The gel perfectly swelled after incubation time, sodium-azide inhibits bacterial growth while fluconazole inhibits fungal growth. After thoroughly rinsing it with distilled water, the glass column was observed for leakage. Solution buffer and gel were sonicated for 30 minutes for degassing. After that, the column was meticulously filled with gel to avoid bubble formation. After loading gel, the column was left undisturbed for 24 hours at room temperature which resulted gel firmly packed in the column. The column flow rate was maintained to 0.33 mL/minute. The Sephadex column was loaded with 3 mL of partially purified enzyme, and then phosphate buffer was constantly added to keep the sample flow going. The fractions were collected and analyzed for total protein at 280 nm (UV light) The enzyme assay and protein estimation were carried out for all fractions. Fractions with high cutinase activity were pooled and then stored at 4°C for further analysis.

### **3.20 Molecular Weight Determination Through SDS-PAGE**

The molecular weight of cutinase enzyme was determined by the method as previously described by Laemmli, (1970).

#### **3.20.1 15% Resolving gel preparation**

For a single resolving gel preparation, distilled water (1.87 mL), 30% acrylamide (3.75 mL), 1.5 M Tris-HCl (1.87 mL) (pH 8.8), 10% SDS (75  $\mu$ L), TEMED (8  $\mu$ L) and 10 % APS (75  $\mu$ L) was carefully mixed. Following that, the gel was immediately poured into the gel assembly, leaving 0.5 inches open for gel stacking. After that 100  $\mu$ L distilled water/isopropanol were added to remove oxygen bubble that inhibits gel polymerization. To achieve full polymerization, the gel was kept at room temperature for 30 minutes.

#### **3.20.2 8% Stacking gel preparation**

For preparation of a single 8% Stacking gel: - 10% SDS (25  $\mu$ L), 30% polyacrylamide gel (400  $\mu$ L), 1M Tris-HCl (pH 6.8) (700  $\mu$ L), TEMED (5  $\mu$ L), distilled water (2 mL) and 33.5  $\mu$ L APS was carefully mixed and poured above the resolving gel. The comb was inserted inside the gel for the formation of wells. Then the gel was left for about 30 minutes at room temperature for complete solidification.

#### **3.20.3 Cutinase treatment**

Before loading the sample, 15  $\mu$ L of cutinase enzyme was mixed with 5  $\mu$ L of loading dye and warmed for 10 minutes at 98°C and then placed at ice box for 10 minutes.

#### **3.20.4 Electrophoresis buffer preparation**

For this purpose, Tris-glycine buffer (5X) was prepared. It comprises 15.1gm of 25 mM tris base and 94gm of glycine. Also included was 50 mL of 10% SDS. With the aid of distilled water, the final volume was set to 1 litre.

#### **3.20.5 Separation of cutinase**

After the stacking gel solidified, the comb was removed and the wells were washed with distilled water. The electrophoresis device's gel tank was carefully kept in a

precise position. 10 µL of denatured cutinase enzyme sample was loaded in each well. Tris-glycine electrophoresis buffer (1X) was carefully poured into the tank without forming any bubbles. The power cable was attached to the apparatus and initially 150 volts current was supplied for 15 minutes followed by a continuous flow of 180 volts current for the next 30 minutes. After 30 minutes the loading and protein marker was reached at the end of gel and protein was separated on the basis of molecular weight, destaining was then carried out.

### 3.20.6 Staining of gel

Once the electrophoresis was completed, the gel was transferred to a separate container filled with a staining solution of Coomassie Brilliant Blue R-250. The gel was gently agitated in the solution for a duration of 1 hour. After staining, the gel was transferred to destaining solution and again kept on shaking for 1 hour. The gel was observed in Coomassie-white Gel Doc imaging system (Universal Hood 2 – S.N. 76S/ 0.4186) for protein bands.

### 3.20.7 Zymograph for cutinase activity

Cutinase activity was confirmed by zymography using  $\alpha$ -naphthyl acetate as substrate. The native gel was incubated in 20 mM Tris-HCl buffer (pH 6.5) with 2% Triton X-100 for 10 minutes followed by incubation in 50 mM phosphate buffer (pH 7.5) supplemented with 1 mM Fast Red TR and 3 mM  $\alpha$ -naphthyl acetate (Sigma) at room temperature for maximum up to 3 hours to observe red color band that will indicate cutinase activity (Karpudhova et al., 2005). The gel was observed in Gel Doc imaging system (Universal Hood 2 – S.N. 76S/ 0.4186) for bands.

### 3.21. Characterization of Purified Cutinase

The purified cutinase was characterized using the method as described by Coral et al. (2002). The relative activity of the enzyme was calculated by using the formula below:

$$\text{Residual Activity (\%)} = \frac{\text{Activity (U/mL) of enzyme}}{\text{Activity (U/mL) of the highest enzyme activity}} \times 100$$

### **3.21.1 Effect of Temperature on the activity and stability**

The effect of temperature on purified enzyme activity was observed under different temperatures range from 30–60°C and activity was calculated in terms of relative activity (%). The thermostability was determined by pre-incubating the enzyme sample in 100 mM phosphate buffer at various temperatures range from 30–60°C in the absence of substrate for the maximum up to 150 minutes. After every 30 minutes' interval substrate was added and again incubated for 30 minutes at optimum temperature. The residual activity was calculated using the standard assay (section 3.11.1).

### **3.21.2 Effect of pH on the activity and stability**

The effect of pH on purified enzyme activity was studied over a wide pH range of 3.0–11.0. The effect of pH was in terms of relative activity (%). The pH stability of enzyme was determined by pre-incubation in different buffer systems (3.0–11.0) at 40°C in the absence of substrate for 150 minutes. After every 30 minutes' substrate was added and again incubated for 30 minutes at optimum temperature and residual activity was measured using the standard assay (section 3.11.1). The following buffer systems (100 mM) were used: sodium acetate buffer, pH 3.0–5.0; potassium phosphate buffer, pH 6.0–8.0; glycine-NaOH buffer, pH 8.0–11.0.

### **3.21.3 Effect of Metals ions**

The influence of various metal ions on the activity of purified cutinase was analyzed by incubating it with two different concentrations of metal ions (2 mM and 15 mM): [Ba<sup>2+</sup>, Cu<sup>2+</sup>, Mg<sup>2+</sup>, Ca<sup>2+</sup>, Zn<sup>2+</sup>, Cu<sup>2+</sup>, K<sup>+</sup>, Hg<sup>2+</sup>, Fe<sup>2+</sup>, Ni<sup>2+</sup>, Co<sup>2+</sup>, Ni<sup>2+</sup>, and Na<sup>2+</sup>]. The results were expressed in terms of residual activity (%) after 30 minutes at 40°C using standard assay protocol.

### **3.21.3. Effect of organic solvents**

The influence of various organic solvents on activity of purified cutinase was analyzed by incubating it with different organic solvents (10 %): [ethanol, methanol, acetonitrile, acetone, ethyl acetate, propanol, butanol, and formaldehyde]. The results

were expressed in terms of residual activity (%) after 120 min at 40°C using standard assay protocol.

#### **3.21.4. Effect of organic surfactant**

The influence of various surfactant on the activity of purified cutinase was analyzed by incubating it with two different concentrations of surfactant (0.5 and 5 %): [sodium dodecyl sulfate (SDS), Tween 40, Triton X-100, Tween 60, Tween-80, and Tween-20]. The results were calculated in terms of residual activity (%) after 30 minutes at 40°C using standard assay protocol.

#### **3.22. Kinetic parameters of purified cutinase enzyme**

The  $V_{max}$  (maximum velocity) and  $K_m$  (Michaelis-Menten constant) were calculated at a temperature of 40°C and pH 8.0. The enzyme assay was performed using a reaction mixture containing 12 mM *p*-NPB at different concentrations (0–300  $\mu$ L/mL), as previously described. The resulting data was plotted in Lineweaver-Burk software to determine the kinetic constants  $V_{max}$  and  $K_m$

#### **3.23 Enzymatic Depolymerization of PET by purified cutinase**

The aim of this experiment was to observe the enzyme activity against PET after every 24 hours. The reaction mixture included PET pieces (50 mg), and purified cutinase (0.7 mg) in 3mL 100 mM potassium phosphate buffer (pH 8.0) in a small beaker and incubated in a table-top shaker incubator for 72 hours at 40°C and 250 rpm (wagner-Egea et al., 2021). The enzyme activity was calculated after every 24 hours using standard assay protocol. The experiment was run in triplicate with a negative control without enzyme is setup in separate.

##### **3.23.1. Sample preparation and investigation of de-polymerization products**

The products of PET hydrolysis by cutinase from strain PRS8 were analysed using reverse phase Liquid Chromatography-Mass Spectrometry (LC-MS). 0.5 ml of sample was collected after incubation and diluted at a 1:1 ratio with dimethyl sulfoxide (DMSO) and filtered through 0.2  $\mu$ m syringe filter. The sample was then transferred to an Amicon Ultra filtration assembly (Pall Life Sciences, Ann Arbor,

MI) and centrifuged at 15,000xg for 20 minutes on a Nanosep 3 K centrifuge to remove the enzyme. The filtrate sample was diluted in 1:2 with Milli-Q water and was used for to analyze the degradation products through LC-MS.

### 3.23.2 Specifications for LC-MS equipment

The LC-MS coupled with HPLC instrument was used to determine the PET degradation product released after treatment with purified cutinase. The instrument consisted of an QExactive mass spectrometer coupled with a HESI source from Agilent and an HPLC system. A hydrophobic C18 column was used to analyze the degradation products in sample. The flow rate of pump was fixed at 400  $\mu\text{L}/\text{minute}$ . Mobile phase consisted of two solvents; A: (20%) consisted of acetonitrile containing 0.1% formic acid and B: (80%) consisted of an aqueous solution containing 0.1% formic acid. The data was further processed by Chromeleon v. 6.8 software. The autosampler temperature was fixed at 4°C with injection volume 15  $\mu\text{L}$ . The sample data was collected in full scan mode between m/z (100-1500) in negative ionization with maximum resolution at 70,000 at 1 Hz, injection time of 200 ms and an AGC target of 3e6.

## 3.24 Analysis of Degradation of enzymatically treated PET

### 3.24.1 Differential Scanning Calorimetry Analysis

The differential scanning calorimetry (DSC) measurements were performed using a TA Instruments DSC Q2000. The thermal transitions of the powders of pristine PET (untreated) and PET treated with PRS8 were studied using nitrogen with a purge rate of 50 mL min<sup>-1</sup> and a heating rate of 10 °C per minute. The samples were heated from room temperature to 280 °C. The glass transition temperature ( $T_g$ ), cold crystallization temperature ( $T_{cc}$ ) and melting temperature <sup>TM</sup> were obtained from the DSC first heating curve. The crystallinity percentage was calculated using the following equation:

$$\text{Crystallinity (\%)} = \frac{|\Delta H_c|}{|\Delta H^{\circ}_m|} \times 100$$



where  $DH_{cc}$  and  $DH_m$  are the heat of the cold crystallization (area under the cold crystallization) and the heat of melting (area under the melting transition), respectively.  $DH^{\circ m}$  is the heat of melting for a 100% crystalline polymer estimated to be 140 J/g (Xi et al., 2021).

#### **3.24.2 Quantitative assay for cutinase activity and Determination of dry weight of residual PET**

About 100  $\mu$ L sample was collected from degradation experiment at different time interval and centrifuged at 10,000 $\times$ g for 10 minutes at 4°C. The supernatant was assayed for cutinase activity using *p*-nitrophenyl Butyrate (*p*-NPB) (12 mM) as substrate. Cutinase activity was expressed in terms of relative activity (%). After enzymatic de-polymerization, PET pieces were recovered and washed 3 time with Milli-Q water and incubated overnight at 60°C. After incubation PET pieces were weighed and observed for weight loss % using the formula below:

$$\text{Percentage of weight loss} = [(Initial\ weight - Final\ weight)/Original\ weight] \times 100.$$

#### **3.24.3 Fourier-transform Infrared (FT-IR) Spectroscopy of Enzymatically treated PET**

PET pieces were analyzed for changes in functional groups after incubation with purified cutinase by *S. maltophilia* PRS8 through FTIR Spectroscopy. The spectra of treated PET pieces were recorded in a frequency range 4000–400  $\text{cm}^{-1}$  wavenumber at a resolution of 4  $\text{cm}^{-1}$  at ambient temperature with a helium–neon laser lamp as a source of IR radiation. Abiotic control was analyzed along with test samples for comparison.

#### **3.24.4 Scanning Electron Microscopy (SEM) of Enzymatically treated PET**

The changes in surface morphology of the PET pieces after incubation with purified cutinase by *S. maltophilia* PRS8 was determined using a scanning electron microscope model JSM-IT100. The pieces were carefully rinsed for a few minutes with 2 % (v/v) aqueous SDS and distilled water, then flushed with ethanol (70%) to remove the buffer and associated protein from the surface and finally gold-painted on

copper stubs. To increase the conductivity of the samples, gold plating was done in vacuum by evaporation. PET piece from control was examined alongside the test sample for comparison.

### 3.25 Cloning and expression of PET degrading enzyme

#### 3.25.1 Preparation of culture media

Luria-Bertani (LB) culture medium is the most favorable and appropriate used for preservation, screening, culturing, and storage of the various native and recombinant clones. Sterilization was carried out in autoclave at 121°C for 20 minutes.

#### 3.25.2 Preparation of antibiotic

50mg/L of Ampicillin (Amp) antibiotic stock solution was prepared in sterile Milli-Q water and filtered by 0.22 µm pore filter paper. The stock solution was stored at -20°C for further use. The antibiotic mode of action and working concentration seen in table 3.6.

**Table 3.6:** Antibiotic used in the present study

Antibiotic	Stock solution	Working concentration	Mechanism of action
Ampicillin (Amp)	50 mg/mL in sterile MilliQ H <sub>2</sub> O	50 µg/mL	Ampicillin inhibit cell wall synthesis by stopping the formation of the peptidoglycan cross-link

#### 3.25.3 Isopropyl-β-D-thiogalactoside stock Preparation

Isopropyl-β-D-thiogalactoside (IPTG) was used in the LB production medium containing Amp in order to stimulate the expression of recombinant protein by inducible strains. About 1M of IPTG stock solution was prepared in sterile Milli-Q water and filtered by 0.22 µm pore sized filter paper. The solution was kept at -20 °C for further use. About 1µM/mL of IPTG was used for expression of protein.

### 3.25.4 X-Gal Stock Preparation

X-Gal is a chromogenic substrate that used for white/blue colony screening to differentiate non-recombinant (blue) from recombinant (white) colonies. About 20mg/mL of X-Gal stock solution was prepared in sterile Milli-Q water and filtered by 0.22  $\mu\text{m}$  pore sized filter paper. The solution was kept at  $-20\text{ }^{\circ}\text{C}$  for further use. About 1 mg/mL of working solution was used to screen out blue and white colonies.

### 3.25.5 Selection of recombinant Strains

Two recombinant bacterial strains were used in the current study for transformation and expression of PET degrading enzyme, shown in table 3.7

**Table 3.7:** *E. coli* strains used for cloning in the present work

Strain	Genotype	Supplier
<i>E. coli</i> DH5 $\alpha$ (D5)	F <sup>-</sup> $\phi$ 80 <i>lacZ</i> $\Delta$ M15 $\Delta$ ( <i>lacZYA-argF</i> ) U169 <i>recA1 endA1 hsdR17</i> (r <sub>K</sub> <sup>-</sup> , m <sub>K</sub> <sup>+</sup> ) <i>phoA supE44 <math>\lambda</math>-thi-</i> 1 <i>gyrA96 relA1</i>	Invitrogen School of Molecular Biology
<i>E. coli</i> BL21 (DE3)	F <sup>-</sup> <i>ompT hsdS<sub>B</sub></i> (r <sub>B</sub> <sup>-</sup> , m <sub>B</sub> <sup>-</sup> ) <i>gal dcm</i> (DE3)	Invitrogen School of Molecular Biology

### 3.25.6 Vectors and plasmids

The plasmids used in the present study are seen in table 3.8

**Table 3.8:** List of vectors used for cloning

Plasmid	Features	Supplier
pUC19	AmpR, <i>E. coli</i> plasmid, 2686 bp in length, 5' lacZ fragment, multiple cloning site (MCS), Plac (lac promoter), pMB1 ori (ColE1 incompatibility group)	New England BioLabs
pET-21b	AmpR expression system, T7 promoter, T7•Tag coding sequence MCS, lacI coding sequence	Novagen

### 3.25.7 Designing of primers

Primers for PET hydrolase gene were designed on sequences of *Stenotrophomonas maltophilia* obtained from GenBank having NdeI (forward) and xhoI (reverse) restriction sites (Table 3.9). ClustalW (MEGA 4.0) program was used by aligning the sequence in order to identify the conserve regions.

**Table 3.9:** Primer for gene amplification

Primer name	Primer sequence	Primer name
PETStM-F	5' catATGCCGGCGCAAATAGCCATTC3' Tm 63.1°C	PETStM-F
PETStM-R	5' ctcgagAAGGGCAGCGGCGAGTT3' Tm 63.5°C	PETStM-R

### 3.26 Extraction of Genomic DNA of Strain PRS8 by QIAamp® DNA Mini Kit (QIAGEN)

**Procedure:** All steps were performed at room temperature

1. Overnight culture of bacterial strain PRS8 was transferred by micropipette into 1.5 mL micro-centrifuge tube and centrifuged at 6000xg for 5 minutes. The supernatant

were discarded and pellets were processed for DNA extraction. The pellets were re-suspended in 180  $\mu$ L ATL buffer by vortexing for 15 seconds. About 20  $\mu$ L of Proteinase K was added into re-suspended pellet and incubated for 2 hours at 56°C in order to lyse the cell completely. The sample was vortexed sporadically during incubation. After incubation, 200  $\mu$ L AL Buffer was added and mixed thoroughly by vortexing for 15 seconds. The tube was gently centrifuged to remove drops from the lid and again incubated for 10 minutes at 70°C. 200  $\mu$ L 200 of 96% ethanol were added, and the mixture was gently vortexed for 15 seconds. The sample was again quick centrifuged to removed drops from the lid. The sample was shifted to the 2 mL collection tube with the help of pipet and centrifuged at 8000 rpm (6000 x g) for 1 minute. The flow-through that was collected in a collection tube was discarded. The QIAamp Mini spin column was transferred in a fresh 2 mL tube and 500  $\mu$ L wash AW1 buffer was also added. The column was again centrifuged at 8000 rpm (6000 x g) for 1 minute and discarded the flow-through. 500  $\mu$ L of AW2 buffer was added to spin column and centrifuged at maximum speed at 14,000 rpm (20,000 x g) for 3 minutes and discarded the flow through. The centrifugation step was repeated twice in order to completely eliminate the buffer AW2. The QIAamp Mini spin column was shifted to new cleaned 1.5 mL micro-centrifuge tube and 50  $\mu$ L elution buffer AE was added and incubated at room temperature for 5 minutes in order to elute the attached DNA. After incubation, the sample was centrifuges at 8000 rpm (6000 x g) for 3 minutes to elute the DNA. Finally the elute DNA was stored at -20°C.

### **3.26.2 Preparation of agarose gel and confirmation of genomic DNA**

About 1g agarose was added into 100 mL TBE buffer 1X (40 mM Tris buffer, 40 mM Boric acid, 1 mM EDTA and 40 mM Tris buffer) and boiled in microwave oven for 1 min at high speed to dissolve it completely. The flask containing agarose solution was cooled down to room temperature and then 5  $\mu$ L GelRed nucleic acid stain was added. The gel was poured into the gel tray (Bio-Rad) and a comb was placed for generation of wells. The gel tray was left undisturbed at room temperature for 15 minutes for solidification. DNA sample was prepared by adding 4  $\mu$ L of DNA into 1  $\mu$ L loading dye (Blue/Orange, promega). 3 $\mu$ L of DNA sample was loaded and the power supply turned on with volatage 90V and 400mA for 50 minutes. 1% agarose gel containing

ethidium bromide was used to validate PCR product amplification. The band was then visualized by comparing it with DNA ladder (1 kb, GeneRuler™) and photograph was taken on a Bio-Rad Gel Doc imaging system (Universal Hood 2 – S.N. 76S/ 0.4186).

### **3.26.3 Nucleic acid quantification by NanoDrop (ND-100)**

Nucleic acid was quantified spectrophotometrically, used ND-100 NanoDrop. About 1.5 µL of DNA sample of strain PRS8 was loaded on the surface of optic fiber cable lens. The source is actually receiving a line. A liquid sample was applied to the source line, an optic fiber cable. Through this process, a space was generated between the two ends. A pulsed xenon flash lamp was used to measure the sample's absorbance along a path length of 0.2 mm. While the concentration is based on OD 260 nm, with a detection limit of 1 ng/µL, the purity of the material is calculated by dividing the absorbance at 260nm/280nm, and regarded as about equal to 1.8 for DNA.

### **3.27 Polymerase Chain Reaction (PCR) to Amplify PET Hydrolase Gene**

iProof™ High-Fidelity Master Mix Kit was used to amplify PET hydrolase gene from bacterial strain PRS8. Primer and template are not included in the iProof high-fidelity PCR master mixes, which are 2x concentrated, ready-to-use supermixes with all of the other ingredients (0.04 U/l iProof polymerase, 3 mM MgCl<sub>2</sub> and 400 M dNTPs). The PCR mixture contained 10 µL of iProof™, 0.6 µL of 3% DMSO, 1 µL forward primer (10 mM) F-(catATGCCGGCGCAAATAGCCATTC), 1 µL reverse primer (10 mM) R-(ctcgagAAGGGCAGCGGCGAGTT), 6.4 µL of autoclaved Mill-Q water and 1 µL DNA template. The PCR conditions were as follows: denaturation of DNA at 98°C for 2 minutes followed by amplification cycle with denaturation at 98°C for 30 seconds, annealing at 63°C for 60 seconds, extension temperature at 72°C for 35 cycles for 1 hour and 28 seconds and one cycle. The reaction was further incubated at 72°C for 7 minutes of final elongation. After PCR, 1% agarose gel containing 5 µL GelRed nucleic acid stain was used to validate PCR product amplification, and the results were evaluated using a Bio-Rad Gel Doc imaging system (Universal Hood 2 – S.N. 76S/ 0.4186).

### **3.27.1 Purification of DNA from polyacrylamide gel by QIAEX II® Gel Extraction Kit (QIAGEN)**

The amplified DNA band was carefully removed from the gel with a sterile scalpel and transferred to a clean 2 mL microfuge tube. The gel containing DNA band was weighted and 3 volumes of QX1 buffer was added according to DNA fragment size. About 20 µL of re-suspension QIAEX II was added and mixed by vortexing for 30 seconds. The sample mixture was incubated for 10 minutes at 50°C to solubilize the agarose gel and DNA bind to QIAEX II. The sample was mixed gently after every 2 minutes during incubation to maintain QIAEX II in suspension. After incubation, the sample was centrifuged at 13000 rpm for 30 seconds and the supernatants was removed carefully with the help of micropipette. 500 µL of QX1 buffer was added again to the pellet and re-suspended by vortexing for 10 seconds. The sample was then centrifuged at 13000 rpm for 30 seconds. The remaining agarose and all traces were removed with the help of pipette. The pellet was rinsed twice with PE buffer (500 µL) and the supernatants obtained after centrifugation was removed by means of pipette. This step removed the residual salts contaminants. The sample was then air-dried for 30 minutes. About 20 µL elution buffer (10 mM Tris·Cl, 1 mM EDTA, pH 8.0) was then added and mixed by vortexing for 15 seconds and then kept at room temperature for 5 minutes to elute the DNA in buffer. The sample was centrifuged for 1 minute at 13000 rpm. The supernatants contained DNA was carefully transferred to new 1.5 mL tube with the help of micropipette.

### **3.27.3 Ligation of PCR purified Products**

The ligation process was carried out in accordance with the instructions given by the manufactures by mean of T4 DNA ligase enzyme. In a double stranded DNA, T4 DNA ligase assembles phosphodiester linkages between the 3' OH and 3' PO<sub>4</sub><sup>-</sup> ends. The amount of components needed to obtain the necessary ratio to carry out the reaction was calculated using a specialized tool (<http://www.gabthon.org/ligate.html>). The amount of vector used in various ligation tests was equal to that of the negative control. The ligation experiment was run at 16°C for 16 hours. The amplified fragment was cloned into pUC19 vector according to the description in the instructor's manual (Table 3.10).

**Table 3.10:** Ligation reaction mixture

Components	Reaction volumes ( $\mu\text{L}$ )
pUC19 Vector	1 (2ng)
T4 DNA ligase Buffer (2X)	4 (2x)
T4 DNA Ligase	1
Insert	10

### 3.28 Cloning and expression experiments

#### 3.28.1 Preparation of competent cells

*E. coli* DH5 $\alpha$  competent cells were prepared for the transformation of gene of interest. *E. coli* DH5 $\alpha$  was added to autoclaved LB, the media was incubated for 16 hours at 37°C. The bacterial culture was transferred into new LB (30 mL) after 16 hours, and it was again incubated at 37°C with constant shaking until the OD of the cells reached to 0.45-0.55 at 600 nm, which was regarded as the exponential phase of cells. The *E. coli* culture was shifted to already sterilized ice-cold falcon tube (50 mL) and kept on ice for 10 minutes. The culture was centrifuged for 5 minutes at 3000 x g at 4°C. After centrifugation, the pellet was homogenized in 10 mL cold CaCl<sub>2</sub> (0.1M) and again incubated on ice for 30 minutes. The already homogenized cells were centrifuged for 5 minutes at 4500 rpm. The supernatants were removed by means of a micropipette and pellet was resuspended in 2 mL CaCl<sub>2</sub> and incubated at 4°C for 2 hours. After incubation the competent cell was used for transformation of gene of interest.

#### 3.28.2 Transformation of *E. coli* competent cells by heat shock method

About 200  $\mu\text{L}$  of *E. coli* competent cells were transferred with the help of pipette into 1.5 mL centrifuge tube contained ligated gene of insert. A control without gene of interest was also run in parallel. The tubes were incubated for 15 minutes on ice followed by heating at 42°C for 2 minutes and then immediately transferred to ice for



maximum up to 10 minutes. 200  $\mu$ L LB medium was added to each tube and then incubated at 37°C for 2 hours so that cell may express and recover antibiotic resistance marker that was encoded on plasmid. After incubation, 200  $\mu$ L sample was shifted to ampicillin (50  $\mu$ g/mL) agar plate supplemented with 1 $\mu$ M IPTG and 1mg/mL X-Gal and spread by mean of disposable VMR sterile spreader. The agar plates were incubated for 14-16 hours in order to observe the blue (non-recombinant) and white (recombinant) colonies.

### **3.28.3 Plasmid extraction of transformed cell by QIAprep® Spin Miniprep Kit - QIAGEN**

Transformed cell from 16 hours fresh culture was shifted to 1.5 mL Eppendorf tube and centrifuged at 6800 xg (8000 rpm) for 3 minutes at room temperature (15–25°C). The supernatant was discarded, and pellet was re-suspend in 250  $\mu$ L P1 buffer. 250  $\mu$ L P2 buffer was then added and gently mixed by inverting the tubes 5–8 times, the solution was turned to blue colored. About 350  $\mu$ L N3 buffer was added to the mixture and mixed immediately by inverting the tubes 5–8 times, the solution was observed colorless. The mixture was centrifuged at  $\sim$ 17,900 x g (13000 rpm) for 10 minutes at room temperature. The supernatant (0.8 mL) was carefully shifted to the QIAprep 2.0 spin column and then centrifuged at maximum speed 13000 rpm for 1 minute, the flow-through was discarded. 500  $\mu$ L PB buffer was added to 2 mL spin column and again centrifuged at maximum speed for 1 minute. The flow-through obtained in tube was discarded. The spin column was placed in a new 2mL tube and 750  $\mu$ L wash buffer PE was added. The sample was centrifuged at maximum speed for 1 minute, the resulted flow through was again discarded. The centrifugation step was repeated twice in order to eliminate the residual buffer. The QIAprep 2.0 spin column was shifted to a new clean 1.5 mL Eppendorf tube. To elute the plasmid DNA, 50  $\mu$ L elution buffer (10 mM Tris, pH 8.5) was added to the center of the spin column and left undisturbed for 1 minute. The plasmid DNA was recovered by centrifugation at 8000 rpm for 3 minutes. The extracted plasmid DNA was examined on 1% agarose gel by mixing loading dye and DNA with a ratio 1:5.

### 3.28.4 Confirmation of cloning with NdeI and XhoI restriction enzymes

The presence of PET hydrolase gene was confirmed by double digestion of plasmid DNA with suitable restriction enzyme. The goal of double digestion is to generate adhesive ends on both the plasmid vector and the inserts. The amount of DNA used in the digestion reaction for PCR amplicons was 100 ng, while 50 ng was used for plasmid vectors. The incubation was done at 37°C for various time intervals. The extracted cloned plasmid containing the insert and pET21b plasmid was cut with NdeI and XhoI restriction enzyme and incubated at 37°C for 3 hours, the reaction mixture is shown in table 3.11. The digestion and cloned fragment was confirmed by gel electrophoresis. After incubation, the digestion of pET21b plasmid and insert was confirmed through electrophoresis.

**Table 3.11:** Digestion of PET hydrolase gene

Reaction	Reaction mixture volumes (μL)
NdeI	1
XhoI	1
Buffer	2
Plasmid DNA	10
Sterilized Milli-Q water	3

### 3.28.5 Purification of double digested band from polyacrylamide gel by QIAEX II® Gel Extraction Kit (QIAGEN)

The double digested cloned DNA and pET21b band was removed carefully from the gel with a sterile scalpel and shifted to a clean 2 mL microfuge tube. Purification was described previously (section 3.27.1).

### 3.29 Ligation of purified pET2b plasmid and cloned gene

The ligation process of double-digested purified PET hydrolase gene and pET21b was carried out in accordance with the instructions given by the manufactures by mean of T4 DNA ligase enzyme. The ligation reaction mixture was incubated at 4°C for 10 hours. The ligation reaction mixture shown in table 3.12.

**Table 3.12:** Ligation of PET hydrolase gene into pET21b

Components	Reaction volume (μL)
pET21b	2 (2ng)
Ligation buffer	2 (2X)
Insert (Gene)	10
T4 DNA ligase	1

#### 3.29.1 Transformation of Insert + pET21b plasmid *E. coli* DH5α competent cells by heat shock method

About 200 μL of *E. coli* DH5α competent cell was added into 1.5 mL micro-centrifuge tube containing ligated PET hydrolase gene of interest in pET21b plasmid. A control without gene of interest was also run in parallel. The tubes were incubated for 15 minutes on ice followed by heating at 42°C for 2 minutes and then immediately transferred to ice for maximum up-to 10 minutes. 200 μL LB medium was added to each tube and then incubated 2 hours at 37°C for so that cell may express and recover antibiotic resistance marker that was encoded on the plasmid. After incubation, 200 μL sample was shifted to ampicillin (50 μg/mL) agar plate. Sample was then spread by mean of disposable VMR sterile spreader. The agar plates were incubated for 14-16 hours in order to observe the colonies.

#### 3.29.2 Plasmid extraction from transformed cell by QIAprep® Spin Miniprep Kit - QIAGEN

Transformed cells, plasmid was extracted by QIApep Spin Miniprep Kit-QIAGEN described previously in section 3.28.3.

### 3.29.3 Verification of PET hydrolase gene Cloning

Double digestion with restriction endonucleases confirmed the presence of the PET hydrolase-cloned fragment. The restriction reaction contained the appropriate restriction buffer (10X), which had been diluted to a final concentration of 1X with Milli-Q water. The reaction mixture was incubated at 37°C for 2 hours, and the digestion of the cloned plasmid was confirmed by 1% agarose gel electrophoresis, as previously described.

### 3.29.4 Confirmation of Cloning with Nde1 and Xho1 restriction enzymes

The presence of PET hydrolase gene was confirmed by double digestion of the plasmid DNA with suitable restriction enzyme. To carry out the process of double digestion, the appropriate buffer (2x) for both types of enzymes was used. The incubation was done at 37°C for 3 hours. The reaction mixture shown in table 3.13. The digestion and cloned fragment was confirmed by gel electrophoresis.

**Table 3.13:** Digestion of PET hydrolase gene

Reaction	Reaction mixture volumes (μL)
Nde1	1
Xho1	1
Buffer	2
Plasmid DNA	10
Sterilized Milli-Q water	3

### 3.29.5 Sequencing of cloned PET hydrolase gene

The PET hydrolase gene in pET21b plasmid was purified by QIAquick® PCR purification Kit (QIAGEN) and sequenced using Mix2Seq kit smart easy quick, according to the instruction provided by manufacturers. The sample was analyzed

with an eurofins genomic, sanger sequencing (Sweden) model Model 370A automatic sequencer.

### 3.30 Bioinformatics analysis

To analyze the nucleotide sequence, BLASTp and BLASTn tools were used respectively (<http://www.ncbi.nlm.nih.gov/BLAST/>). CLUSTALW program was used for Multiple sequence alignment (MSA) of PET hydrolase gene. Phylogenetic analysis and dendrogram construction for StmPRS8PET was carried out using MEGA 6.0 software.

### 3.31 Growth Conditions and Expression of PET Hydrolase Gene *E. coli* BL21

Protein expression was carried out after verification of the recombinant clone of DNA sequence. About 10 mL of LB broth was inoculated with recombinant *E. coli* strain amended with ampicillin (50 µg/mL) and incubated in shaking incubator at 37 °C for 16 hours. About 1% of the overnight seed inoculum was transferred to another 2 L Erlenmeyer flask containing 600 mL LB medium amended with ampicillin (50 µg/mL) and incubated at 37 °C for several hours till the OD was observed 0.72 at 600 nm. At this stage 1mM of IPTG was added to the medium to induce protein expressions and re-incubated at 20°C in shaker incubator for 16 hours. After incubation, the cells were harvested by centrifugation at 12,000 rpm for 15 minutes and re-suspended in 60 mL buffer (tris-HCl 100Mm, NaCl 0.5M, pH 7.4). Cells were sonicated for 30 minutes to release intracellularly produced PET hydrolase protein using ultrasonic homogenizer. After sonication, the cell debris was removed by centrifugation at 10,000 rpm for 30 minutes and supernatants were collected.

### 3.32 Purification of Recombinant Protein

#### 3.32.1 Protein purification by HiPrep 16/60 Sephacryle S-300 high-resolution gel filtration column Chromatography

HiPrep 16/60 Sephacryle S-300 is pre-packed gel permeation column chromatography actually designed for separation of proteins, peptides and larger molecules according to their sizes. The column length and size was: L × 60 cm × 16 mm, with 50 µm

average part size. The HiPrep 16/60 Sephacryle S-300 column was directly connected to AKTA™ start (29022094) GE Healthcare BioSciences AB 71584 Uppsala Sweden. UNICORN software was used for calibration and maintenance of column flow rate. Initially the column was calibrated by eluting 120 mL of buffer (tris-HCl 100Mm, NaCl 0.5M, pH 7.4). The column flow rate was maintained to 0.5 mL/minute with a total volumes of 260 mL. Subsequently 1 mL of partially purified recombinant enzyme was loaded to the Sephacryle column. About 500 mL buffer was placed in injection valves to maintain continuous flow of sample. A total of 28 fractions were collected and protein concentration was determined spectrophotometrically at 280 nm by UV in UNICORN (AKTA start). Then enzyme assay of all fractions was checked and fractions that showed high activity were combined and concentrated by Macrosep advance centrifugal device with 10K MWCO and stored at 4°C for further analysis.

### **3.32.2 Mini- protein TGX Staining-free SDS polyacrylamide gels for protein**

Before loading the sample, 15 µL of recombinant enzyme was mixed with 5 µL of loading dye and heated for 10 minutes at 98°C and then placed in icebox for 10 minutes. The gel was made by the method as described previously and 10 µL of denatured recombinant enzyme was loaded in each well. The power cables were attached to the apparatus and 150 volt current was provided for 15 minutes. After 15 minutes, the voltage was increased up to 200 volt and run for 30 minutes. After completion of electrophoresis, the stain-free gel was shifted to another box and directly observed without staining under UV black tray Gel Doc imaging system (Universal Hood 2 – S.N. 76S/ 0.4186) for protein bands with protein marker standard.

## **3.33 Characterization of Purified Recombinant Cutinase**

### **3.33.1 Effect of Temperature on the activity and stability**

The effect of temperature on recombinant enzyme activity was observed under different temperatures range from 30–80°C and activity was calculated in terms of relative activity (%). The thermostability was determined by pre-incubating enzyme sample in 100 mM phosphate buffer at various temperatures (30–80°C) in the absence of substrate for the maximum up to for 150 min. Substrate was added after every 30

min interval and again incubated for 30 minutes at optimum temperature. The residual activity was measured using the standard assay.

### **3.33.2 Effect of pH on the activity and stability**

The effect of pH on recombinant enzyme activity was studied over a pH range of 3.0–11.0 and activity was calculated in terms of relative activity (%). The pH stability of enzyme was determined by pre-incubation in different buffer systems (3.0–11.0.) at 40°C in the absence of substrate for 150 min. Substrate was added after every 30 min interval and again incubated for 30 minutes at optimum temperature and residual activity was measured using the standard assay.

### **3.33.3. Effect of Metals ions**

The influence of various metal ions on the activity of recombinant enzyme was analyzed by incubating it with two different concentrations of metal ions (2 mM and 10 mM). [Ba<sup>2+</sup>, Ca<sup>2+</sup>, Cu<sup>2+</sup>, Mg<sup>2+</sup>, Zn<sup>2+</sup>, Cu<sup>2+</sup>, K<sup>+</sup>, Na<sup>2+</sup>, Hg<sup>2+</sup>, Fe<sup>2+</sup>, Ni<sup>2+</sup>, K<sub>2</sub><sup>2+</sup>, Co<sup>2+</sup>, Ni<sup>2+</sup>, and Na<sup>2+</sup>]. The results were expressed in terms of residual activity (%) after 30 min at 40°C using standard assay protocol.

### **3.33.4. Effect of Organic Solvents**

The influence of various organic solvent on the activity of recombinant enzyme was analyzed by incubating it with different organic solvent (10 %): [ethanol, methanol, acetonitrile, acetone, ethyl acetate, propanol, butanol, and formaldehyde]. The results were expressed in terms of residual activity (%) after 120 min at 40°C using standard assay protocol.

### **3.33.5. Effect of Surfactant**

The influence of various surfactants on activity of recombinant enzyme was analyzed by incubating it with two different concentrations of surfactant (0.5 and 5 %): [sodium dodecyl sulfate (SDS), Tween 40, Triton X-100 Tween 80, Tween-20 and Tween-60]. The results were expressed in terms of residual activity (%) after 30 min at 40°C using standard assay protocol.

### **3.34. Enzymatic Depolymerization of PET by Recombinant Enzyme**

The aim of experiment was to observe the recombinant enzyme activity against PET after every 24 hours. The reaction mixture included: PET (20 mg), 1.6 mL recombinant enzyme (1.3 mg), 0.2 mL 100 mM Glycine-NaOH buffer (pH 9.0) and 0.2 mL DMSO in final volume 2 mL were taken in a glass tube and incubated in a small table-top shaker incubator for 72 hours at 40 °C and 200 rpm. The experiment was run in triplicate with a negative control without enzyme setup in separate.

#### **2.34.1. Sample preparation**

1 mL of sample was collected after incubation and diluted at a 1:1 ratio with dimethyl sulfoxide (DMSO), vortexed and then filtered through 0.2 µm syringe filter. The sample was then transferred to an Amicon Ultra filtration assembly (Pall Life Sciences, Ann Arbor, MI) and centrifuged at 15,000xg for 20 minutes on a Nanosep 3 K centrifuge to remove the enzyme.

#### **3.34.2 Analysis of de-polymerization products by HPLC**

The products released as a result of hydrolysis of PET by recombinant enzyme from strain PRS8, were analyzed by HPLC. A hydrophobic C18 column was used to analyze the degradation products in sample. The pump flow rate was fixed at 400 µL/minute. Mobile phase consisted of two solvents; A: (100%) consisted of acetonitrile and B: consisted of an aqueous solution containing 0.1% formic acid. The data was further processed by Chromeleon v. 6.8 software. The TPA product was quantified by using TPA standard curve in a range from 830 µg/L to 2 g/L.

#### **2.34.3 LC-MS analysis of de-polymerization products**

The sample preparation was performed as previously described (section 3.34.2) The LTQ Velos Pro Ion trap mass spectrum coupled with Ultimate 3000 RS HPLC-system instrument using heated electrospray ionization source (HESI-II) to determine the PET degradation product released after treatment with recombinant enzyme. The sample data was collected in full scan mode between m/z (60-500) in negative ionization while providing a spray voltage of -3 kV.



### 3.35 Degradation Analysis of Enzymatically Treated PET

#### 3.35.1 Differential Scanning Calorimetry Analysis

Differential scanning calorimetry (DSC) measurements were employed using a TA DSC Q2000 Instruments. The PET sample was analyzed with a 10°C/minute of heat rate with a purge rate of nitrogen 50 mL/minute. The heating ramp was maintained from 25-280°C. The analysis was run for 90 minutes and the crystallinity of PET was observed after precipitation–dissolution. Following equation was used for crystallinity calculation

$$\text{Crystallinity (\%)} = |\Delta H_m| - |\Delta H_c| / |\Delta H_m^\circ| \times 100$$

Whereas  $\Delta H_m$  showed melting crystallization and  $\Delta H_c$  represent cold crystallization and  $\Delta H_m^\circ$  is the heat of melting for a 100% crystalline polymer (Xi et al., 2021).

#### 3.35.2 Determination of dry weight of residual PET

After enzymatic de-polymerization PET pieces were recovered and washed with detergent (1% SDS) followed by washing with Milli-Q water and finally dried under airflow for 72 hours. PET pieces were weighted and observed for weight loss % using the formula below:

$$\text{Percentage of weight loss} = [(Initial\ weight - Final\ weight)/Original\ weight] \times 100.$$

#### 3.35.3 Fourier-transform Infrared (FT-IR) Spectroscopy of Enzymatically treated PET

PET pieces were analyzed for changes in functional groups after incubation with recombinant enzyme by *S. maltophilia* PRS8 through Fourier-transform Infra-red (FTIR) Spectroscopy. The spectra of treated PET pieces were recorded in a frequency range 4000–400  $\text{cm}^{-1}$  wavenumber at a resolution of 4  $\text{cm}^{-1}$  at ambient temperature with helium–neon laser lamp as a source of IR radiation. Abiotic control was analyzed along with test samples for comparison.

***CHAPTER 4***  
***RESULTS***

---

## Results

### 4.1 Collection of Sample

Polyethylene terephthalate (PET) bottle and soil samples were collected from a garbage dumping site located in Peshawar, Ring road (Peshawar, Khyber Pakhtunkhwa) at N 34.0074° and E 71.6194° (Fig 4.1). Temperature and pH was recorded as 37.0°C and 7.0 respectively. The physical features of samples are described in table 4.1.

### 4.2 Isolation of bacteria

Plastic contaminated soil was screened for isolation of PET degrading bacterial strains. A total of 24 bacterial strains were isolated on nutrient agar plates, 19 from soil while 05 from PET bottle sample. Colonies forming unit/ml were calculated as  $5 \times 10^{-6}$  for soil sample, whereas  $3 \times 10^{-5}$  for PET bottle.

### 4.3 Screening of bacterial isolates for PET degradation

The 24 bacterial strains were screened for polyethylene terephthalate (PET) biodegradation. The bacterial strains were inoculated into minimal salt medium (MSM) containing PET as the sole carbon source and then incubated for 28 days at 35°C. By the end of experiment, only 03 bacterial strains designated as PRS3, PRS6 and PRS8 could survive and grew well during the rigorous screening period while utilizing PET as sole carbon source. Among the above 3 strains, strain PRS8 was selected on the basis of rapid growth in the presence of PET for further study (Fig 4.2).

### 4.4 Identification of PET degrading bacterial strain PRS8

#### 4.4.1 Growth of Bacterial strain

Bacterial strain PRS8 was grown on nutrient agar (NA) and nutrient broth (NB). Rapid and highest growth was observed at 35°C within 24 hours.

#### 4.4.2 Macroscopic and Microscopic Characteristics

The colonial characteristics were considered to examine the cellular morphology of strain PRS8. The bacterium was yellowish in color with pointed and small colonies on nutrient agar plates. Gram's staining results indicated that strain PRS8 was gram negative upon microscopic examination.

#### 4.4.3 Biochemical characteristics

Biochemical properties of PET degrading bacterial strain PRS8 are presented in table 4.2. Biochemical characteristics revealed that strain was citrate, urease, and catalase positive while negative for oxidase and indole test.

#### 4.4.4 Molecular identification os strain PRS8

16S rRNA gene sequencing of strain PRS8 demonstrated closest alignment to the phylum *Pseudomonadota*, genus *Stenotrophomonas*. A phylogenetic tree constructed by Neighbor-Joining method presented 100% similarity of strain PRS8 with *Stenotrophomonas maltophilia*. The sequence was submitted to NCBI database under accession number OK510364 (Fig. 4.3).



**Figure 4.1:** Samples from plastic disposal site for isolation of PET degrading bacteria

**Table 4.1:** Soil physical characteristics at the time of sampling

S No	Physical features	Results
1	Temperature	37.0 °C
2	pH	7.0
3	Texture	Grey moisture soil

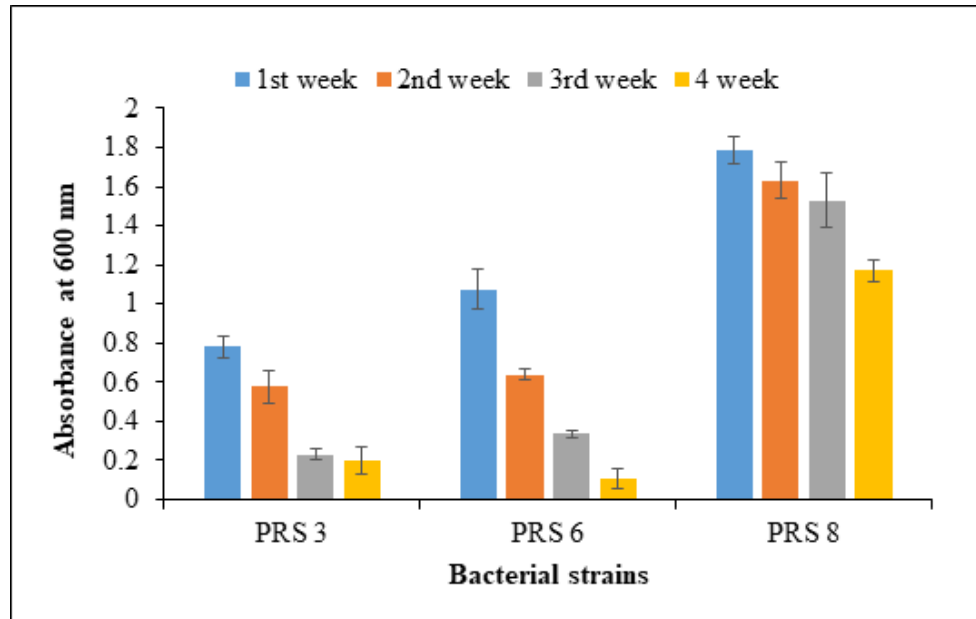


**Figure 4.2:** Bacterial growth in the minimal salt medium containing PET as the sole carbon source after 28 days of incubation

**Table 4.2:** Physiological and biochemical properties of bacterial strain PRS8

Tests	Result
Colony Morphology	Yellowish, pointed and small colonies with regular margins
Shape	Rod shaped
Temperature (°C)	30 °C – 45 °C
pH Range	6.0 – 8.0
Gram's Stain	Gram-negative
Urease	Positive (+ve)
Catalase	Positive (+ve)
Citrate	Positive (+ve)
Triple Sugar Iron	No Glucose fermenter
Maconkey's Agar	Non Lactose Fermenter
Oxidase	Negative (-ve)
Indole Test	Negative (-ve)

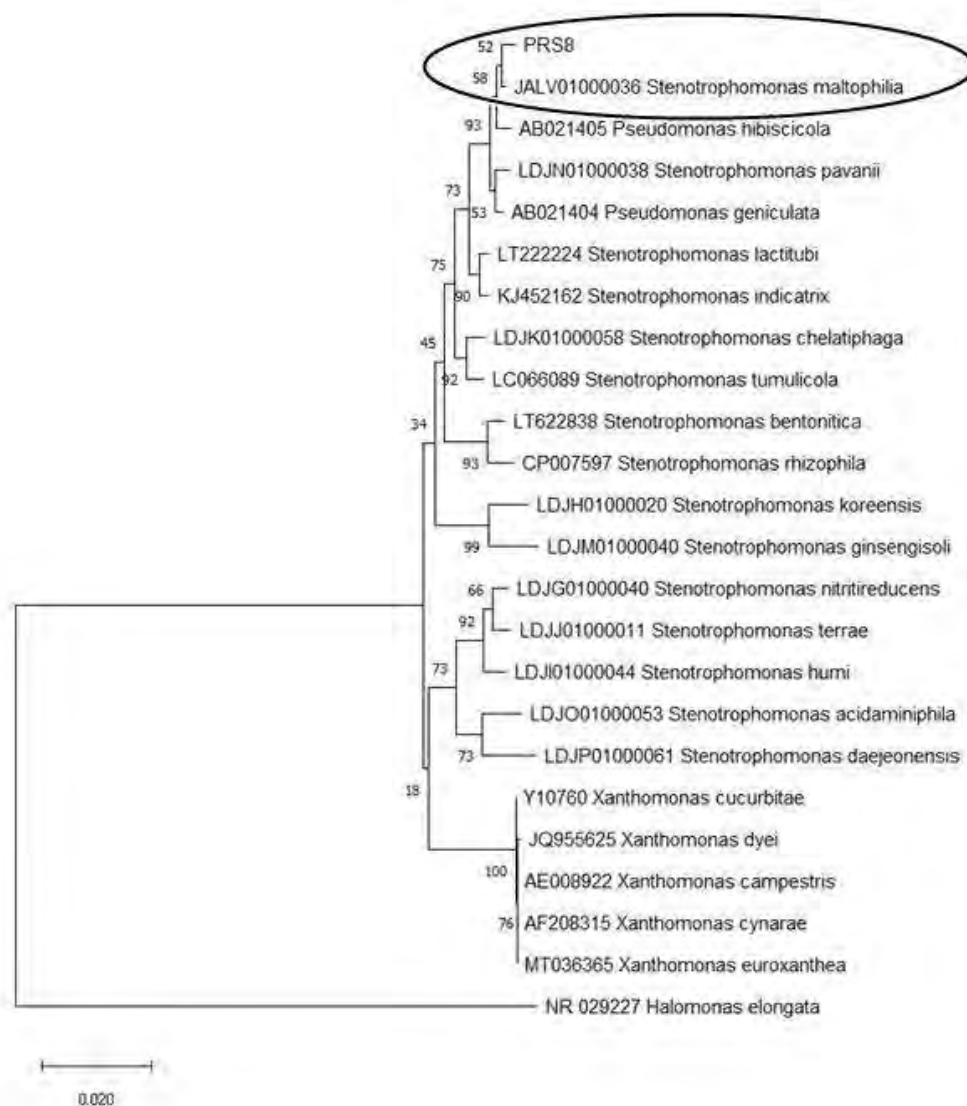


**Figure. 4.3:** Neighbour-joining tree based on 16S rRNA gene sequences showing the phylogenetic position of strain PRS8 and representatives of some other related taxa. For out group *Halomonas elongata* was used. Bootstrap standards were analyzed as % of 1200 replications not <50% are shown at the branching points bar 0.02 substitutions per nucleotide position was identified *Stenotrophomonas maltophilia*.

## 4.5 Biofilm Assays of *S. maltophilia* PRS8

### 4.5.1 Congo red agar

*S. maltophilia* strain PRS8 was streaked on congo red plate containing brain heart infusion agar (BHIA) along with sucrose, congo red dye showed results as light brown colonies on its surface indicating their ability to produce biofilm. The standard set is from red (weak biofilm former) to brown (strong biofilm former) colonies. The light brown colonies that appeared on the surface of congo red agar indicated that strain PRS8 was moderate biofilm former (Fig. 4.4).

### 4.5.2 Microtitre Plate Assay

Biofilm formation ability of *S. maltophilia* strain PRS8 was determined in a microtiter plate with a positive and negative control. After 48 hours of incubation, a good amount of biofilm was detected in microtiter plate wells inoculated with *S. maltophilia* strain PRS8 and *Pseudomonas aeruginosa* (positive control), while no biofilm was observed in un-inoculated wells (negative control) (Fig 4.5). The wells containing strain PRS8 showed an absorbance (600 nm) of 1.18 and positive control (*Pseudomonas aeruginosa*) 1.39 respectively. Similarly, the un-inoculated wells as negative control value was recorded 0.1. The biofilm ability on the surface of PET with bacterial strain PRS8 was monitored 1.94 at 600 nm (Fig 4.6). The results indicated that *S. maltophilia* PRS8 strain demonstrated biofilm formation even at the surface of PET pieces thus showing its ability to attach to PET that could be helpful in its degradation.

## 4.6 Evaluation bacterial Hydrophobicity

*S. maltophilia* PRS8 strain clearly showed higher hydrophobicity as evident from bacterial adhesion to hexadecane hydrocarbon (BATH) assay. The adhesion of strain PRS8 to hexadecane was high even at low hydrocarbon concentration (0.32 mL), which resulted in to a decrease of more than 17% turbidity of culture in mid-logarithmic phase (Fig. 4.7 A and B). It was confirmed that bacterial strain PRS8 was more hydrophobic in nature. As PET is hydrophobic in nature, so this hydrophobic-hydrophobic interaction was helpful in bacterial adhesion to the surface of PET piece and ultimately facilitated the degradation of PET films.





**Figure 4.4:** *S. maltophilia* strain PRS8 biofilm on the surface of BHI Congo red agar

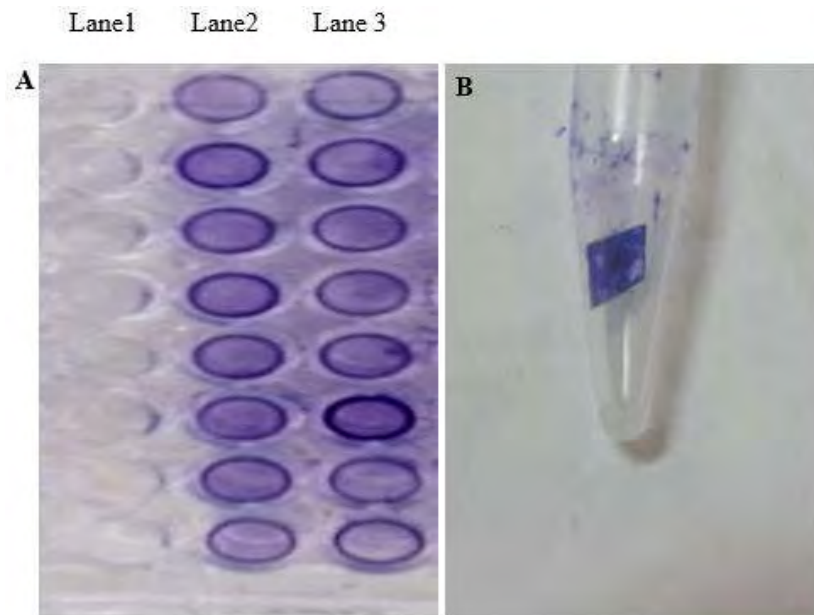


**Figure 4.5:** *S. maltophilia* PRS8 strain biofilm forming on Microtiter plate and on PET piece after crystal violet fixation(A) The biofilm forming ability of *S. maltophilia* PRS8 on Microtiter plate after treatment with crystal violet, (Lane 1), Negative control; (Lane 2), Positive control *Pseudomonas aeruginosa*; (Lane 3), *S. maltophilia* PRS8 biofilm in the wells (B) The biofilm forming ability of PRS8 strain on the surface of PET

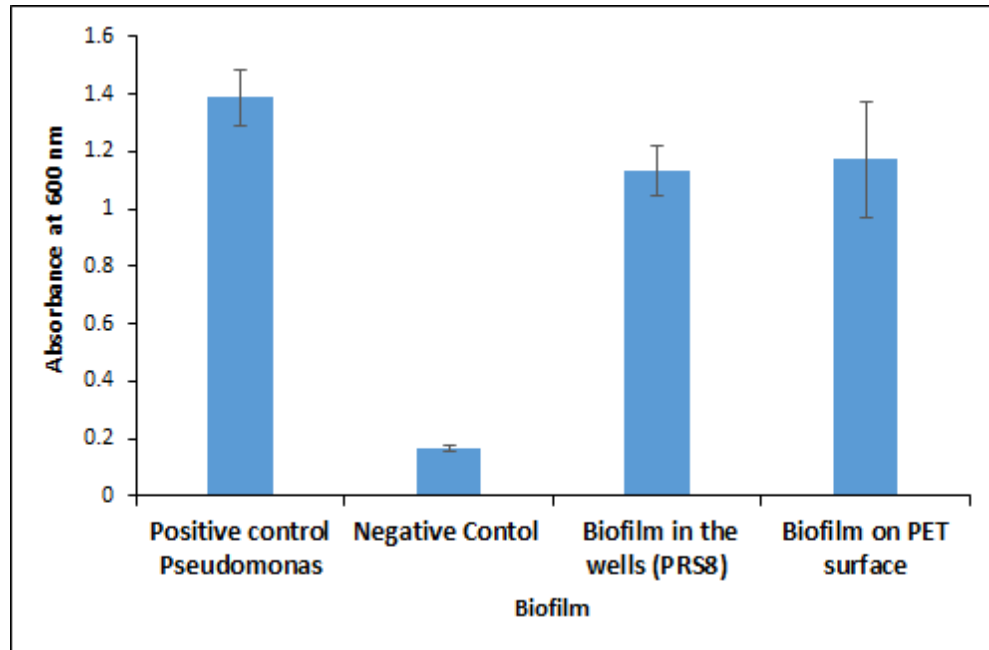


**Figure 4.6:** The biofilm forming ability of *S. maltophilia* PRS8 strain on microtiter plate and on PET piece

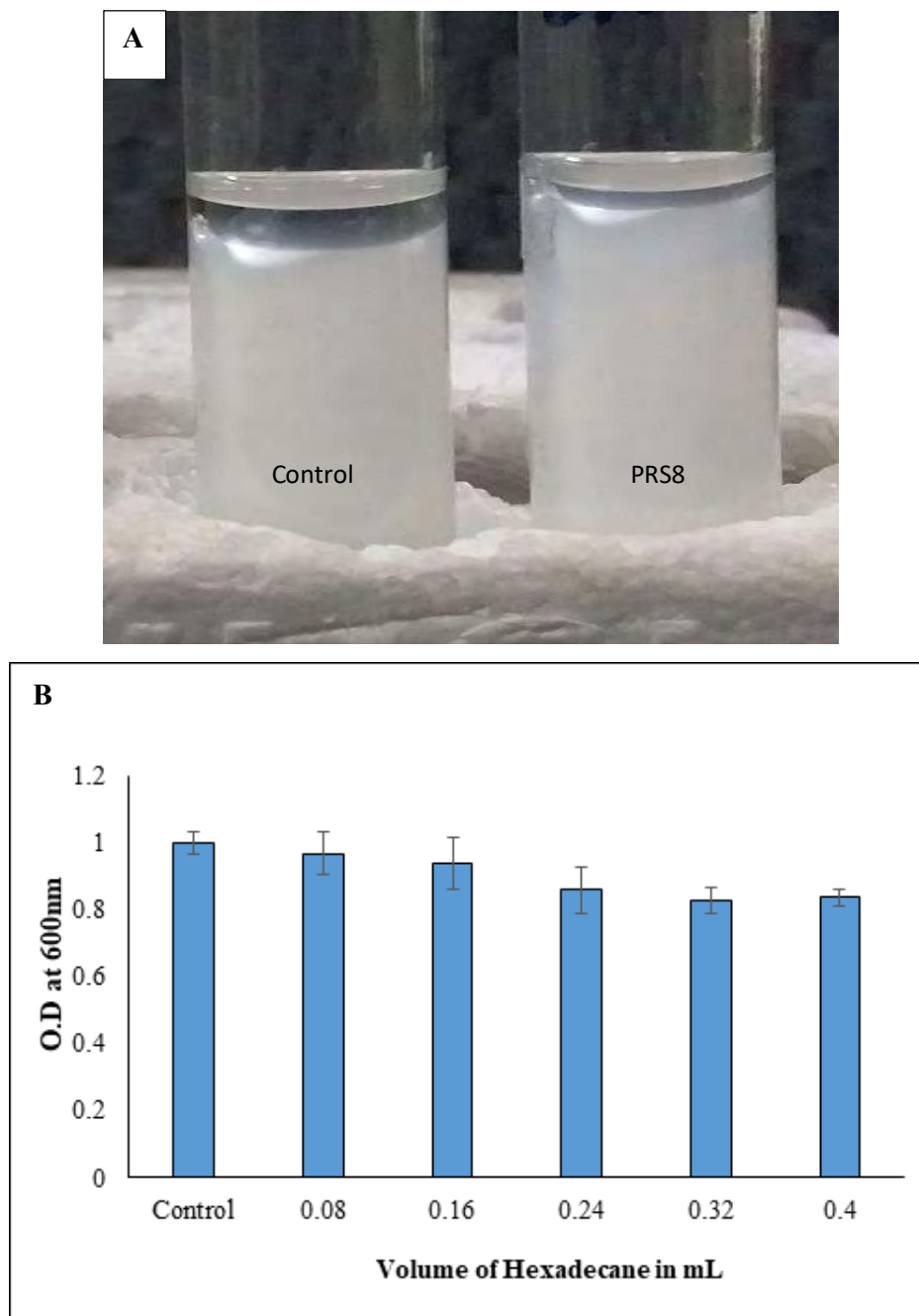


**Figure 4.7:** Hydrophobicity of *S. maltophilia* PRS8 strain resulted by the bacterial cells adhesion to hexadecane hydrocarbon. (A) Phase separation of aqueous phase and organic phase after the addition of hexadecane in comparison with control. (B) Hydrophobic cells moved from the aqueous phase to the hexadecane phase, reflecting as a decreased in the turbidity of the bacterial suspension.

#### 4.7 Qualitative Cutinase Assay using PCL agar plate

Cutinase activity was determined on polycaprolactone agar plate (PCL). *S. maltophilia* PRS8 was inoculated on PCL agar plate and incubated at 35 °C for 48 h. After incubation, clear zones were observed around bacterial colonies that revealed hydrolytic action of cutinase against PCL (Fig. 4.8).

#### 4.8 Analysis of Degradation of PET by *S. maltophilia* PRS8

The degradation experiment was carried out with *S. maltophilia* PRS8 against PET (30 mg) pieces as the sole carbon source in the degradation medium and incubated for 28 days.

##### 4.8.1 Determination of dry weight of residual PET

The measurement of weight reduction is an easy and quick method to measure the degradation of PET by desired bacterial strain. The PET pieces were recovered from both test and control flasks at the end of the experiment after 28 days and their weight was measured. Approximately 1.2% reduction in weight of PET pieces was measured in comparison to control where no loss was found (Fig. 4.9).

##### 4.8.2 Fourier-transform infrared (FT-IR) spectroscopy

The PET treated with *S. maltophilia* PRS8 and the untreated PET (control) were analyzed using FTIR. The FTIR spectra were normalized at 1410 cm<sup>-1</sup> (aromatic ring vibrations), according to the literature (Drobot et al., 2013). The characteristic peaks (722, 870, 1016, 1098, 1244, and 1713 cm<sup>-1</sup>) were clearly observed. The treated PET slightly reduced the intensity of the FTIR peaks at 722, 1098, 1242, and 1714 cm<sup>-1</sup> (Figure 4.10) compared to the untreated PET, indicating a surface degradation by *S. maltophilia* PRS8.

##### 4.8.3 Scanning Electron Microscopy (SEM)

The changes in surface morphology of PET pieces after incubation with *S. maltophilia* PRS8 were visualized through SEM. In comparison to control, SEM images of test samples showed clear deterioration of PET pieces with holes, cracks and roughness of its surface at different points. The untreated PET piece was observed

clear and smooth without any roughness on surface. These changes clearly indicate enzymatic hydrolysis of PET pieces during incubation with *S. maltophilia* PRS8 (Figure 4.11).

#### 4.8.4 Quantitative Assay for Cutinase activity and total protein by *S. maltophilia* PRS8

The enzyme activity and total protein was determined in samples collected from degradation experiment after every 48 hours. A gradual increase in cutinase activity and protein content was observed during first few weeks followed by a gradual reduction near the end of the experiment. The maximum cutinase activity was measured as 39.74 U/mL with protein content 0.066 mg/mL after 22 days of incubation (Fig. 4.12).

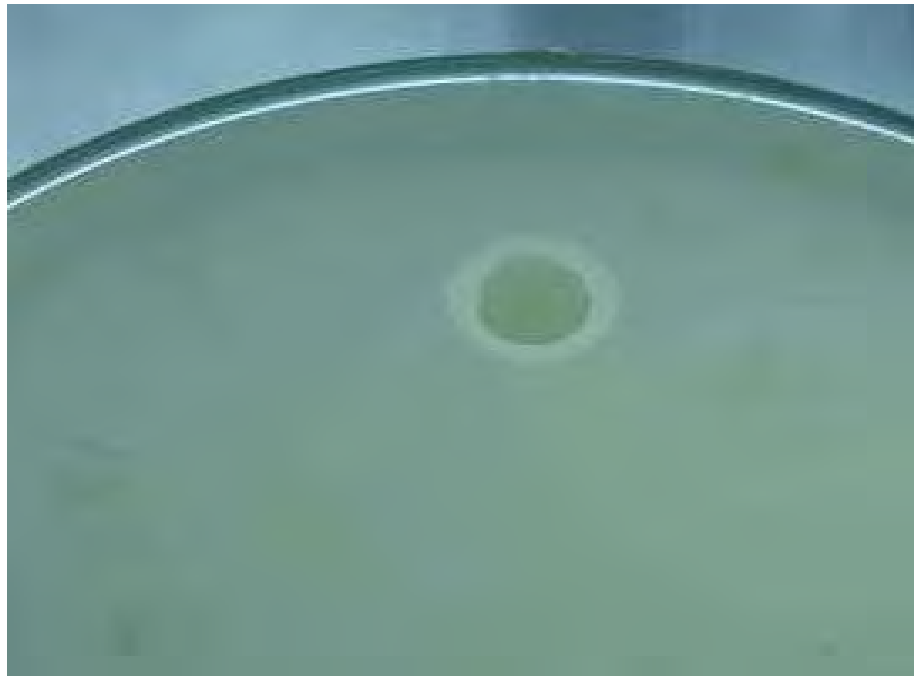


**Figure 4.8:** Expression of cutinase activity by *S. maltophilia* PRS8 strain, clear zone around colony on PCL agar showed cutinase activity

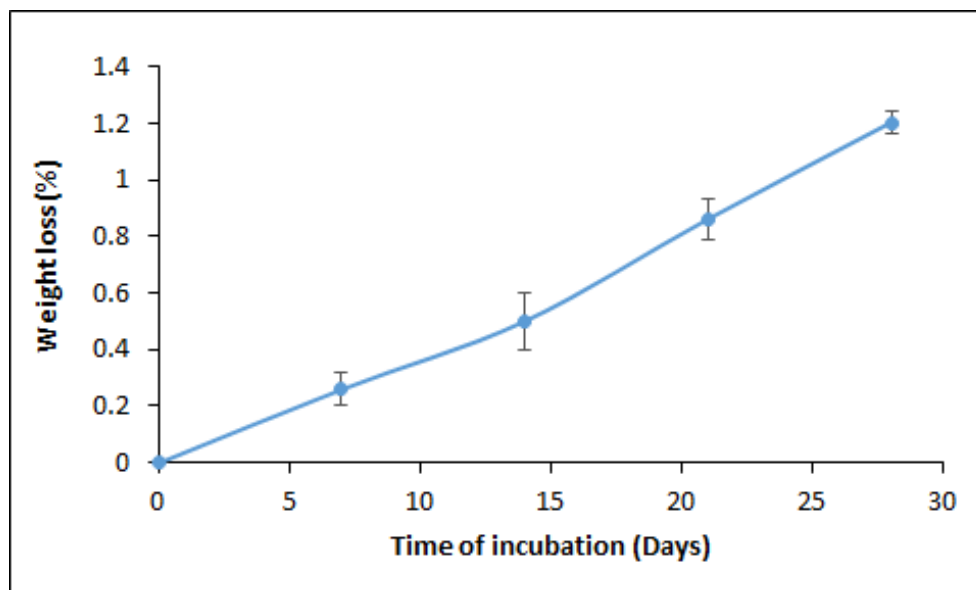


**Figure. 4.9:** Percent of weight reduction in PET by *S. maltophilia* PRS8 strain

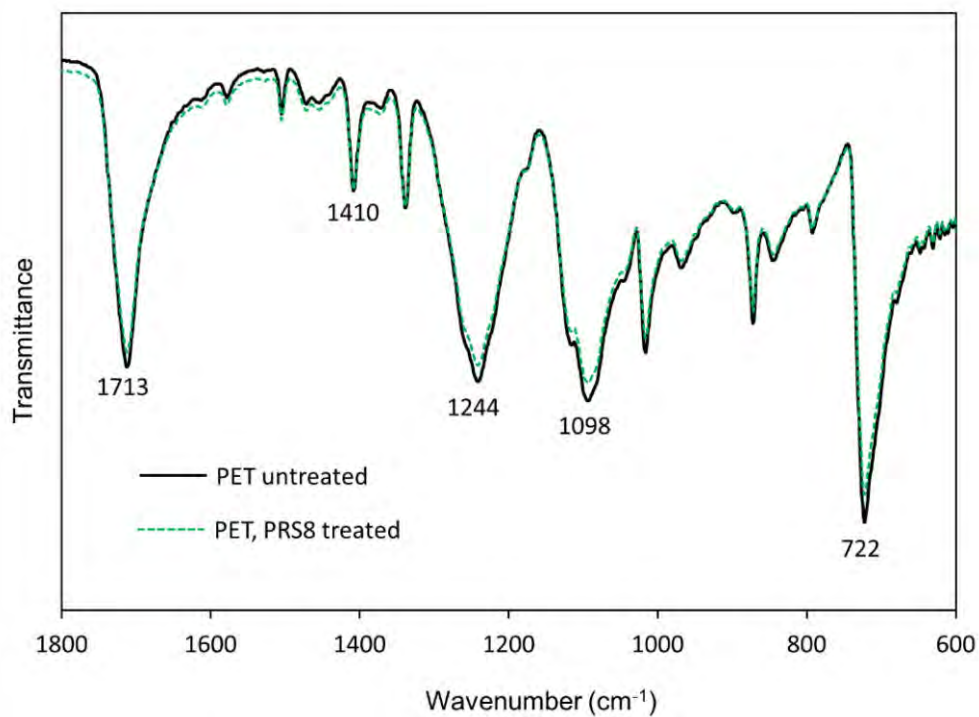


**Figure: 4.10** Expanded FT-IR spectra of PET after 28 days, abiotic control untreated (black solid curve) and PET treated with *S. maltophilia* PRS8 strain (Green dotted curve).

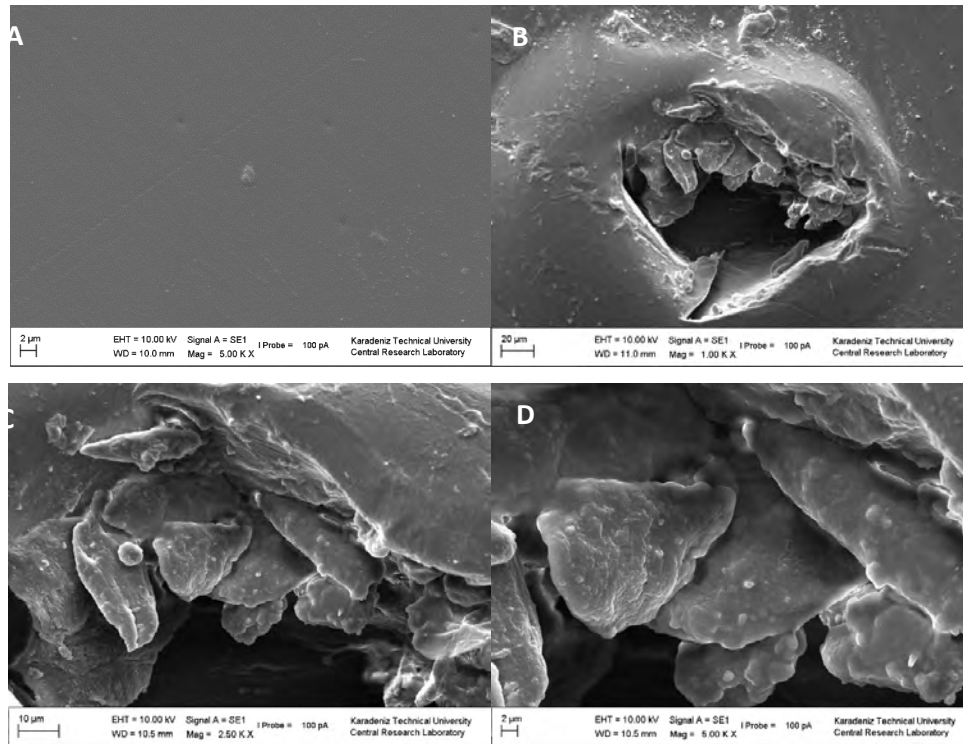


**Fig 4.11** SEM images of *S. maltophilia* PRS8 treated PET compared with untreated PET 28 days (A) Control un-treated (x5.00K) (BCD) Micrographs of biodegraded PET (x1.0K, x2.5K, x5.00K).

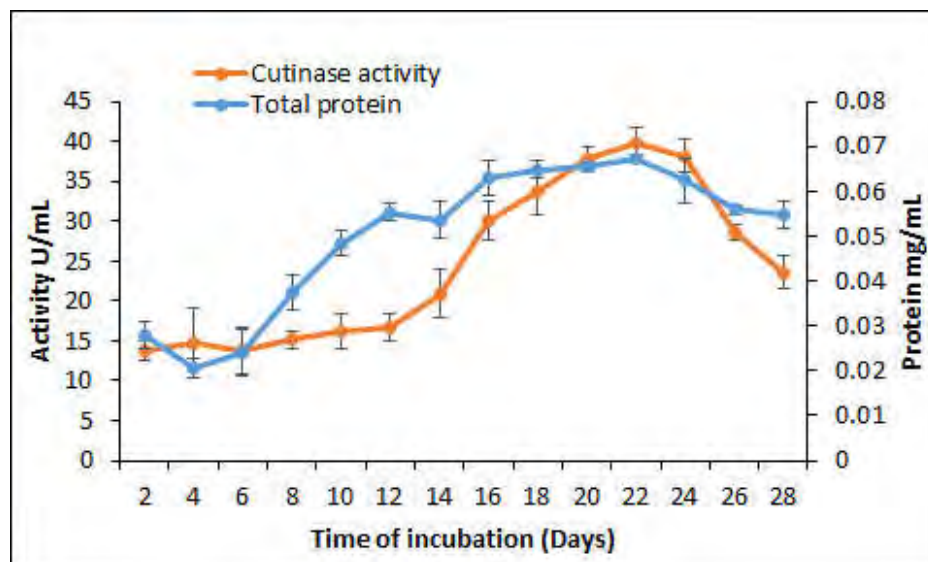


**Figure 4.12:** Cutinase enzyme activity and total protein in cell free supernatant by *S. maltophilia* PRS8 strain during biodegradation of PET piece as a carbon source in MSM media.



#### 4.9 Standardization of enzyme assay conditions

After verification of cutinase production by *S. maltophilia* PRS8, the enzyme conditions were optimized. Maximum activity was achieved after 30 minutes of incubation. Temperature and pH was recorded as 40.0°C and 8.0 respectively, while enzyme concentration and substrate concentration was achieved as 200  $\mu$ L and 80  $\mu$ L respectively.

#### 4.10 Optimization of physico-chemical parameters for Cutinase production by *S. maltophilia* PRS8

##### 4.10.1 Effect of temperature

The production of cutinase from *S. maltophilia* PRS8 strain was observed by incubating the production medium at temperatures ranges from 25 to 45°C. The samples were taken at every 24 hours interval upto the period of 72 hours for protein estimation and enzyme assay. Maximum specific activity (56.68 U/mg) was achieved at 35°C after 48 hours, while the activity was dropped at temperatures above 35°C and below 30°C (Fig. 4.13).

##### 4.10.2 Effect of pH

The production of cutinase from strain PRS8 was observed by incubating in the production medium at a wide range of pH (5.0 to 10.0). *S. maltophilia* PRS8 strain displayed maximum activity between pH 6.0 to 8.0 with highest specific activity (71.88 U/mg) at pH 8.0 after 48 hours of incubation. A decline in enzyme activity was observed at above or below this pH range (Fig. 4.14).

##### 4.10.3 Effect of Incubation Time

The effect of incubation time on production of enzyme from *S. maltophilia* PRS8 strain was analyzed after every 24 hours up to the maximum of 72 hours. Maximum specific activity was achieved after 48 hours of incubation (44.83 U/mg) along with other optimum conditions such as pH and temperature (Fig. 4.15).



#### **4.10.4 Effect of inoculum size**

The production of cutinase was analyzed at different concentrations of inoculum size ranging from 0.1% to 3%. The samples were withdrawn after every 24 hours for a period of 72 hours for protein estimation and enzyme assay. Maximum specific activity 52.82 U/mg was achieved at 2% inoculum size after 48 hours of incubation. A considerable decrease in enzyme activity was determined at below and above 48 hours (Fig. 4.16).

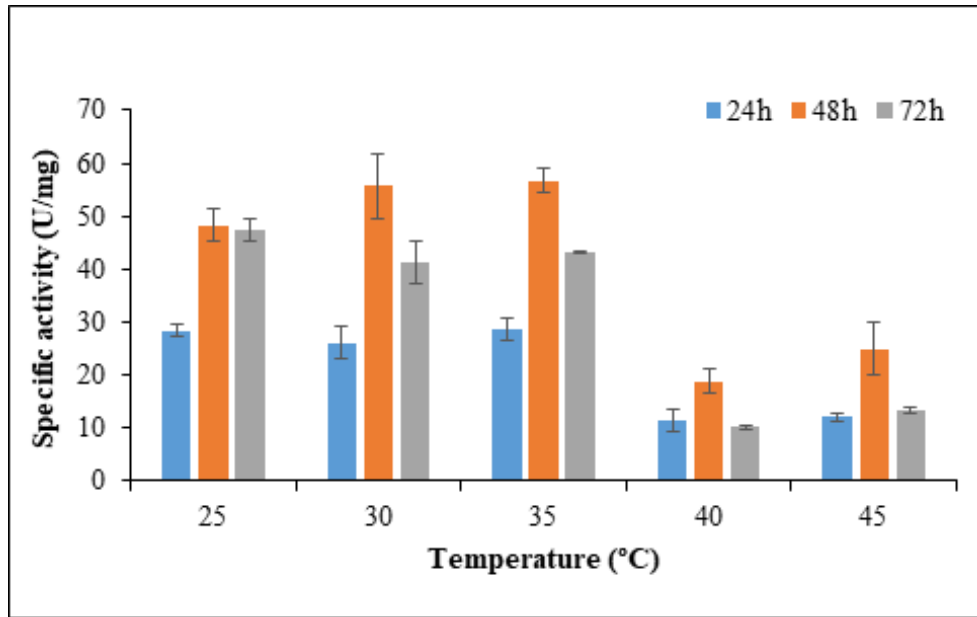


**Figure 4.13:** Effect of temperature on production of cutinase from *S. maltophilia* PRS8 strain within 24–72 hours of incubation

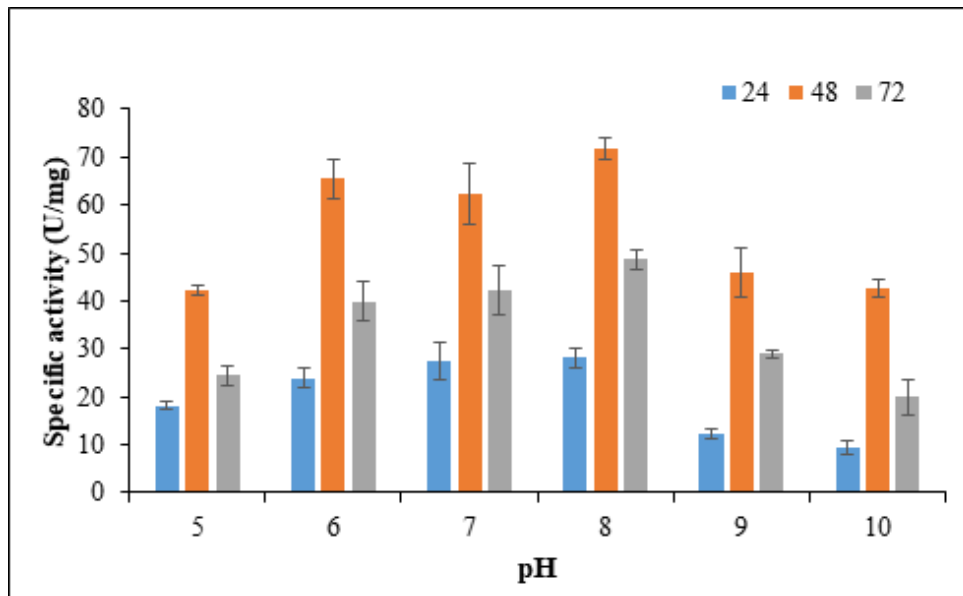


**Figure 4.14:** Effect of pH on production of cutinase from *S. maltophilia* PRS8 strain within 24–72 hours of incubation

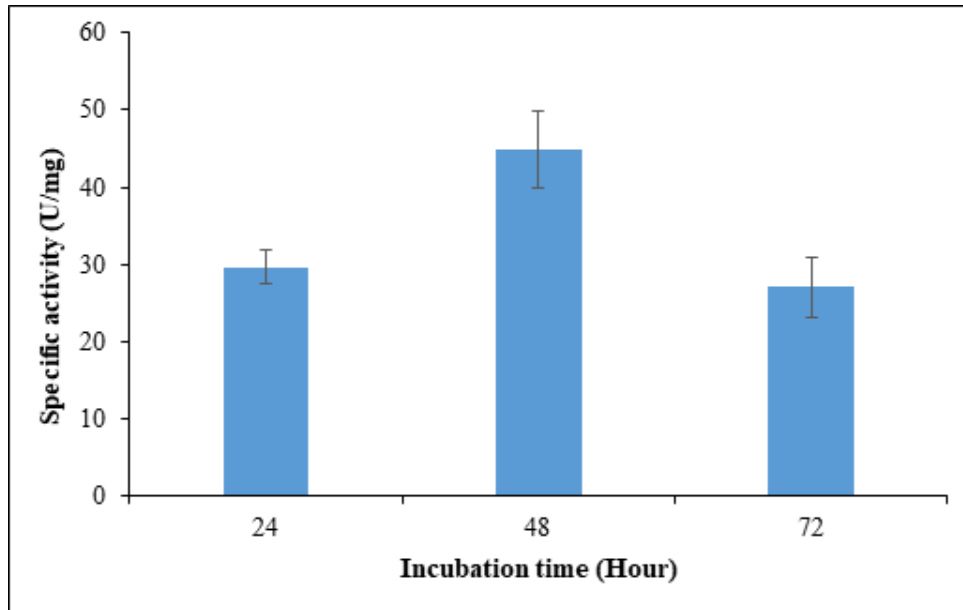


**Figure 4.15:** Effect of incubation time on production of cutinase from *S. maltophilia* PRS8 strain within 24–72 hours of incubation

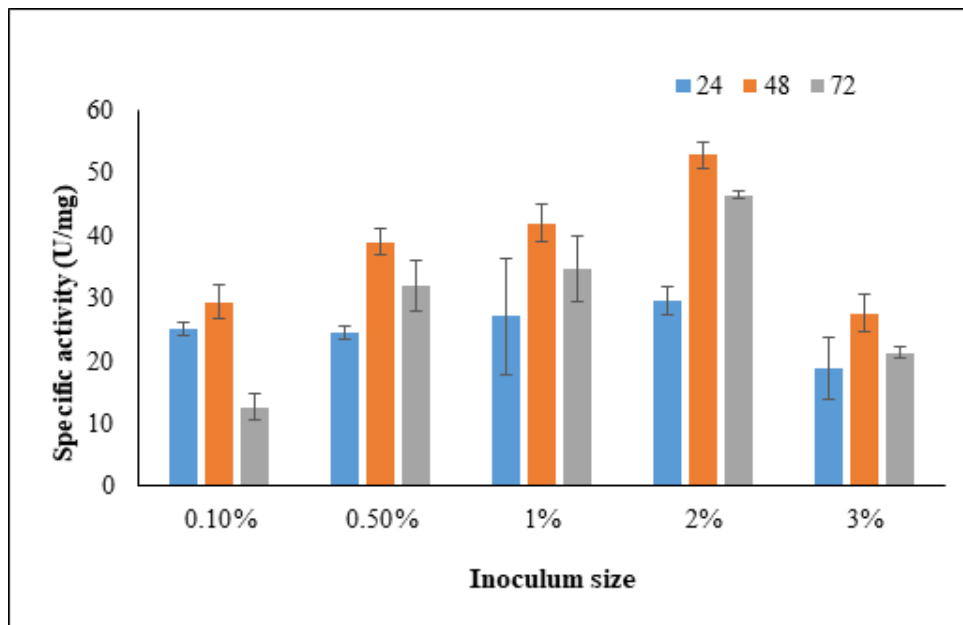


**Figure 4.16:** Effect of inoculum size on production of cutinase from *S. maltophilia* PRS8 strain within 24–72 hours of incubation

#### 4.11 Plackett Burman Design for optimizing of nutritional condition

Plackett-Burman Design (PBD) was employed for independent variables that had an effect on cutinase production from *S. maltophilia* PRS8 (Table.4.3). In this design, total 11 nutritional factors were evaluated in 15 trials and maximum cutinase activity was obtained in trial 14 (313.96 U/mg) and lowest activity (46.85 U/mg) was found in run number 7 (Fig. 4.17). All trails were conducted in triplicates according to the software's instructions. Out of 11 factors, Cutin, NaNO<sub>3</sub>, and (NH<sub>4</sub>)<sub>2</sub>SO<sub>4</sub> were found to have a considerable influence on cutinase synthesis as apparent from the values of "Prob > F" of each element (Fig. 4.18).

The model equation for cutinase activity (U/mg) (R) could be stated as follows:

$$\text{Specific activity (R)} = (169.39) + (20.51A) + (5.78B) + (-2.27C) + (34.34D) + (11.90E) + (2.74G) + (4.27H) + (46.82J) + (-6.53K) + (22.26L)$$

The model F-value was calculated as 9.56 with "Prob F" values < 0.050 identified that the model is significant statistically. Values in the model showed higher than 0.1000 are not significant terms in model. If the insignificant terms in model are many (not including those mandatory to the maintenance hierarchy), model reduction may improve the model. The "Curvature F-value" of 12.59 suggests in the model significant curvature (as calculated by alteration between the normal of the center points and factorial points of the average) in the design space. According to the model, 3.81% high "F-Value" could occur due to noise. "Prob F" values < 0.050 also showed that model is significant (Table 4.4).

#### 4.12 Optimization of significant variable using Central Composite Design (CCD)

A two-level CCD was run to screen the significant components obtained by Plackett-Burman Design. The model included 3 elements and their influence on cutinase activity was investigated in total 20 runs (Table 4.5). The model included three factors, specified by their codes, obtained from PBD and their effect was studied in 20 runs. Maximum specific activity 369.93 U/mg was achieved at run number 3 (Fig. 4.19). In this model, the linear terms A, B, C and interactive terms AB, AC and BC were significant model terms, whereas A represent cutin, B represent NaNO<sub>3</sub> while, C

represent  $(\text{NH}_4)_2\text{SO}_4$ . ANOVA was used to assess the model's significant elements (Table 4.6). The following second order polynomial equation was applied by multiple regression analysis on the experimental data to describe the cutinase activity (U/mg).

$$\text{Specific Activity (U/mg)} = +221.45 + 31.51A + 51.23B - 14.30C + 77.22AB + 51.02AC - 51.51BC$$

Factors A-C shows linear terms and AB, AC and BC represent interactive terms. Response surface plot (AB) in (Fig 4.20) shows an increase in cutin and  $\text{NaNO}_3$  potentially enhanced enzyme activity, both factors had positive effect on enzyme activity. Same response plot (AC) in (Fig 4.21) shows the highest cutinase activity by increasing cutin and decreasing  $(\text{NH}_4)_2\text{SO}_4$  concentration. Cutin had positive effect and  $(\text{NH}_4)_2\text{SO}_4$  had negative effect on cutinase activity. Similarly, response surface plot (BC) in (Fig 4.22) shows, that increase in  $\text{NaNO}_3$  and  $(\text{NH}_4)_2\text{SO}_4$  potentially enhanced enzyme activity, both had positive effect on enzyme activity. The F-value of 6.70 ( $p > 0.050$ ) showed the model was found to be statistically significant. In the model, 0.21% chance that such a high "F-Value" could be due to noise. Response surface plot (AB, AC and BC) shows both factors had potential influence on cutinase activity with maximum regression coefficient, AB (77.22) followed by AC (51.02) and BC (51.19). Values are higher than 0.1000 which shows that model is not significant. If the insignificant terms in model are many (not including those mandatory to maintenance hierarchy), model reduction may improve it.

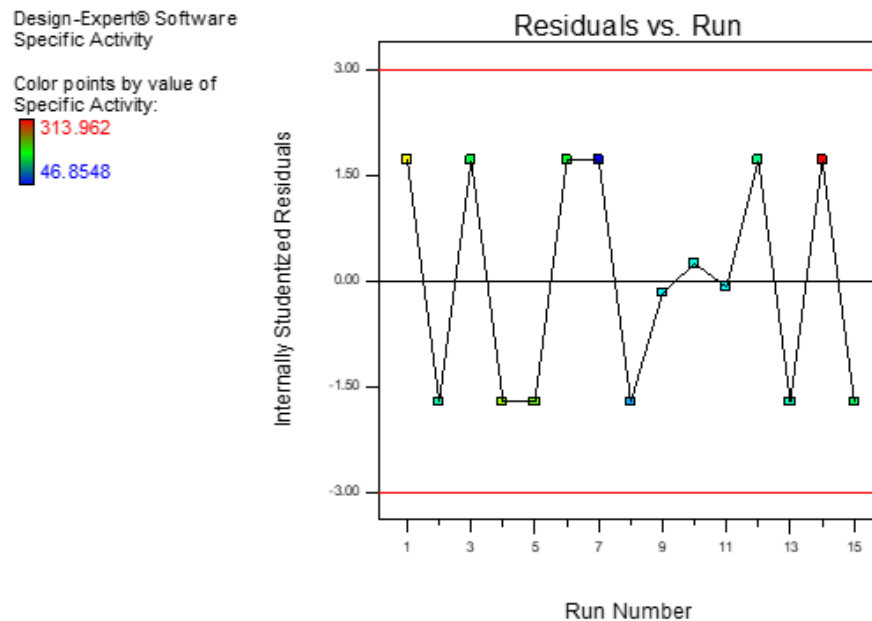


**Figure. 4.17** Plackett Burman design of residuals vs run showed color point by value of specific enzyme activity (U/mg) as response of run number.

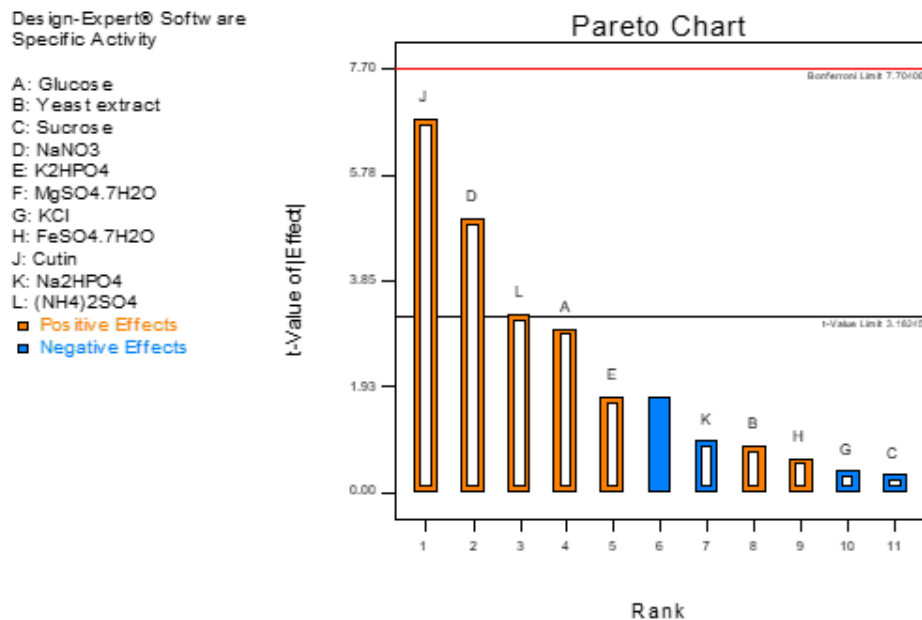


**Figure 4.18** Pareto chart showing the effect of t value by important factors [J, cutin; D, NaNO<sub>3</sub> and L (NH<sub>4</sub>)<sub>2</sub>SO<sub>4</sub>] generated by the PBD with respect to the effect on the cutinase enzyme production

**Table 4.3:** Plackett Burman design of factors with specific enzyme activity (U/mg) as response

Run	Glucose (%)	Yeast Extract (%)	Sucrose (%)	NaNO <sub>3</sub> (%)	K <sub>2</sub> HPO <sub>4</sub> (%)	MgSO <sub>4</sub> 7H <sub>2</sub> O (%)	KCl (%)	FeSO <sub>4</sub> 7H <sub>2</sub> O (%)	Cutin (%)	Na <sub>2</sub> HPO <sub>4</sub> (%)	(NH <sub>4</sub> ) <sub>2</sub> SO <sub>4</sub> (%)	Response Specific Activity U/mg
1	0.7	0.9	0.50	0.50	0.20	0.02	0.90	0.01	0.60	0.20	0.30	247.59
2	0.7	0.3	1.10	0.10	0.20	0.08	0.03	0.01	0.60	0.60	0.30	131.65
3	0.7	0.9	1.10	0.50	0.08	0.02	0.03	0.01	0.20	0.60	0.50	162.54
4	1.3	0.9	0.50	0.10	0.08	0.08	0.03	0.01	0.60	0.20	0.50	222.53
5	0.7	0.3	0.50	0.50	0.08	0.08	0.90	0.00	0.60	0.60	0.50	211.55
6	1.3	0.9	1.10	0.10	0.08	0.02	0.90	0.00	0.60	0.60	0.30	169.97
7	0.7	0.3	0.50	0.10	0.08	0.02	0.03	0.00	0.20	0.20	0.30	46.85
8	0.7	0.9	1.10	0.10	0.20	0.08	0.90	0.00	0.20	0.20	0.50	93.1
9	1.0	0.6	0.80	0.30	0.14	0.05	0.47	0.00	0.40	0.40	0.40	111.51
10	1.0	0.6	0.80	0.30	0.14	0.05	0.47	0.00	0.40	0.40	0.40	119.65
11	1.0	0.6	0.80	0.30	0.14	0.05	0.47	0.00	0.40	0.40	0.40	113.09
12	1.3	0.3	0.50	0.10	0.20	0.02	0.90	0.01	0.20	0.60	0.50	146.20
13	1.3	0.3	1.10	0.50	0.08	0.08	0.90	0.01	0.20	0.20	0.30	131.46
14	1.3	0.3	1.10	0.50	0.20	0.02	0.03	0.00	0.60	0.20	0.50	313.96
15	1.3	0.9	0.50	0.50	0.20	0.08	0.03	0.00	0.20	0.60	0.30	155.26

**Table 4.4:** ANNOVA for Plackett-Burman Design

Source	Sum of Squares	Degree of Freedom	Means Square	F Value	p-value prob>F
Model	54429.80	10	5442.98	9.56	0.0445
A-Glucose	5046.98	1	5046.98	8.87	0.0587
B-Yeast extract	400.49	1	400.49	0.70	0.4631
C-Sucrose	62.07	1	62.07	0.11	0.7629
D-NaNO <sub>3</sub>	14149.43	1	14149.43	24.86	0.0155
E-K <sub>2</sub> HPO <sub>4</sub>	1700.50	1	1700.50	2.99	0.1823
F-MgSO <sub>4</sub> .7H <sub>2</sub> O	713.02	1	713.02	6.60	0.124
G-KCl	90.24	1	90.24	0.16	0.7171
H-FeSO <sub>4</sub> .7H <sub>2</sub> O	219.18	1	219.18	0.39	0.5788
I-(NH <sub>4</sub> ) <sub>2</sub> SO <sub>4</sub>	5944.86	1	5944.86	10.45	0.0481
J-Cutin	26304.84	1	26304.84	46.22	0.0065
K-Na <sub>2</sub> HPO <sub>4</sub>	511.21	1	511.21	0.90	0.4132



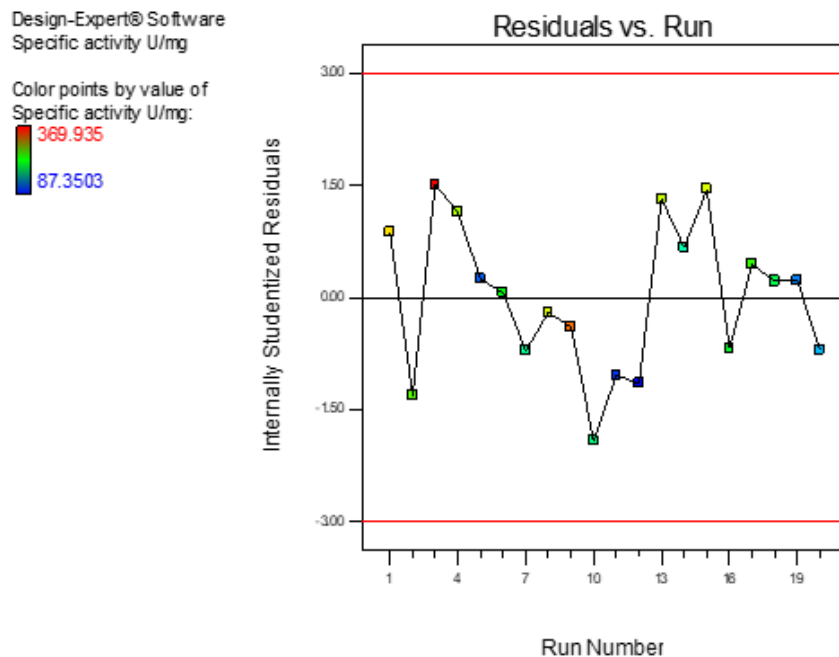


**Figure 4.19:** Central Composite design of residuals vs run showed color point by value of specific enzyme activity (U/mg) as response of run number

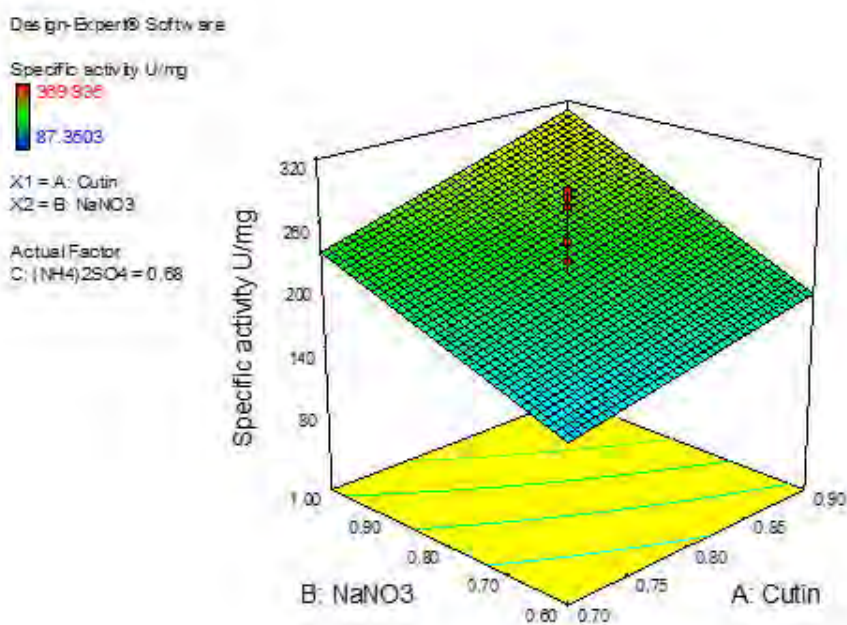


**Figure 4.20:** Three-dimensional response surface plot between Cutin and NaNO<sub>3</sub> showing the significant factor with respect to the effect on the cutinase enzyme in terms of specific activity (U/mg).

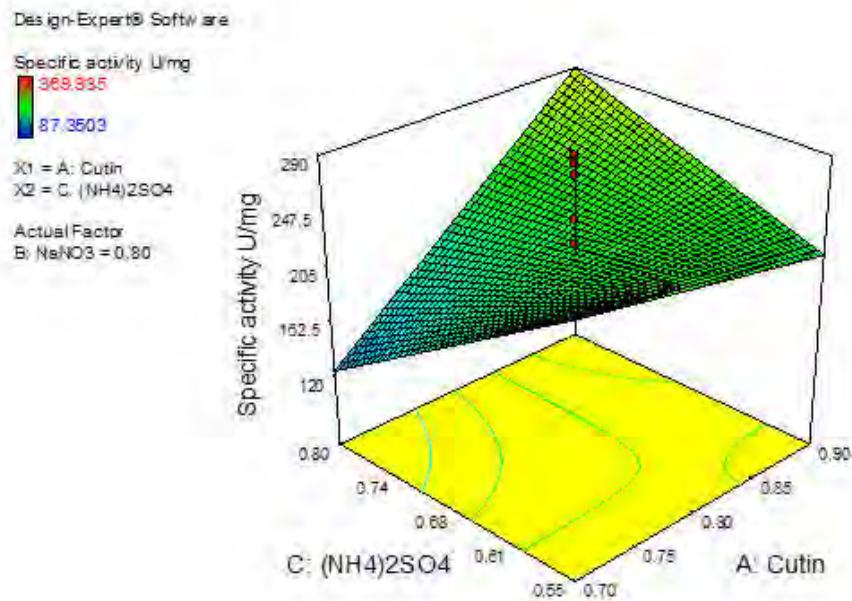


**Figure 4.21.** Three-dimensional response surface plot between cutin and (NH<sub>4</sub>)<sub>2</sub>SO<sub>4</sub> showing the significant factor with respect to the effect on the cutinase enzyme in terms of specific activity (U/mg).

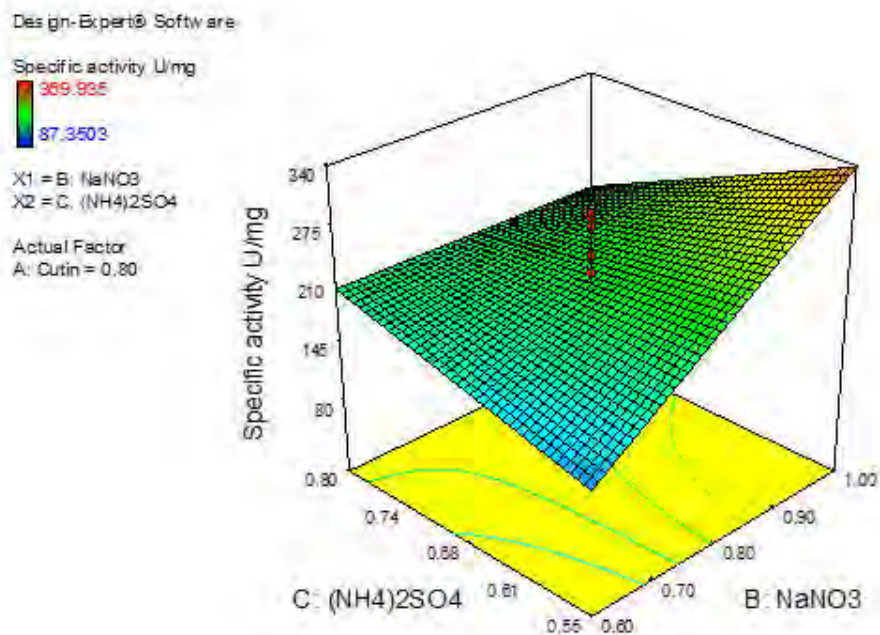


**Figure 4.22:** Three-dimensional response surface plot between NaNO<sub>3</sub> and (NH<sub>4</sub>)<sub>2</sub>SO<sub>4</sub> showing the significant factor with respect to the effect on the cutinase enzyme in terms of specific activity (U/mg).

**Table 4.5:** Central Composite design of factors with specific activity (U/mg)

Run	Factor 1	Factor 2	Factor 3	Response 1
	Cutin (%)	NaNO <sub>3</sub> (%)	(NH <sub>4</sub> ) <sub>2</sub> SO <sub>4</sub> (%)	Specific Activity U/mg
1	0.90	0.60	0.80	307.95
2	0.80	1.14	0.68	253.05
3	0.90	1.00	0.55	369.93
4	0.80	0.80	0.68	275.63
5	0.90	0.60	0.55	113.50
6	0.80	0.80	0.68	224.54
7	0.80	0.80	0.68	187.81
8	0.90	1.00	0.80	290.91
9	0.70	1.00	0.55	339.32
10	0.97	0.80	0.68	194.22
11	0.70	0.60	0.80	102.15
12	0.80	0.46	0.68	87.35
13	0.80	0.80	0.68	283.91
14	0.70	0.60	0.55	179.21
15	0.80	0.80	0.68	289.95
16	0.80	0.80	0.46	217.34
17	0.80	0.80	0.68	242.56
18	0.80	0.80	0.89	206.63
19	0.70	1.00	0.80	123.63
20	0.63	0.80	0.68	139.29

**Table 4.6:** ANNOVA for Central Composite design

Source	Sum of Squares	Degree of Freedom	Means Square	F Value	p-value prob>F
Model	8031.59	6	15778.90	6.70	0.002
A-Cutin	535.90	1	13561.64	5.75	0.0322
B- NaNO <sub>3</sub>	45.66	1	35845.94	15.21	0.0018
C-(NH <sub>4</sub> ) <sub>2</sub> SO <sub>4</sub>	1667.59	1	2794.08	1.19	0.2960
AB	1432.53	1	417.48	0.18	0.0468
AC	13.99.10	1	20825.80	8.84	0.0108
BC	406.85	1	21228.48	9.01	0.0102

### 4.13 Purification of Cutinase from *S. maltophilia* PRS8 strain

About 1000 mL cutinase production media was prepared in 2 L flask with the following composition: g/L [glucose, 13.0; (NH<sub>4</sub>)<sub>2</sub>SO<sub>4</sub>, 5.5; sucrose, 11.0; NaNO<sub>3</sub>, 11.0; K<sub>2</sub>HPO<sub>4</sub>, 2.0; Yeast Extract, 3.0; MgSO<sub>4</sub>.7H<sub>2</sub>O, 2.0; KCl, 3.0; cutin, 9.0; and Na<sub>2</sub>HPO<sub>4</sub>, 3.0]. The Flask was incubated with already optimized condition described previously.

#### 4.13.1 Precipitation with ammonium sulfate

Ammonium sulfate was used in various concentrations and dissolved in cell free supernatant for maximum precipitation of proteins. Maximum precipitation was obtained at 70% concentration, whereas further addition of ammonium sulfate resulted in to a drop-in enzyme activity, while enzyme activity was low at below 70% ammonium sulfate concentration. 70% of ammonium sulfate precipitation was optimum for cutinase with specific activity was 128.71 U/mg (Fig. 4.23).

#### 4.13.2 Protein purification (Sephadex G-100) column Chromatography

After dialysis, partially purified dialyzed enzyme was subjected for additional purification by column chromatography technique using Sephadex G-100 gel resin and depending on the size of their molecules, the proteins were eluted. 30 fractions were collected and all fractions were analyzed at 280 nm for total protein content and assayed for cutinase activity. Highest cutinase activity was observed in fraction 9 to 15. All of these fractions were combined up to concentrate the cutinase for highest activity (Fig. 4.24).

#### 4.13.3 Purification steps

The purification fold and total yield for precipitated and gel filtered cutinase from *S. maltophilia* PRS8 was estimated. Total yield was 48.64% and purification fold was 6.39. Table 4.7 shows various steps during purification to measure specific activity, purification fold and maximum yield.

#### 4.13.4 Molecular Weight determination (SDS-PAGE)

The fractions that contained highest activity were pooled and subjected to SDS PAGE and zymography on 10% gel. A single band of protein was appeared after staining

with Coomassie Brilliant Blue R-250. The molecular size of enzyme was determined approximately 58 kDa using standard denaturing protein marker (Fig. 4.25).

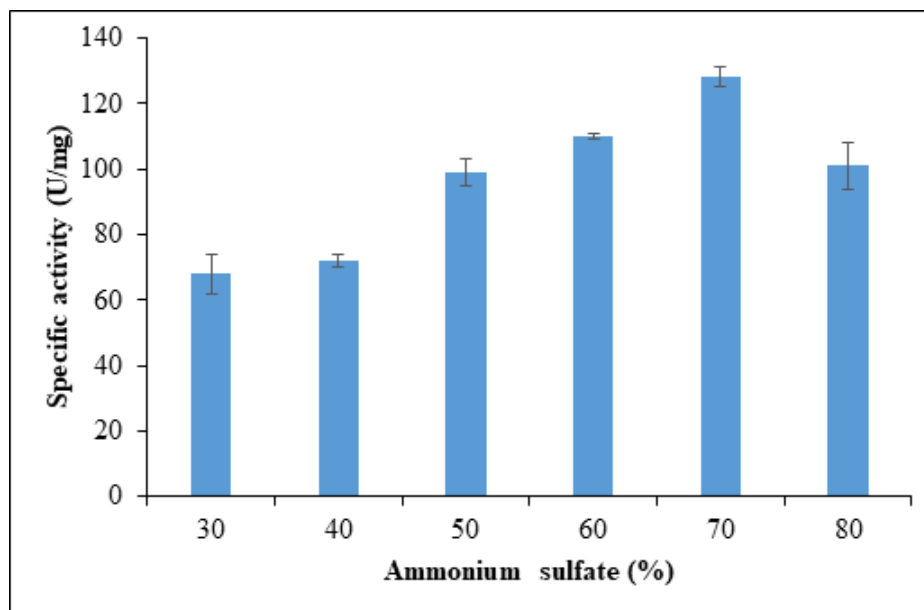


**Figure 4.23:** Ammonium Sulfate precipitation of crude cutinase from *S. maltophilia* PRS8 and evaluation of specific activities of pellet at varying ammonium sulphate precipitation percentages

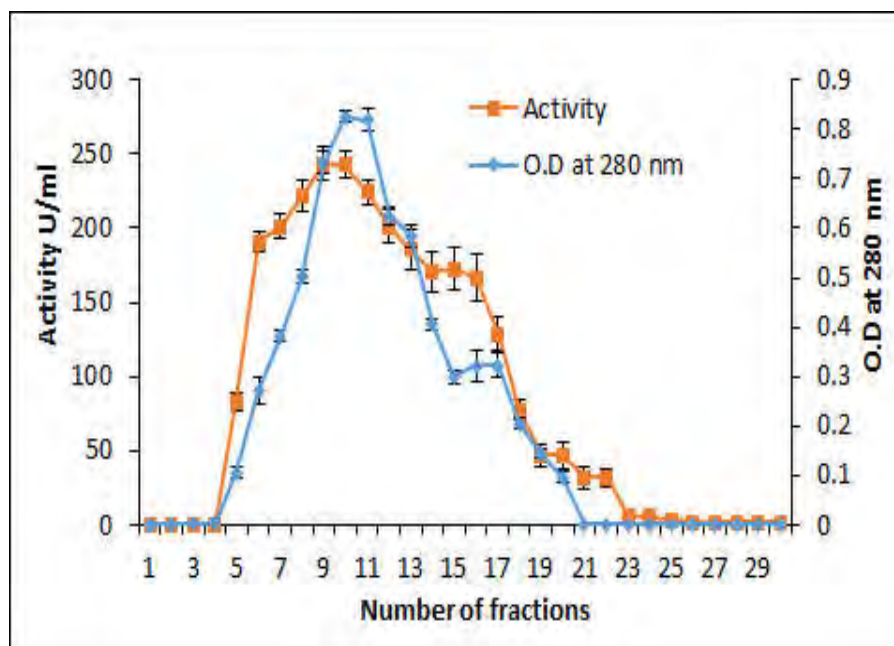


**Figure 4.24:** Total protein and cutinase activity profile by *S. maltophilia* PRS8 through Sephadex G-100 gel filtration column

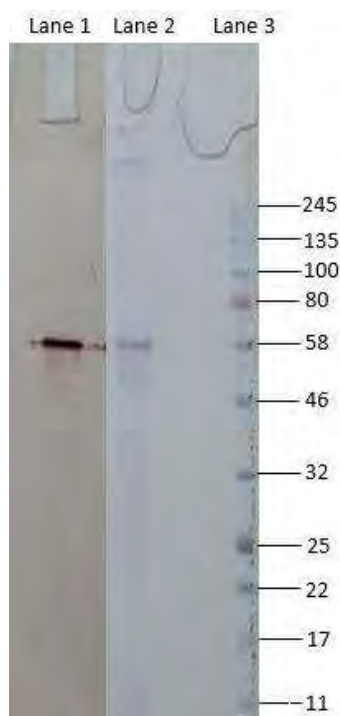


**Figure 4.25:** SDS-PAGE of cutinase from *S. maltophilia* PRS8 strain after purification by column chromatography. Lane 1, Zymogram; Lane 2, eluate from Sephadex G 100; Lane 3, (Color Prestained Protein Standard) 11-245 kDa.

**Table 4.7:** Purification steps of cutinase by *S. maltophilia* PRS8 strain

Purification Steps	Activity (U/mL)	Total Activity (Units)	Protein (mg/mL)	Specific activity (U/mg)	Yield (%)	Purification Fold
Crude Extract	138.13	69068.18	1.65	70.47	100	1
(NH <sub>4</sub> ) <sub>2</sub> SO <sub>4</sub>	260.40	52081.82	1.18	153.42	75.40	2.17
Sephadex(G 100)	373.28	33595.91	0.75	450.58	48.64	6.39

#### **4.14. Characterization of purified Cutinase**

##### **4.14.1 Effect of temperature on the activity and stability**

The effect of temperature on activity of purified cutinase from *S. maltophilia* PRS8 was analyzed by incubating enzyme in the presence of substrate at different temperatures (30 to 60°C) for 30 minutes. The purified cutinase showed maximum activity at temperature between 30-40°C with optimum achieved at 40 °C (Fig. 4.26). While the stability of purified cutinase was calculated by incubating enzyme at different temperatures (30 to 60°C) for 150 minutes. The enzyme was found stable at 40°C and retaining 95% of its activity for 150 minutes, while retained only 55% of its activity at 45°C for 150 minutes. The activity was reduced upto 10% at temperatures 50-60°C for 150 minutes (Fig. 4.27).

##### **4.14.2 Effect of pH on the Activity and Stability**

The influence of pH on activity of purified cutinase from *S. maltophilia* PRS8 was analyzed by incubating enzyme at different pH (3.0-10.0) for 30 minutes. The purified cutinase showed maximum activity at pH between 7.0-9.0 with optimum activity achieved at pH 8.0 (Fig. 4.28). While the stability of purified cutinase was calculated by incubating enzyme at different pH (3.0-10.0) for 150 minutes. The purified cutinase revealed maximum activity at wide range of pH (7.0-9.0) with optimum at pH 8.0 and retained 93% stability. The enzyme retained more than 72% of its activity at pH 6.0 and 10.0 for 150 minutes. The activity was greatly reduced at pH below 5.0 (Fig. 4.29).

##### **4.14.3 Effect of metal ions on the activity of enzyme**

Effects of the various monovalent and divalent metals on the cutinase activity were evaluated at 2 and 15 mM. CaSO<sub>4</sub>, ZnSO<sub>4</sub>, KCl, and MgSO<sub>4</sub> enhanced 10% of the enzyme activity at either concentration, while HgCl<sub>2</sub> and CdCl<sub>2</sub> strongly inhibited cutinase activity at both concentrations. Exposure to BaSO<sub>4</sub> and CoCl<sub>2</sub> enzyme retained only 50% activity. No significant effect was observed in the presence of FeSO<sub>4</sub>, NiSO<sub>4</sub> and NaSO<sub>4</sub> at both concentrations 2 mM and 15 mM (Fig 4.30).



#### 4.14.4 Effect of Surfactants on the activity of enzyme

The effect of the surfactants on the enzyme activity was evaluated by treating of purified enzymes with 0.5 and 5% of each surfactant. Among surfactants, Tween-20, Triton X-100, Tween-40, Tween-60 and Tween-80 strongly enhanced cutinase activity at both concentrations (0.5% and 5%), while CTAB and SDS suppressed cutinase activity (Fig. 4.31).

#### 4.14.5 Effect of organic solvents on the activity of enzyme

The influence of various organic solvents on cutinase activity was analyzed by incubating enzyme in a solution with 10% solvent concentration for 120 minutes. Among solvents; methanol, propanol, ethyle acetate and acetone greatly increased cutinase activity with the increase of time. Acetonitrile, DMSO and ethanol had no effect on cutinase activity and retained 100% activity for 120 minutes. Organic solvents such as ethanol and butanol suppressed enzyme activity with the passage of time and retained only 50% activity after 120 minutes (Fig. 4.32).

#### 4.14.6. Kinetic parameter of Cutinase

Lineweaver and Burk's plot was used to calculate the Michaelis Menten constant ( $K_m$ ) and rate of enzyme reaction ( $V_{max}$ ) of purified cutinase. A constant amount of enzyme was incubated with various concentrations of substrate and activity was determined.  $K_m$  and  $V_{max}$  values were recorded to be 0.703  $\mu\text{M}$  and 370.37 (U/mg), respectively (Fig. 4.33). A low  $K_m$  of enzyme revealed high affinity of cutinase toward substrate.

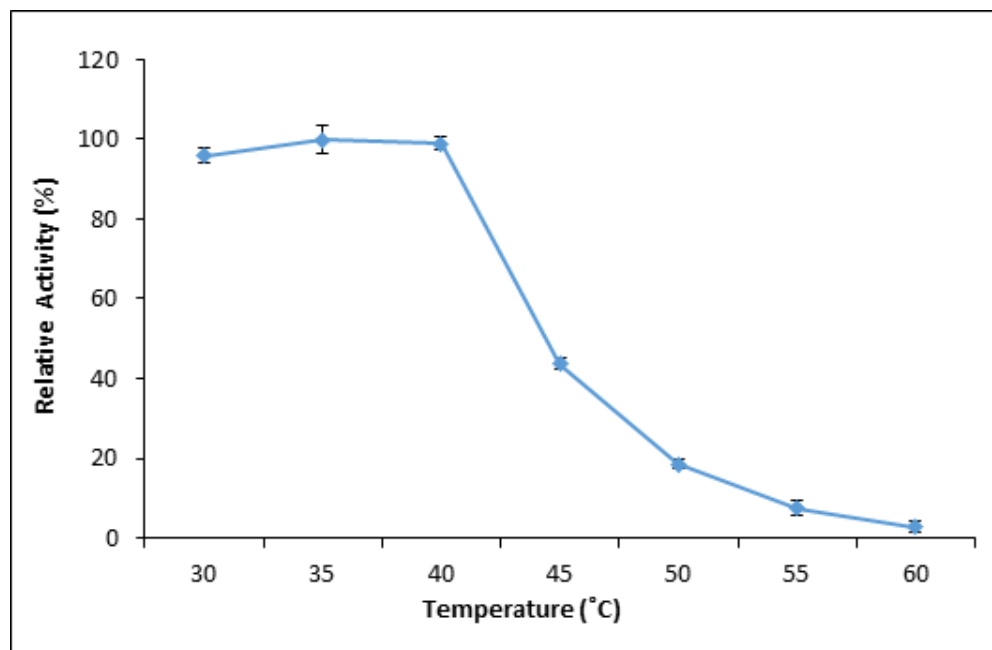


**Figure 4.26:** Effect of temperature on specific activity of purified cutinase *S. maltophilia* PRS8 strain

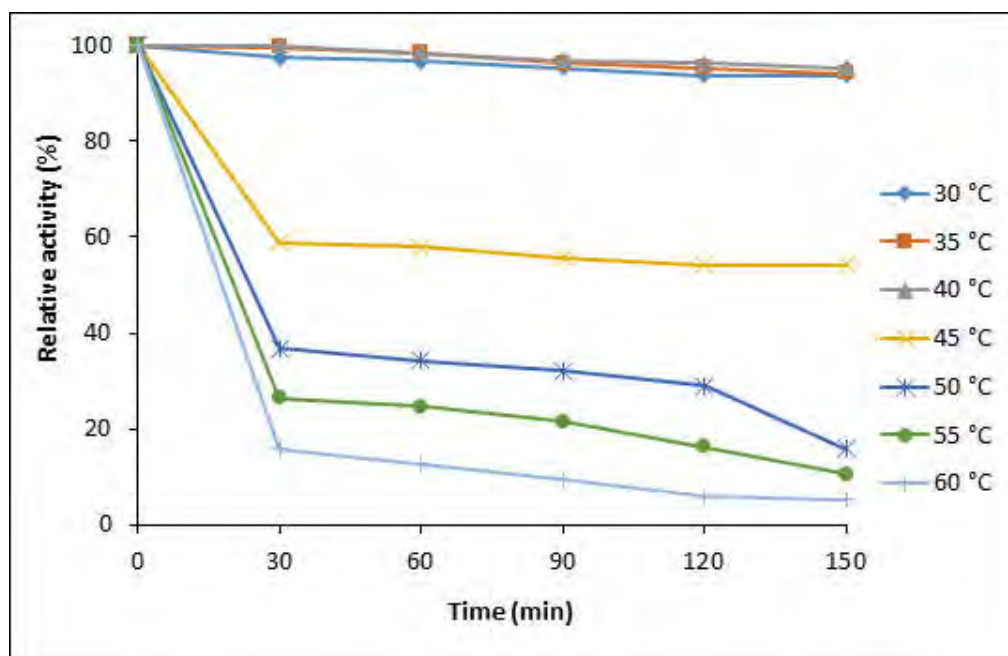


**Figure 4.27:** Effect of temperature on stability of purified cutinase from *S. maltophilia* PRS8 strain

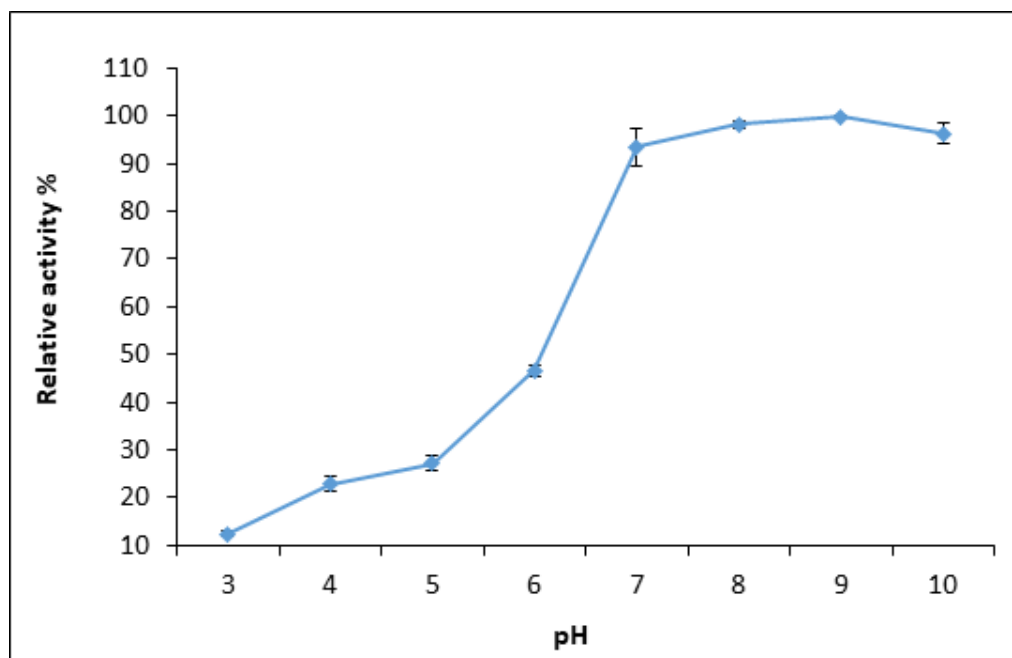


**Figure 4.28:** Effect of pH on the activity of purified cutinase from *S. maltophilia* PRS8 strain

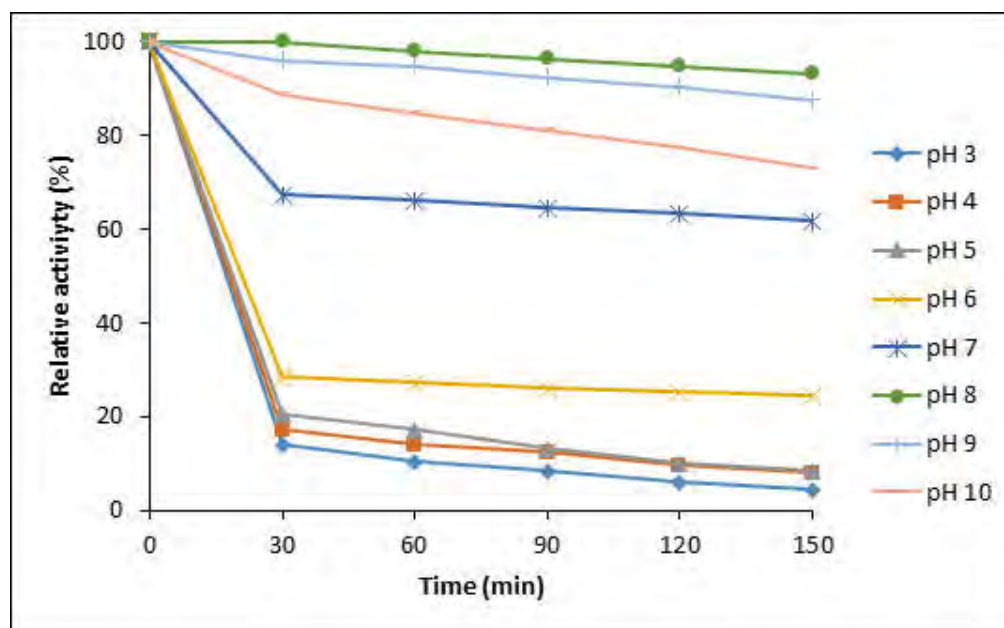


**Figure 4.29:** Effect of pH on stability of purified cutinase from *S. maltophilia* PRS8 strain

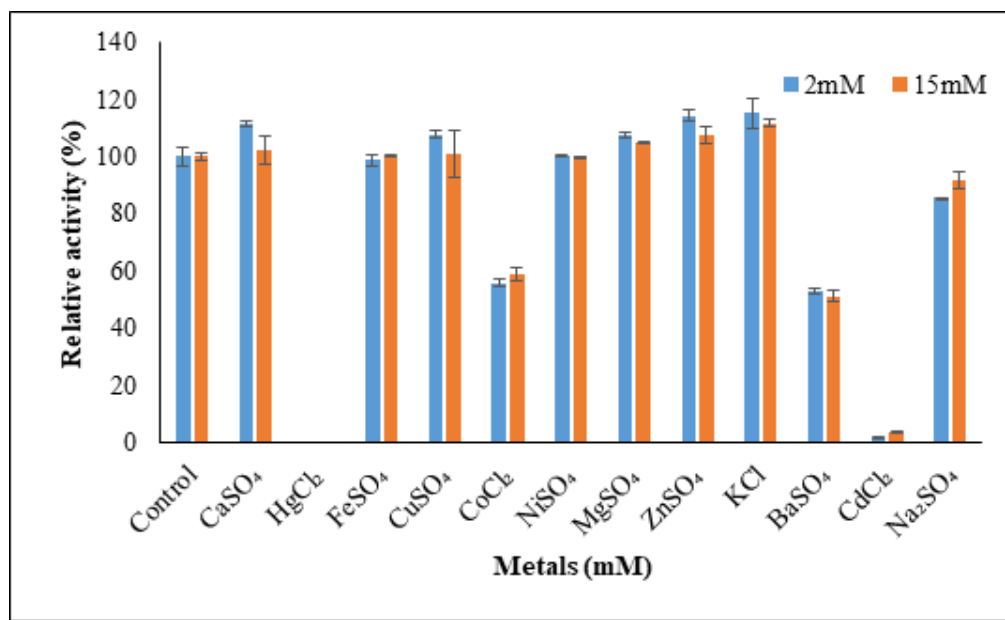


**Figure 4.30:** Effect of metals on the activity of cutinase from *S. maltophilia* PRS8 strain

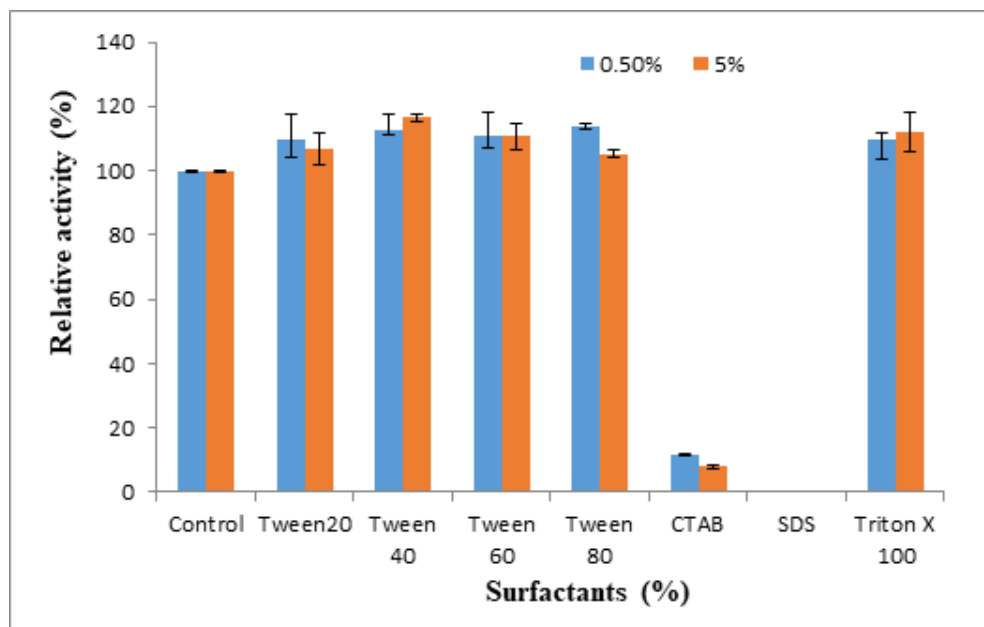


**Figure 4.31:** Effect of surfactants on the activity of cutinase from *S. maltophilia* PRS8 strain

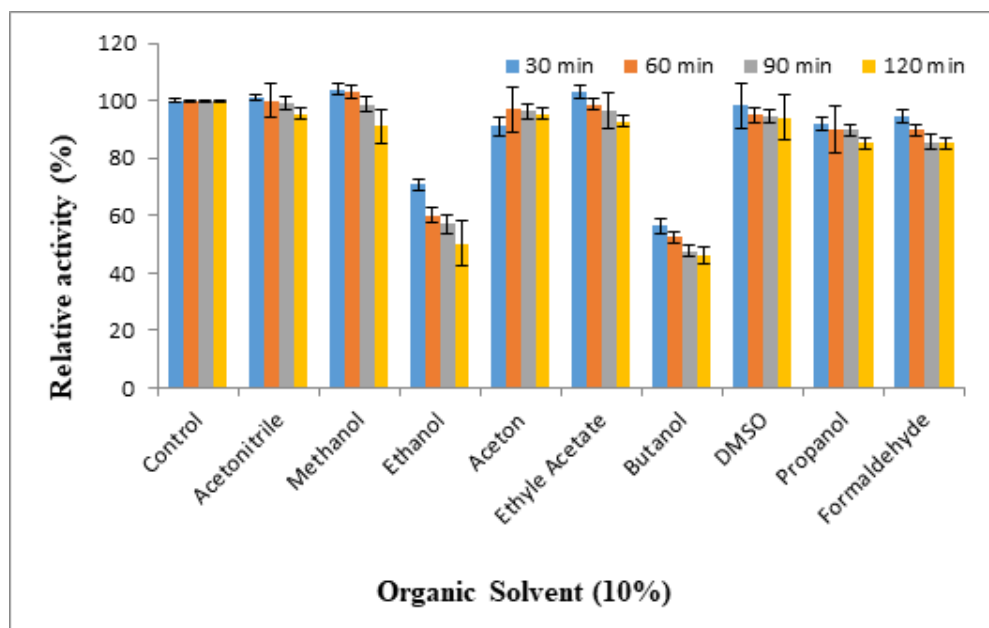


**Figure 4.32:** Effect of organic solvents on the activity of cutinase from *S. maltophilia* PRS8 strain

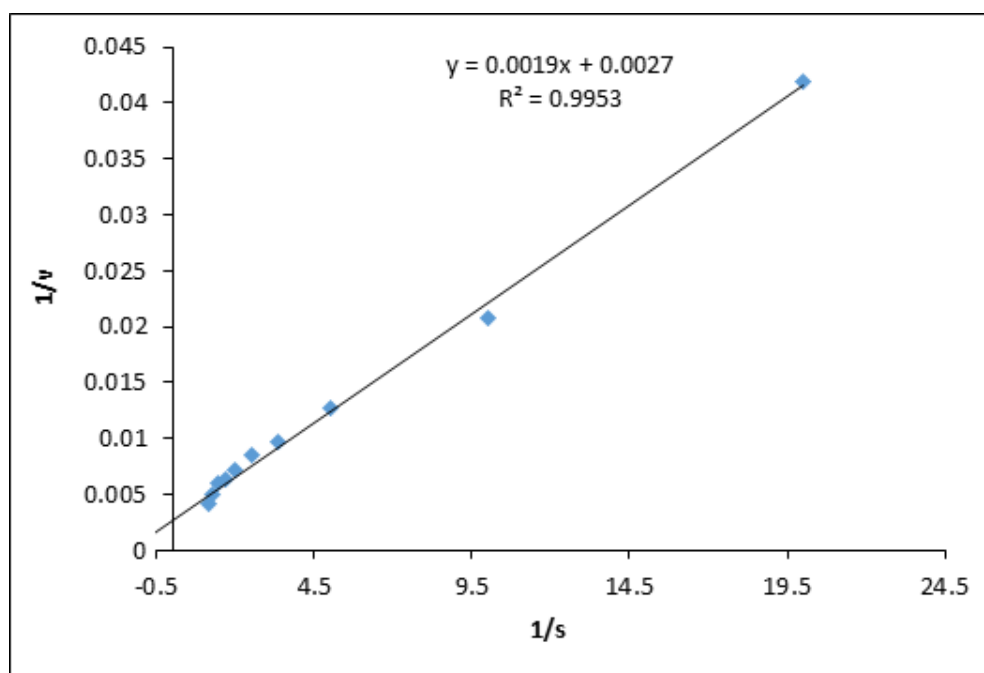


**Figure 4.33:** Kinetics analysis of cutinase-like enzyme from *S. maltophilia* PRS8 strain ( $K_m$  and  $V_{max}$ ) value were calculating by Lineweaver-burk plot using *p*-nitrophenyl Butyrate (*p*-NPB) as substrate

#### 4.15 Cutinase activity on PET and analysis of Depolymerization by HPLC

The cutinase activity against semi-crystalline PET was assessed after 72 hours of reaction at 40°C and pH 9.0. The products terephthalic acid (TPA), mono-(2-hydroxyethyl) terephthalate (MHET), and bis-(2-hydroxyethyl) terephthalate (BHET) peaks were detected by HPLC. The chromatogram in figure 4.34 shows the product profiles. TPA eluted after ~0.66 min, while other products such as MHET and trace amount of BHET, were eluted after ~0.81 and ~1.02 min, respectively (Fig 4.34 B). DMSO was used as a co-solvent for maximum solubility of depolymerized products. No products were detected in the negative control comprising DMSO, PET, and buffer under the same conditions (Fig 4.34 A). Thus, the total amount of degraded polymer can be calculated by the TPAeq and the molecular weight 192 g/mol corresponding to the PET repeating unit (Wagner-Egea et al., 2021). The enzyme concentration was estimated from the total protein concentration and enzyme fraction (58 kDa band) in the SDS-PAGE. The PET depolymerization yield resulted in 18.3 %, with the main product MHET, followed by TPA and a small fraction of BHET (Table 4.8). Interestingly, these results are comparable with the thermostable cutinase HiCut from *Humicola insolens* (Aristizábal-Lanza et al., 2022) (Table 4.8).

##### 4.15.1 Identification of Degradation Products by LC-MS

The PET was incubated with purified cutinase in 100 mM potassium phosphate buffer (pH 8.0) at 40 °C. PET degradation products (BHET, MHET and TPA) have less solubility in water, therefore DMSO was used as a solvent for maximum solubility of depolymerized products. Purified cutinase depolymerized PET polymer and products such as BHET, MHET and TPA were separated in C18 column and analyzed by LC-MS.

The chromatogram in figure 4.35A showed the product profiles. TPA eluted after ~02.51 min, while other product such as MHET and trace amount of BHET, were eluted after ~3.93 and ~20.60 min, respectively. The degradation products TPA, MHET, and BHET were detected and confirmed by mean of mass-to-charge ratio (m/z). The TPA peak in the MS was identified at 165.91 m/z with negative ionization, while main product MHET was found at 211.06 m/z. Similarly; small amount of BHET was detected at 253.65 (Fig 4.35B).

#### **4.15.2 Fourier-transform infrared (FT-IR) spectroscopy of enzymatically treated PET**

The PET pieces were subjected to FT-IR spectroscopy for determining chemical changes in its structure after treated with purified enzyme. FT-IR spectrum for both treated and untreated control samples showed potential differences in their functional groups as shown in figure 4.36. The area of 750–1000  $\text{cm}^{-1}$  resembles to OH bends showing shift of peaks that depicts the clear difference between treated and untreated piece. In control, a peak at 1525 was shifted to 1517 in test piece after treatment with strain PRS8 that shows C-H stretch. The area of 1550–1800  $\text{cm}^{-1}$  resembles to  $\text{CH}_2$  and OH bends showing the appearance of new peaks after microbial treatment. A peak at 1926  $\text{cm}^{-1}$  was disappeared in test spectrum that indicates C-C group stretching in aromatic ring as a result of breaks in polymer chain and new peak at region 2318  $\text{cm}^{-1}$  was appeared, that represents OH bend (Fig 4.36). This clearly indicates splitting of ester linkages in polymer chain after its degradation.

#### **4.15.3 Scanning Electron Microscopy (SEM) of enzymatically treated PET**

The changes in surface morphology of PET pieces after treated by purified enzyme were visualized through SEM. SEM images of test samples showed clear deterioration of PET pieces with cracks and roughness of its surface at different points. The untreated PET piece was observed clear and smooth without any roughness on surface. These changes clearly indicate enzymatic hydrolysis of PET pieces during incubation with purified enzyme (Figure 4.37).

#### **3.15.4. Thermal properties and crystallinity of PET after treatment with purified Enzyme**

The crytallinity and thermal properties of PET treated with PRS8 were analyzed by Differential Scanning Calorimetry (DSC) (Fig 4.38 and Table 4.9). The glass transition for the untreated (control) sample was clearly observed in the first heating curve ( $T_g \sim 83^\circ\text{C}$ ). Whereas in case of treated sample,  $T_g$  of PET was not clearly observed on the first heating curve, probably due to overlapping with the onset of the cold crytallization process ( $\sim 85^\circ\text{C}$ ). The  $T_g$  of treated PET powder was found in the second heating curve. It was observed that the temperature for the cold crytallization

peak ( $T_{cc}$ ) became lower after the enzyme treatment (110 °C compared to 125 °C for untreated PET, which was accompanied by a lowered enthalpy for cold crystallization ( $\Delta H_{cc} \sim 2.9$  J/g compared to 9.0 J/g for pristine PET, Table 4.9). In addition, a decrease in  $T_m$  (247 °C) and crystallinity (18.3%) was observed after treatment of PET with purified enzyme in comparison to untreated PET ( $T_m \sim 242$  °C and crystallinity of 19.1%). This result suggested that the degradation of bulk PET materials presumably occurred (or occurred faster) in the amorphous region of PET, which decreased 3.4% of the relative content of the crystalline region.

Crystallinity is calculated using Equation

$$\text{Crystallinity \% (first heating cycle)} = \frac{(\Delta H_m - \Delta H_{cc})}{(\Delta H_m^0)} \times 100$$



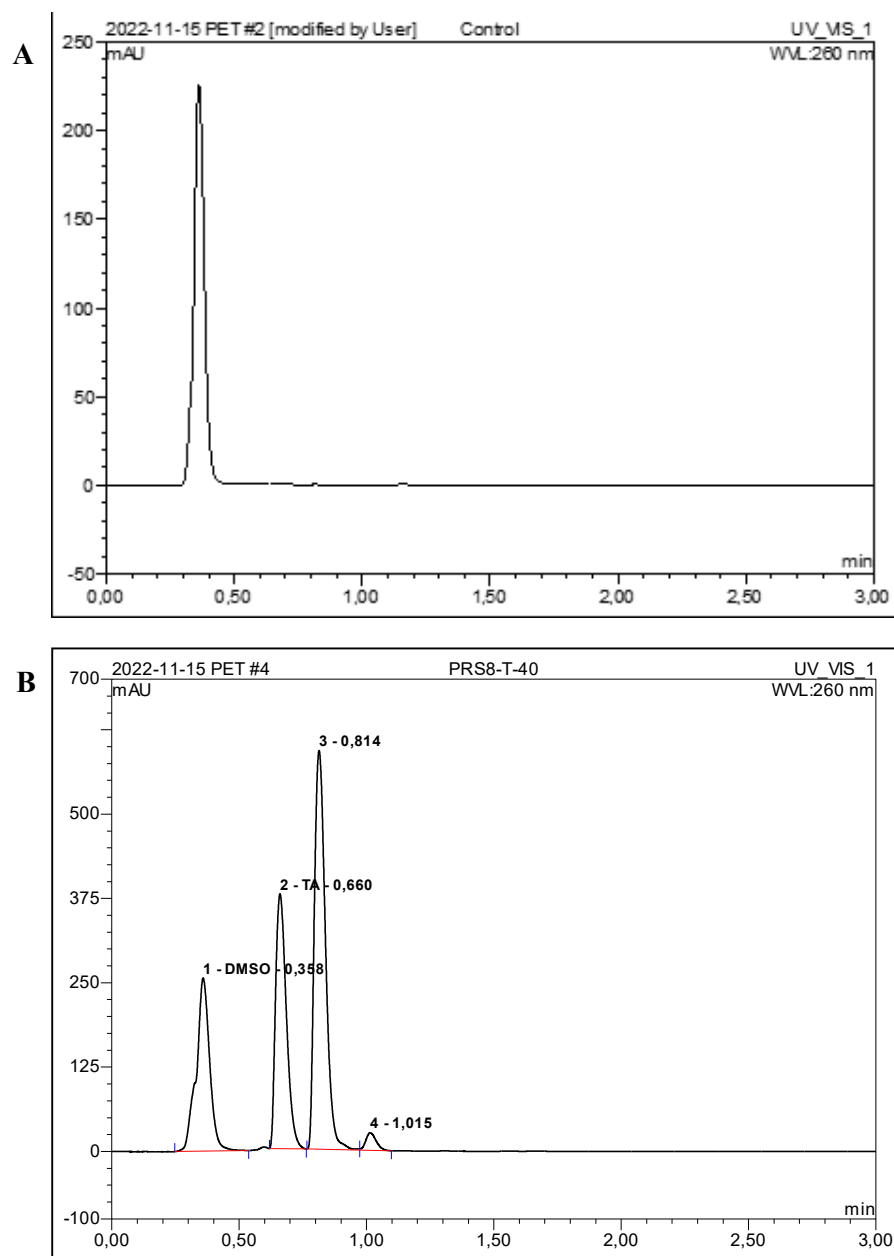


**Figure 4.34:** HPLC analysis of the degradation products of the cutinase enzyme activity on PET, The Chromatogram showed the time course of product profile where the main product is MHET, followed by TPA and a small fraction of BHET. (A) Untreated (control) PET chromatogram. (B) PRS8 enzyme treated PET chromatogram

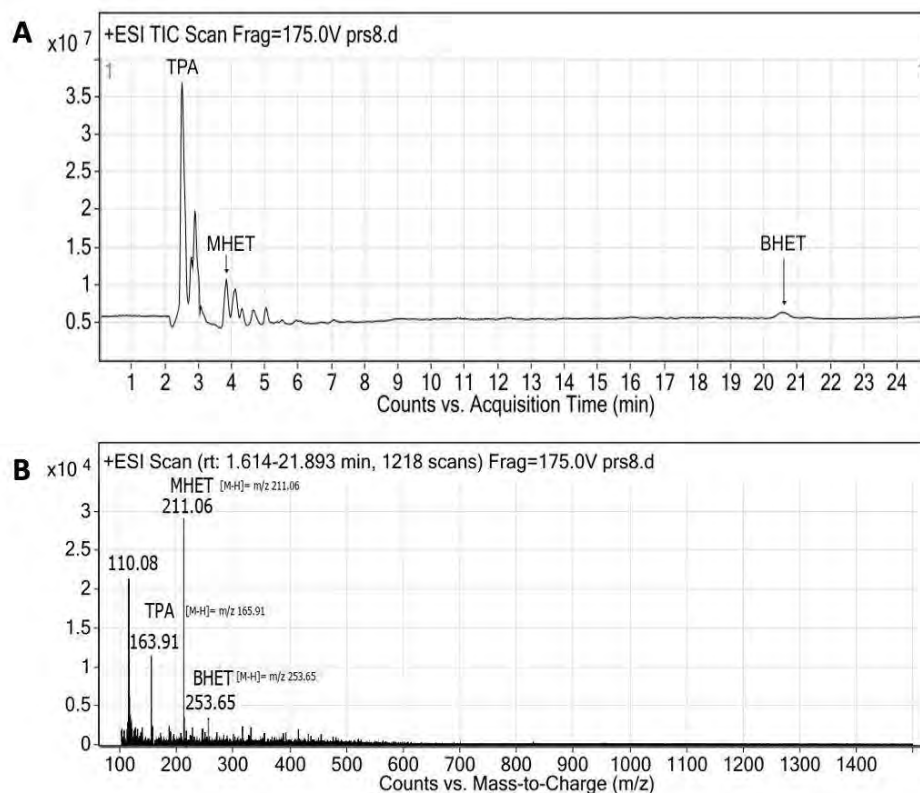


**Figure 4.35:** Analysis of the degradation products of the cutinase activity on PET (A) The Chromatogram showed the time course of product profile (B) The Mass spectrum confirmed the identity of TA, MHET, and BHET

**Table 4.8:** PET depolymerization activity of the cutinase of *S. maltophilia* PRS8 compared with enzymes. The reaction time was between 72 and 73 hours.

Enzyme	T (°C)	pH	Degradatio n Products (mg/L)	Relative Production (%)			PET depolyme rization (%)
				TPA	MHE T	BHET	
Cutinase	40	9	1935	35	56	1.8	18.3
HiCut (HiC)	70	7.5	437	100	38	0.9	12.7

\* Estimated ratio based on the cutinase enzyme.

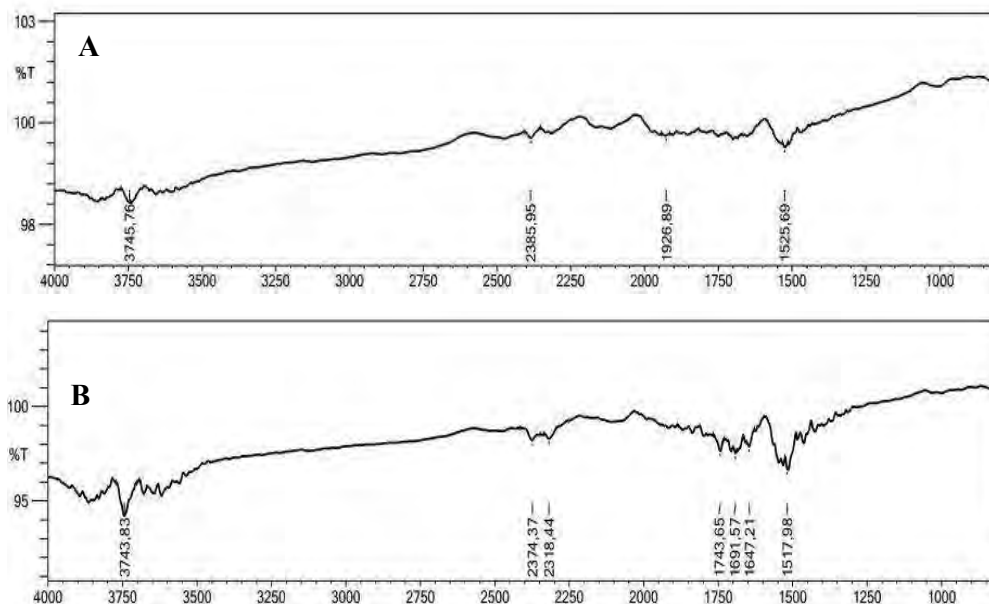


**Figure 4.36:** The Fourier Transform Infra-Red (FT-IR) absorption pattern of PET (A) Control un-treated PET (B) Enzyme treated PET

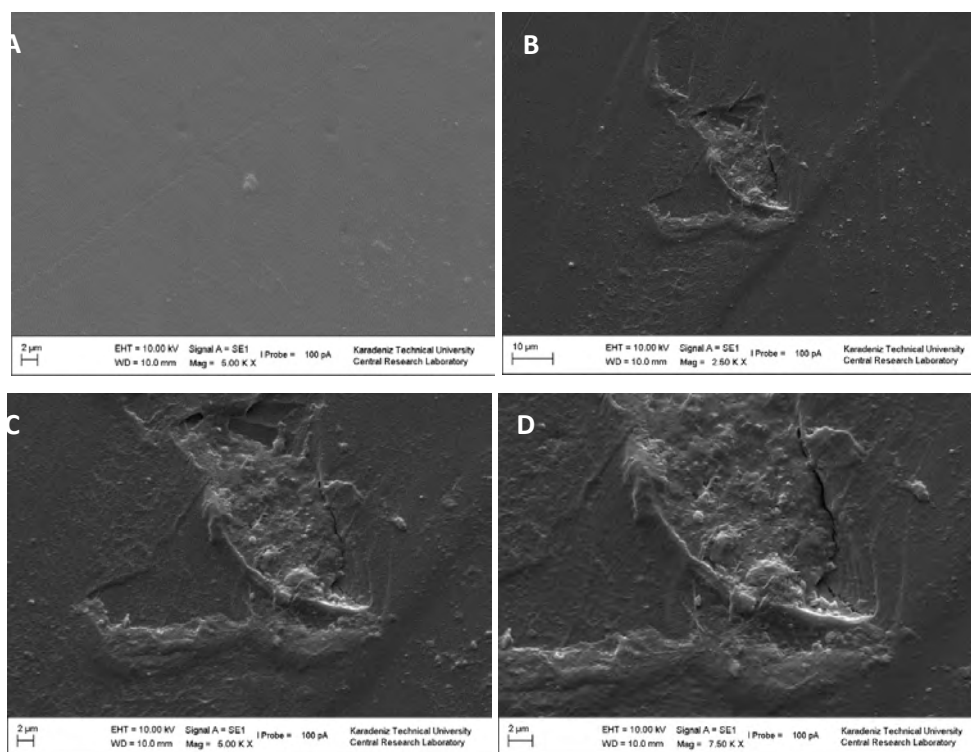


**Figure 4.37:** SEM images of enzymatically treated PET compared with untreated PET (A) Control un-treated (x5.00K) (BCD) Micrographs of biodegraded PET (x2.5K, x5.00K, x7.5K)

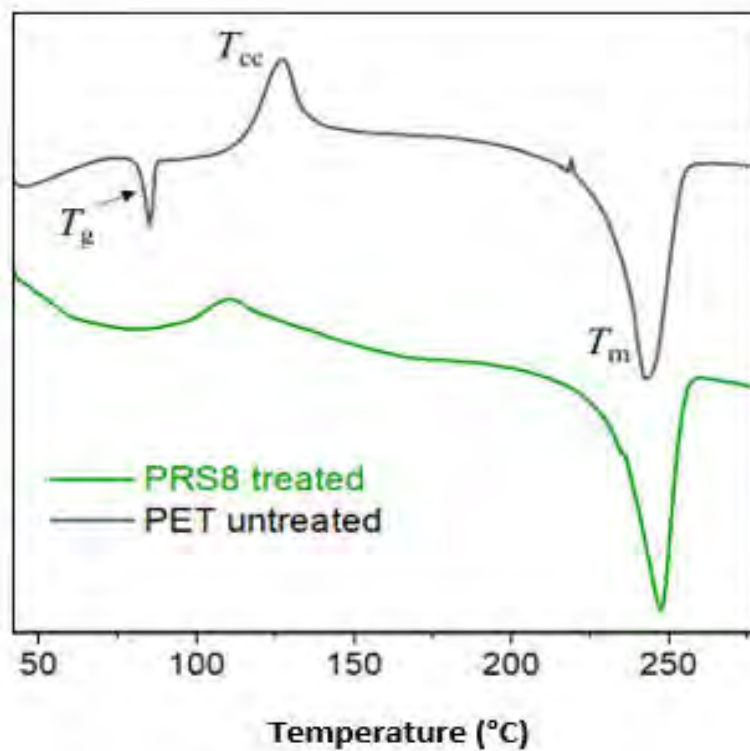


**Figure 4.38:** DSC heating curves of untreated and enzymatically treated PET. The  $T_g$ ,  $T_{cc}$  and  $T_m$  are shown on the untreated PET curve.

**Table 4.9:** Properties and crystallinity of the untreated and enzymatically treated PET

Polymer	$T_g$ (°C)	$T_{cc}$ (°C)	$T_m$ (°C)	$\Delta H_{cc}$ (J/g)	$\Delta H_m$ (J/g)	Crystallinity (%)
PET (untreated)	83	125	241	9.0	35.9	19.1
PET (treated)	-	110	248	2.9	32.4	18.3

## **4.16 Cloning and Expression of PET hydrolase gene**

### **4.16.1 Isolation of genomic DNA**

*S. maltophilia* genomic DNA was isolated by QIAamp® DNA Mini Kit (QIAGEN). The extracted DNA band was visualized by comparing it with DNA ladder (10 kb, GeneRuler™) (Fig 4. 39). The pure DNA was used as template for amplification of PET hydrolase gene in PCR reaction.

### **4.16.2 PCR optimization for PET hydrolase gene**

PET hydrolase encoding gene of *S. maltophilia* PRS8 amplification was optimized at various temperatures level (54-64°C). Optimization of annealing temperature clearly indicated that 60°C is the optimum annealing temperature for amplification of PET hydrolase gene (Fig. 4.40).

### **4.16.3 PCR amplification of PET hydrolase gene**

PET hydrolase encoding gene of strain PRS8 was amplified by using *S. maltophilia* PRS8 as a template with a translation codon (ATG) and termination codon (TAG) in the presence of a newly designed primer. PET hydrolase gene of approximately 1.8 kb was amplified for *S. maltophilia* PRS8 shown in lane 1 and 2, while negative control containing all the reagents except the DNA template is shown in lane 3 (Fig. 4.41).

### **4.16.4 Purification of amplified band from polyacrylamide gel**

The amplified cloned PET hydrolase gene was cut from the agarose gel with a sterile scalpel and transferred to a clean 2 mL microfuge tube. The band from gel was purified by QIAEX II® Gel Extraction Kit (QIAGEN) and confirmed by agarose gel electrophoresis by comparing it with DNA ladder (10 kb, GeneRuler™). Approximately 1.8 kb size for PET hydrolase gene was determined under Gel Doc imaging system (Fig 4. 42).

### **4.16.5 Cloning of PET hydrolase gene in cloning vector**

PET hydrolase coding gene was ligated in the pUC19 cloning vector. The overnight ligated gene product was transferred in *E. coli* DH5 $\alpha$  competent cells. White/blue screening method was used for confirmation of cloning gene having recombinant PET hydrolase gene product (Fig. 4.43). Amp-LB agar medium was used for cultivation of

10 white colonies (recombinant) and one blue colony (non-recombinant), pUC19 cloning contained ampicillin resistant gene. The plasmids from both white and blue colonies were isolated by QIAprep® Spin Miniprep Kit. Cloning of PET hydrolase gene was confirmed by double digestion with restriction enzymes NdeI and XhoI. Sequencing was used to clarify the cloning of PET hydrolase gene to pUC19 vector. The desired band of PET hydrolase gene size approximately 1.8 kb for *S. maltophilia* PRS8 after digestion with restriction enzyme along with 2686 bp of its own size (Fig. 4.44).

#### **4.16.6 Preparation of pET21b and PET hydrolase gene product for expression**

pET21b vector and pUC19 cloned PET hydrolase gene plasmid of *S. maltophilia* PRS8 was isolated and confirmed by gel electrophoresis (Fig. 4.45 and 4.46). These plasmids were double digested with appropriate restriction enzymes NdeI and XhoI for 3 hours at 37°C and the digestion was confirmed by gel electrophoresis. The digested pET21b plasmid showed approximately 5442 bp size of single band while *S. maltophilia* PRS8 strain gene showed 1800 bp under gel doc system (Fig. 4.47).

#### **4.16.7 Purification of amplified band from polyacrylamide gel**

The digested PET hydrolase gene and pET21b vector was cut from the agarose gel with a sterile scalpel and transferred to a clean 2 mL microfuge tube. The band from gel was purified by QIAEX II® Gel Extraction Kit (QIAGEN) and confirmed by electrophoresis by comparing it with DNA ladder (10 kb, GeneRuler™). Approximately 1.8 kb size for PET hydrolase gene and 5442 kb size for pET21b was determined under Gel Doc imaging system (Fig 4. 48).

#### **4.16.8 Cloning of PET hydrolase gene in expression vector**

The gel purified PET hydrolase coding gene was ligated in the pET21b cloning vector. The overnight ligated gene product was transferred in *E-coli* DH5α competent cells. The transformed coding gene in pET21b vector was observed in Amp-LB agar plate. (Fig. 4.49). Amp-LB broth media was used for cultivation of 10 colonies. pET21b cloning vector contain ampicillin resistant gene. The plasmids from recombinant colonies were isolated by QIAprep® Spin Miniprep Kit. Cloning of PET hydrolase gene was confirmed by double digestion with restriction enzymes NdeI and

XhoI. Sequencing was used to clarify the cloning of PET hydrolase gene to pET21b vector. The desired band of PET hydrolase gene size approximately 1.8 kb for *S. maltophilia* PRS8 strain after digestion with restriction enzyme along with size of pET21b plasmid (Fig. 4.50).

#### **4.17 Bioinformatics analysis**

Phylogenetic relationship of PET hydrolase of *S. maltophilia* PRS8 with other PET hydrolase available at NCBI database showed highest identity with polyethylene terephthalate hydrolase of *stentrophomonas* sp HBG88740 (Fig 4.51).

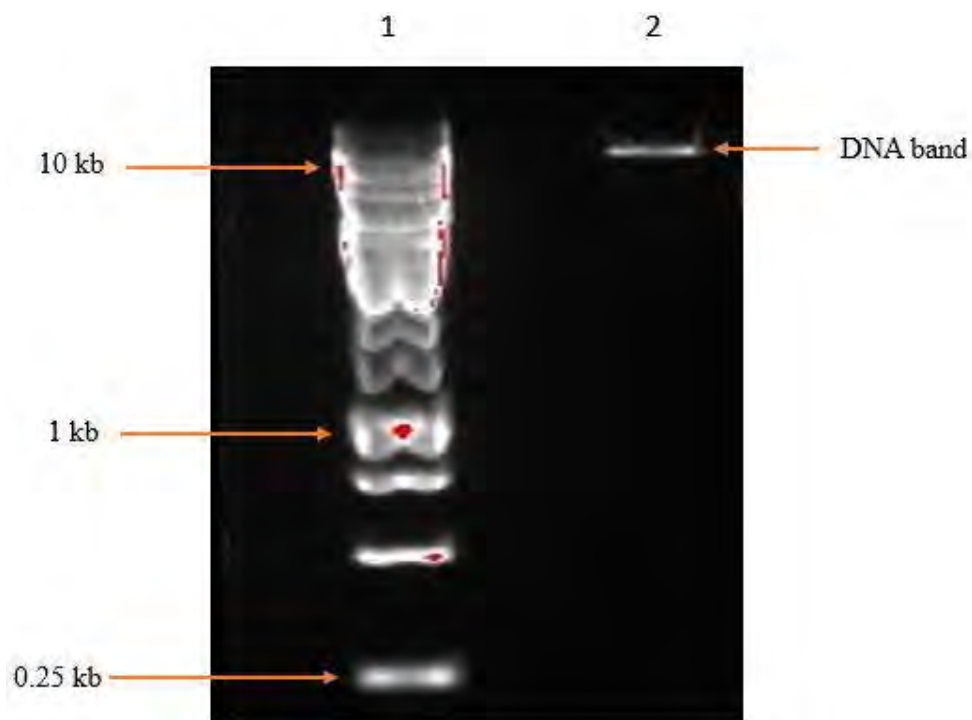


**Figure 4.39:** Gel electrophoresis of extracted genomic DNA; 1, DNA ladder (10 kb, GeneRuler); 2, *S. maltophilia* genomic DNA

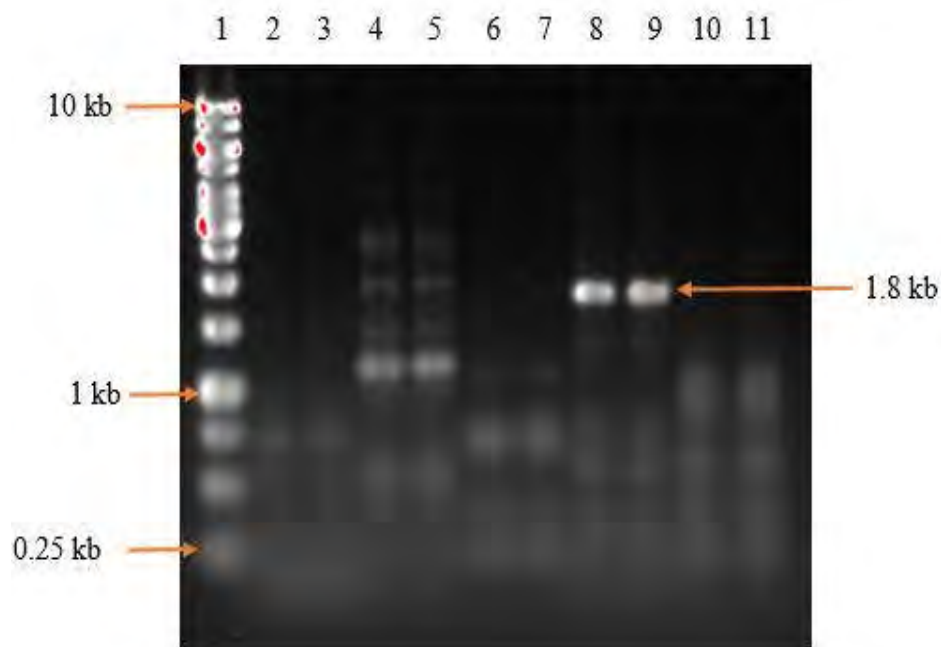


**Figure 4.40:** PCR optimization for PET hydrolase gene (54 to 64°C); 1, DNA ladder (10 kb, GeneRuler); 2-11, Temperatures from 54°C to 62°C



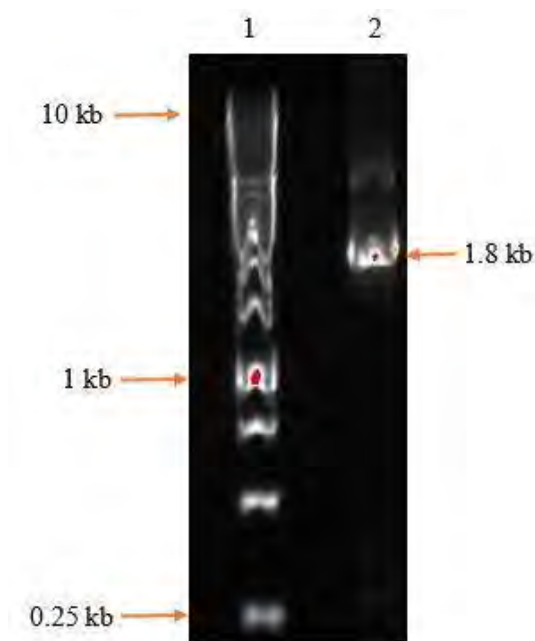


**Figure 4.41:** PCR amplification of *S. maltophilia* PRS8 PET hydrolase gene; 1, DNA ladder (10 kb, GeneRuler); 2, PRS8 PCR amplified PET hydrolase gene product 1.8 kb approximately

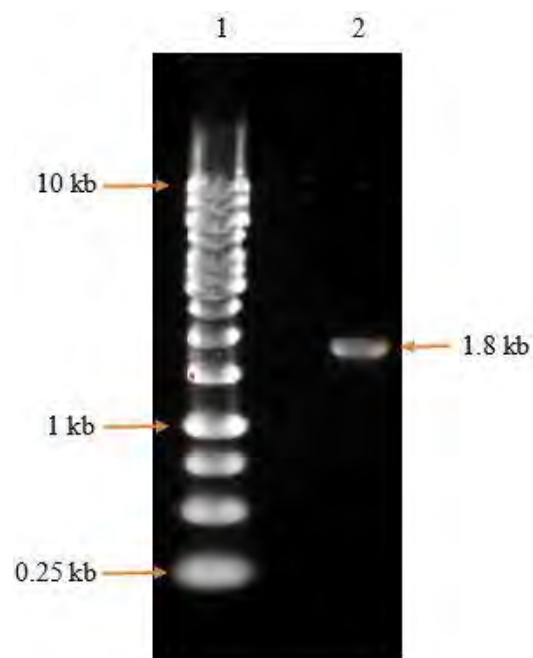


**Figure 4.42:** Purification of PCR amplified PET hydrolase gene product from polyacrylamide gel; 1, DNA ladder (10 kb, GeneRuler); 2, PRS8 PCR amplified PET hydrolase gene product 1800 bp approximately

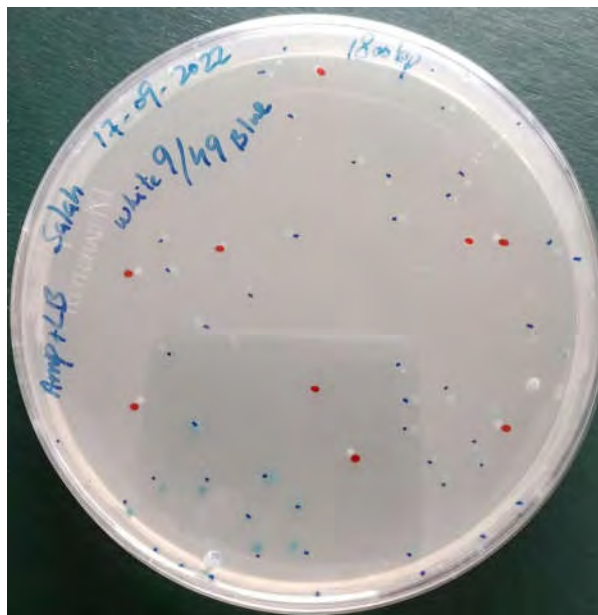


**Figure 4.43:** White/blue screening of pUC19 with *S. maltophilia* PRS8 strain PET hydrolase gene

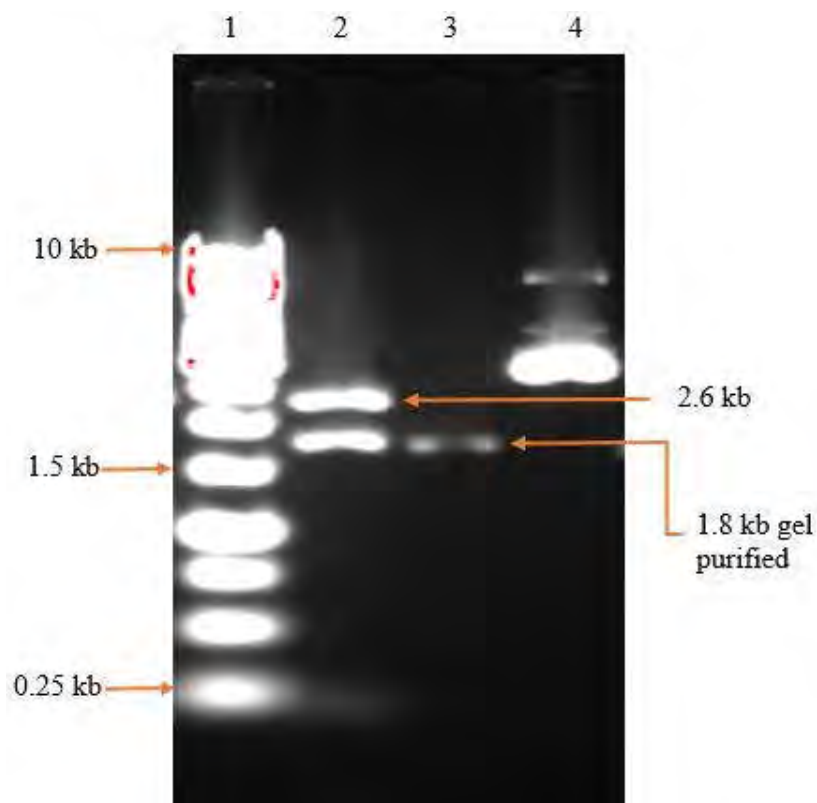


**Figure 4.44:** Confirmation of PET hydrolase gene into pUC19 vector; 1, DNA ladder (10 kb, GeneRuler); 2, Digested PET hydrolase clone; 3, Purified PRS8 gene amplicon; 4, Undigested PRS8 gene clone

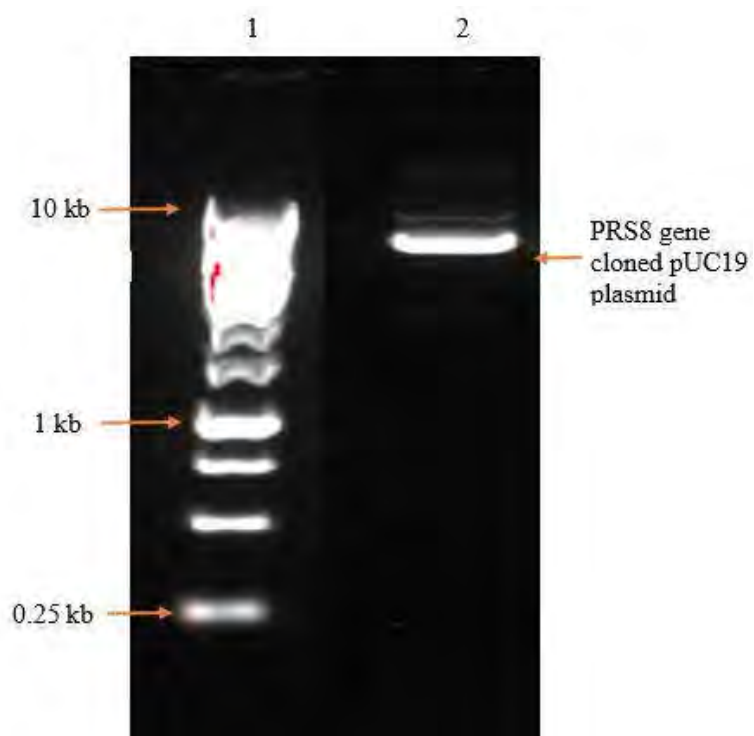


**Figure 4.45:** Isolation of PET hydrolase cloned pUC19 plasmid; 1 DNA ladder (10 kb, GeneRuler); 2, PET hydrolase cloned pUC19 plasmid

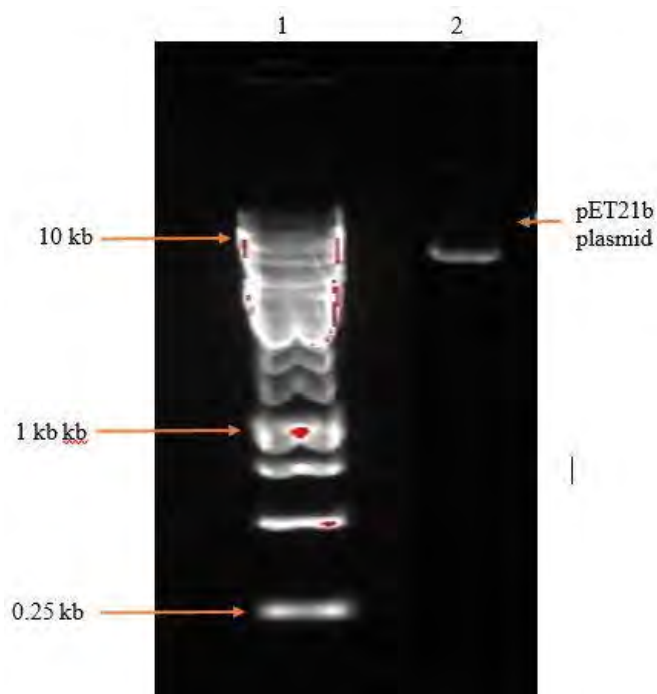


**Figure 4.46:** Isolation of pET21b plasmid; 1 DNA ladder (10 kb, GeneRuler); 2, pET21b plasmid vector

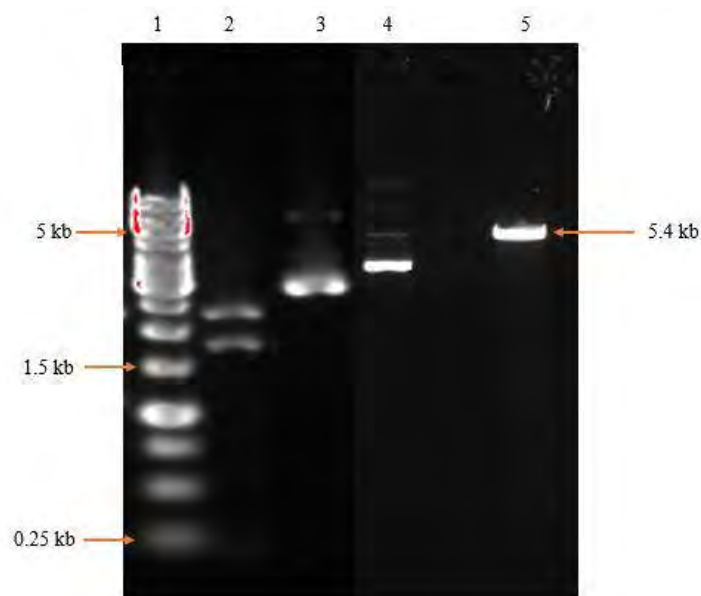


**Figure 4.47:** Confirmation of double-digested PET hydrolase gene into pUC19 vector; 1, DNA ladder (10 kb, GeneRuler); 2, double-digested PET hydrolase gene into pUC19 product; 3, un-digested PET hydrolase gene into pUC19 vector; 4, un-digested pET21b plasmid; 5, double digested pET21b plasmid

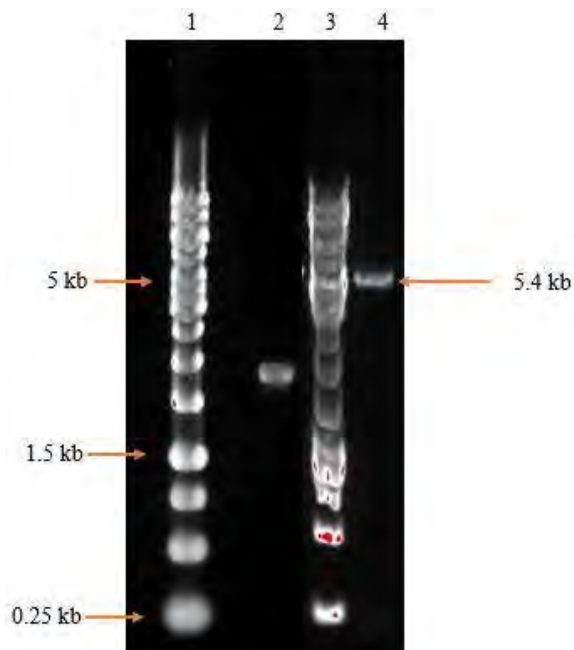


**Figure 4.48:** Purification of double digested amplified PET hydrolase gene product and pET21b product from polyacrylamide gel; 1, DNA ladder (10 kb, GeneRuler); 2, PRS8 double digested PET hydrolase gene product; 3, DNA ladder (10 kb, GeneRuler); 4, double digested pET21b product

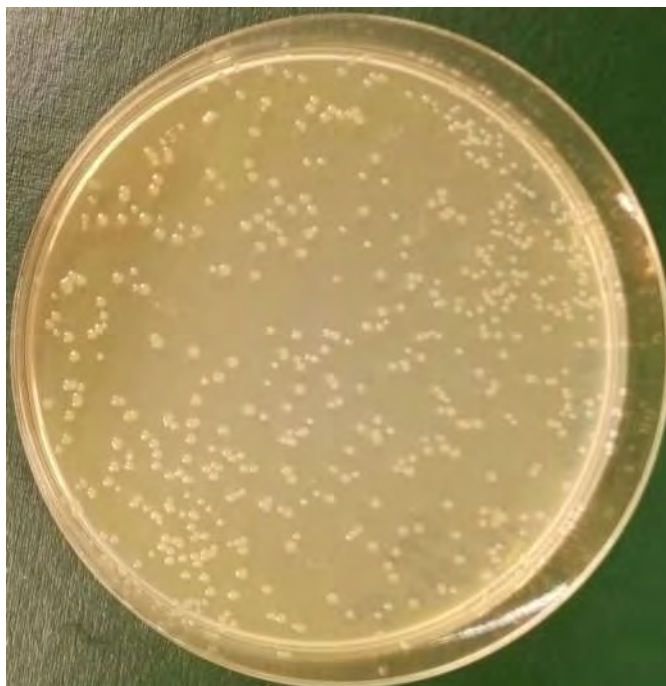


**Figure 4.49:** Recombinant colonies of pET21b with *S. maltophilia* PRS8 strain PET hydrolase gene

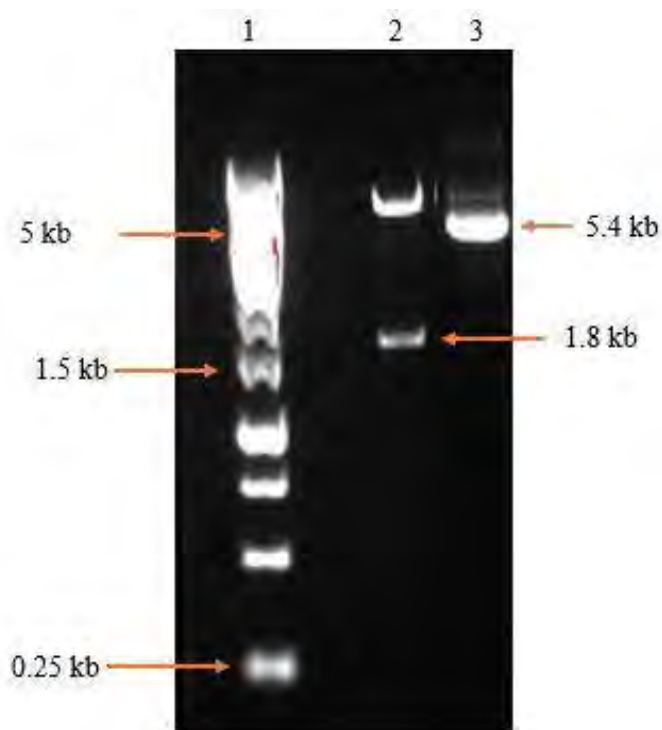


**Figure 4.50:** Confirmation of double-digested PET hydrolase gene into pET21b vector; 1, DNA ladder (10 kb, GeneRuler); 2, double-digested PET hydrolase gene into pET21b product; 3, un-digested PET hydrolase gene into pET21b plasmid

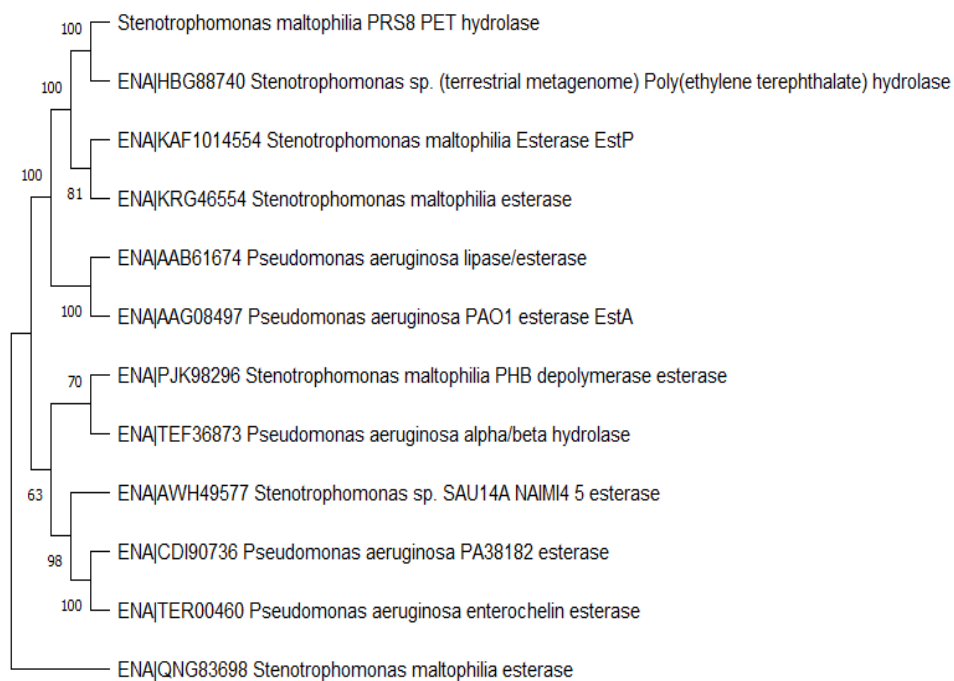


**Figure 4.51** Phylogenetic relationship of *S. maltophilia* PRS8 PET hydrolase with other PET hydrolase available in NCBI database, Neighbor-joining tree showed maximum identity with polyethylene terephthalate hydrolase of *Stenotrophomonas* sp HBG88740.

#### 4.18 Induction of recombinant PET hydrolase enzyme

Production of recombinant PET hydrolase enzyme was performed by 1mM IPTG and protein expression band was confirmed by SDS-PAGE analysis. A 58 kDa expressed band was directly observed without staining and de- staining under UV black tray Gel Doc imaging system (Universal Hood 2 – S.N. 76S/ 0.4186) for recombinant PET hydrolase with molecular weight standard 10-250 kDa (Fig. 4.52).

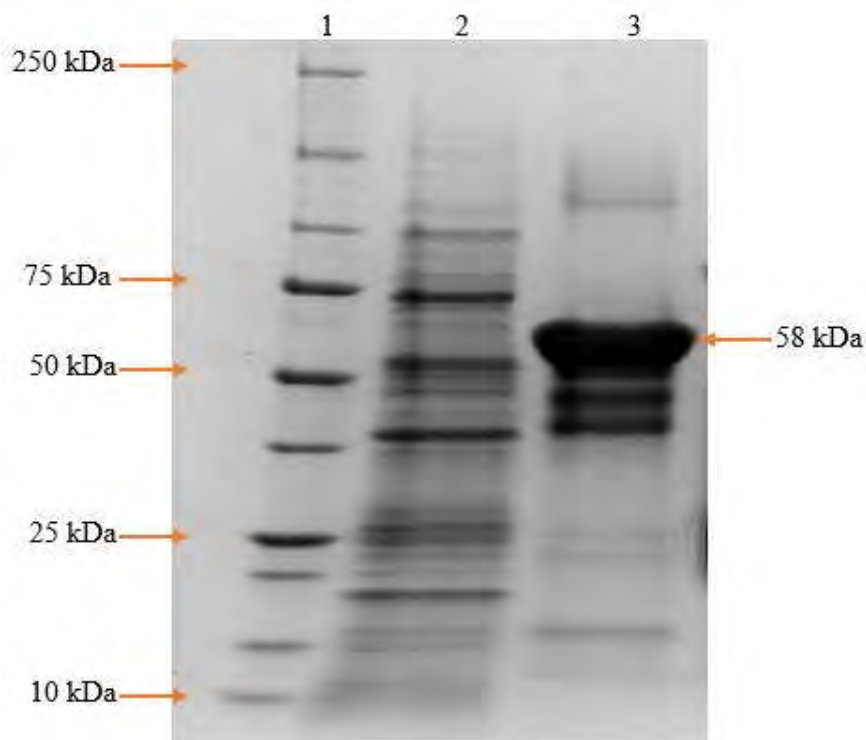


**Figure 4.52** Recombinant PET hydrolase enzyme expression by SDS-PAGE.

**1:** Protein marker (10 – 250 kDa; **2,** Induced protein of *E. coli* BL 21 (DE3) with pET21b; **3,** Induced protein of *E. coli* BL21 (DE3) with pET21b and PET hydrolase

#### **4.19 Protein purification by HiPrep 16/60 Sephacryle S-300 High Resolution Gel Filtration Column Chromatography**

Partially purified recombinant enzyme was subjected to additional purification by HiPrep 16/60 Sephacryle S-300 High resolution gel filtration column chromatography resin and the proteins were eluted on the basis of its molecular sized. 28 fraction were collected each fraction contain 10 mL after every 20 minutes. During purification, total proteins were determined spectrophotometrically at 280 nm by UV in UNICORN (AKTA start) (Fig 4.53). All fractions were analyzed at 410 nm for recombinant PET hydrolase activity. Highest enzyme activity was determined in fraction 19 (Fig. 4.54).

##### **4.19.1 Purification steps**

The recombinant PET hydrolase was purified to homogeneity and its specific, total yield and purification fold was calculated. The specific activity of purified enzyme was determined as 595.93 U/mg with 23.89% total yield and 6.19 purification fold. Table 4.10 shows various steps during purification to measure specific activity, purification fold and maximum yield.

##### **4.19.2 Recombinant enzyme Molecular Weight determination (SDS-PAGE)**

Purification of recombinant PET hydrolase enzyme was confirmed by SDS-PAGE analysis. Approximately, 58 kDa single band was directly observed without staining and de-staining under UV black tray Gel Doc imaging system (Universal Hood 2 – S.N. 76S/ 0.4186) for recombinant PET hydrolase with molecular weight standard, 10-250 kDa (Fig. 4.55).



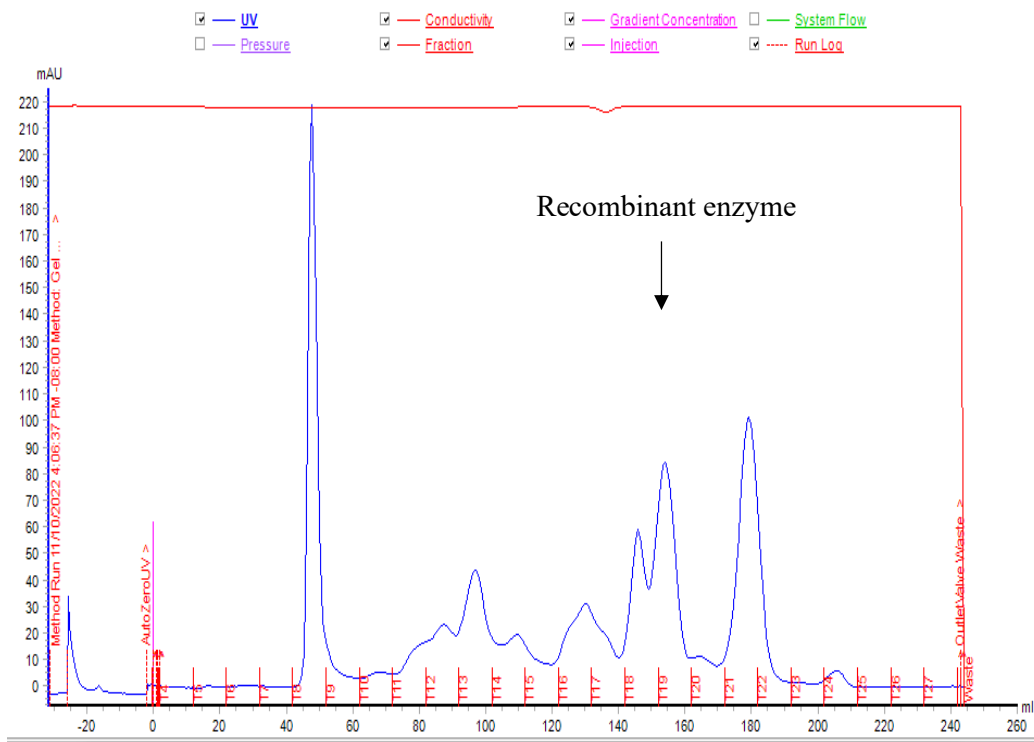


**Figure 4.53:** Total protein profile by *S. maltophilia* PRS8 through HiPrep 16/60 Sephacryle S-300 High resolution gel filtration column

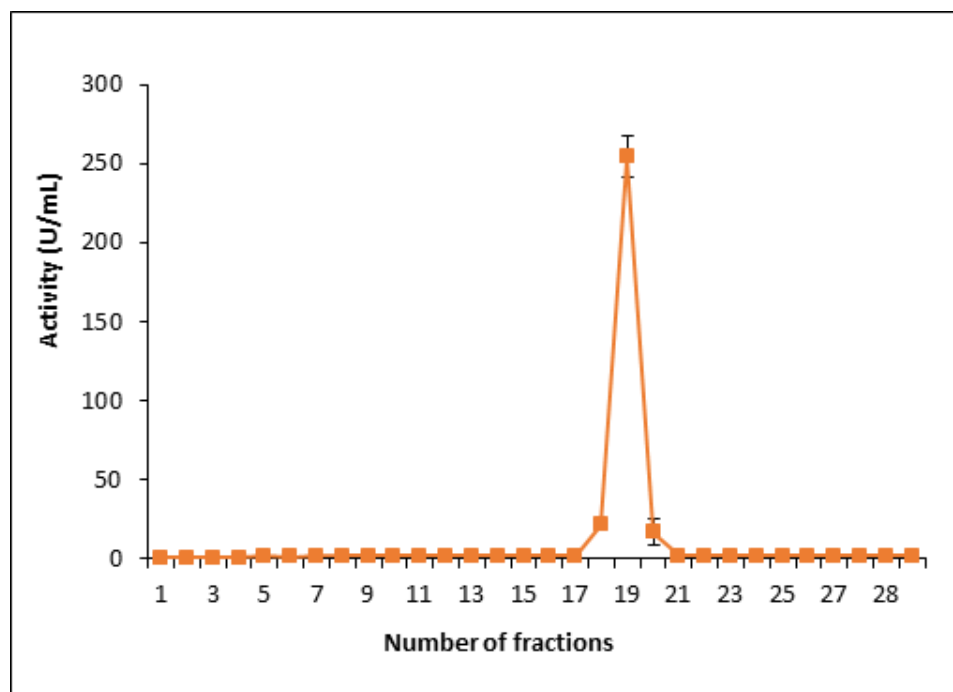


**Figure 4.54:** PET hydrolase enzyme activity profile by *S. maltophilia* PRS8 through HiPrep 16/60 Sephacryle S-300 High resolution gel filtration column

**Table 4.10:** Purification steps of recombinant PET hydrolase by *S. maltophilia* PRS8 strain

Purification Steps	Activity (U/mL)	Total Activity (Units)	Protein (mg/mL)	Specific activity (U/mg)	Yield (%)	Purification Fold
Crude Extract	260.40	15624.55	2.71	96.17	100	1
Sephacryle S-300	373.28	3732.87	0.65	595.93	23.89	6.19

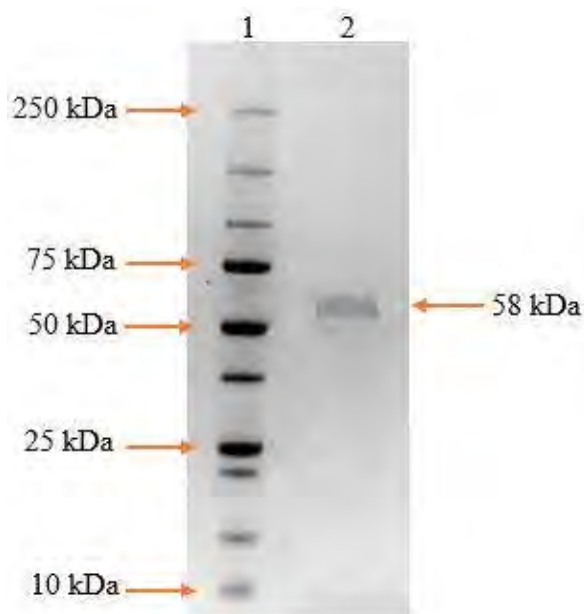


**Figure 4.55:** SDS-PAGE of Recombinant PET hydrolase from *S. maltophilia* PRS8 strain after purification by HiPrep 16/60 Sephacryle S-300 High resolution Gel filtration column Chromatography. Lane 1, Protein Standard (10-250 kDa); Lane 2, 58 kDa recombinant PET hydrolase enzyme eluate from Sephacryle S-300 gel chromatography

## **4.20. Characterization of Recombinant PET hydrolase**

### **4.20.1 Temperature effect on the activity and stability**

The effect of temperature on the activity of recombinant enzyme from *S. maltophilia* PRS8 was analyzed by incubating enzyme at different temperatures (30-70°C) for 30 minutes. The purified cutinase showed maximum activity at temperature between 30-45°C with optimum activity observed at 40°C (Fig. 4.56). While, the stability of purified recombinant enzyme was calculated by incubating enzyme at different temperatures (30-70°C) for 150 minutes. The enzyme retained 100% of its activity at 40°C followed by a significant decrease up to 55% at 50°C for 150 minutes. The enzyme retained only 15% of its activity at 60-70°C for 150 minutes (Fig. 4.57).

### **4.20.2 pH effect on the activity and stability**

The effect of pH on activity of recombinant enzyme from *S. maltophilia* PRS8 was calculated by incubating enzyme with substrate at different pH (4.0 to 11.0) for 30 minutes. The recombinant enzyme showed maximum activity at pH between 8.0 and 9.0 with optimum activity achieved at 8.0 (Fig. 4.58). While, the stability of recombinant enzyme was calculated by incubating enzyme at different pH (4.0 to 11.0) for 150 minutes. The recombinant enzyme retained 98 % of its activity at pH 8.0-9.0 with optimum at pH 9.0. The activity was reduced upto 60% after incubation at pH 6.0 and 7.0 for 150 minutes. The enzyme activity was significantly reduced upto 12% at pH below 6.0 for 150 minutes (Fig. 4.59).

### **4.20.3 Effect of Metal Ions**

Effects of the various monovalent and divalent metals on the cutinase activity were evaluated at 2 and 10 mM. CaSO<sub>4</sub>, ZnSO<sub>4</sub>, KCl, and MgSO<sub>4</sub> enhanced 10% of the enzyme activity at either concentration, while HgCl<sub>2</sub> and CdCl<sub>2</sub> strongly inhibited cutinase activity at both concentrations (2 mM and 10 mM). Exposure to BaSO<sub>4</sub>, the enzyme retained only 50% of its activity. No significant effect was observed in the presence of FeSO<sub>4</sub>, NiSO<sub>4</sub> and NaSO<sub>4</sub> at both concentrations (Fig 4.60).

### **4.20.4 Effect of Surfactants**

The effect of the surfactants on the enzyme activity was evaluated by treating of purified enzymes with 0.5 and 5% of each surfactant. Among surfactants, Tween-20,

Triton X-100, Tween-40, Tween-60 and Tween-80, enhanced enzyme activity at both concentrations, while CTAB and SDS strongly suppressed enzyme activity (Fig. 4.61).

#### 4.20.5 Effect of organic solvents

The influence of various organic solvents on recombinant enzyme activity was analyzed by incubating enzyme in a solution with 15% solvent concentration for 120 minutes. Among solvents; methanol, propanol, ethyl acetate and acetone greatly increased cutinase activity with time. Acetonitrile, butanol, DMSO and ethanol had no effect and the enzyme retained 100% of its activity for 120 minutes. Organic solvents such as ethanol suppressed enzyme activity with the passage of time and retained only 35% activity after 120 minutes (Fig. 4.62).

#### 3.20.6. Kinetic parameter of Cutinase

Lineweaver and Burk's plot was used to calculate the Michaelis Menten constant ( $K_m$ ) and rate of enzyme reaction ( $V_{max}$ ) of purified recombinant enzyme. A constant amount of enzyme was incubated with various concentrations of substrate and activity was determined.  $K_m$  and  $V_{max}$  values were recorded to be 0.521  $\mu\text{M}$  and 434.78 (U/mg), respectively (Fig. 4.63). A low  $K_m$  of enzyme revealed high affinity of enzyme toward substrate.

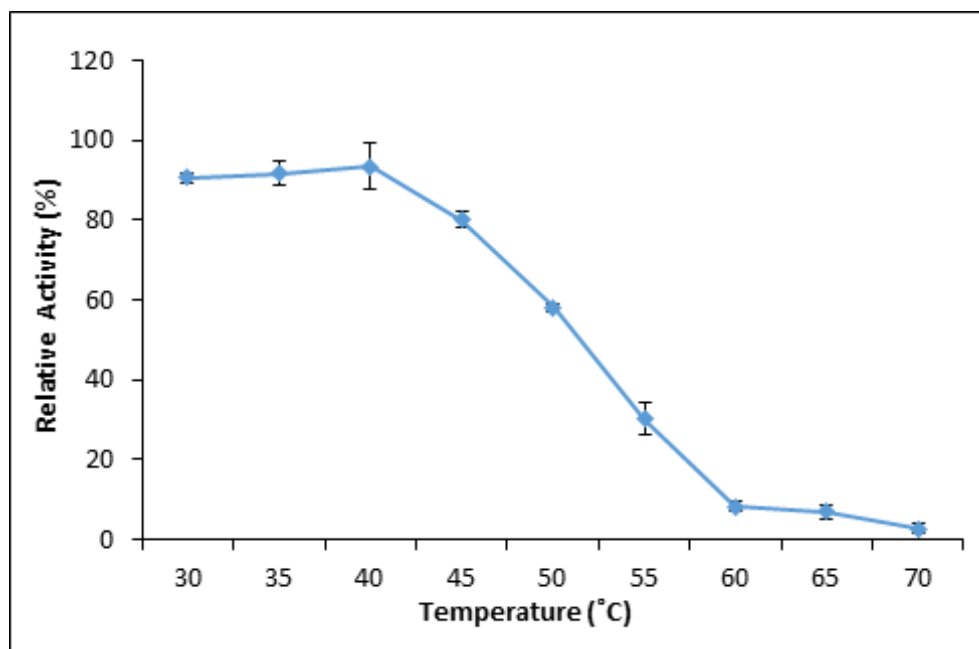


**Figure 4.56.** Effect of temperature on activity of recombinant enzyme *S. maltophilia* PRS8 strain

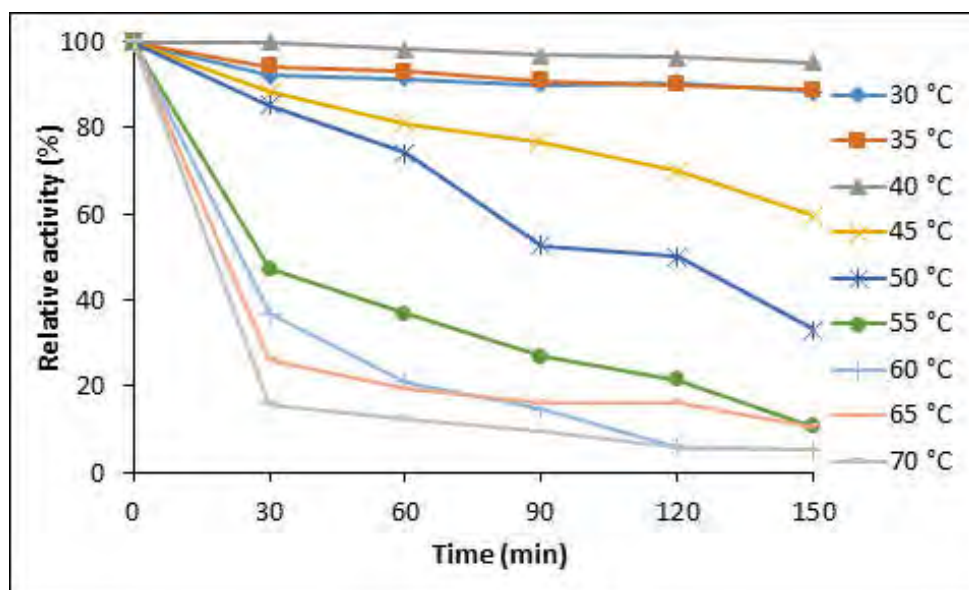


**Figure 3.57** Effect of temperature on stability of recombinant enzyme from *S. maltophilia* PRS8 strain

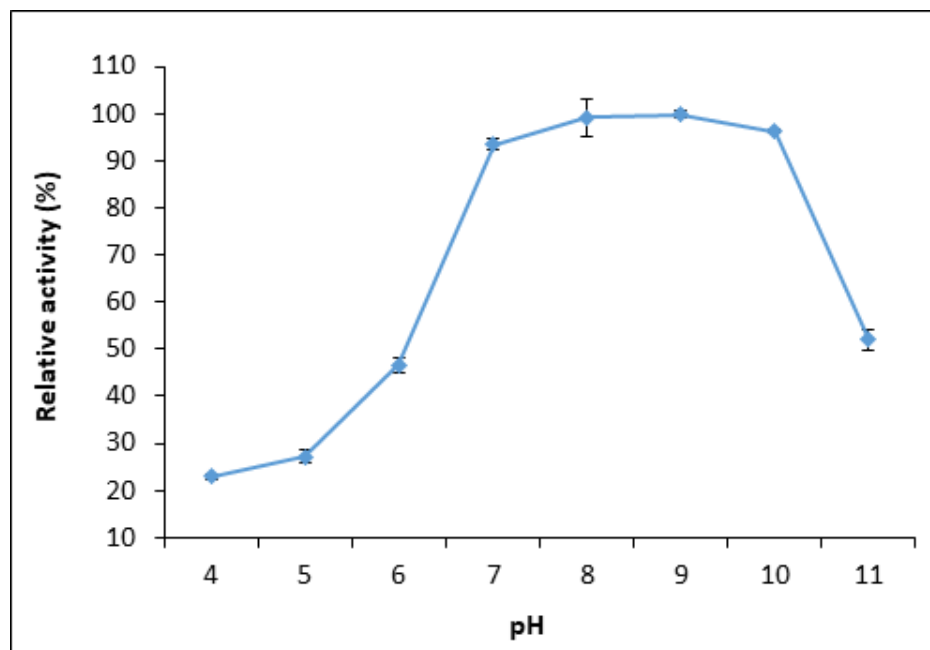


**Figure 4.58:** Effect of pH on activity of recombinant enzyme from *S. maltophilia* PRS8 strain

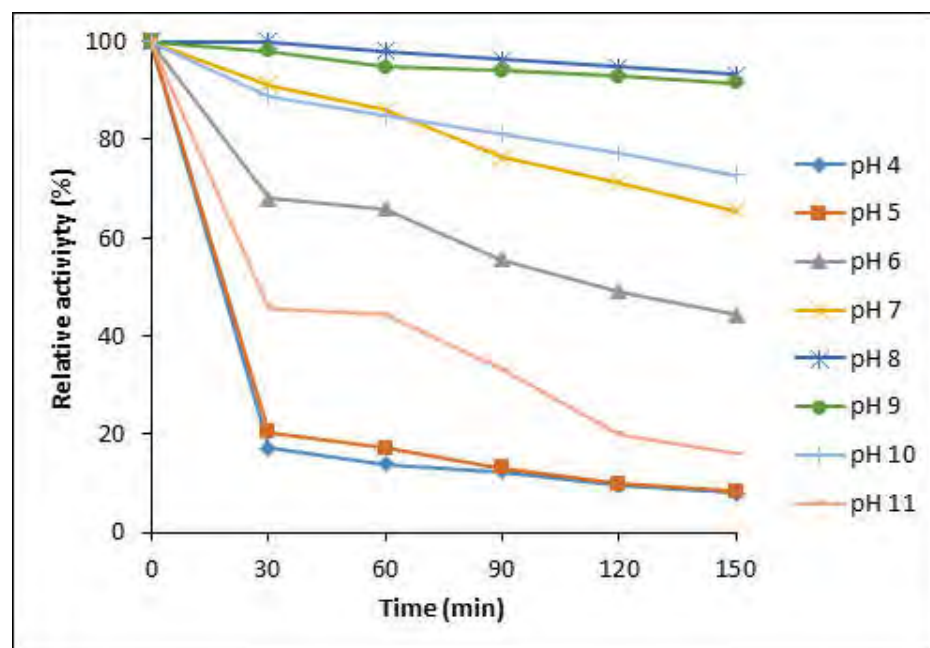


**Figure 4.59:** Effect of pH on stability of recombinant enzyme from *S. maltophilia* PRS8 strain

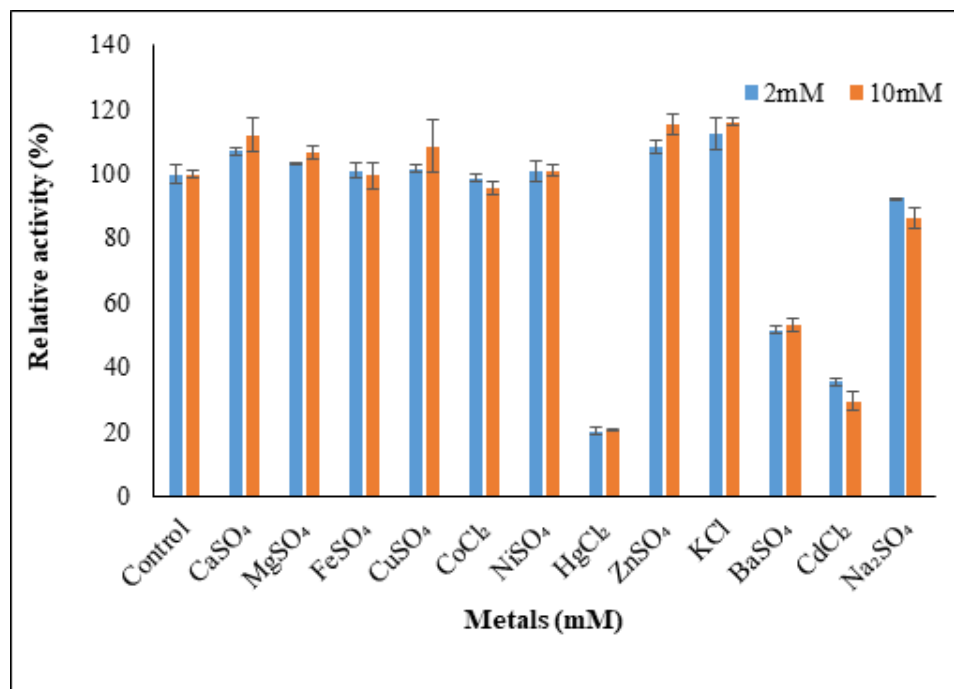


**Figure 4.60:** Effect of metals on the activity of recombinant enzyme from *S. maltophilia* PRS8 strain

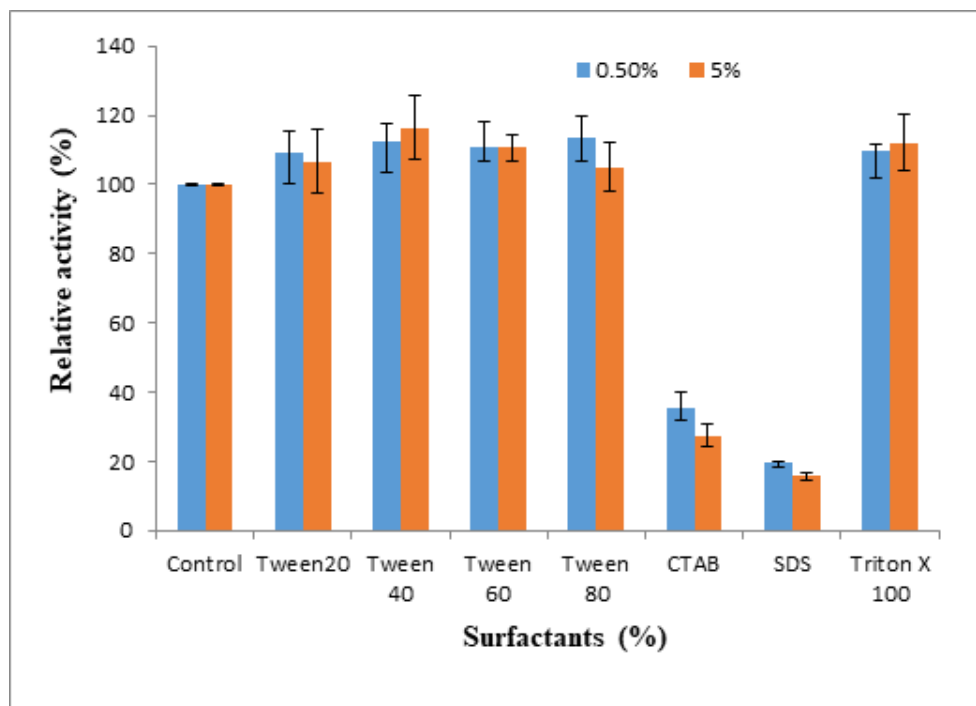


**Figure 4.61:** Effect of surfactants on the activity of recombinant enzyme from *S. maltophilia* PRS8 strain

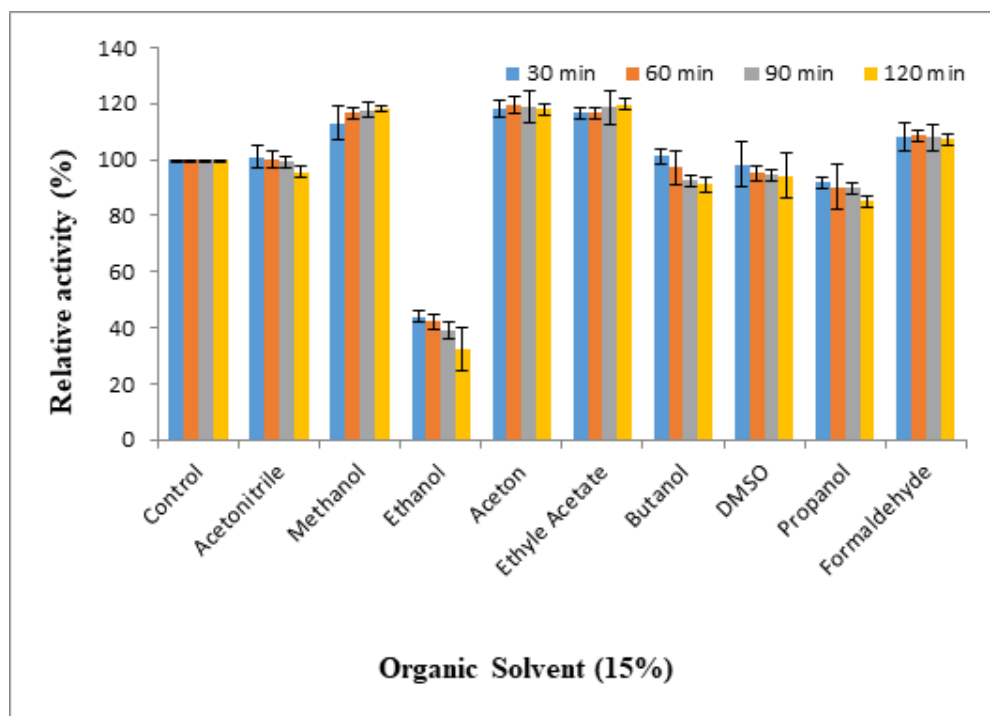


**Figure 4.62:** Effect of organic solvents on the activity of recombinant enzyme from *S. maltophilia* PRS8 strain

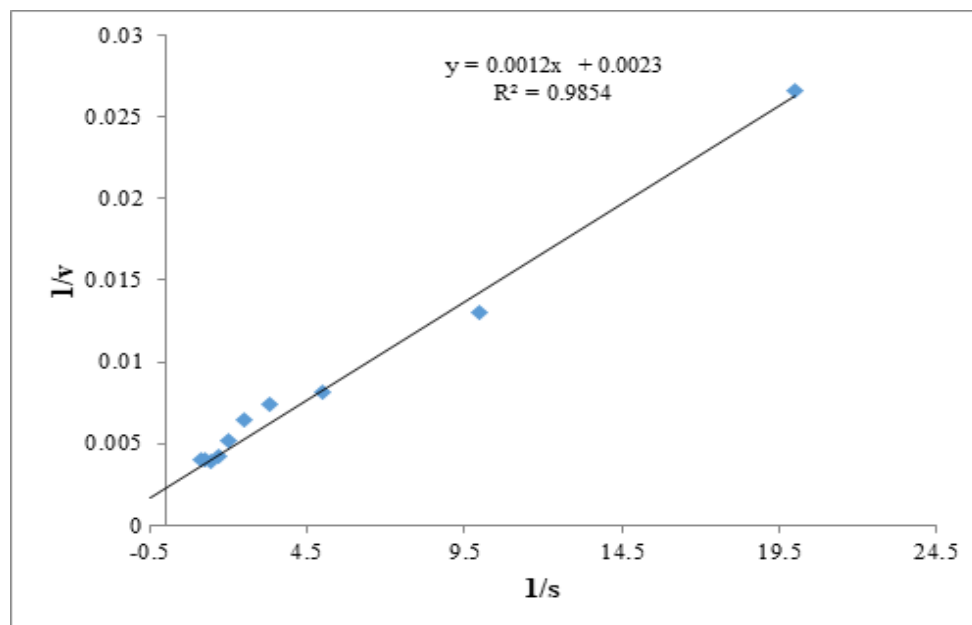


**Figure 4.63:** Kinetics analysis of recombinant enzyme from *S. maltophilia* PRS8 strain ( $K_m$  and  $V_{max}$ ) value were calculating by Lineweaver-burk plot using *p*-nitrophenyl Butyrate (*p*-NPB) as substrate.



#### 4.21 Recombinant Enzyme Activity on PET and Degradation Analysis by HPLC

The recombinant enzyme activity against semi-crystalline PET was assessed after 72 hours of reaction at 40°C and pH 9.0. The peaks for degradation products BHET, MHET, and TPA were detected through HPLC as indicated by HPLC chromatograms of degradation products. TPA eluted after ~0.677 min, while other product such as MHET and trace amount of BHET, were eluted after ~0.837 and ~1.042 min, respectively. (Fig 4.64B). DMSO was used as an additive for maximum solubility of depolymerized products. No products were detected in the negative control comprising DMSO, PET, and buffer under the same conditions (Fig 4.64A). Thus, the total amount of degraded polymer can be calculated by the TPAeq and the molecular weight 192 g/mol corresponding to the PET repeating unit (Wagner-Egea et al., 2021). The enzyme concentration was estimated by Nano-drop at 280 nm. The PET depolymerization yield was 22.5% with the main product MHET, followed by TPA and a small fraction of BHET (Table 4.11). Interestingly, these results are comparable with the *Ideonella sakaiensis* IsPETase, and superior to the thermostable cutinase HiCut from *Humicola insolens* (Table 4.11).

##### 4.21.1 Identification of degradation product by LCMS

The PET bottle pieces were incubated with purified cutinase-like enzyme in 100 mM potassium phosphate buffer (pH 8.0) at 40 °C. PET degradation products (BHET, MHET and TPA) have less solubility in water, therefore DMSO was used as a solvent for maximum solubility of depolymerized products. The PET polymer and its degradation products were separated in C18 column and analyzed by LC-MS.

The chromatogram in Fig 4.65 A shows the product profiles. TPA eluted after ~2.51 min, while other product such as MHET and trace amount of BHET, were eluted after ~3.93 and ~20.60 min, respectively. The degradation products TPA, MHET, and BHET were detected and confirmed by means of mass-to-charge ratio (m/z). The TPA peak in the MS was identified at 164.97 m/z with negative ionization, while the main product MHET was found at 209.06 m/z. Similarly, a small amount of BHET was detected at 253.08 (Fig 4.65B). This is the confirmation of PET hydrolyzing potential of purified recombinant enzyme from *S. maltophilia* PRS8.

### 4.21.2 Fourier-transform infrared (FT-IR) spectroscopy

The PET was subjected to FT-IR spectroscopy for determining chemical changes in its structure after incubation with recombinant PET hydrolase. FT-IR spectrum for both treated and untreated control samples showed potential differences in their functional groups as shown in figure 4.66. The area between 750–1000  $\text{cm}^{-1}$  corresponds to OH bends showing shift of peaks that depicts a clear difference between treated and untreated piece. A peak at 1103 in control was shifted to 1098 in test sample after treatment of PET recombinant PET hydrolase that shows C–C stretch. A peak at 1253  $\text{cm}^{-1}$  was moved to 1244  $\text{cm}^{-1}$  in test spectrum that indicates C-H group stretching in aromatic ring as result of breaks in polymer chain. A peak in the region 1713  $\text{cm}^{-1}$  corresponding C=O group, slightly altered in its position after microbial treatment. This clearly indicates splitting of ester linkages in polymer chain after its degradation.

### 4.21.3 Thermal properties and crystallinity of PET

The crystallinity and the thermal properties of untreated PET powder and PET powder treated with recombinant PET hydrolase were analyzed by DSC (Fig 4.67 and Table 4.12). The glass transition for the untreated PET was clearly observed in the first heating curve ( $T_g \sim 83^\circ\text{C}$ ). In case of PET treated with recombinant PET hydrolase,  $T_g$  was not clearly observed on the first heating curve, probably due to overlapping with the onset of the cold crystallization process ( $\sim 85^\circ\text{C}$ ). The  $T_g$  of treated PET was observed in the second heating curve. It was observed that the temperature for the cold crystallization peak ( $T_{cc}$ ) became lower after the enzyme treatment ( $110^\circ\text{C}$  compared to  $127^\circ\text{C}$  for untreated PET), which was accompanied by a lowered enthalpy for cold crystallization ( $\Delta H_{cc} \sim 2.9 \text{ J/g}$  compared to  $9.0 \text{ J/g}$  for pristine PET powder, Table 4.12). In addition, increased  $T_m$  ( $247^\circ\text{C}$ ) and crystallinity (21.1%) were observed after the PET powder was treated with PRS8 (compared to  $T_m \sim 242^\circ\text{C}$  and crystallinity of 19.3% for the pristine PET). This result suggested that the degradation of bulk PET materials presumably occurred (or occurred faster) in the amorphous region of PET.

Crystallinity is calculated using Equation

$$\text{Crystallinity \% (first heating cycle)} = \frac{(\Delta H_m - \Delta H_{cc})}{(\Delta H_m^o)} \times 100$$

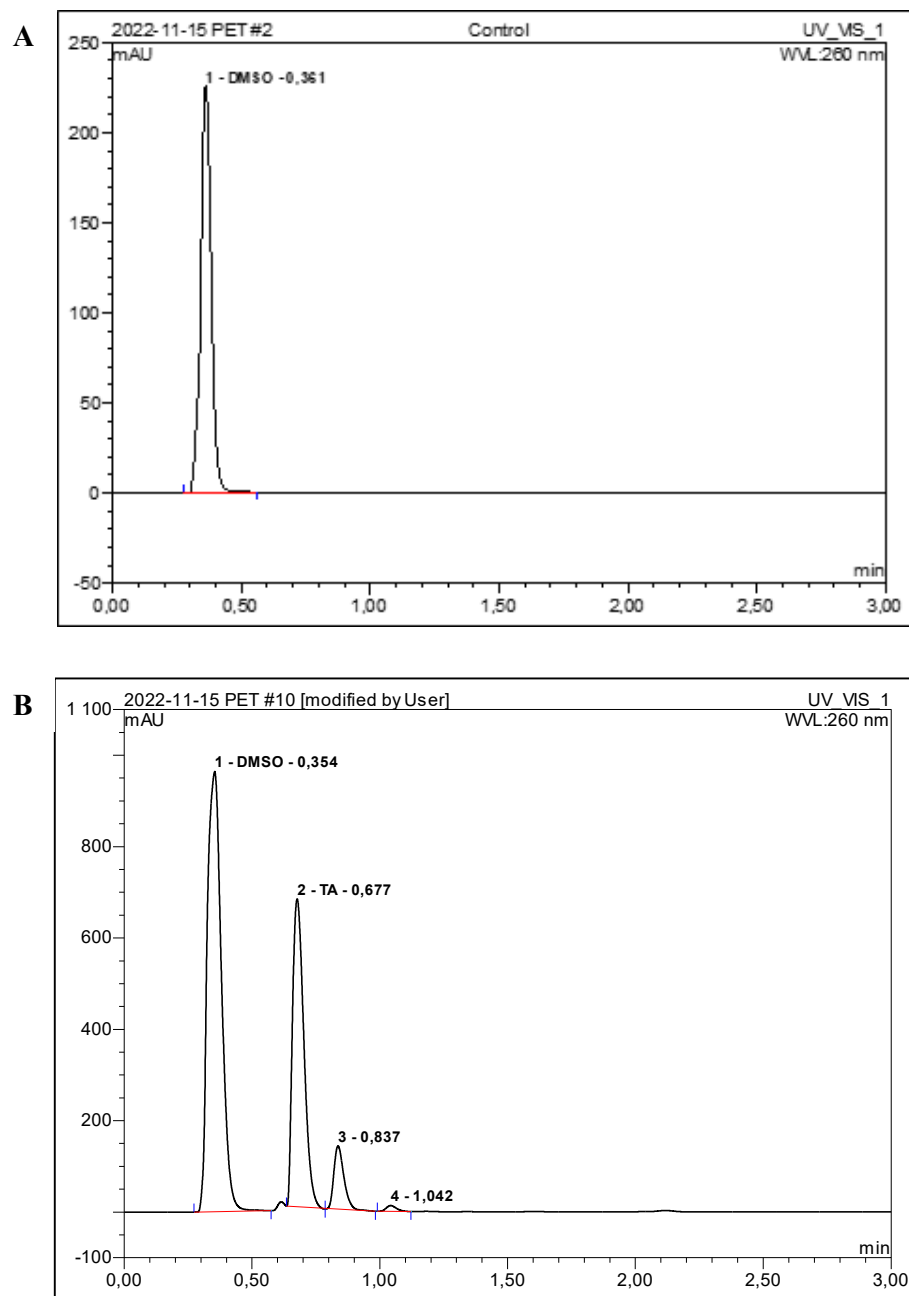


**Figure 4.64:** HPLC analysis of the degradation products of the recombinant enzyme activity on PET. The chromatogram showed the time course of product profile where the main product is MHET, followed by TPA and a small fraction of BHET. (A) Untreated (control) PET chromatogram. (B) PRS8 recombinant enzyme treated PET chromatogram

**Table 4.11:** PET depolymerization activity of the recombinant PET hydrolase of *S. maltophilia* PRS8 compared with enzymes after 72 hours

Enzyme	T (°C)	pH	Degradat ion Products (mg/L)	Relative Production (%)			PET depoly merizatio n (%)
				TPA	MHET	BHET	
Recombinant enzyme	40	8	2246	38	60	2	22.5
<i>Is</i> PETase	37	7.2	2304	24.2	73.7	2.1	23
Trx- <i>Is</i> PETase	37	7.2	3230	31.5	66.7	1.8	32
HiCut (HiC)	70	7.5	437	100	38	0.9	12.7

\* Estimated ratio based on the recombinant enzyme.

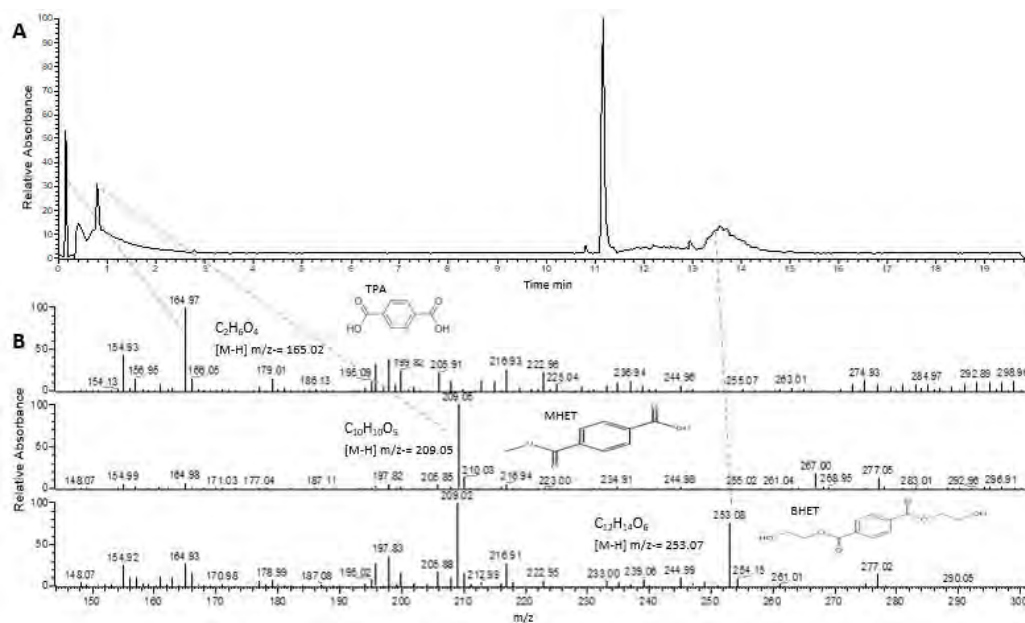


**Figure 4.66.** LC-MS analysis of the degradation products of the recombinant PET hydrolase activity on PET. (A) The Chromatogram showed the time course of product profile. (B) The Mass spectrum confirmed the identity of TA, MHET, and BHET.

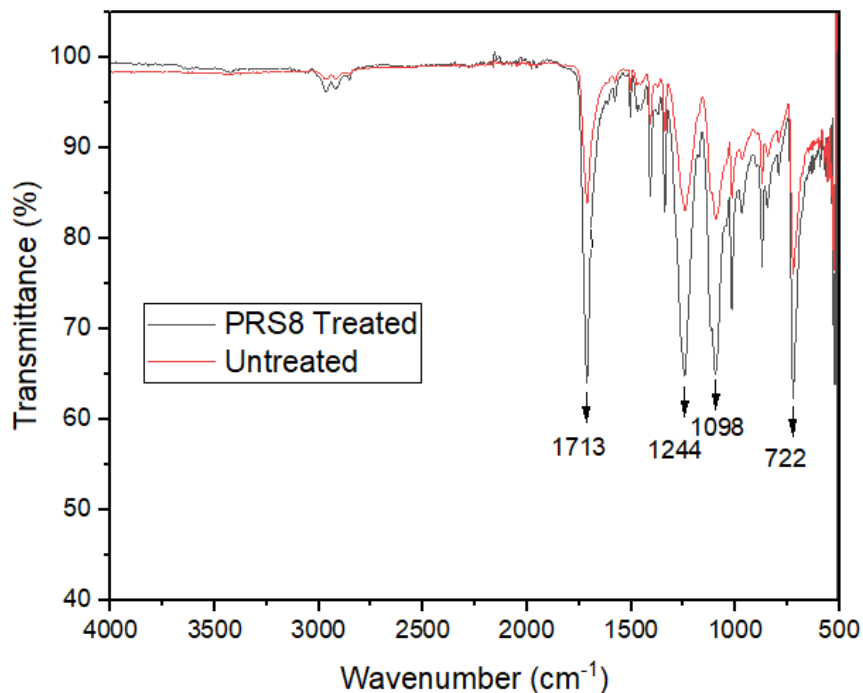


**Figure. 4.65:** The Fourier Transform Infra-Red (FT-IR) absorption pattern of recombinant PET hydrolase treated PET and untreated PET after 72 hours

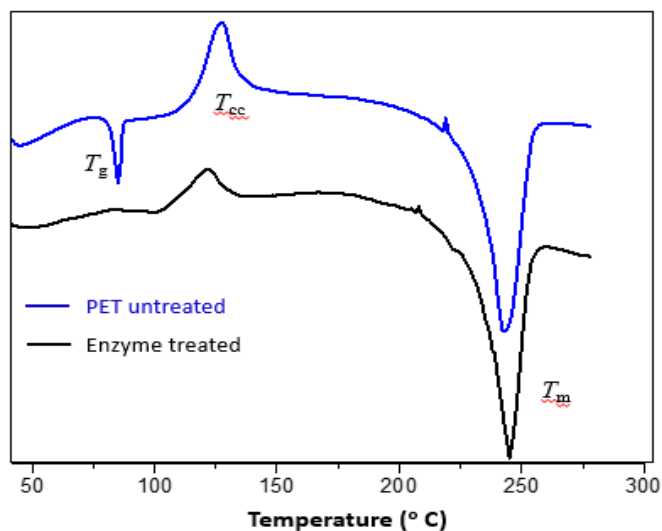


**Figure 4.67:** DSC heating curves of untreated PET and PET treated with PRS8 recombinant PET hydrolase. The  $T_g$ ,  $T_{cc}$  and  $T_m$  are shown on the PET untreated curve.

**Table 4.12:** Properties and crystallinity of the untreated PET and treated with recombinant PET hydrolase enzyme

<b>Polymer</b>	<b><math>T_g</math> (°C)</b>	<b><math>T_{cc}</math> (°C)</b>	<b><math>T_m</math> (°C)</b>	<b><math>\Delta H_{cc}</math> (J/g)</b>	<b><math>\Delta H_m</math> (J/g)</b>	<b>Crystallinity (%)</b>
PET (untreated)	83	110	247	2.9	32.4	21.1
PET (treated)	83	127	242	9.0	35.9	19.3

***CHAPTER 5***  
***DISCUSSION***

---

## Discussion

The study on biodegradation of synthetic polymer has received a lot of attention since early 1990s as a result of widespread concern over the international environmental crisis. Therefore, biodegradable polymer consumption and manufacturing have steadily increased, yet it accounts for a small percentage of overall plastic production. There's an urgent need for assessment of the potential ecosystem levels that have been occupied by plastic waste (microplastics) and their adverse effect on the life that invades our oceans and freshwaters and even land (Cózar et al., 2014). About 5 trillion pieces of plastic in the oceans, weighing up to 0.25 million tons, and research has revealed aquatic habitats where plastic debris is abundant (Eriksen et al., 2014). This man-made pollutant is also found in marine sediments and some of the world's most remote and largest freshwater reservoirs (Alqattaf, 2020).

Moreover, polyethene, polypropylene, polystyrene, polyvinyl chloride, polyurethane and polyethylene terephthalate (PET) are some others. PET is one of the most pervasive, extensive, and essential synthetic polymers. PET is widely used, and this overuse of synthetic PET has raised several health and environmental issues. PET adds to the urban solid waste and plastic waste in the oceans, which is the most alarming situation on a global level for the environment (Danso et al., 2019; Rajmohan et al., 2019). This situation has caused severe damage to marine life and is threatening all life forms. Most of the land plastic ends in water bodies (Barboza et al., 2020). So, to combat the nuisance created by PET, the enzymatic breakdown of PET seems to be a feasible and viable option. The polymeric material tends to aggregate in the environment and up till now no enzymes with high potential to degrade plastic has been discovered. Plastics are recalcitrant to biological degradation, and at present, only a small number of fungi and bacteria have been found to partially degrade PET to monomers (Danso et al., 2019).

PET crystallinity is one of the main obstacles to its biodegradation. The PET hydrolyzing enzymes involved in the breakdown are typical serine hydrolases, e.g., carboxylesterases, cutinases, and lipases. Usually, PET and cutin share small structural characteristics (Danso et al., 2019), they have ester bonds, which are



assaulted and cleaved by the enzyme. Thus, cutinases play an important part in hydrolyzing polyesters (Duan et al., 2017; Kawai et al., 2019; Aristizábal-Lanza et al., 2022). Cutinases enzymes are gaining interest because some showed activity on polyethylene terephthalate (PET). Although the first report on a PET active cutinase was published a long time ago (Müller et al., 2005). However, mesophilic enzymes and microorganisms could play an important role in systems where high temperatures are not suitable, for example, wastewater plants. Still, a few of these enzymes have been thoroughly studied so far. It is not only necessary to put focus on discovering possible new PET hydrolyzing microbial strains, but it is essential to study the efficient and effective enzymatic mechanism, their characterization, and other important factors that support maximum production of the enzymes.

In the current study a total of 3 bacterial strains were isolated, a bacterium designated as strain PRS8 was selected on the basis maximum growth in MSM medium containing PET pieces as sole carbon source. Strain PRS8 was identified as a member of genus *Stenotrophomonas* with 100% similarity with *Stenotrophomonas maltophilia*. In this study *Stenotrophomonas maltophilia* PRS8 was screened for degradation of PET and characterization of PET hydrolase enzymes. *Stenotrophomonas maltophilia* PRS8 is a gram-negative bacterium and belongs to  $\gamma$ -proteobacteria. It is mostly present in water, soil, and considered opportunistic pathogen. *Stenotrophomonas* have diverse metabolic machinery and utilize various carbon sources for survival in stressed condition. *S. maltophilia* has previously been reported for its major role in bioremediation of various pollutants including xenobiotic compounds, oil, dyes and poly aromatic hydrocarbons (PAHs) (An et al., 2021). Some of the PET degrading bacterial and fungal strains such as *Delftia* sp. WL-3 (Liu et al., 2018), *Thermobifida* species (Ribitsch et al., 2012), *Thermomyces insolens* (Ronkvist et al., 2009), and *Fusarium* species (Alisch-Mark., 2006), have been reported in the previous studies but their number is limited. Using PET as the sole carbon source, our strain PRS8 developed exceptionally well during rigorous screening period. *Ideonella sakaiensis* 201-F6 was recently isolated as a unique bacterium that can use PET as a main carbon source and erode the surface of PET pieces (Yoshida et al., 2016).

Serine hydrolases such lipases, cutinases or carboxylesterases, have typically been involved in degradation of polyethylene terephthalate (e.g., PET hydrolase, MHETase, tannase,). Cutinases belong to hydrolases superfamily, have a catalytic triad of aspartate, histidine, and serine (Danso et al., 2019). PETase (PET-digesting enzyme) is an enzyme that converts PET into mono(2-hydroxyethyl) terephthalic acid (MHET) along with terephthalic acid (TPA) and bis(2-hydroxyethyl)-TPA in trace concentrations. In the current study *S. maltophilia* PRS8 was screened for cutinase enzyme using PCL plate assay. The presence of zone of hydrolysis on PCL plate was an indication of cutinase production in the medium. The role of cutinase enzyme in degradation of PET has already been reported in the literature (Müller et al., 2005). Cutinase from *Trichoderma harzianum*, *Bacillus* SP KYP701 and *Pseudomonas cepacia* also hydrolyzed PET oligomer and displayed high hydrolytic activity against PET fiber (Adıgüzel and Tunçer 2017; Dutta et al., 2015; Rubio et al., 2008). Cutinase enzymes belong to hydrolases family with the capability to breakdown short-chain fatty acids by hydrolyzing ester bonds.

*S. maltophilia* PRS8 demonstrated its ability to form biofilm on PET film surface that could be helpful in its degradation. Previously reported *Delftia* sp. WL-3 which was fixed and developed a thin biofilm over the surface of PET (Liu et al., 2018). Biofilms can help microorganisms for better adaptation and adherence to the target surface and contribute to their tolerance to different environmental stresses. Microorganisms that are involved in the degradation of solid polymers require attachment, biofilm formation and thus enabling them to utilize non-soluble polymer efficiently (Hadar et al., 2004).

Bacterial adhesion to hexadecane hydrocarbon (BATH) assay was analyzed to determine bacterial hydrophobicity to assess the capacity of bacteria that have an affinity for organic hydrocarbons like hexadecane. The larger the hydrophobicity of the bacterial cells, the higher affinity is to the hydrocarbons, this causes the transfer of bacteria from the suspended state in the aqueous phase to the organic phase, hence decreasing the turbidness of the culture (Rosenberg et al., 1980). The *S. maltophilia*

PRS8 exhibited high hydrophobicity, the adherence of bacteria to hexadecane at low concentration was also significant, 0.32 mL which contributed to a 17% reduction in turbidity of culture during the log phase. Hence, confirming that, *S. maltophilia* PRS8 has hydrophobic nature. The hydrophobic-hydrophobic interaction aids in the adhesion of bacteria to PET surface, which as a result supports the degradation of PET pieces. The reduction in the turbidity of bacterial suspension (400 nm) indicates the transfer of hydrophobic cells from the aqueous to the organic phase. This assay confirmed the polymer adhesion capacity of the *S. maltophilia* PRS8.

*S. maltophilia* PRS8 exhibited extracellular cutinase activity in culture medium during degradation experiment. Expression of cutinase from *Pseudomonas cepacia* has previously been reported to be involved in degradation of PET (Dutta et al. 2015). The structural elucidation is crucial to determine changes that occurred as a result of deterioration. For this purpose, PET pieces were processed for SEM and FTIR analysis for structural changes. The FTIR analysis of PET pieces treated with strain PRS8 showed some changes in peaks at different wavenumbers in comparison to control. A decrease in value of peak at position  $2922\text{ cm}^{-1}$  corresponds to stretching of C-H group in the aromatic ring (Dąbrowska et al., 2021). Peak at  $1713\text{ cm}^{-1}$ , corresponds to vibration of C=O group, slightly altered that indicates splitting of ester bond in the polymer as a result of its degradation (Dang et al., 2018). SEM analysis revealed a clear roughness and cracks in PET piece after degradation by microorganism (Liu et al. 2018). Engineered *Clostridium thermocellum* exhibited marked changes in SEM and FTIR results of PET film at the end of experiment (Yan et al., 2021).

Cutinases are extracellular enzymes and have significantly been affected by physicochemical parameters (Maruthiah et al., 2014). In our study, the optimum activity on *p*-NPB was achieved at  $35^{\circ}\text{C}$  and pH 8.0 after 48 hours. The nutritional parameters were optimized using statistical tools such as Plackett-Burman and Central Composite design for effective cutinase-like enzyme production. These statistical tools have effectively been used in previous studies for optimum enzyme production (Muroi et al., 2017; Noor et al., 2020; Patil and Jena, 2015).

The involvement of each ingredient in production of cutinase is depicted in a Pareto chart acquired from Plackett Burman's Design (PBD). Cutin,  $\text{NaNO}_3$ , and  $[(\text{NH}_4)_2\text{SO}_4]$  were discovered to have a considerable influence on cutinase synthesis. In this report,  $\text{NaNO}_3$ , cutin and  $[(\text{NH}_4)_2\text{SO}_4]$  have positive effect on cutinase enzyme production because microorganisms favor organic nitrogen source for maximum production of enzymes (Das and Chandran, 2011). The reciprocal interaction of the factors on maximum cutinase enzyme production was further studied in response surface plot achieved from Central Composite design (CCD). Response surface plot (AB) in Figure 4.20 shows the action of  $\text{NaNO}_3$  and cutin on the activity of enzyme. An increase in the concentrations of both factors potentially enhanced enzyme specific activity. Same response plot for cutin and  $(\text{NH}_4)_2\text{SO}_4$  (AC) in Figure 4.21 indicated that the enzyme activity was enhanced as a result of increase in concentration of cutin while decrease in  $(\text{NH}_4)_2\text{SO}_4$  concentration had positive effect on enzyme activity. Similar interaction between  $\text{NaNO}_3$  and  $(\text{NH}_4)_2\text{SO}_4$  in response plot (BC) was observed that maximum specific activity was achieved at high concentrations of both components, respectively. Both components have a positive effect on enzyme production (Fig. 4.22). Similar result was previously reported for esterase production from *Pseudomonas aeruginosa* S3 (Noor et al., 2020). In numerous comparable experiments, both the PBD and CCD have been used to maximise the medium components for the synthesis of pectinase from *Bacillus pumilus*. (Sharma and Satyanarayana, 2006). It is important to employ an experimental design that can take into account the interactions between various operational factors since these interactions affect each operational variable's impact on the response (Kumar et al. 2009). Prior to now, *P. cepacia* NRRL B 2320 cutinase was optimized via CCD, which led to a twofold increase in enzyme activity, or 336 mol/min/ml. (Dutta et al., 2013). When *Fusarium oxysporum* produced cutinase, the enzyme activity increased by twofold (22.68 mol/min/ml) and the enzyme activity was optimized via CCD (Dutta et al., 2013).

The cutinase enzyme from *S. maltophilia* PRS8 was purified to homogeneity, which enhanced its specific activity from 70.47 to 450.58 U/mg with 6.39 purification fold.

The molecular weight of cutinase from *S. maltophilia* PRS8 was found to be approximately 58 kDa which is quite higher, cutinase from *F. solani* (20–22 kDa) (Kwon et al., 2009), *P. cepacia* NRRL B 2320 (26.5 kDa) (Dutta et al., 2013), *T. terrestris* (25.3 kDa) (Yang et al., 2013), *F. oxysporum* (20.0 kDa) (Degani et al., 2015) and *A. nidulans* (29 kDa) (Castro-Ochoa et al., 2012). The enzyme activity was optimum at 40 °C and pH 8.0 and found stable at wide range of temperature (30 to 40 °C) and pH (8.0 to 10.0). The optimal temperature of cutinase is lower, previously reported from *P. cepacia* NRRL B 2320 (Dutta et al., 2013), *T. terrestris* (Yang et al., 2013), *T. vulgaris* NRRL B-16177 (Fett et al., 2000) and *T. fusca* KW3 (Billig et al., 2010). The exposure to temperatures and pH above or below optimum level negatively affect the enzyme activity due to structural changes in protein that ultimately leads to denaturation of the enzyme. The enzyme from *Thermoactinomyces vulgaris* was found to be stable at temperature ranges from 20-40°C and pH from 8.0-11.0 (Fett et al., 2000).

The enzyme activity is usually affected in the presence of metals and chemicals such as surfactants and organic solvents (Adıgüzel and Tunçer, 2017). Metal ions keep enzyme structure stable and active by binding to negatively charged amino acid residues. They are also known to modify solubility and catalytic properties of enzymes (Çolak et al., 2005). The enzyme activity was slightly stimulated by various metals ions (mono and divalent cationic) except  $\text{Cd}^{2+}$ ,  $\text{Co}^{2+}$  and  $\text{Hg}^{2+}$  that strongly inhibited. Activity limitation in the presence of  $\text{Cd}^{2+}$  and  $\text{Hg}^{2+}$  can reveal the presence of critical vicinal sulfhydryl gathering (Kawai et al., 2019; Then et al., 2015). Since the metals can act as co-factors, the enzyme was stable in the presence of  $\text{Cu}^{2+}$  and  $\text{Ni}^{2+}$ , with enhanced relative activity (Geyer et al., 2016). Likewise, Thumarat et al., (2012) observed that  $\text{Mg}^{2+}$  and  $\text{Ca}^{2+}$  ions slightly affect cutinase activity from *T. alba* AHK119.

Similarly, surfactants have a positive effect on cutinase enzyme activity that might be due to increase in oil–water interfacial area, which in turn promoted cutinase activity. It has been reported that non-ionic surfactants have a major role in stimulating cutinase activity (Degani, 2015). SDS and CTAB strongly inhibited the enzyme

activity that might be due to its interaction with enzyme hydrophobic region that ultimately leads to modification in 3-D structure. Although Hegde and Veeranki, (2013) and Chen et al. (2010) previously reported that some surfactants chemicals such as Triton X-100, Tween 80, and Tween 20, strongly inhibited the cutinase activity from *T. fusca*, while in our study these surfactants enhanced the cutinase activity from *S. maltophilia* PRS8. The enzyme was stable in the presence of various solvents except ethanol and butanol that might be due to change in structure of bound substrate or active site polarity. Similarly, Adıgüzel & Tunçer, (2017) reported that some chemicals such as propanol, ethanol, chloroform, benzene DMSO and methanol slightly inhibited cutinase activity with increase of time. The  $K_m$  and  $V_{max}$  of the purified enzyme for *p*-NP-butyrate was found to be 0.703  $\mu$ M and 370.37 U/mg, respectively, as calculated by Lineweaver and Burk's plot. A very low  $K_m$  showed high affinity of enzyme toward substrate (Kim et al., 2006).

The DSC analysis of PET indicated a reduction in crystallinity by 3.1% following treatment with the enzyme derived from *S. maltophilia* PRS8. This finding suggests that the enzymatic degradation of PET primarily targeted the amorphous region. as reported in the literature (Carr et al., 2020). Previous similar results were reported *F. solani* and *T. fusca* cutinase that hydrolyzed PET and decreased only 1 % crystallinity (Aristizábal-Lanza et al., 2022). While using synthetic IsPETase from *Ideonella sakaiensis* that hydrolyzed PET into monomers and decreased only 0.1 % of the crystallinity (Wagner-Egea et al., 2021). Previously, it was noted that the use of IsPETase from *Ideonella sakaiensis* for enzymatic degradation of PET led to a marginal decrease in crystallinity. This decrease was attributed to the formation of dimers during the degradation process, which likely contributed to the disruption of the crystalline structure. (Menzel et al., 2021). In our result, no dimer (melting or crystallization) peak was observed using DSC, which was consistent with the decreased crystallinity after the enzymatic degradation by *S. maltophilia* PRS8. Thus, the cutinase enzyme activity seemed restricted to the amorphous part.

The role of the cutinase enzyme from *S. maltophilia* PRS8 in depolymerization of PET (18.3 % after 72 hours) was determined through analysis of degradation products released into the medium by LC-MS. The degradation products TA, MHET and BHET were detected released as a result of enzyme de-polymerization of PET. Previous similar results were reported *F. solani* and *T. fusca* cutinase that hydrolyzed PET as model substrate and produced degradation fragments comprised TA, MHET and BHET (Aristizábal-Lanza et al., 2022). Similarly Cloning and expression of PET degrading enzyme in *E. coli* host was previously reported by several researchers. Wagner-Egea et al. (2021) reported synthetic IsPETase that de-polymerized PET and confirmed the degradation products such as TA, MHET and BHET by HPLC and LC-MS. This confirms PET-hydrolyzing ability of cutinase from *S. maltophilia* PRS8 that can be used to develop new PET waste recovery processes.

PET hydrolyzing enzyme from *S. maltophilia* PRS8 was successfully expressed in *E. coli* BL21 cell. Interestingly, the enzymatic activity of PET hydrolyzing enzyme was observed to be higher in *E. coli* compared to the native bacterial strains PRS8. This difference in activity could be attributed to the elevated protein expression levels in *E. coli*. Moreover, the PET hydrolyzing enzyme secreted by *E. coli* exhibited functional activity, effectively degrading PET. The first characterized lipase for this genus was named LipSM54 and was described as cold-active, solvent-tolerant, and alkaline (Li et al., 2016). A thermostable lipase, LipSm (Parapouli et al., 2018), and a thermostable-alkaline-stable esterase (Gao et al., 2019) were also cloned and characterized. Cloning and expression of PET degrading enzyme in *E. coli* host was previously reported by several researchers (Wagner-Egea et al., 2021; Aristizábal-Lanza et al., 2022). The cloned PET hydrolyzing enzyme from *S. maltophilia* PRS8 was 1.8 kb. Yang et al., (2023) reported previously 0.9 kb PET degrading engineered cutinase. Similarly, Wagner-Egea et al., (2021) reported purified IsPETase that was 0.8 kb have a potential role in degradation of PET.

The recombinant PET hydrolyzing enzyme from *S. maltophilia* PRS8 was purified to homogeneity, which enhanced its activity from 70.47 to 595.93 U/mL with 6.19 purification fold. The enzyme exhibited a molecular weight of approximately 58 kDa. Its activity was most favorable at a temperature of 40°C and a pH range of 8.0-9.0.



Additionally, it displayed stability over a broad temperature range (30 to 40 °C) and pH range (8.0 to 10.0). The exposure to temperatures and pH below or above optimum level negatively affect the enzyme activity due to structural changes in protein that ultimately leads to denaturation of the enzyme. This study suggests that the alkaline pH range of 8 to 10 provides a suitable chemical environment for the cutinase enzyme to exhibit its highest catalytic activity. Enzymes are sensitive to pH changes because the pH affects their three-dimensional structure, which in turn influences their active sites and interactions with substrates (Aristizábal-Lanza et al., 2022). The mesophilic temperature and high pH are more suitable for potential degradation of PET. The cutinase from *Humicola insolens* was found to be stable at temperature ranges from 62-77°C and pH from 8.0-9.0 (Aristizábal-Lanza et al., 2022). Finally, the *S. maltophilia* PRS8 recombinant PET hydrolyzing enzyme showed a PET-depolymerizing activity comparable to IsPETase and significantly higher than the thermostable HiCut (HiC) from *Humicola insolens*.

Some metal ions, surfactants, and organic solvents could be used as additives to increase the enzyme activity. Some metal ions could stabilize the enzyme structure, and the surfactants and organic solvents could facilitate the interaction with the hydrophobic polymers. The cutinase enzyme activity was slightly increased by the various metal ions (mono and divalent cationic) except for Cd<sup>2+</sup>, Co<sup>2+</sup>, and Hg<sup>2+</sup>, which strongly inhibited the activity. The activity limitation in the presence of Cd<sup>2+</sup> and Hg<sup>2+</sup> revealed the presence of a gathering of critical vicinal sulfhydryl (Then et al., 2015). However, Cu<sup>2+</sup> and Ni<sup>2+</sup> enhanced the relative activity (Geyer et al., 2016). Regarding surfactants, nonionic surfactants were reported to have an important role in promoting cutinase activity (Degani et al., 2015). Tween and Triton-100 showed a positive effect, but the SDS and CTAB strongly inhibited the enzyme activity. Although Hegde and Veeranki, (2013) and Chen et al. (2010) previously reported that some surfactants chemicals such as Triton X-100, Tween 80, and Tween 20, strongly inhibited the cutinase activity from *T. fusca*, while in our study these surfactants enhanced the cutinase activity from *S. maltophilia* PRS8. The enzyme was stable in the presence of the various solvents except for ethanol and butanol, which might be due to a change in the structure of the bound substrate or the active site polarity (Kim



et al., 2006). Similarly, Adıgüzel & Tunçer, (2017) reported that some chemicals such as propanol, ethanol, chloroform, benzene DMSO and methanol slightly inhibited cutinase activity with increase of time.

The degradation rate with recombinant PET hydrolase from *S. maltophilia* PRS8 was recorded as 22.5% after 72 hours. The enzyme could not retain its activity and dropped to 50% after this time. The primary product derived from PET was MHET, with subsequent formation of TPA, along with a minor portion of BHET. A similar product profile was also found after the treatment of PET with PETases (Joo et al., 2018; Wagner-Egea et al., 2021) and cutinases (Kawai, 2021; Aristizábal-Lanza et al., 2022). The stability of Trx-IsPETase was assessed by calculating the amounts of products after 72 hours. The concentration of degradation products increased over time and reached saturation after 72 hours. The saturation was attributed to the inactivation of the enzyme and not to the completion of the reaction, since the substrate conversion reached ~35%, according to kinetics with the coexistence of a sufficient substrate (20 mg PET) (Wagner-Egea et al., 2021). The DSC analysis of PET indicated a reduction in crystallinity following treatment with the enzyme derived from *S. maltophilia* PRS. This finding suggests that the enzymatic degradation of PET predominantly targeted the amorphous region, as reported in the literature (Carr et al., 2020). Previously, it was noted that the use of IsPETase from *Ideonella sakaiensis* for enzymatic degradation of PET led to a slight reduction of 0.9% in crystallinity. This decrease was attributed to the formation of dimers during the degradation process, which could potentially disrupt the overall crystalline structure (Menzel et al., 2021). In our result, no dimer (melting or crystallization) peak was observed using DSC, which was consistent with the decreased 4.1 % crystallinity after the enzymatic degradation by *S. maltophilia* PRS8. Thus, the recombinant PET hydrolyzing enzyme activity seemed restricted to the amorphous part.

PET, however, is an aromatic polyester, and several cutinases have also shown the depolymerizing activity on PET (Liang, X.; Zou, 2022). The PET treated with *S. maltophilia* PRS8 showed a slightly reduced intensity of the characteristic PET peaks

between 700 and 1800  $\text{cm}^{-1}$  in the FTIR analysis, compared to the non-treated PET. These results provide physical and chemical evidence of the PET degradation capability of *S. maltophilia* PRS8 with the participation of a cutinase enzyme. *Engineered Clostridium thermocellum* exhibited marked changes in FTIR results of PET film at the end of experiment (Yan et al., 2021). Enzymatic treatment of PET led to a noticeable decrease in the intensity of FTIR peaks at 720 and 1240  $\text{cm}^{-1}$  when compared to the negative control. This change in intensity is in line with the evidence of surface degradation (Ioakeimidis et al., 2016).

Finally, the *S. maltophilia* PRS8 containing the PET hydrolyzing enzyme showed a PET-depolymerizing activity comparable to IsPETase and significantly higher than the thermostable HiCut (HiC) from *Humicola insolens*. In a practical sense, these results indicated that the *S. maltophilia* PRS8 enzyme under optimal conditions could be used in the PET degradation processes, with the advantage of degrading PET at mesophilic temperature.

# ***CONCLUSION***

**Conclusion**

- i. A total of 24 bacterial strains were isolated from both soil and PET piece sample. 3 bacterial isolates from soil sample exhibited good growth after 28 days of incubation utilizing PET as a sole carbon source. Bacterial strain PRS8 was identified, characterized and further investigated for degradation of PET.
- ii. Bacterial strain *Stenotrophomonas maltophilia* PRS8 degraded PET piece with 1.8% reduction in weight loss after 28 days of incubation, used 60% crystalline PET plastic from nestle water bottle. The biodegradation potential was confirmed through FTIR and SEM.
- iii. *S. maltophilia* PRS8 is more hydrophobic in nature and was able to effectively colonize on the surface of PET in the form of biofilm.
- iv. Native *S. maltophilia* PRS8 was explored for production of cutinase. Maximum production of enzyme by *S. maltophilia* PRS8 was achieved at temperature 40°C and pH 8.0, while retained 100% of the enzyme activity for 150 minutes. A total of 18.2% reduction in PET was achieved for 72 hours after treatment with purified cutinase.
- v. PET degradation product Terephthalic acid, Mono (2-hydroxyethyl) terephthalate and Bis 2-hydroxyethyl) terephthalate were identified through HPLC and LC-MS
- vi. PET hydrolyzing gene from *S. maltophilia* PRS8 was successfully cloned into intracellular PET-21b and expressed into BL 21 (DE3). The recombinant enzyme was purified by HiPrep 16/60 Sephacryle S-300 High resolution Gel filtration column Chromatography and used for degradation of PET. The efficiency of enzyme was enhanced and 22.5% reduction in PET was achieved after 72 hours with recombinant enzyme.
- vii. PET degradation product TPA, MHET and BHET were identified through LC-MS. About 4.1 % reduction in crystallinity was observed after the PET was treated with recombinant enzyme.

# ***FUTURE PROSPECTS***

**Future prospects**

- i. Diversity of sampling sites for isolation of more significant PET degrading strains.
- ii. Enhancing the activity of *S. maltophilia* PRS8 PET hydrolyzing enzyme by regulating the flexibility of the hinge region.
- iii. N-terminal amino acid sequence of purified enzyme can also be carried out for checking multiple alignment.
- iv. Thermal stability of PET hydrolase can be enhanced by molecular biology techniques such as adding proline tag to the protein.
- v. PET degradation enzyme can be more efficiently tailored through site directed mutagenesis for efficient PET degradation.
- vi. Enzymes can be engineered to have improved substrate specificity and catalytic activity for certain types of plastics, such as PET. Reducing the crystallinity of PET can enhance their biodegradability. Engineered enzymes could target and break down the regions of higher crystallinity, enabling better access to the polymer chains for further degradation.

## ***REFERENCES***

---

## References

1. Aday, M. S., & Yener, U. (2014). Consumer behaviours in Turkey. *International Journal of Consumer Studies*, 38, 385-393.
2. Adıgüzel, A. O., & Tunçer, M. (2017). Purification and characterization of cutinase from *Bacillus* sp. KY0701 isolated from plastic wastes. *Preparative Biochemistry and Biotechnology*, 47(9), 925-933.
3. Alisch-Mark, M., Herrmann, A., & Zimmermann, W. (2006). Increase of the hydrophilicity of polyethylene terephthalate fibres by hydrolases from *Thermomonospora fusca* and *Fusarium solani* f. sp. *Biotechnology letters*, 28, 681-685.
4. Alqattaf, A. (2020). Plastic waste management: Global facts, challenges and solutions. In *2020 Second International Sustainability and Resilience Conference: Technology and Innovation in Building Designs (51154)* (pp. 1-7). IEEE.
5. An, Q., Deng, S., Liu, M., Li, Z., Wu, D., Wang, T., & Chen, X. (2021). Study on the aerobic remediation of Ni (II) by *Pseudomonas hibiscicola* strain L1 interaction with nitrate. *Journal of Environmental Management*, 299, 113641.
6. Anderson, A. G., Grose, J., Pahl, S., Thompson, R. C., & Wyles, K. J. (2016). Microplastics in personal care products: Exploring perceptions of environmentalists, beauticians and students. *Marine pollution bulletin*, 113(1-2), 454-460.
7. Arena, M., Abbate, C., Fukushima, K., & Gennari, M. (2011). Degradation of poly (lactic acid) and nanocomposites by *Bacillus licheniformis*. *Environmental Science and Pollution Research*, 18, 865-870.
8. Aristizábal-Lanza, L., Mankar, S. V., Tullberg, C., Zhang, B., & Linares-Pastén, J. A. (2022). Comparison of the enzymatic depolymerization of polyethylene terephthalate and Akestra TM using *Humicola insolens* cutinase. *Frontiers in Chemical Engineering*, 4.
9. Aryan, Y., Yadav, P., & Samadder, S. R. (2019). Life Cycle Assessment of the existing and proposed plastic waste management options in India: A case study. *Journal of Cleaner Production*, 211, 1268-1283.



10. Aslam, M., Kalyar, M. A., & Raza, Z. A. (2018). Polyvinyl alcohol: A review of research status and use of polyvinyl alcohol based nanocomposites. *Polymer Engineering & Science*, 58(12), 2119-2132.
11. Ayeleru, O. O., Dlova, S., Akinribide, O. J., Ntuli, F., Kupolati, W. K., Marina, P. F., ... & Olubambi, P. A. (2020). Challenges of plastic waste generation and management in sub-Saharan Africa: A review. *Waste Management*, 110, 24-42.
12. Badia, J. D., Gil-Castell, O., & Ribes-Greus, A. (2017). Long-term properties and end-of-life of polymers from renewable resources. *Polymer Degradation and Stability*, 137, 35-57.
13. Bahl, S., Dolma, J., Singh, J. J., & Sehgal, S. (2021). Biodegradation of plastics: A state of the art review. *Materials Today: Proceedings*, 39, 31-34.
14. Baker, P. J., Poultney, C., Liu, Z., Gross, R., & Montclare, J. K. (2012). Identification and comparison of cutinases for synthetic polyester degradation. *Applied microbiology and biotechnology*, 93, 229-240.
15. Barboza, L. G. A., Lopes, C., Oliveira, P., Bessa, F., Otero, V., Henriques, B., ... & Guilhermino, L. (2020). Microplastics in wild fish from North East Atlantic Ocean and its potential for causing neurotoxic effects, lipid oxidative damage, and human health risks associated with ingestion exposure. *Science of the Total Environment*, 717, 134625.
16. Barnes, D. K., Galgani, F., Thompson, R. C., & Barlaz, M. (2009). Accumulation and fragmentation of plastic debris in global environments. *Philosophical transactions of the royal society B: biological sciences*, 364(1526), 1985-1998.
17. Barros, M. V., Salvador, R., Piekarski, C. M., & de Francisco, A. C. (2019). Mapping of main research lines concerning life cycle studies on packaging systems in Brazil and in the world. *The International Journal of Life Cycle Assessment*, 24, 1429-1443.
18. Barth, M., Honak, A., Oeser, T., Wei, R., Belisário-Ferrari, M. R., Then, J., ... & Zimmermann, W. (2016). A dual enzyme system composed of a polyester hydrolase and a carboxylesterase enhances the biocatalytic degradation of polyethylene terephthalate films. *Biotechnology Journal*, 11(8), 1082-1087.

19. Becidan, M. (2007). Experimental studies on municipal solid waste and biomass pyrolysis.
20. Bhardwaj, H., Gupta, R., & Tiwari, A. (2013). Communities of microbial enzymes associated with biodegradation of plastics. *Journal of Polymers and the Environment*, *21*, 575-579.
21. Bher, A., Mayekar, P. C., Auras, R. A., & Schvezov, C. E. (2022). Biodegradation of Biodegradable Polymers in Mesophilic Aerobic Environments. *International Journal of Molecular Sciences*, *23*(20), 12165.
22. Billig, S., Oeser, T., Birkemeyer, C., & Zimmermann, W. (2010). Hydrolysis of cyclic poly (ethylene terephthalate) trimers by a carboxylesterase from *Thermobifida fusca* KW3. *Applied microbiology and biotechnology*, *87*, 1753-1764.
23. Borrelle, S. B., Ringma, J., Law, K. L., Monnahan, C. C., Lebreton, L., McGivern, A., ... & Rochman, C. M. (2020). Predicted growth in plastic waste exceeds efforts to mitigate plastic pollution. *Science*, *369*(6510), 1515-1518.
24. Boucher, J., & Billard, G. (2019). The challenges of measuring plastic pollution. *Field Actions Science Reports. The Journal of Field Actions*, (Special Issue 19), 68-75.
25. Browne, M. A., Crump, P., Niven, S. J., Teuten, E., Tonkin, A., Galloway, T., & Thompson, R. (2011). Accumulation of microplastic on shorelines worldwide: sources and sinks. *Environmental science & technology*, *45*(21), 9175-9179.
26. Browne, M. A., Niven, S. J., Galloway, T. S., Rowland, S. J., & Thompson, R. C. (2013). Microplastic moves pollutants and additives to worms, reducing functions linked to health and biodiversity. *Current biology*, *23*(23), 2388-2392.
27. Burnley, S., Coleman, T., & Peirce, A. (2015). Factors influencing the life cycle burdens of the recovery of energy from residual municipal waste. *Waste management*, *39*, 295-304.
28. Carr, C. M., Clarke, D. J., & Dobson, A. D. (2020). Microbial polyethylene terephthalate hydrolases: current and future perspectives. *Frontiers in Microbiology*, *11*, 571265.

- 
29. Castro-Ochoa, D., Peña-Montes, C., González-Canto, A., Alva-Gasca, A., Esquivel-Bautista, R., Navarro-Ocaña, A., & Farrés, A. (2012). AN CUT2, an extracellular cutinase from *Aspergillus nidulans* induced by olive oil. *Applied biochemistry and biotechnology*, *166*, 1275-1290.
30. Cataldo, F., & Angelini, G. (2006). Some aspects of the ozone degradation of poly (vinyl alcohol). *Polymer Degradation and Stability*, *91*(11), 2793-2800.
31. Chen, S., Su, L., Billig, S., Zimmermann, W., Chen, J., & Wu, J. (2010). Biochemical characterization of the cutinases from *Thermobifida fusca*. *Journal of Molecular Catalysis B: Enzymatic*, *63*(3-4), 121-127
32. Chen, S., Su, L., Chen, J., & Wu, J. (2013). Cutinase: characteristics, preparation, and application. *Biotechnology advances*, *31*(8), 1754-1767.
33. Chen, Y., Tan, L., Chen, L., Yang, Y., & Wang, X. (2008). Study on biodegradable aromatic/aliphatic copolyesters. *Brazilian journal of chemical engineering*, *25*, 321-335.
34. Chinthapalli, R., Skoczinski, P., Carus, M., Baltus, W., de Guzman, D., Käß, H., ... & Ravenstijn, J. (2019). Biobased building blocks and polymers—global capacities, production and trends, 2018–2023. *Industrial Biotechnology*, *15*(4), 237-241.
35. Cleary, J. (2014). A life cycle assessment of residential waste management and prevention. *The International Journal of Life Cycle Assessment*, *19*, 1607-1622.
36. Coates, G. W., & Getzler, Y. D. (2020). Chemical recycling to monomer for an ideal, circular polymer economy. *Nature Reviews Materials*, *5*(7), 501-516.
37. Çolak, A., Şişik, D., Sağlam, N., Güner, S., Çanakçı, S., & Beldüz, A. O. (2005). Characterization of a thermoalkalophilic esterase from a novel thermophilic bacterium, *Anoxybacillus gonensis* G2. *Bioresource technology*, *96*(5), 625-631.
38. Cox, K. D., Covernton, G. A., Davies, H. L., Dower, J. F., Juanes, F., & Dudas, S. E. (2019). Human consumption of microplastics. *Environmental science & technology*, *53*(12), 7068-7074.
39. Cózar, A., Echevarría, F., González-Gordillo, J. I., Irigoien, X., Úbeda, B., Hernández-León, S., ... & Duarte, C. M. (2014). Plastic debris in the open

- ocean. *Proceedings of the National Academy of Sciences*, 111(28), 10239-10244.
40. Dąbrowska, G. B., Janczak, K., & Richert, A. (2021). Combined use of *Bacillus* strains and *Miscanthus* for accelerating biodegradation of poly (lactic acid) and poly (ethylene terephthalate). *PeerJ*, 9, e10957.
41. Dang, T. C. H., Nguyen, D. T., Thai, H., Nguyen, T. C., Hien Tran, T. T., Le, V. H., ... & Nguyen, Q. T. (2018). Plastic degradation by thermophilic *Bacillus* sp. BCBT21 isolated from composting agricultural residual in Vietnam. *Advances in Natural Sciences: Nanoscience and Nanotechnology*, 9(1), 015014.
42. Danso, D., Chow, J., & Streit, W. R. (2019). Plastics: environmental and biotechnological perspectives on microbial degradation. *Applied and environmental microbiology*, 85(19), e01095-19.
43. Das, N., & Chandran, P. (2011). Microbial degradation of petroleum hydrocarbon contaminants: an overview. *Biotechnology research international*, 2011.
44. Dauvergne, P. (2018). The power of environmental norms: marine plastic pollution and the politics of microbeads. *Environmental Politics*, 27(4), 579-597.
45. Degani, O. (2015). Production and purification of cutinase from *Fusarium oxysporum* using modified growth media and a specific cutinase substrate. *Advances in Bioscience and Biotechnology*, 6(04), 245.
46. Determann, H. (2012). *Gel Chromatography Gel Filtration· Gel Permeation· Molecular Sieves: A Laboratory Handbook*. Springer Science & Business Media.
47. Devi, R. S., Kannan, V. R., Natarajan, K., Nivas, D., Kannan, K., Chandru, S., & Antony, A. R. (2016). The role of microbes in plastic degradation. *Environ Waste Manage*, 341, 341-370.
48. Dhawan, R., Bisht, B. M. S., Kumar, R., Kumari, S., & Dhawan, S. K. (2019). Recycling of plastic waste into tiles with reduced flammability and improved tensile strength. *Process Safety and Environmental Protection*, 124, 299-307.

- 
49. Driedger, A. G., Dürr, H. H., Mitchell, K., & Van Cappellen, P. (2015). Plastic debris in the Laurentian Great Lakes: a review. *Journal of Great Lakes Research*, *41*(1), 9-19.
50. Drobot, M., Persin, Z., Zemljic, L. F., Mohan, T., Stana-Kleinschek, K., Doliska, A., ... & Coseri, S. (2013). Chemical modification and characterization of poly (ethylene terephthalate) surfaces for collagen immobilization. *Central European Journal of Chemistry*, *11*, 1786-1798.
51. Duan, X., Liu, Y., You, X., Jiang, Z., Yang, S., & Yang, S. (2017). High-level expression and characterization of a novel cutinase from *Malbranchea cinnamomea* suitable for butyl butyrate production. *Biotechnology for biofuels*, *10*, 1-14.
52. Dutta, K., Dasu, V. V., & Hegde, K. (2013). Development of medium and kinetic modeling for enhanced production of cutinase from *Pseudomonas cepacia* NRRL B-2320. *Advances in Microbiology*, *2013*.
53. Dutta, K., Krishnamoorthy, H., & Dasu, V. V. (2013). Novel cutinase from *Pseudomonas cepacia* NRRL B 2320: Purification, characterization and identification of cutinase encoding genes. *The Journal of General and Applied Microbiology*, *59*(3), 171-184.
54. Dutta, K., Venkata Dasu, V., Mahanty, B., & Anand Prabhu, A. (2015). Substrate inhibition growth kinetics for cutinase producing *Pseudomonas cepacia* using tomato-peel extracted cutin. *Chemical and Biochemical Engineering Quarterly*, *29*(3), 437-445.
55. Eerkes-Medrano, D., Thompson, R. C., & Aldridge, D. C. (2015). Microplastics in freshwater systems: a review of the emerging threats, identification of knowledge gaps and prioritisation of research needs. *Water research*, *75*, 63-82.
56. Eriksen, M., Lebreton, L. C., Carson, H. S., Thiel, M., Moore, C. J., Borerro, J. C., ... & Reisser, J. (2014). Plastic pollution in the world's oceans: more than 5 trillion plastic pieces weighing over 250,000 tons afloat at sea. *PloS one*, *9*(12), e111913.

- 
57. Fett, W. F., Wijey, C., Moreau, R. A., & Osman, S. F. (2000). Production of cutinolytic esterase by filamentous bacteria. *Letters in applied microbiology*, *31*(1), 25-29.
58. Gao, X., Mao, X., Lu, P., Secundo, F., Xue, C., & Sun, J. (2019). Cloning, expression, and characterization of a novel thermostable and alkaline-stable esterase from *Stenotrophomonas maltophilia* OUC\_Est10 catalytically active in organic solvents. *Catalysts*, *9*(5), 401.
59. Gardette, J.-L.; Rivaton, A.; Therias, S. Photodegradation Processes In Polymeric Materials. In *Photochemistry and Photophysics of Polymer Materials*; John Wiley & Sons, Inc.: Hoboken, NJ, USA, 2010; pp. 569–601, ISBN 9780470137963.
60. Gawande, A., Zamre, G. S., Renge, V. C., Bharsakale, G. R., & Tayde, S. (2012). Utilization of waste plastic in asphaltting of roads. *Scientific Reviews & chemical communications*, *2*(2), 147-157.
61. Geyer, B., Lorenz, G., & Kandelbauer, A. (2016). Recycling of poly (ethylene terephthalate)—A review focusing on chemical methods. *Express Polymer Letters*, *10*(7), 559-586.
62. Geyer, R., Jambeck, J. R., & Law, K. L. (2017). Production, use, and fate of all plastics ever made. *Science advances*, *3*(7), e1700782.
63. Ghasemlou, M., Daver, F., Ivanova, E. P., & Adhikari, B. (2019). Bio-based routes to synthesize cyclic carbonates and polyamines precursors of non-isocyanate polyurethanes: A review. *European Polymer Journal*, *118*, 668-684.
64. Gong, J., Kong, T., Li, Y., Li, Q., Li, Z., & Zhang, J. (2018). Biodegradation of microplastic derived from poly (ethylene terephthalate) with bacterial whole-cell biocatalysts. *Polymers*, *10*(12), 1326.
65. Gorrasi, G., & Pantani, R. (2018). Hydrolysis and Biodegradation of Poly (lactic acid). *Synthesis, Structure and Properties of Poly (lactic acid)*, 119-151.
66. Gregson, N., & Crang, M. (2019). Made in China and the new world of secondary resource recovery. *Environment and Planning A: Economy and Space*, *51*(4), 1031-1040.

- 
67. Gricajeva, A., Nadda, A. K., & Gudiukaite, R. (2022). Insights into polyester plastic biodegradation by carboxyl ester hydrolases. *Journal of Chemical Technology & Biotechnology*, 97(2), 359-380.
68. Gug, J., Cacciola, D., & Sobkowicz, M. J. (2015). Processing and properties of a solid energy fuel from municipal solid waste (MSW) and recycled plastics. *waste management*, 35, 283-292.
69. Hadar, Y., & Sivan, A. (2004). Colonization, biofilm formation and biodegradation of polyethylene by a strain of *Rhodococcus ruber*. *Applied microbiology and biotechnology*, 65, 97-104.
70. Hajighasemi, M., Nocek, B. P., Tchigvintsev, A., Brown, G., Flick, R., Xu, X., ... & Yakunin, A. F. (2016). Biochemical and structural insights into enzymatic depolymerization of polylactic acid and other polyesters by microbial carboxylesterases. *Biomacromolecules*, 17(6), 2027-2039.
71. Harding, K. G., Gounden, T., & Pretorius, S. (2017). "Biodegradable" plastics: a myth of marketing?. *Procedia manufacturing*, 7, 106-110.
72. Hegde, K., & Veeranki, V. D. (2013). Production optimization and characterization of recombinant cutinases from *Thermobifida fusca* sp. NRRL B-8184. *Applied biochemistry and biotechnology*, 170, 654-675.
73. Heidbreder, L. M., Bablok, I., Drews, S., & Menzel, C. (2019). Tackling the plastic problem: A review on perceptions, behaviors, and interventions. *Science of the total environment*, 668, 1077-1093.
74. Hermabessiere, L., Dehaut, A., Paul-Pont, I., Lacroix, C., Jezequel, R., Soudant, P., & Duflos, G. (2017). Occurrence and effects of plastic additives on marine environments and organisms: a review. *Chemosphere*, 182, 781-793.
75. Herrero Acero, E., Ribitsch, D., Steinkellner, G., Gruber, K., Greimel, K., Eiteljoerg, I., ... & Guebitz, G. (2011). Enzymatic surface hydrolysis of PET: effect of structural diversity on kinetic properties of cutinases from *Thermobifida*. *Macromolecules*, 44(12), 4632-4640.
76. Herzog, K., Müller, R. J., & Deckwer, W. D. (2006). Mechanism and kinetics of the enzymatic hydrolysis of polyester nanoparticles by lipases. *Polymer degradation and stability*, 91(10), 2486-2498.

- 
77. Hopewell, J., Dvorak, R., & Kosior, E. (2009). Plastics recycling: challenges and opportunities. *Philosophical Transactions of the Royal Society B: Biological Sciences*, 364(1526), 2115-2126.
78. Horton, A. A., Walton, A., Spurgeon, D. J., Lahive, E., & Svendsen, C. (2017). Microplastics in freshwater and terrestrial environments: evaluating the current understanding to identify the knowledge gaps and future research priorities. *Science of the total environment*, 586, 127-141.
79. Howard, G. T., & Blake, R. C. (1998). Growth of *Pseudomonas fluorescens* on a polyester–polyurethane and the purification and characterization of a polyurethanase–protease enzyme. *International Biodeterioration & Biodegradation*, 42(4), 213-220.
80. Idumah, C. I., & Nwuzor, I. C. (2019). Novel trends in plastic waste management. *SN Applied Sciences*, 1, 1-14.
81. Jamieson, A. J., Malkocs, T., Piertney, S. B., Fujii, T., & Zhang, Z. (2017). Bioaccumulation of persistent organic pollutants in the deepest ocean fauna. *Nature ecology & evolution*, 1(3), 1-4.
82. Jâms, I. B., Windsor, F. M., Poudevigne-Durance, T., Ormerod, S. J., & Durance, I. (2020). Estimating the size distribution of plastics ingested by animals. *Nature Communications*, 11(1), 1594.
83. Jayasekara, R., Harding, I., Bowater, I., & Lonergan, G. (2005). Biodegradability of a selected range of polymers and polymer blends and standard methods for assessment of biodegradation. *Journal of Polymers and the Environment*, 13, 231-251.
84. Jeon, H. J., & Kim, M. N. (2015). Functional analysis of alkane hydroxylase system derived from *Pseudomonas aeruginosa* E7 for low molecular weight polyethylene biodegradation. *International Biodeterioration & Biodegradation*, 103, 141-146.
85. Jiang, J. Q. (2018). Occurrence of microplastics and its pollution in the environment: a review. *Sustain Prod Consumption* 13: 16–23.
86. Joshi, R., & Ahmed, S. (2016). Status and challenges of municipal solid waste management in India: A review. *Cogent Environmental Science*, 2(1), 1139434.



- 
87. Karpushova, A.; Brümmer, F.; Barth, S.; Lange, S.; Schmid, R. (2005). Cloning, recombinant expression and biochemical characterization of novel esterases from *Bacillus* sp. associated with the marine sponge *Aplysina aerophoba*. *Appl. Microbiol. Biotechnol*, *67*, 59–69.
88. Kawai, F. (2021). The current state of research on PET hydrolyzing enzymes available for biorecycling. *Catalysts*, *11*(2), 206.
89. Kawai, F., Kawabata, T., & Oda, M. (2019). Current knowledge on enzymatic PET degradation and its possible application to waste stream management and other fields. *Applied microbiology and biotechnology*, *103*, 4253-4268.
90. Khan, S., Nadir, S., Shah, Z. U., Shah, A. A., Karunarathna, S. C., Xu, J., ... & Hasan, F. (2017). Biodegradation of polyester polyurethane by *Aspergillus tubingensis*. *Environmental pollution*, *225*, 469-480.
91. Kijchavengkul, T., Auras, R., Rubino, M., Ngouajio, M., & Fernandez, R. T. (2008). Assessment of aliphatic–aromatic copolyester biodegradable mulch films. Part I: Field study. *Chemosphere*, *71*(5), 942-953.
92. Kim, J. H., Choi, S. H., Park, M. G., Park, D. H., Son, K. H., & Park, H. Y. (2022). Polyurethane biodegradation by *Serratia* sp. HY-72 isolated from the intestine of the Asian mantis *Hierodula patellifera*. *Frontiers in Microbiology*, *13*.
93. Kim, J. W., Park, S. B., Tran, Q. G., Cho, D. H., Choi, D. Y., Lee, Y. J., & Kim, H. S. (2020). Functional expression of polyethylene terephthalate-degrading enzyme (PETase) in green microalgae. *Microbial Cell Factories*, *19*(1), 1-9.
94. Kim, Y. J., Choi, G. S., Kim, S. B., Yoon, G. S., Kim, Y. S., & Ryu, Y. W. (2006). Screening and characterization of a novel esterase from a metagenomic library. *Protein expression and purification*, *45*(2), 315-323.
95. Knoblauch, D., Mederake, L., & Stein, U. (2018). Developing countries in the lead—what drives the diffusion of plastic bag policies?. *Sustainability*, *10*(6), 1994.
96. Konduri, M. K., Koteswarareddy, G., Rohini Kumar, D. B., Venkata Reddy, B., & Lakshmi Narasu, M. (2011). Effect of pro-oxidants on biodegradation of polyethylene (LDPE) by indigenous fungal isolate, *Aspergillus oryzae*. *Journal of Applied Polymer Science*, *120*(6), 3536-3545.
-

- 
97. Kong, H. G., Kim, H. H., Chung, J. H., Jun, J., Lee, S., Kim, H. M., ... & Ryu, C. M. (2019). The *Galleria mellonella* hologenome supports microbiota-independent metabolism of long-chain hydrocarbon beeswax. *Cell Reports*, *26*(9), 2451-2464.
98. Konieczna, A., Rachoń, D., Owczarek, K., Kubica, P., Kowalewska, A., Kudłak, B., ... & Namieśnik, J. (2018). Serum bisphenol A concentrations correlate with serum testosterone levels in women with polycystic ovary syndrome. *Reproductive Toxicology*, *82*, 32-37.
99. Krueger, M. C., Harms, H., & Schlosser, D. (2015). Prospects for microbiological solutions to environmental pollution with plastics. *Applied microbiology and biotechnology*, *99*, 8857-8874.
100. Kumar, P. (2018). Role of plastics on human health. *The Indian Journal of Pediatrics*, *85*(5), 384-389.
101. Kumar, S., Pakshirajan, K., & Venkata Dasu, V. (2009). Development of medium for enhanced production of glutaminase-free L-asparaginase from *Pectobacterium carotovorum* MTCC 1428. *Applied microbiology and biotechnology*, *84*, 477-486.
102. Kwon, M. A., Kim, H. S., Yang, T. H., Song, B. K., & Song, J. K. (2009). High-level expression and characterization of *Fusarium solani* cutinase in *Pichia pastoris*. *Protein expression and purification*, *68*(1), 104-109.
103. Kyaw, B. M., Champakalakshmi, R., Sakharkar, M. K., Lim, C. S., & Sakharkar, K. R. (2012). Biodegradation of low density polythene (LDPE) by *Pseudomonas* species. *Indian journal of microbiology*, *52*, 411-419.
104. Kyaw, B. M., Champakalakshmi, R., Sakharkar, M. K., Lim, C. S., & Sakharkar, K. R. (2012). Biodegradation of low density polythene (LDPE) by *Pseudomonas* species. *Indian journal of microbiology*, *52*(3), 411-419
105. Laemmli, U. K. (1970). Cleavage of structural proteins during the assembly of the head of bacteriophage T4. *nature*, *227*(5259), 680-685.
106. Lahens, L., Strady, E., Kieu-Le, T. C., Dris, R., Boukerma, K., Rinnert, E., Gasperi, J., & Tassin, B. (2018). Macroplastic and microplastic contamination assessment of a tropical river (Saigon River, Vietnam) transversed by a developing megacity. *Environmental Pollution*, *236*, 661-671

- 
107. Lau, W. W., Shiran, Y., Bailey, R. M., Cook, E., Stuchtey, M. R., Koskella, J., ... & Palardy, J. E. (2020). Evaluating scenarios toward zero plastic pollution. *Science*, *369*(6510), 1455-1461.
108. Law, K. L., & Narayan, R. (2022). Reducing environmental plastic pollution by designing polymer materials for managed end-of-life. *Nature Reviews Materials*, *7*(2), 104-116.
109. Laycock, B., Nikolić, M., Colwell, J. M., Gauthier, E., Halley, P., Bottle, S., & George, G. (2017). Lifetime prediction of biodegradable polymers. *Progress in Polymer Science*, *71*, 144-189.
110. Lebreton, L., & Andrady, A. (2019). Future scenarios of global plastic waste generation and disposal. *Palgrave Communications*, *5*(1), 1-11.
111. Lee, S. H., & Kim, M. N. (2010). Isolation of bacteria degrading poly (butylene succinate-co-butylene adipate) and their lip A gene. *International Biodeterioration & Biodegradation*, *64*(3), 184-190.
112. Lefèvre, C., Tidjani, A., Vander Wauven, C., & David, C. (2002). The interaction mechanism between microorganisms and substrate in the biodegradation of polycaprolactone. *Journal of applied polymer science*, *83*(6), 1334-1340.
113. Leja, K., & Lewandowicz, G. (2010). Polymer Biodegradation and Biodegradable Polymers-a Review. *Polish Journal of Environmental Studies*, *19*(2).
114. Li, M., Yang, L. R., Xu, G., & Wu, J. P. (2016). Cloning and characterization of a novel lipase from *Stenotrophomonas maltophilia* GS11: the first member of a new bacterial lipase family XVI. *Journal of Biotechnology*, *228*, 30-36.
115. Liang, X., & Zou, H. (2022). Biotechnological Application of Cutinase: A Powerful Tool in Synthetic Biology. *SynBio*, *1*(1), 54-64.
116. Lim, H. A., Raku, T., & Tokiwa, Y. (2005). Hydrolysis of polyesters by serine proteases. *Biotechnology Letters*, *27*, 459-464.
117. Lineweaver, H., & Burk, D. (1934). The determination of enzyme dissociation constants. *Journal of the American chemical society*, *56*(3), 658-666.

- 
118. Liu, J., Xu, G., Dong, W., Xu, N., Xin, F., Ma, J., ... & Jiang, M. (2018). Biodegradation of diethyl terephthalate and polyethylene terephthalate by a novel identified degrader *Delftia* sp. WL-3 and its proposed metabolic pathway. *Letters in Applied Microbiology*, 67(3), 254-261.
119. Lowry, O. H., Rosebrough, N. J., Farr, A. L., & Randall, R. J. (1951). Protein measurement with the Folin phenol reagent. *Journal of biological chemistry*, 193(1), 265-275.
120. Lucas, N., Bienaime, C., Belloy, C., Queneudec, M., Silvestre, F., & Nava-Saucedo, J. E. (2008). Polymer biodegradation: Mechanisms and estimation techniques—A review. *Chemosphere*, 73(4), 429-442.
121. MacLeod, M., Arp, H. P. H., Tekman, M. B., & Jahnke, A. (2021). The global threat from plastic pollution. *Science*, 373(6550), 61-65.
122. Mao, H., Liu, H., Gao, Z., Su, T., & Wang, Z. (2015). Biodegradation of poly (butylene succinate) by *Fusarium* sp. FS1301 and purification and characterization of poly (butylene succinate) depolymerase. *Polymer degradation and stability*, 114, 1-7.
123. Marten, E., Müller, R. J., & Deckwer, W. D. (2005). Studies on the enzymatic hydrolysis of polyesters. II. Aliphatic–aromatic copolyesters. *Polymer degradation and stability*, 88(3), 371-381.
124. Maruthiah, T., Esakkiraj, P., Prabakaran, G., Palavesam, A., & Immanuel, G. (2014). Purification and characterization of moderately halophilic alkaline serine protease from marine *Bacillus subtilis* AP-MSU 6. *Biocatalysis and Agricultural Biotechnology*, 2(2), 116-119.
125. Mason, S. A., Welch, V. G., & Neratko, J. (2018). Synthetic polymer contamination in bottled water. *Frontiers in chemistry*, 407.
126. Melo, E. P., Baptista, R. P., & Cabral, J. M. S. (2003). Improving cutinase stability in aqueous solution and in reverse micelles by media engineering. *Journal of Molecular Catalysis B: Enzymatic*, 22(5–6), 299–306
127. Mendenhall, E. (2018). Oceans of plastic: a research agenda to propel policy development. *Marine Policy*, 96, 291-298.

- 
128. Menzel, T., Weigert, S., Gagsteiger, A., Eich, Y., Sittl, S., Papastavrou, G., ... & Höcker, B. (2021). Impact of enzymatic degradation on the material properties of poly (ethylene terephthalate). *Polymers*, *13*(22), 3885.
129. MoEFCC, 2018. Plastics in Life and Environment. Retrieved from New Delhi: [http:// envfor.nic.in/sites/default/files/press-releases/Lo\\_Book01.pdf](http://envfor.nic.in/sites/default/files/press-releases/Lo_Book01.pdf)
130. Mohee, R., & Unmar, G. (2007). Determining biodegradability of plastic materials under controlled and natural composting environments. *Waste management*, *27*(11), 1486-1493.
131. Mohee, R., Unmar, G. D., Mudhoo, A., & Khadoo, P. (2008). Biodegradability of biodegradable/degradable plastic materials under aerobic and anaerobic conditions. *Waste Management*, *28*(9), 1624-1629
132. Moog, D., Schmitt, J., Senger, J., Zarzycki, J., Rexer, K. H., Linne, U., ... & Maier, U. G. (2019). Using a marine microalga as a chassis for polyethylene terephthalate (PET) degradation. *Microbial cell factories*, *18*(1), 1-15.
133. Moss, B. (2017). Marine reptiles, birds and mammals and nutrient transfers among the seas and the land: an appraisal of current knowledge. *Journal of Experimental Marine Biology and Ecology*, *492*, 63-80.
134. Mowla, D., & Ahmadi, M. (2007). Theoretical and experimental investigation of biodegradation of hydrocarbon polluted water in a three phase fluidized-bed bioreactor with PVC biofilm support. *Biochemical Engineering Journal*, *36*(2), 147-156.
135. Mueller, R. J. (2006). Biological degradation of synthetic polyesters—Enzymes as potential catalysts for polyester recycling. *Process Biochemistry*, *41*(10), 2124-2128.
136. Müller, R. J., Schrader, H., Profe, J., Dresler, K., & Deckwer, W. D. (2005). Enzymatic degradation of poly (ethylene terephthalate): rapid hydrolyse using a hydrolase from *T. fusca*. *Macromolecular rapid communications*, *26*(17), 1400-1405.
137. Muroi, F., Tachibana, Y., Soulethone, P., Yamamoto, K., Mizuno, T., Sakurai, T., ... & Kasuya, K. I. (2017). Characterization of a poly (butylene

- adipate-co-terephthalate) hydrolase from the aerobic mesophilic bacterium *Bacillus pumilus*. *Polymer Degradation and Stability*, 137, 11-22.
138. Nakajima-Kambe, T., Onuma, F., Kimpara, N., & Nakahara, T. (1995). Isolation and characterization of a bacterium which utilizes polyester polyurethane as a sole carbon and nitrogen source. *FEMS Microbiology Letters*, 129(1), 39-42.
139. Nakajima-Kambe, T., Toyoshima, K., Saito, C., Takaguchi, H., Akutsu-Shigeno, Y., Sato, M., ... & Uchiyama, H. (2009). Rapid monomerization of poly (butylene succinate)-co-(butylene adipate) by *Leptothrix* sp. *Journal of bioscience and bioengineering*, 108(6), 513-516.
140. Narancic, T., Verstichel, S., Reddy Chaganti, S., Morales-Gamez, L., Kenny, S. T., De Wilde, B., ... & O'Connor, K. E. (2018). Biodegradable plastic blends create new possibilities for end-of-life management of plastics but they are not a panacea for plastic pollution. *Environmental science & technology*, 52(18), 10441-10452.
141. Nielsen, T. D., Hasselbalch, J., Holmberg, K., & Stripple, J. (2020). Politics and the plastic crisis: A review throughout the plastic life cycle. *Wiley Interdisciplinary Reviews: Energy and Environment*, 9(1), e360.
142. Nikolaidis, P., & Poullikkas, A. (2017). A comparative overview of hydrogen production processes. *Renewable and sustainable energy reviews*, 67, 597-611.
143. Noor, H., Satti, S. M., ud Din, S., Farman, M., Hasan, F., Khan, S., ... & Shah, A. A. (2020). Insight on esterase from *Pseudomonas aeruginosa* strain S3 that depolymerize poly (lactic acid)(PLA) at ambient temperature. *Polymer Degradation and Stability*, 174, 109096.
144. Ocegüera-Cervantes, A., Carrillo-García, A., López, N., Bolanos-Nunez, S., Cruz-Gómez, M. J., Wachter, C., & Loza-Tavera, H. (2007). Characterization of the polyurethanolytic activity of two *Alicyclophilus* sp. strains able to degrade polyurethane and N-methylpyrrolidone. *Applied and Environmental Microbiology*, 73(19), 6214-6223.

- 
145. Olewnik-Kruszkowska, E., Nowaczyk, J., & Kadac, K. (2017). Effect of compatibilizing agent on the properties of polylactide and polylactide based composite during ozone exposure. *Polymer Testing*, *60*, 283-292.
146. Onundi, Y., Drake, B. A., Malecky, R. T., DeNardo, M. A., Mills, M. R., Kundu, S., ... & Collins, T. J. (2017). A multidisciplinary investigation of the technical and environmental performances of TAML/peroxide elimination of Bisphenol A compounds from water. *Green Chemistry*, *19*(18), 4234-4262.
147. Orr, R. J., Rutter, S. M., Yarrow, N. H., Champion, R. A., & Rook, A. J. (2004). Changes in ingestive behaviour of yearling dairy heifers due to changes in sward state during grazing down of rotationally stocked ryegrass or white clover pastures. *Applied Animal Behaviour Science*, *87*(3-4), 205-222.
148. Osman, M., Satti, S. M., Luqman, A., Hasan, F., Shah, Z., & Shah, A. A. (2018). Degradation of polyester polyurethane by *Aspergillus* sp. strain S45 isolated from soil. *Journal of Polymers and the Environment*, *26*, 301-310.
149. Owczarek, K., Kubica, P., Kudłak, B., Rutkowska, A., Konieczna, A., Rachoń, D., ... & Wasik, A. (2018). Determination of trace levels of eleven bisphenol A analogues in human blood serum by high performance liquid chromatography–tandem mass spectrometry. *Science of the total environment*, *628*, 1362-1368.
150. Ozen, B. F., Mauer, L. J., & Floros, J. D. (2002). Effects of ozone exposure on the structural, mechanical and barrier properties of select plastic packaging films. *Packaging Technology and Science: An International Journal*, *15*(6), 301-311.
151. Pan, W., Bai, Z., Su, T., & Wang, Z. (2018). Enzymatic degradation of poly (butylene succinate) with different molecular weights by cutinase. *International journal of biological macromolecules*, *111*, 1040-1046.
152. Parapouli, M., Foukis, A., Stergiou, P. Y., Koukouritaki, M., Magklaras, P., Gkini, O. A., ... & Hatziloukas, E. (2018). Molecular, biochemical and kinetic analysis of a novel, thermostable lipase (LipSm) from *Stenotrophomonas maltophilia* Psi-1, the first member of a new bacterial lipase family (XVIII). *Journal of Biological Research-Thessaloniki*, *25*, 1-12.

- 
153. Patil, S. S., & Jena, H. M. (2015). Statistical optimization of phenol degradation by *Bacillus pumilus* OS1 using plackett–burman design and response surface methodology. *Arabian Journal for Science and Engineering*, *40*(8), 2141-2151.
154. Pelch, K., Wignall, J. A., Goldstone, A. E., Ross, P. K., Blain, R. B., Shapiro, A. J., ... & Thayer, K. A. (2019). A scoping review of the health and toxicological activity of bisphenol A (BPA) structural analogues and functional alternatives. *Toxicology*, *424*, 152235.
155. Pérez-Arauz, A. O., Aguilar-Rabiela, A. E., Vargas-Torres, A., Rodríguez-Hernández, A. I., Chavarría-Hernández, N., Vergara-Porras, B., & López-Cuellar, M. R. (2019). Production and characterization of biodegradable films of a novel polyhydroxyalkanoate (PHA) synthesized from peanut oil. *Food Packaging and Shelf Life*, *20*, 100297.
156. Plastics Europe Plastics—The Facts 2021. Available online: <https://plasticseurope.org/wp-content/uploads/2021/12/Plastics-the-Facts-2021-web-final.pdf> (accessed on 31 January 2022).
157. PlasticsEurope. (2018). PlasticsEurope, plastics—the facts 2018: an analysis of European plastics production, demand and waste data. PlasticsEurope, Brussels, Belgium
158. Poortinga, W., & Whitaker, L. (2018). Promoting the use of reusable coffee cups through environmental messaging, the provision of alternatives and financial incentives. *Sustainability*, *10*(3), 873
159. Prata, J. C. (2018). Microplastics in wastewater: State of the knowledge on sources, fate and solutions. *Marine pollution bulletin*, *129*(1), 262-265.
160. Priyanka, M., & Dey, S. (2018). Ruminant impaction due to plastic materials-An increasing threat to ruminants and its impact on human health in developing countries. *Veterinary world*, *11*(9), 1307.
161. Qasaimeh, A., Abdallah-Qasaimeh, M. R., & Hani, F. B. (2016). A review on biogas interception processes in municipal landfill. *Journal of Environmental Science and Technology*, *9*(1), 1-25.
162. Quartinello, F., Vajnhandl, S., Volmajer Valh, J., Farmer, T. J., Vončina, B., Lobnik, A., ... & Guebitz, G. M. (2017). Synergistic chemo-enzymatic



- hydrolysis of poly (ethylene terephthalate) from textile waste. *Microbial biotechnology*, 10(6), 1376-1383.
163. Rajmohan, K. V. S., Ramya, C., Viswanathan, M. R., & Varjani, S. (2019). Plastic pollutants: effective waste management for pollution control and abatement. *Current Opinion in Environmental Science & Health*, 12, 72-84.
164. Ribitsch, D., Acero, E. H., Greimel, K., Dellacher, A., Zitzenbacher, S., Marold, A., ... & Guebitz, G. M. (2012). A new esterase from *Thermobifida halotolerans* hydrolyses polyethylene terephthalate (PET) and polylactic acid (PLA). *Polymers*, 4(1), 617-629.
165. Richert, A., & Dąbrowska, G. B. (2021). Enzymatic degradation and biofilm formation during biodegradation of polylactide and polycaprolactone polymers in various environments. *International Journal of Biological Macromolecules*, 176, 226-232.
166. Rizzarelli, P., Impallomeni, G., & Montaudo, G. (2004). Evidence for selective hydrolysis of aliphatic copolyesters induced by lipase catalysis. *Biomacromolecules*, 5(2), 433-444.
167. Ronkvist, Å. M., Xie, W., Lu, W., & Gross, R. A. (2009). Cutinase-catalyzed hydrolysis of poly (ethylene terephthalate). *Macromolecules*, 42(14), 5128-5138.
168. Rosenberg, E., & DeLong, E. F. (1980). The prokaryotes. Rosenberg E DE, Thompson F, Lory S, Stackebrandt E., editor.
169. Ruan, J., Qin, B., & Huang, J. (2018). Controlling measures of microplastic and nano pollutants: A short review of disposing waste toners. *Environment international*, 118, 92-96.
170. Ruan, L., Yao, X., Chang, Y., Zhou, L., Qin, G., & Zhang, X. (2018). Properties and applications of the  $\beta$  phase poly (vinylidene fluoride). *Polymers*, 10(3), 228.
171. Rubio, M. B., Cardoza, R. E., Hermosa, R., Gutiérrez, S., & Monte, E. (2008). Cloning and characterization of the *Thec1* gene encoding a cutinase of *Trichoderma harzianum* T34. *Current genetics*, 54, 301-312.

- 
172. Sadri, S. S., & Thompson, R. C. (2014). On the quantity and composition of floating plastic debris entering and leaving the Tamar Estuary, Southwest England. *Marine pollution bulletin*, *81*(1), 55-60.
173. Samak, N. A., Jia, Y., Sharshar, M. M., Mu, T., Yang, M., Peh, S., & Xing, J. (2020). Recent advances in biocatalysts engineering for polyethylene terephthalate plastic waste green recycling. *Environment international*, *145*, 106144.
174. Sepperumal, U., Markandan, M., & Palraja, I. (2013). Micromorphological and chemical changes during biodegradation of polyethylene terephthalate (PET) by *Penicillium* sp. *J Microbiol Biotechnol Res*, *3*(4), 47-53.
175. Shafei, A., Ramzy, M. M., Hegazy, A. I., Husseny, A. K., El-Hadary, U. G., Taha, M. M., & Mosa, A. A. (2018). The molecular mechanisms of action of the endocrine disrupting chemical bisphenol A in the development of cancer. *Gene*, *647*, 235-243.
176. Shah, A. A., Eguchi, T., Mayumi, D., Kato, S., Shintani, N., Kamini, N. R., & Nakajima-Kambe, T. (2013). Degradation of aliphatic and aliphatic–aromatic co-polyesters by depolymerases from *Roseateles depolymerans* strain TB-87 and analysis of degradation products by LC-MS. *Polymer degradation and stability*, *98*(12), 2722-2729.
177. Shah, A. A., Hasan, F., Hameed, A., & Ahmed, S. (2008). Biological degradation of plastics: a comprehensive review. *Biotechnology advances*, *26*(3), 246-265.
178. Sharma, D. C., & Satyanarayana, T. (2006). A marked enhancement in the production of a highly alkaline and thermostable pectinase by *Bacillus pumilus* dcsr1 in submerged fermentation by using statistical methods. *Bioresource Technology*, *97*(5), 727-733.
179. Shi, K., Jing, J., Song, L., Su, T., & Wang, Z. (2020). Enzymatic hydrolysis of polyester: Degradation of poly ( $\epsilon$ -caprolactone) by *Candida antarctica* lipase and *Fusarium solani* cutinase. *International Journal of Biological Macromolecules*, *144*, 183-189.

- 
180. Siewe, F. B., Kudre, T. G., & Narayan, B. (2021). Optimisation of ultrasound-assisted enzymatic extraction conditions of umami compounds from fish by-products using the combination of fractional factorial design and central composite design. *Food Chemistry*, *334*, 127498.
181. Simon, B., Amor, M. B., & Földényi, R. (2016). Life cycle impact assessment of beverage packaging systems: focus on the collection of post-consumer bottles. *Journal of Cleaner Production*, *112*, 238-248.
182. Singh, A. K., & Mukhopadhyay, M. (2012). Overview of fungal lipase: a review. *Applied biochemistry and biotechnology*, *166*, 486-520.
183. Singh, B., & Sharma, N. (2008). Mechanistic implications of plastic degradation. *Polymer degradation and stability*, *93*(3), 561-584.
184. Siracusa, V. (2019). Microbial degradation of synthetic biopolymers waste. *Polymers*, *11*(6), 1066.
185. Sivan, A. (2011). New perspectives in plastic biodegradation. *Current opinion in biotechnology*, *22*(3), 422-426.
186. Skleničková, K., Abbrent, S., Halecký, M., Kočí, V., & Beneš, H. (2022). Biodegradability and ecotoxicity of polyurethane foams: a review. *Critical Reviews in Environmental Science and Technology*, *52*(2), 157-202.
187. Smith, R. (2005). *Biodegradable polymers for industrial applications*. CRC Press
188. Song, J. H., Murphy, R. J., Narayan, R., & Davies, G. B. H. (2009). Biodegradable and compostable alternatives to conventional plastics. *Philosophical transactions of the royal society B: Biological sciences*, *364*(1526), 2127-2139.
189. Sruthy, S., & Ramasamy, E. V. (2017). Microplastic pollution in Vembanad Lake, Kerala, India: the first report of microplastics in lake and estuarine sediments in India. *Environmental pollution*, *222*, 315-322.
190. Steensgaard, I. M., Syberg, K., Rist, S., Hartmann, N. B., Boldrin, A., & Hansen, S. F. (2017). From macro-to microplastics-Analysis of EU regulation along the life cycle of plastic bags. *Environmental Pollution*, *224*, 289-299.

- 
191. Suzuki, K., Noguchi, M. T., Shinozaki, Y., Koitabashi, M., Sameshima-Yamashita, Y., Yoshida, S., ... & Kitamoto, H. K. (2014). Purification, characterization, and cloning of the gene for a biodegradable plastic-degrading enzyme from Paraphoma-related fungal strain B47-9. *Applied microbiology and biotechnology*, *98*, 4457-4465.
192. Suzuki, K., Sakamoto, H., Shinozaki, Y., Tabata, J., Watanabe, T., Mochizuki, A., ... & Kitamoto, H. K. (2013). Affinity purification and characterization of a biodegradable plastic-degrading enzyme from a yeast isolated from the larval midgut of a stag beetle, *Aegus laevicollis*. *Applied microbiology and biotechnology*, *97*, 7679-7688.
193. Then, J., Wei, R., Oeser, T., Barth, M., Belisário-Ferrari, M. R., Schmidt, J., & Zimmermann, W. (2015). Ca<sup>2+</sup> and Mg<sup>2+</sup> binding site engineering increases the degradation of polyethylene terephthalate films by polyester hydrolases from *Thermobifida fusca*. *Biotechnology Journal*, *10*(4), 592-598.
194. Thompson, R. C., Moore, C. J., Vom Saal, F. S., & Swan, S. H. (2009). Plastics, the environment and human health: current consensus and future trends. *Philosophical transactions of the royal society B: biological sciences*, *364*(1526), 2153-2166.
195. Thumarat, U., Nakamura, R., Kawabata, T., Suzuki, H., & Kawai, F. (2012). Biochemical and genetic analysis of a cutinase-type polyesterase from a thermophilic *Thermobifida alba* AHK119. *Applied microbiology and biotechnology*, *95*, 419-430.
196. Tokiwa, Y., Calabia, B. P., Ugwu, C. U., & Aiba, S. (2009). Biodegradability of plastics. *International journal of molecular sciences*, *10*(9), 3722-3742.
197. Torres-Mura, J. C., Lemus, M. L., & Hertel, F. (2015). Plastic material in the diet of the turkey vulture (*Cathartes aura*) in the Atacama Desert, Chile. *The Wilson Journal of Ornithology*, *127*(1), 134-138.
198. Tournier, V., Topham, C. M., Gilles, A., David, B., Folgoas, C., Moya-Leclair, E., ... & Marty, A. (2020). An engineered PET depolymerase to break down and recycle plastic bottles. *Nature*, *580*(7802), 216-219.
-

- 
199. Tsuji, H., Echizen, Y., & Nishimura, Y. (2006). Photodegradation of biodegradable polyesters: A comprehensive study on poly (l-lactide) and poly ( $\epsilon$ -caprolactone). *Polymer degradation and stability*, *91*(5), 1128-1137.
200. Tulashie, S. K., Boadu, E. K., Kotoka, F., & Mensah, D. (2020). Plastic wastes to pavement blocks: A significant alternative way to reducing plastic wastes generation and accumulation in Ghana. *Construction and Building Materials*, *241*, 118044.
201. Vaughan, R., Turner, S. D., & Rose, N. L. (2017). Microplastics in the sediments of a UK urban lake. *Environmental Pollution*, *229*, 10-18.
202. Vethaak, A. D., & Legler, J. (2021). Microplastics and human health. *Science*, *371*(6530), 672-674.
203. Vought, V., & Wang, H. S. (2018). Impact of common environmental chemicals bisphenol A and bisphenol S on the physiology of *Lumbricus variegatus*. *Environmental Toxicology and Pharmacology*, *60*, 225-229.
204. Wagner-Egea, P., Tosi, V., Wang, P., Grey, C., Zhang, B., & Linares-Pastén, J. A. (2021). Assessment of Is PETase-Assisted Depolymerization of Terephthalate Aromatic Polyesters and the Effect of the Thioredoxin Fusion Domain. *Applied Sciences*, *11*(18), 8315.
205. Wang, Z., Wang, Y., Guo, Z., Li, F., & Chen, S. (2011). Purification and characterization of poly (L-lactic acid) depolymerase from *Pseudomonas* sp. strain DS04-T. *Polymer Engineering & Science*, *51*(3), 454-459.
206. Warner, M., Mocarelli, P., Brambilla, P., Wesselink, A., Samuels, S., Signorini, S., & Eskenazi, B. (2013). Diabetes, metabolic syndrome, and obesity in relation to serum dioxin concentrations: the Seveso women's health study. *Environmental health perspectives*, *121*(8), 906-911.
207. Watanabe, T., Suzuki, K., Shinozaki, Y., Yarimizu, T., Yoshida, S., Sameshima-Yamashita, Y., ... & Kitamoto, H. K. (2015). A UV-induced mutant of *Cryptococcus flavus* GB-1 with increased production of a biodegradable plastic-degrading enzyme. *Process Biochemistry*, *50*(11), 1718-1724.
208. Webb, H. K., Arnott, J., Crawford, R. J., & Ivanova, E. P. (2012). Plastic degradation and its environmental implications with special reference to poly (ethylene terephthalate). *Polymers*, *5*(1), 1-18.

- 
209. Wei, R., & Zimmermann, W. (2017). Biocatalysis as a green route for recycling the recalcitrant plastic polyethylene terephthalate. *Microbial biotechnology*, *10*(6), 1302.
210. Wei, R., & Zimmermann, W. (2017). Microbial enzymes for the recycling of recalcitrant petroleum-based plastics: how far are we?. *Microbial biotechnology*, *10*(6), 1308-1322.
211. Wei, R., Oeser, T., Schmidt, J., Meier, R., Barth, M., Then, J., & Zimmermann, W. (2016). Engineered bacterial polyester hydrolases efficiently degrade polyethylene terephthalate due to relieved product inhibition. *Biotechnology and Bioengineering*, *113*(8), 1658-1665.
212. Werner, S., Budziak, A., Van Franeker, J. A., Galgani, F., Hanke, G., Maes, T., ... & Vlachogianni, T. (2016). Harm caused by marine litter.
213. Wilcox, C., Van Sebille, E., & Hardesty, B. D. (2015). Threat of plastic pollution to seabirds is global, pervasive, and increasing. *Proceedings of the national academy of sciences*, *112*(38), 11899-11904.
214. Willis, K., Maureaud, C., Wilcox, C., & Hardesty, B. D. (2018). How successful are waste abatement campaigns and government policies at reducing plastic waste into the marine environment?. *Marine Policy*, *96*, 243-249.
215. Woodard, L. N., & Grunlan, M. A. (2018). Hydrolytic degradation and erosion of polyester biomaterials.
216. World Economic Forum. (2016). The New Plastics Economy: Rethinking the future of plastics, Cologny, Switzerland
217. Wu, W. M., Yang, J., & Criddle, C. S. (2017). Microplastics pollution and reduction strategies. *Frontiers of Environmental Science & Engineering*, *11*, 1-4.
218. Xie, F., Zhang, T., Bryant, P., Kurusingal, V., Colwell, J. M., & Laycock, B. (2019). Degradation and stabilization of polyurethane elastomers. *Progress in Polymer Science*, *90*, 211-268.
219. Yan, F., Wei, R., Cui, Q., Bornscheuer, U. T., & Liu, Y. J. (2021). Thermophilic whole-cell degradation of polyethylene terephthalate using engineered *Clostridium thermocellum*. *Microbial biotechnology*, *14*(2), 374-385.

- 
220. Yang, S., Xu, H., Yan, Q., Liu, Y., Zhou, P., & Jiang, Z. (2013). A low molecular mass cutinase of *Thielavia terrestris* efficiently hydrolyzes poly (esters). *Journal of Industrial Microbiology and Biotechnology*, *40*(2), 217-226.
221. Yang, Y., Min, J., Xue, T., Jiang, P., Liu, X., Peng, R., ... & Guo, R. T. (2023). Complete bio-degradation of poly (butylene adipate-co-terephthalate) via engineered cutinases. *Nature Communications*, *14*(1), 1645.
222. Yoshida, S., Hiraga, K., Takehana, T., Taniguchi, I., Yamaji, H., Maeda, Y., ... & Oda, K. (2016). A bacterium that degrades and assimilates poly (ethylene terephthalate). *Science*, *351*(6278), 1196-1199.
223. Yousif, E., & Haddad, R. (2013). Photodegradation and photostabilization of polymers, especially polystyrene. *SpringerPlus*, *2*(1), 1-32.
224. Zhang, Y., Chen, S., Xu, M., Cavoco-Paulo, A., Wu, J., & Chen, J. (2010). Characterization of *Thermobifida fusca* cutinase-carbohydrate-binding module fusion proteins and their potential application in bioscouring. *Applied and environmental microbiology*, *76*(20), 6870-6876.
225. Zheng, Y., Yanful, E. K., & Bassi, A. S. (2005). A review of plastic waste biodegradation. *Critical reviews in biotechnology*, *25*(4), 243-250.
226. Zubris, K. A. V., & Richards, B. K. (2005). Synthetic fibers as an indicator of land application of sludge. *Environmental pollution*, *138*(2), 201-211.

# ***APPENDICES***



### Appendix 1: Composition of nutrient agar

Nutrient broth	0.8 g
Agar	1.5 g
Water	100 mL

### Appendix 2: Composition of MSM

$K_2HPO_4$	1.0 g
$KH_2PO_4$	0.2 g
NaCl	1.0 g
$CaCl_2 \cdot 2H_2O$	0.002 g
$(NH_4)_2 SO_4$ , 1.0	1.0 g
$MgSO_4 \cdot 7H_2O$ , 0.5	0.5 g
Distilled Water	100 mL
$FeSO_4 \cdot 7 H_2O$	0.01 g

### Appendix 3: Composition of Production Media

Glucose	13 g
Sucrose	11 g
Yeast Extract	3 g
$NaNO_3$	11.0 g
$K_2HPO_4$	2 g
$(NH_4)_2SO_4$	5.5 g
$MgSO_4 \cdot 7H_2O$	2 g
KCL	2 g
Cutin	4 g
$Na_2HPO_4$	3 g
Distilled Water	1 L

**Appendix 4: Composition of PCL agar**

PCL	0.5 g
Acetone	50 mL
Agar	2 g
Water	100 mL

**Appendix 5: 20mM Stock Preparation of Substrate**

Isopropanol	50 m
<i>p</i> -Nitrophenyl Butyrate ( <i>p</i> -NP-B)	91 $\mu$ L

**Appendix 6: 100mM Phosphate Buffer**

Distilled Water	100mL
K <sub>2</sub> HPO <sub>4</sub>	1.74 g
KH <sub>2</sub> PO <sub>4</sub>	1.36 g

**Appendix 7: Standard curve development for bovine serum albumin**

Test Tube #	Distilled Water (mL)	BSA Stock Solution (mL)	Protein Conc. (mg/mL)	Absorbance
1	0.00	1	1	0.987
2	0.1	0.9	0.9	0.901
3	0.2	0.8	0.8	0.836
4	0.3	0.7	0.7	0.746
5	0.4	0.6	0.6	0.632
6	0.5	0.5	0.5	0.564
7	0.6	0.4	0.4	0.423
8	0.7	0.3	0.3	0.307
9	0.8	0.2	0.2	0.266
10	0.9	0.1	0.1	0.112
11	1	0.00	0.00	0

**Appendix 8: Standard curve development for *p*-nitrophenol (*p*NP)**

Test Tube #	Distilled Water (mL)	<i>p</i> NP Stock Solution (μL)	<i>p</i> NP Conc. (μg/mL)	Absorbance
1	0.00	100	100	0
2	0.1	90	90	0.0506
3	0.2	80	80	0.1161
4	0.3	70	70	0.18514
5	0.4	60	60	0.2633
6	0.5	50	50	0.3297
7	0.6	40	40	0.4008
8	0.7	30	30	0.4636
9	0.8	20	20	0.514
10	0.9	10	10	0.5761
11	1	0.0	0.0	0.6664

**Appendix 9: Running gel**

Serial number	Gel %	15%	12.5%
1	30% Acrylamide/bis	4.9 mL	4.2 mL
2	Tris (1.5 M pH 6.8)	2.5 mL	2.5 mL
3	SDS 10%	100 μL	100 μL
4	TEMED	20 μL	20 μL
5	10% APS	50 μL	50 μL
6	Water	2.4 mL	3.4 mL

**Appendix 10: Stacking gel**

Serial number	Gel %	Volume
1	30% Acrylamide/bis	696 $\mu$ L
2	Tris (1.5 M pH 6.8)	650 $\mu$ L
3	SDS 10%	100 $\mu$ L
4	TEMED	10 $\mu$ L
5	10% APS	50 $\mu$ L
6	Water	3.65 mL

**Appendix 11: Protein dye solution**

Water	40 mL
Methanol	50 mL
Acetic acid	10 mL
Commasi brilliant blue R-250	0.125 g

**Appendix 12: Distaining solution 1**

Water	40 mL
Methanol	50 mL
Acetic acid	10 mL

**Appendix 13: Distaining solution 2**

Water	132 mL
Methanol	7.5 mL
Acetic acid	10.5 mL

**Appendix 14: Temperature optimization (Fermentation condition)**

<b>Specific activity (U/mg)</b>			
<b>Temperature</b>	<b>24</b>	<b>48</b>	<b>72</b>
25	28.43303	48.30156	47.36715
30	26.12603	55.64449	41.15081
35	28.53798	56.68346	43.18093
40	11.54999	18.83078	10.22473
45	12.12959	24.93349	13.41036

**Appendix 15: pH optimization (Fermentation condition)**

<b>Specific activity (U/mg)</b>			
<b>pH</b>	<b>24</b>	<b>48</b>	<b>72</b>
5	18.23101	42.23326	24.41045
6	23.88125	65.47494	39.89454
7	27.49802	62.36197	42.24628
8	28.25695	71.6867	48.73385
9	12.12959	45.99434	28.9986
10	9.524584	42.48683	19.88207

**Appendix 16: Temperature optimization (Fermentation condition)**

<b>Specific activity (U/mg)</b>			
<b>Inoculum size</b>	<b>24</b>	<b>48</b>	<b>72</b>
0.10%	25.17995	29.36747	12.66887
0.50%	24.39593	38.93709	32.01476
1%	27.07029	41.94877	34.6447
2%	29.48373	52.80125	46.44383
3%	18.83369	27.56295	21.29808

**Appendix 17: Time of incubation optimization (Fermentation condition)**

<b>Time (h)</b>	<b>Specific Activity (U/mg)</b>
<b>24</b>	29.60996
<b>48</b>	44.83896
<b>72</b>	27.01402

**Appendix 18: *S. maltophilia* PRS8 Sephadex (G-100) profile**

<b>Fraction</b>	<b>O.D at 280 nm</b>	<b>O.D at 410 nm</b>
1	0	0.198364
2	0	0.198364
3	0	0.198364
4	0	0.198364
5	0.54	83.13636
6	1.251	190.8636
7	1.318	201.0152
8	1.455	221.7727
9	1.599	243.5909
10	1.591	242.3788
11	1.472	224.3485
12	1.32	201.3182
13	1.214	185.2576
14	1.117	170.5606
15	1.13	172.5303
16	1.09	166.4697
17	0.84	128.5909
18	0.5	77.07576
19	0.3	46.77273
20	0.3	46.77273
21	0.2	31.62121
22	0.2	31.62121
23	0.03	5.863636
24	0.024	4.954545
25	0.01	2.833333
26	0.0001	1.333333
27	0.00001	1.319697
28	0.00001	1.319697
29	0.0001	1.333333
30	0.0001	1.333333

**Appendix 19: *S. maltophilia* PRS8 Cutinase temperature profile**

<b>Temperature (°C)</b>	<b>O.D</b>	<b>Relative Activity</b>
30	2.138067	95.87743
35	2.227333	99.88042
40	2.204033	98.83558
45	0.973333	43.64723
50	0.411	18.43049
55	0.166667	7.473842
60	0.0634	2.843049

**Appendix 20: *S. maltophilia* PRS8 Cutinase pH profile**

<b>pH</b>	<b>O.D</b>	<b>Relative Activity</b>
<b>3</b>	0.246333	12.44108
<b>4</b>	0.453333	22.89562
<b>5</b>	0.536667	27.10438
<b>6</b>	0.923333	46.633
<b>7</b>	1.85	93.43434
<b>8</b>	1.946	98.28283
<b>9</b>	1.976667	99.83165
<b>10</b>	1.906333	96.27946
<b>11</b>	1.03	52.0202



**Appendix 21: *S. maltophilia* PRS8 Cutinase temperature stability profile**

PRS8 Relative activity							
Time (minutes)	Temperature (°C)						
	30	35	40	45	50	55	60
<b>0</b>	100	100	100	100	100	100	100
<b>30</b>	97.52	99.57	100	58.94	36.84	26.31	15.78
<b>60</b>	96.73	98.42	98.42105	57.89	34.21	24.73	12.63
<b>90</b>	95.26	96.31	96.84211	55.78	32.10	21.57	9.473
<b>120</b>	93.73	95.26	96.31	54.21	28.94	16.31	5.78
<b>150</b>	93.73	94.21	95.26	54.21	15.78	10.52	5.26

**Appendix 22: *S. maltophilia* PRS8 Cutinase pH stability profile**

PRS8 Relative activity									
Time (minutes)	pH								
	3	4	5	6	7	8	9	10	11
<b>0</b>	100	100	100	100	100	100	100	100	100
<b>30</b>	14	17.2	20.4	28.4	67.2	100	96	88.8	73.6
<b>60</b>	10.44	14	17.2	27.2	66	98	94.8	84.8	64.4
<b>90</b>	8.4	12.4	13.2	26	64.4	96.4	92.4	81.2	57.2
<b>120</b>	6	9.6	10	25.2	63.2	94.8	90.4	77.2	50
<b>150</b>	4.4	8	8.4	24.4	61.6	93.2	87.6	72.8	40.8

**Appendix 23: *S. maltophilia* PRS8 Cutinase metal ions profile**

<b>Metals</b>	<b>2mM</b>	<b>10mM</b>
Control	100	100
CaSO <sub>4</sub>	111.3281	102.3438
HgCl <sub>2</sub>	0	0
FeSO <sub>4</sub>	98.82813	100.3906
CuSO <sub>4</sub>	107.8125	100.7813
CoCl <sub>2</sub>	55.85938	58.98438
NiSO <sub>4</sub>	100.3906	100
MgSO <sub>4</sub>	107.4219	105.0781
ZnSO <sub>4</sub>	114.4531	107.4219
KCl	115.2344	111.7188
BaSO <sub>4</sub>	52.73438	51.17188
CdCl <sub>2</sub>	1.953125	3.515625
Na <sub>2</sub> SO <sub>4</sub>	85.54688	91.79688
MgSO <sub>4</sub>	107.4219	105.0781
HgCl <sub>2</sub>	0	0
CuCl <sub>2</sub>	0.24576	0.205824
CaSO <sub>4</sub>	0.226048	0.177664

**Appendix 24: *S. maltophilia* PRS8 Cutinase surfactants profile**

<b>Surfactants</b>	<b>0.50%</b>	<b>1%</b>
Control	100	100
Tween20	109.4118	106.6667
Tween 40	112.549	116.4706
Tween 60	110.9804	110.5882
Tween 80	113.7255	105.098
CTAB	11.76471	7.843137
SDS	0	0
Triton X 100	109.8039	112.1569

**Appendix 25: *S. maltophilia* PRS8 Cutinase organic solvents profile**

<b>PRS8 Relative activity</b>				
<b>Time</b>	<b>30</b>	<b>60</b>	<b>90</b>	<b>120</b>
Control	100	100	100	100
Acetonitrile	100.8969	100	99.10314	95.5157
Methanol	104.0359	103.139	98.65471	91.03139
Ethanol	70.85202	60.08969	56.95067	50.22422
Aceton	91.03139	96.86099	96.41256	95.5157
Ethyle Acetate	103.139	98.65471	96.41256	92.82511
Butanol	56.50224	52.46637	47.53363	46.18834
DMSO	98.20628	95.06726	94.61883	94.1704
Propanol	91.92825	90.13453	89.6861	85.20179
Formaldehyde	94.61883	89.6861	85.65022	85.20179

**Appendix 26: *S. maltophilia* PRS8 Cutinase kinetic profile**

PRS8 kinetics					
Substrate	Absorbance at 540 nm	Activity (U/ml)	Specific activity U/mg	I/s	I/v
				-0.7037	0
0.05	0.07	11.92424	23.84848	20	0.041931
0.1	0.15	24.04545	48.09091	10	0.020794
0.2	0.25	39.19697	78.39394	5	0.012756
0.3	0.33	51.31818	102.6364	3.333333	0.009743
0.4	0.38	58.89394	117.7879	2.5	0.00849
0.5	0.45	69.5	139	2	0.007194
0.6	0.51	78.59091	157.1818	1.666667	0.006362
0.7	0.54	83.13636	166.2727	1.428571	0.006014
0.8	0.65	99.80303	199.6061	1.25	0.00501
0.9	0.78	119.5	239	1.111111	0.004184

**Appendix 27: *S. maltophilia* PRS8 recombinant PET hydrolase temperature profile**

Temperature (°C)	O.D	Relative Activity
30	2.204	90.62127
35	2.227333	91.58066
40	2.2707	93.36376
45	1.946667	80.04057
50	1.411	58.01571
55	0.733333	30.15227
60	0.196733	8.089031
65	0.166667	6.852788
70	0.0634	2.606801

**Appendix 28: *S. maltophilia* PRS8 recombinant PET hydrolase pH profile**

<b>pH</b>	<b>O.D</b>	<b>Relative Activity</b>
3	0.246333	12.44108
4	0.453333	22.89562
5	0.536667	27.10438
6	0.923333	46.633
7	1.85	93.43434
8	1.946	99.15825
9	1.976667	99.83165
10	1.906333	96.27946
11	1.03	52.0202

**Appendix 29: *S. maltophilia* PRS8 recombinant PET hydrolase temperature stability profile**

<b>PRS8 Relative activity</b>									
<b>Time (minutes)</b>	<b>Temperature (°C)</b>								
	30	35	40	45	50	55	60	66	70
<b>0</b>	100	100	100	100	100	100	100	100	100
<b>30</b>	92.26	94.31	100	88.42	85.26	47.36	36.84	26.31	15.78
<b>60</b>	91.47	93.15	98.42	81.05	74.21	36.84	21.05	19.47	12.63
<b>90</b>	90	91.05	96.84	76.84	52.68	26.84	14.73	16.31	9.47
<b>120</b>	90.57	90	96.31	70	50	21.57	5.789	16.31	5.78
<b>150</b>	88.47	88.94	95.26	59.47	33.15	10.52	5.263	10.52	5.26

**Appendix 30: *S. maltophilia* PRS8 recombinant PET hydrolase pH stability profile**

PRS8 Relative activity									
Time (minutes)	pH								
	3	4	5	6	7	8	9	10	11
<b>0</b>	100	100	100	100	100	100	100	100	100
<b>30</b>	14	17.2	20.4	68	91.2	100	98	88.8	45.6
<b>60</b>	10.44	14	17.2	66	86	98	94.8	84.8	44.4
<b>90</b>	8.4	12.4	13.2	55.6	76.4	96.4	94	81.2	33.2
<b>120</b>	6	9.6	10	49.2	71.2	94.8	92.8	77.2	20
<b>150</b>	4.4	8	8.4	44.4	65.6	93.2	91.6	72.8	16

**Appendix 31: *S. maltophilia* PRS8 recombinant PET hydrolase surfactants profile**

Surfactants	0.50%	1%
Control	100	100
Tween20	109.4118	106.6667
Tween 40	112.549	116.4706
Tween 60	110.9804	110.5882
Tween 80	113.7255	105.098
CTAB	35.29412	27.45098
SDS	19.60784	15.68627
Triton X 100	109.8039	112.1569

**Appendix 32: *S. maltophilia* PRS8 recombinant PET hydrolase metal ions profile**

<b>Metals</b>	<b>2mM</b>	<b>10mM</b>
Control	100	100
CaSO <sub>4</sub>	107.0866	112.2047
MgSO <sub>4</sub>	103.5433	106.6929
FeSO <sub>4</sub>	101.1811	99.6063
CuSO <sub>4</sub>	101.5748	108.6614
CoCl <sub>2</sub>	98.8189	95.66929
NiSO <sub>4</sub>	100.7874	101.1811
HgCl <sub>2</sub>	20.07874	20.86614
ZnSO <sub>4</sub>	108.2677	115.3543
KCl	112.5984	116.1417
BaSO <sub>4</sub>	51.5748	53.14961
CdCl <sub>2</sub>	35.43307	29.52756
Na <sub>2</sub> SO <sub>4</sub>	92.51969	86.22047
MgSO <sub>4</sub>	105.9055	108.2677
HgCl <sub>2</sub>	0	19.68504
CuCl <sub>2</sub>	0.24576	0.205824
CaSO <sub>4</sub>	0.226048	0.177664

**Appendix 33: *S. maltophilia* PRS8 recombinant PET hydrolase organic solvents profile**

<b>PRS8 Relative activity</b>				
<b>Time</b>	30	60	90	120
Control	100	100	100	100
Acetonitrile	100.8969	100	99.10314	95.5157
Methanol	113.0045	116.5919	117.5785	117.9372
Ethanol	43.94619	42.15247	39.01345	32.287
Aceton	117.9372	119.2825	118.8341	117.9372
Ethyle Acetate	116.5919	116.5919	118.8341	119.7309
Butanol	101.3453	97.30942	92.37668	91.03139
DMSO	98.20628	95.06726	94.61883	94.1704
Propanol	91.92825	90.13453	89.6861	85.20179
Formaldehyde	108.0717	108.5202	108.0717	107.1749

**Appendix 34: *S. maltophilia* PRS8 recombinant PET hydrolase kinetic profile**

<b>PRS8 kinetics</b>					
<b>substrate</b>	<b>Absorbance at 540 nm</b>	<b>Activity (U/ml)</b>	<b>Specific activity U/mg</b>	<b>I/s</b>	<b>I/v</b>
				-0.7037	0
<b>0.05</b>	0.17	27.07576	54.15152	20	0.018467
<b>0.1</b>	0.25	39.19697	78.39394	10	0.012756
<b>0.2</b>	0.35	54.34848	108.697	5	0.0092
<b>0.3</b>	0.43	66.4697	132.9394	3.333333	0.007522
<b>0.4</b>	0.48	74.04545	148.0909	2.5	0.006753
<b>0.5</b>	0.55	84.65152	169.303	2	0.005907
<b>0.6</b>	0.61	93.74242	187.4848	1.666667	0.005334
<b>0.7</b>	0.74	113.4394	226.8788	1.428571	0.004408
<b>0.8</b>	0.75	114.9545	229.9091	1.25	0.00435
<b>0.9</b>	0.75	114.9545	229.9091	1.111111	0.00435





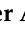




**Appendix 35: *S. maltophilia* PRS8 16S gene**

CCATGGCTCAGAGTGAACGCTGGCGGTAGGCCTAACACATGCAAGTCGAA  
CGGCAGCACAGGAGAGCTTGCTCTCTGGGTGGCGAGTGGCGGACGGGTG  
AGGAATACATCGGAATCTACTTTTTTCGTGGGGGATAACGTAGGGAACTT  
ACGCTAATAACGCATACGACCTACGGGTGAAAGCAGGGGATCTTCGGACC  
TTGCGCGATTGAATGAGCCGATGTCGGATTAGCTAGTTGGCGGGGTAAAG  
GCCCACCAAGGCGACGATCCGTAGCTGGTCTGAGAGGATGATCAGCCACA  
CTGGAAGTGAACACGGTCCAGACTCCTACGGGAGGCAGCAGTGGGGAA  
TATTGGACAATGGGCGCAAGCCTGATCCAGCCATACCGCGTGGGTGAAGA  
AGGCCTTCGGGTGTAAAGCCCTTTTGTGGGAAAGAAATCCAGCTGGCT  
AATACCCGGCTGGGATGACGGTACCCAAAGAATAAGCACCGGCTAACTTC  
GTGCCAGCAGCCGCGTAATACGAAGGGCGCAAGCGTACTCGGAATTAC  
TGGGCGTAAAGCGTGCGTAGGTGGTCGTTAAGTCCGTTGTGAAAGCCCT  
GGGCTCAACCTGGGAACTGCAGTGGATACTGGGCGACTAGAATGTGGTAG  
AGGGTAGCGGAATTCCTGGTGTAGCAGTGAAATGCGTAGAGATCAGGAG  
GAACATCCATGGCGAAGGCAGCTACCTGGACCAACATTGACACTGAGGCA  
CGAAAGCGTGGGGAGCAAACAGGATTAGATACCCTGGTAGTCCACGCCCT  
AAACGATGCGAACTGGATGTTGGGTGCAATTTGGCACGCAGTATCGAAGC  
TAACGCGTTAAGTTCGCCGCCTGGGGAGTACGGTCGCAAGACTGAAACTC  
AAAGGAATTGACGGGGGCCCGCACAAAGCGGTGGAGTATGTGGTTAATTC  
GATGCAACGCGAAGAACCTTACCTGGCCTTGACATGTCGAGAACTTTCCA  
GAGATGGATTGGTGCCTTCGGGAACTCGAACACAGGTGCTGCATGGCTGT  
CGTCAGCTCGTGTGTCGTGAGATGTTGGGTAAAGTCCCGCAACGAGCGCAAC  
CCTTGTCCTTAGTTGCCAGCACGTAATGGTGGGAACTCTAAGGAGACCGC  
CGGTGACAAACCGGAGGAAGGTGGGGATGACGTCAAGTCATCATGGCCC  
TTACGGCCAGGGCTACACACGTACTACAATGGTAGGGACAGAGGGCTGCA  
AGCCGGCGACGGTAAGCCAATCCCAGAAACCCTATCTCAGTCCGGATTGG  
AGTCTGCAACTCGACTCCATGAAGTCGGAATCGCTAGTAATCGCAGATCA  
GCATTGCTGCGGTGAATACGTTCCCGGGCCTTG

## Article

# The Purification and Characterization of a Cutinase-like Enzyme with Activity on Polyethylene Terephthalate (PET) from a Newly Isolated Bacterium *Stenotrophomonas maltophilia* PRS8 at a Mesophilic Temperature

Salah Ud Din <sup>1,2,3</sup>, Kalsoom <sup>1</sup>, Sadia Mehmood Satti <sup>4</sup> , Salah Uddin <sup>1</sup> , Smita V. Mankar <sup>5</sup>, Esmā Ceylan <sup>2</sup>, Fariha Hasan <sup>1</sup>, Samiullah Khan <sup>1</sup> , Malik Badshah <sup>1</sup>, Ali Osman Beldüz <sup>2</sup> , Sabriye Çanakçı <sup>2</sup>, Baozhong Zhang <sup>5</sup> , Javier A. Linares-Pastén <sup>3,\*</sup>  and Aamer Ali Shah <sup>1,\*</sup> 

<sup>1</sup> Department of Microbiology, Faculty of Biological Sciences, Quaid-i-Azam University, Islamabad 45320, Pakistan

<sup>2</sup> Department of Biology, Karadeniz Technical University, Trabzon 61080, Turkey

<sup>3</sup> Division of Biotechnology, Department of Chemistry, Faculty of Engineering (LTH), Lund University, P.O. Box 124, SE-22100 Lund, Sweden

<sup>4</sup> Department of Microbiology, Kohsar University Murree, Murree 47150, Pakistan

<sup>5</sup> Centre for Analysis and Synthesis, Department of Chemistry, Faculty of Engineering (LTH), Lund University, SE-22100 Lund, Sweden

\* Correspondence: javier.linares\_pasten@biotek.lu.se (J.A.L.-P.); alishah@qau.edu.pk (A.A.S.)

**Featured Application:** The potential use of bacteria and their enzymes for the degradation of plastic waste and the recovery of value-added products considering bio-up recycling for the circular economy.



**Citation:** Din, S.U.; Kalsoom; Satti, S.M.; Uddin, S.; Mankar, S.V.; Ceylan, E.; Hasan, F.; Khan, S.; Badshah, M.; Beldüz, A.O.; et al. The Purification and Characterization of a Cutinase-like Enzyme with Activity on Polyethylene Terephthalate (PET) from a Newly Isolated Bacterium *Stenotrophomonas maltophilia* PRS8 at a Mesophilic Temperature. *Appl. Sci.* **2023**, *13*, 3686. <https://doi.org/10.3390/app13063686>

Academic Editor: Philippe Michaud

Received: 7 December 2022

Revised: 4 March 2023

Accepted: 9 March 2023

Published: 14 March 2023



**Copyright:** © 2023 by the authors. Licensee MDPI, Basel, Switzerland. This article is an open access article distributed under the terms and conditions of the Creative Commons Attribution (CC BY) license (<https://creativecommons.org/licenses/by/4.0/>).

**Abstract:** A polyethylene terephthalate (PET)-degrading bacterium identified as *Stenotrophomonas maltophilia* PRS8 was isolated from the soil of a landfill. The degradation of the PET bottle flakes and the PET prepared as a powder were assessed using live cells, an extracellular medium, or a purified cutinase-like enzyme. These treated polymers were analyzed using Fourier transform infrared spectroscopy (FTIR) and scanning electron microscopy (SEM). The depolymerization products, identified using HPLC and LC-MS, were terephthalic acid (TPA), mono(2-hydroxyethyl)-TPA (MHET), and bis(2-hydroxyethyl)-TPA (BHET). Several physicochemical factors were optimized for a better cutinase-like enzyme production by using unique single-factor and multi-factor statistical models (the Plackett–Burman design and the central composite design software). The enzyme was purified for homogeneity through column chromatography using Sephadex G-100 resin. The molecular weight of the enzyme was approximately 58 kDa. The specific activity on para nitrophenyl butyrate was estimated at 450.58 U/mg, with a purification of 6.39 times and a yield of 48.64%. The enzyme was stable at various temperatures (30–40 °C) and pH levels (8.0–10.0). The enzyme activity was significantly improved by the surfactants (Triton X-100 and Tween-40), organic solvent (formaldehyde), and metals (NiCl<sub>2</sub> and Na<sub>2</sub>SO<sub>4</sub>). The extracellular medium containing the cutinase-type enzyme showed a depolymerization yield of the PET powder comparable to that of *Idonella skaiensis* IsPETase and significantly higher than that of *Humicola insolens* thermostable HiCut (HiC) cutinase. This study suggests that *S. maltophilia* PRS8 is able to degrade PET at a mesophilic temperature and could be further explored for the sustainable management of plastic waste.

**Keywords:** biodegradation; PET; *Stenotrophomonas maltophilia*; cutinase; Plackett–Burman design; central composite design

## 1. Introduction

Cutinase-like enzymes are gaining interest because some exhibit degradation activity on polyethylene terephthalate (PET). Since the first report on a PET-active cutinase was published in 2005 [1], reports on PET-depolymerizing enzymes have significantly increased in recent years, after the publication of the *Ideonella sakaiensis* bacterium that was able to grow using PET as the sole carbon source [2]. It is worth emphasizing that the amorphous domain of PET can be more accessible to an enzyme attack than crystalline domains. Indeed, thermostabilized PETase, acting at temperatures closer to the glass transition temperature of PET, has shown a better depolymerizing performance [3]. However, mesophilic enzymes and microorganisms could play an important role in the systems where high temperatures are not suitable, such as in wastewater plants.

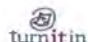
The annual production of plastics was estimated to be 348 million tons in 2017, of which ~90% was derived from fossil fuels [4,5]. By 2030, it is expected to increase to 590 million tons [6]. Owing to their expanding use and versatility, plastic products have become a part of everyday life [7]. Polyethylene terephthalate (PET) consists of ethylene glycol (EG) and terephthalic acid (TPA) monomers linked by ester bonds. It is considered one of the most widely used synthetic polymers and has many applications in drinking bottles, food packaging, and textile fiber materials [8,9]. In 2017, PET production exceeded 30 million tons. Packaging materials always rank high, accounting for ~40% of the total plastics produced [4]. They accumulate in urban solid waste, landfills, and oceans, causing global environmental pollution [10]. This situation has caused severe damage to marine life and threatened some species as most plastic waste on land ends up in water bodies [11].

Plastics are recalcitrant materials for biological degradation. However, 30,000 non-redundant enzyme homologs with putative activity in 10 different plastic types were recently found using bioinformatics methods [12], supporting the current trend of developing enzymatic processes for plastic recycling. Nevertheless, only a small number of fungi and bacteria capable of partially depolymerizing PET have been experimentally studied [13]. The crystallinity of PET is one of the main obstacles to its biodegradation. The enzymes that hydrolyze PET are serine hydrolases, such as cutinases, lipases, and carboxylesterases. The *I. sakaiensis* enzyme, PETase (PET-active enzyme), mainly produces mono(2-hydroxyethyl) terephthalic acid (MHET) and, to a lesser extent, terephthalic acid (TPA) and bis(2-hydroxyethyl)-TPA [2]. The cutinases are part of the  $\alpha/\beta$  family of serine hydrolases that perform ester bond hydrolysis using the canonical Ser-His-Asp catalytic triad. PET and cutin generally share small structural features; they have ester bonds that can be cleaved by cutinases [14,15].

Plastic pretreatment is an important process before enzymatic depolymerization. Plastic crystallinity is one of the main obstacles to an enzymatic attack [16]. Therefore, several pretreatment strategies focus on increasing the amorphization. For example, extrusion and micronization are processes widely used in the plastic industries that amorphize and increase the exchange surface of plastics, facilitating an enzymatic attack. These technologies have maximized PET depolymerization by using an outperforming engineered leaf-branch compost cutinase (LCC), resulting in an outstanding depolymerization yield in a few hours [3]. At the laboratory level and for research purposes, as in this work, PET and other polyesters can also be dissolved in organic solvents and then precipitated as powders [17]. These polyester powders have a lower crystallinity and are suitable for assessing enzymatic activities. On the other hand, green plastic pretreatments should be developed for practical purposes and industrial processes.

In the present study, a bacterial strain capable of growing in a saline medium containing PET as the sole carbon source was isolated from landfill soil. This strain was identified as *Stenotrophomonas maltophilia*. *S. maltophilia* is a gram-negative bacterium and belongs to the  $\gamma$ -proteobacteria. It is present in water, soil, and plant rhizospheres and is considered an opportunistic pathogen [18]. This species has previously been reported to play a role in the bioremediation of various contaminants, including xenobiotics, oils, dyes,

## Turnitin Originality Report

Biodegradation of Poly (Ethylene Terephthalate) by Bacteria Isolated from Soil  
Salah Udinby  turnitin

From PhD (PhD DRSMML)

- Processed on 01-Nov-2023 13:47 PKT
- ID: 2214018489
- Word Count: 41066

## Similarity Index

18%

## Similarity by Source

## Internet Sources:

14%

## Publications:

10%

## Student Papers:

7%

  
PROFESSOR  
Department of Microbiology  
Quaid-i-Azam University, Islamabad

  
Focal Person (Turnitin)  
Quaid-i-Azam University  
Islamabad

**sources:**

- 1 1% match (student papers from 17-Mar-2023)  
[Submitted to Higher Education Commission Pakistan on 2023-03-17](#)
- 2 1% match (student papers from 08-Feb-2017)  
[Submitted to Higher Education Commission Pakistan on 2017-02-08](#)
- 3 1% match (Internet from 15-Oct-2022)  
<http://pr.hec.gov.pk/spul/bitstream/123456789/8233/1/Muhammad%20Irfan%20Thesis%20Complete%20in%201%20File.pdf>
- 4 1% match (Internet from 19-Oct-2022)  
<https://www.mdpi.com/2076-3417/11/18/8315/htm>
- 5 < 1% match (student papers from 12-Jun-2023)  
[Submitted to Higher Education Commission Pakistan on 2023-06-12](#)
- 6 < 1% match (student papers from 07-May-2013)  
[Submitted to Higher Education Commission Pakistan on 2013-05-07](#)
- 7 < 1% match (student papers from 25-May-2023)  
[Submitted to Higher Education Commission Pakistan on 2023-05-25](#)
- 8 < 1% match (student papers from 08-Mar-2011)  
[Submitted to Higher Education Commission Pakistan on 2011-03-08](#)
- 9 < 1% match (student papers from 09-Aug-2010)  
[Submitted to Higher Education Commission Pakistan on 2010-08-09](#)
- 10 < 1% match (student papers from 01-Feb-2011)  
[Submitted to Higher Education Commission Pakistan on 2011-02-01](#)
- 11 < 1% match (student papers from 09-Feb-2023)  
[Submitted to Higher Education Commission Pakistan on 2023-02-09](#)
- 12 < 1% match (student papers from 09-Aug-2011)  
[Submitted to Higher Education Commission Pakistan on 2011-08-09](#)
- 13 < 1% match (student papers from 18-Dec-2009)  
[Submitted to Higher Education Commission Pakistan on 2009-12-18](#)
- 14 < 1% match (student papers from 08-Feb-2022)  
[Submitted to Higher Education Commission Pakistan on 2022-02-08](#)
- 15 < 1% match (student papers from 08-Apr-2022)  
[Submitted to Higher Education Commission Pakistan on 2022-04-08](#)
- 16 < 1% match (Internet from 14-Dec-2022)